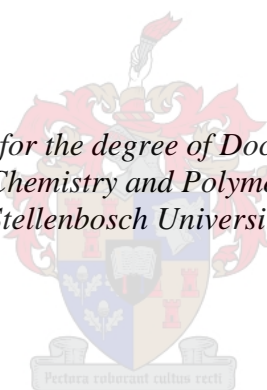


**The use of mononuclear and multinuclear
complexes of rhodium and ruthenium in
catalytic olefin hydroformylation and
hydroaminomethylation reactions**

by
Jacquin October

*Dissertation presented for the degree of Doctor of Philosophy in the
Faculty of Chemistry and Polymer Science at
Stellenbosch University*



Supervisor: Prof Selwyn Frank Mapolie

March 2020

Declaration

By submitting this dissertation electronically, I declare that the entirety of the work contained therein is my own, original work, that I am the sole author thereof (save to the extent explicitly otherwise stated), that reproduction and publication thereof by Stellenbosch University will not infringe any third party rights and that I have not previously in its entirety or in part submitted it for obtaining any qualification.

.....

Jacquin October

March 2020

Copyright © 2020 Stellenbosch University

All rights reserved

Abstract

A range of imino-pyridine ligands (**L1-L8**) were synthesized via Schiff-base condensation reactions. These ligands were subsequently complexed to Rh(I) and Ru(II) using $[\text{Rh}(\text{COD})\text{Cl}]_2$ and $[\text{RuCl}_2(\text{p-cymene})]_2$, to form five novel Rh(I) (**C1-C5**) and three novel Ru(II) (**C6-C8**) imino-pyridine complexes. The rhodium complexes contained both electron-withdrawing (F) and electron-donating groups (CH_3 and OH). In the case of the Ru(II) complexes, **C6** and **C7** were mononuclear in nature while **C8** was binuclear. These complexes were fully characterized using a range of analytical techniques, including IR and NMR (^1H and ^{13}C) spectroscopy, mass spectrometry, elemental analysis and melting point measurements.

The Rh(I) complexes (**C1-C4**) were evaluated as catalyst precursors in the hydroformylation of 1-octene. Full conversion of 1-octene was achieved after only 1 h reaction time, however, poor chemoselectivities towards aldehydes were obtained (only ~52 %) at 30 bar $\text{CO}:\text{H}_2$ (1:1), 0.05 mol% catalyst loading and reaction temperature of 75 °C, with slight regioselectivity towards the linear aldehyde (58 %). Therefore, the effect of pressure was evaluated. However, as the pressure was decreased from 30 to 10 bar, the yield of the aldehydes decreased further. High chemoselectivity towards the aldehydes (~75 %) was obtained when the temperature was decreased from 75 to 55 °C, albeit at moderate conversions (~49 %) of the substrate. This also produced an increase in the regioselectivity towards the linear aldehyde (70 %).

The R groups (F, CH_3 , OH) had no significant effect on the catalytic activity. The hydroformylation of 2-octene was also performed which showed as expected that the rate of hydroformylation of internal olefins is much slower than that of terminal olefins.

The hydroformylation of 1-octene was also attempted using a syngas surrogate, such as formaldehyde. However, no aldehydic products were obtained since with 1-octene. Isomerization to internal olefins (~80 %) and hydrogenation to octane (~20 %) were detected.

The rhodium complexes, **C4** and **C5** were then used as catalyst precursors in the hydroaminomethylation of 1-octene in the presence of amines (piperidine, aniline and benzylamine). High chemoselectivities towards *N*-alkyl piperidines were obtained (~80 %) at 30 bar $\text{CO}:\text{H}_2$ (1:1), 0.1 mol% catalyst loading, 75 °C and 2 h, forming the linear amine in 75 % selectivity. The hydroaminomethylation activity of **C4** and **C5** was found to be superior to that of the well-known complex, $\text{HRhCO}(\text{PPh}_3)_3$. Performing the hydroaminomethylation reaction in the presence of excess piperidine, dramatically influenced the catalytic activity since higher conversions and yields of amines were obtained. Piperidine appears to partially inhibit side reactions such as the isomerization and hydrogenation of 1-octene. The influence of pressure and temperature was also investigated and it was

observed that this promoted the chemoselective synthesis of *N*-alkyl piperidines (~90 %) at 30 bar CO:H₂ (1:1), 0.1 mol % catalyst loading, 2 h and 85 °C.

The focus was then shifted to the use of primary amine, aniline, as co-reagent in the hydroaminomethylation reaction. The initial reaction conditions were chosen as those optimized for the hydroaminomethylation of 1-octene in the presence of piperidine (30 bar CO:H₂ (1:1), 0.1 mol%, 1 h, and 85 °C). As a result of the lower basicity of aniline in comparison to piperidine, the yield of the *N*-alkylated anilines were initially low, even though 1-octene was completely consumed during the reaction. The reaction conditions had to be optimized in order to increase the yield of the *N*-alkylated anilines. We specifically focussed on the partial pressure of H₂. Using a 1:3 ratio of CO:H₂ (50 bar) and extending the reaction time to 6 h, secondary amines could be synthesized in ~45 % yield. When the hydroaminomethylation reaction was performed in the presence of excess aniline (1.5 eq), *N*-alkylated anilines could be synthesized chemoselectively (~95 %), albeit at moderate regioselectivity towards the linear amine (56 %).

Using benzylamine in the hydroaminomethylation of 1-octene, the reaction was significantly faster in comparison to the use of aniline. This was attributed to the higher basicity and thus higher nucleophilicity of benzylamine. *N*-alkylated benzylamines were thus also synthesized chemoselectively while also proceeding at moderate regioselectivities.

The Ru(II) complexes, **C6-C8**, were also evaluated as catalyst precursors in the hydroaminomethylation of 1-octene in the presence of benzylamine. Although these complexes require slightly higher temperatures (110 °C) in comparison to rhodium, they also efficiently mediate the hydroaminomethylation of 1-octene with benzylamine. During the hydroaminomethylation reaction, aldehyde intermediates were not observed even when there were still unreacted olefins (terminal and internal) present in the reaction mixture. This suggest that the hydroformylation reaction is slower than the reductive amination reaction for these ruthenium complexes.

The potential of hydroaminomethylation in the synthesis of value-added chemicals was also demonstrated. In this regard, hydroaminomethylation was used to synthesize primary fatty amines in high yields from cheap olefin feedstocks. Using a similar methodology, dopamine-analogues were synthesized from eugenol. The synthesis of bifunctional biopolymer precursors was also demonstrated via the hydroaminomethylation of methyl 10-undecenoate in the presence of amino acid esters (L-proline methyl ester and methyl piperidine-4-carboxylate). The hydroaminomethylation of 1-octene with these amino acid ester provided access to biosurfactants. It was found that the pyrrolidyl and piperidyl moieties contribute towards the hydrophobicity of the alkyl chain. We also found that the position of the hydrophilic group relative to the alkyl chain can also influence the critical micelle concentration (CMC).

Opsomming

'n Reeks imino-pyridien ligande (**L1-L8**) was gesintetiseer deur middel van Schiff-basis kondensasie reaksies. Hierdie ligande was vervolgens aan Rh(I) en Ru(II) gekomplekseer, deur gebruik te maak van $[\text{Rh}(\text{COD})\text{Cl}]_2$ en $[\text{RuCl}_2(\text{p-cymene})]_2$, om vyf nuwe Rh(I) (**C1-C5**) en drie nuwe Ru(II) (**C6-C8**) imino-pyridien komplekse te vorm. Die rhodium komplekse bevat beide elektron-onttrekkende (F) en elektron-donerende groepe (CH_3 en OH). In die geval van die Ru(II) komplekse, was **C6** en **C7** mono-kernagtig van aard, terwyl **C8** bi-nukleêr is. Hierdie komplekse was volledig gekarakteriseer deur van 'n reeks analitiese tegnieke gebruik te maak. Dit sluit in IR en KMR (^1H en ^{13}C) spektroskopie, massaspektrometrie, elementêre analiese en die bepaling van hul smeltpunte.

Die Rh(I) komplekse (**C1-C4**) was daarna geëvalueer as katalisator-voorlopers in die hidroformulering van 1-okteen. Na 'n reaksietyd van slegs 1 uur was die volledige omskakeling van 1-okteen bereik, maar lae chemoselektiwiteit ten opsigte van aldehyede was verkry (~52 %) by 30 bar $\text{CO}:\text{H}_2$ (1: 1), 0,05 mol% katalisator-lading en 75 °C, met geringe regioselektiwiteit teenoor die lineêre aldehyede (58%). Die effek van druk was dus verder geëvalueer. Met 'n verlaging in druk vanaf 30 na 10 bar het die opbrengs van aldehyede verder gedaal. Hoë chemoselektiwiteit ten opsigte van aldehyede (~75 %) was verkry met 'n verlaging in temperatuur vanaf 75 na 55 °C, al was dit teen matige omskakelings (~49 %) van die substraat. Dit het ook 'n toename in die regioselektiwiteit teenoor die lineêre aldehyd (70%) teweeg gebring.

Die R-groepe (F, CH_3 , OH) het geen noemenswaardige uitwerking op die katalitiese aktiwiteit gehad nie. Die hidroformulering van 2-okteen was ook uitgevoer en het soos verwag getoon dat die hidroformulering van interne alkene baie stadiger is as terminale alkene.

Die hidroformulering van 1-okteen was ook met behulp van 'n singas-surrogaat, formaldehyd, probeer. Geen aldehydiese produkte was egter verkry nie, aangesien die 1-okteen isomerisering na interne alkene (~80 %) en hidrogenering na oktaan (~20 %) ondergaan het.

Die rhodium komplekse, **C4** en **C5** was daarna as katalisator-voorlopers in die hidroaminometielering van 1-okteen in die teenwoordigheid van amiene (piperidien, anilien en bensielamien) gebruik. Hoë chemoselektiwiteit ten opsigte van *N*-alkielpiperidien is verkry (~80 %) by 30 bar $\text{CO}:\text{H}_2$ (1:1), 0,1 mol% katalisator-lading, 75 °C en 2 uur, waar die lineêre amien met 75 % selektiwiteit vorm. Die hidroaminometielering aktiwiteit van **C4** en **C5** was beter as die van die wel-bekende kompleks, $\text{HRhCO}(\text{PPh}_3)_3$. Die uitvoering van die hidroaminometielering reaksie in die teenwoordigheid van 'n oormaat piperidien het die katalitiese aktiwiteit positief beïnvloed, aangesien hoër omskakelings en opbrengste van amiene verkry was. Op die oog af verhoed piperidien nuwe-reaksies, soos die isomerisering en hidrogenering van 1-okteen gedeeltelik. Die invloed van druk en temperatuur was ook

ondersoek en dit het die chemoselektiewe sintese van *N*-alkielpiperidene (~90 %) teweeg gebring by 30 bar CO: H₂ (1: 1), 0,1 mol% katalisator-lading, 2 uur reaksie tyd en 85 ° C.

Die fokus was daarna verskuif na die gebruik van 'n primêre amien, anilien. Die reaksie kondisies wat geoptimeer was vir die hidroaminometielering van 1-okteen in die teenwoordigheid van piperidien (30 bar CO:H₂ (1:1), 0,1 mol%, 1 uur en 85 ° C) was gekies as die aanvanklike kondisies. As gevolg van die laer basisiteit van anilien in vergelyking met die van piperidien, was die opbrengs van die *N*-gealkieerde anilene aanvanklik laag, alhoewel al die 1-okteen heeltemal omgeskakel was. Die reaksie kondisies moes geoptimeer word om die opbrengste van die *N*-alkieerde anilene te verhoog. Ons het spesifiek gefokus op die gedeeltelike druk van H₂. Met behulp van 'n 1:3 verhouding van CO:H₂ (50 bar) en 'n reaksie tyd van 6 uur kon sekondêre amiene in ~45 % opbrengs gesintetiseer word. Uitvoering van die hidroaminometielering reaksie in die teenwoordigheid van oormaat anilien (1,5 ekw.), kon *N*-alkieerde anilene chemoselektief (~95 %) gesintetiseer word, alhoewel teen matige regioselektiwiteit na die lineêre amien (56 %).

In die gebruik van bensielamien in die hidroaminometielering van 1-okteen, was die reaksie aansienlik vinniger in vergelyking met die gebruik van anilien. Dit word toegeskryf aan die hoër basisiteit en dus die hoër nukleofilisiteit van bensielamien. *N*-gealkieerde bensielamiene was dus chemoselektief gesintetiseer, alhoewel teen matige regioselektiwiteit na die lineêre amien.

Die Ru(II) komplekse, **C6-C8**, was ook geëvalueer as katalisator-voorlopers in die hidroaminometielering van 1-okteen in die teenwoordigheid van bensielamien. Alhoewel hierdie komplekse effens hoër temperature (110 °C) benodig in vergelyking met rhodium, bemiddel hulle ook die hidroaminometielering van 1-okteen met bensielamien doeltreffend. Tydens die hidroaminometielerings reaksie was die aldehiede tussenprodukte nooit waargeneem nie, alhoewel alkene (terminaal en intern) nog teenwoordig was. Dit dui daarop dat die hidroformuliserings reaksie vir hierdie ruthenium komplekse stadiger is as die reduktiewe aminering reaksie.

Die potensiaal van hidroaminometielering in die sintese van waardevolle chemikalieë was ook getoon. In hierdie opsig was hidroaminometielering gebruik om primêre amiene in hoë opbrengste te sintetiseer vanaf goedkoop olefien voermiddels. Deur gebruik te maak van dieselfde metodologie, is dopamien-analoë van eugenol gesintetiseer. Die sintese van biopolymeer-voorlopers is ook gedemonstreer deur middel van die hidroaminometielering van metiel-10-undesenoaat in die teenwoordigheid van amino suur esters (*L*-prolien-metielester en metiel piperidien-4-karboksilaat). Die hidroaminometielering van 1-okteen met hierdie amino suur esters het toegang gegee tot bio-surfaktante. Daar was gevind dat die pirrolidiel- en piperidiel-groepe bydra tot die hidrofobisiteit van die alkielketting. Ons het ook gevind dat die posisie van die hidrofiliese groep relatief tot die alkielketting ook die kritieke misel konsentrasie (CMC) kan beïnvloed.

Acknowledgement

My deepest gratitude towards my supervisor, Prof. Selwyn Mapolie, for being an exceptional supervisor. This project would definitely not have been a success without his excellent guidance, fruitful discussions and his exceptional way of teaching.

A huge thank you to my colleagues in the Organometallic Research Group, past and present. I specifically want to thank Derik, Sean, Ené, Annick, Laura and Nicole. The contribution by the RME-nano and Luckay research groups is also much appreciated.

A special thank you to Emile, Sameera and Cassiem for being great friends and colleagues. A day is not complete without having a good laugh with them.

The technical staff of the Inorganic Chemistry building is also acknowledged, especially the assistance by Peta and Ayanda.

I would also like to thank CAF (Central Analytical Facility) for their exceptional service. A special thanks to Elsa and Jaco at the NMR facility.

Financial contribution by the National Research Foundation (NRF), the DST-NRF Centre of Excellence in Catalysis (c*change) and Stellenbosch University is gratefully acknowledged.

My hard-working Mom, my never-stop-praying Grandmother and my loving and late Grandfather deserves the greatest acknowledgement. They made me the person I am today. My broader family is thanked for their contribution.

Last but not least, the greatest praise belongs to our Heavenly Father for providing me with the strength and perseverance each day. I wouldn't have made it without Him!

Conference Contributions and Publications

Poster Presentations

J. October and S.F. Mapolie

Functionalized N-Phenyl-2-pyridylmethanimine complexes of Rh(I) as Catalyst Precursors in Octene Hydroformylation. Catalysis Society of South Africa (CATSA) annual conference at Champagne Sports Resort, Central Drakensberg, 2016.

Conventional vs Microwave-assisted hydroformylation of 1-Octene catalyzed by Functionalized N-Phenyl-2-pyridylmethanimine complexes of Rh(I). Catalysis Society of South Africa (CATSA) annual conference at Kwa Maritane Bush Lodge, Pilanesberg, 2017.

Application of Functionalized Rh(I) N-Phenyl-2-pyridylmethanimine Complexes as Pre-catalysts in Alkene Hydroformylation. 28th International Conference on Organometallic Chemistry at the Congress and Exhibition Centre, Firenze, Italy, 2018.

Oral Presentation

J. October and S.F. Mapolie

Tandem synthesis of Amines from Alkenes. Cape Organometallic Symposium (COS) at the University of Cape-Town (UCT), Cape-Town, 2019.

Publications

Synthesis and characterization of novel rhodium and ruthenium based iminopyridyl complexes and their application in 1-octene hydroformylation. J. October and S. F. Mapolie, *J. Organomet. Chem.*, 2017, **840**, 1-10.

Alkylation of Amines Via Tandem Hydroaminomethylation Using Imino-pyridine Complexes of Rhodium as Catalyst Precursors. J. October and S. F. Mapolie, *Catal. Lett.* (2019). <https://doi.org/10.1007/s10562-019-02998-y>

Table of Contents

Declaration	i
Abstract	ii
Opsomming	iv
Acknowledgement	vi
Conference Contributions and Publications	vii
Table of Contents	viii
List of Figures	xii
List of Tables	xvii
List of Schemes	xviii
Abbreviation and Symbols	xix

Chapter 1: Literature Review of Olefin Hydroformylation and Hydroaminomethylation

1.1 The discovery of Hydroformylation	1
1.2 Hydroformylation with formaldehyde as Syngas Surrogate	1
1.3 Indirect Reductive Amination of Imine/Enamines catalyzed by Ir, Ru and Rh Metal Complexes ...	4
1.3.1 Iridium catalyzed imine/enamine hydrogenation	4
1.3.2 Ruthenium catalyzed imine/enamine hydrogenation	9
1.3.3 Rhodium catalyzed imine/enamine hydrogenation	12
1.4 Hydroaminomethylation	16
1.4.1 Synthesis of medicinal compounds via hydroaminomethylation	29
1.4.2 Synthesis of polymers and surfactants via hydroaminomethylation	33
1.5 Concluding Remarks and Project Objectives	35
1.6 Overview of thesis	36
1.7 References	36

Chapter 2: Synthesis and Characterization of Novel Iminopyridyl Rh(I) and Ru(II) Complexes

2.1 Introduction	42
2.2 Synthesis and characterization of Rh(I) complexes	42
2.2.1 Synthesis of iminopyridyl ligands (L1-L5).....	42
2.2.2 Synthesis of novel iminopyridyl Rh(I) complexes (C1-C5)	44
2.3 Synthesis and characterization of Ru(II) complexes	47
2.3.1 Synthesis of iminopyridyl ligands (L6-L8).....	47
2.3.2 Synthesis of novel iminopyridyl Ru(II) complexes (C6-C8).....	48
2.4 Conclusion.....	51
2.5 Experimental	52
2.6 References	56

Chapter 3: Hydroformylation of 1-Octene by Iminopyridyl Rh(I) Complexes

3.1 Introduction	58
3.2 Hydroformylation of 1-octene.....	61
3.2.1 Hydroformylation of 1-octene using four different Rh(I) iminopyridyl complexes	61
3.2.2 Effect of time on the hydroformylation of 1-octene.....	63
3.2.3 Effect of pressure on the hydroformylation of 1-octene.....	65
3.2.4 Effect of temperature on the hydroformylation of 1-octene.....	67
3.2.5 Effect of time on the hydroformylation of 1-octene at 65 °C.....	68
3.2.6 Comparing the catalytic activity of C1 with that of C2	69
3.3 Hydroformylation using paraformaldehyde as syngas surrogate	70
3.4 Conclusion.....	74
3.5 Experimental Section	74
3.6 References	75

Chapter 4: Hydroaminomethylation of Olefins with Primary and Secondary Amines

4.1 Introduction	78
4.2 Hydroaminomethylation of 1-octene and piperidine catalyzed by Rh(I) catalyst precursors	79
4.2.1 Influence of catalyst loading on catalytic activity	80
4.2.2 Influence of time on the catalytic activity	81

4.2.3 Evaluating different catalysts in the hydroaminomethylation of 1-octene and piperidine	82
4.2.4 Influence of olefin:amine ratio on the activity and selectivity of the hydroaminomethylation of 1-octene with piperidine	84
4.2.5 Influence of pressure on the activity and selectivity of the hydroaminomethylation of 1-octene and piperidine	85
4.2.6 Influence of temperature on the activity and selectivity of the hydroaminomethylation of 1-octene and piperidine	86
4.3 Hydroaminomethylation of 1-octene in the presence of primary amines (Aniline and Benzylamine)	88
4.3.1 Effect of temperature and catalyst concentration on the yield of <i>N</i> -alkylated anilines	89
4.3.2 Influence of pressure (total and partial) on the yield of <i>N</i> -alkylated anilines	91
4.3.3 Influence of time on the yield of <i>N</i> -alkylated anilines	93
4.3.4 Influence of the olefin:amine ratio on the yield of secondary <i>N</i> -alkylated anilines	94
4.3.5 The hydroaminomethylation of aniline vs benzylamine	95
4.4 Hydroaminomethylation of 1-octene with benzylamine catalyzed by Ru(II) catalyst precursors ..	97
4.4.1 Influence of temperature on the hydroaminomethylation of 1-octene with benzylamine	98
4.4.2 Comparing the activity of different Ru(II) catalysts in the hydroaminomethylation of 1-octene with benzylamine	99
4.4.3 Influence of time on the Ru(II) catalyzed hydroaminomethylation of 1-octene with benzylamine	100
4.4.4 Possible mechanism for the Ru-catalyzed hydrogenation of imines	101
4.5 Conclusion	102
4.6 Experimental	103
4.6.1 General Considerations	103
4.6.2 Instrumentation	103
4.6.3 General method for the hydroaminomethylation reaction	104
4.6.3.1 Hydroaminomethylation of 1-octene in the presence of piperidine	104
4.6.3.2 Hydroaminomethylation of 1-octene in the presence of aniline	104
4.6.3.3 Hydroaminomethylation of 1-octene in the presence of benzylamine	104
4.7 References	105

Chapter 5: The synthesis of primary amines, polymer precursors and surfactants via hydroaminomethylation

5.1 Introduction	107
5.2 The synthesis of primary amines via hydroaminomethylation.....	107
5.3 The synthesis of novel bio-polymer precursors via hydroaminomethylation	113
5.4 The synthesis of biosurfactants via hydroaminomethylation	122
5.5 Conclusion.....	131
5.6 Experimental	131
5.6.1 General Considerations	131
5.6.2 Synthesis of primary amines	132
5.6.3 Synthesis of novel biopolymer precursors	133
5.6.4 Synthesis of novel bio-surfactants.....	135
5.7 References	138

Chapter 6: Concluding Remarks and Future Prospects

6.1 Concluding Remarks	141
6.2 Future Prospects	142

List of Figures***Chapter 1: Literature Review of Olefin Hydroformylation and Hydroaminomethylation***

Figure 1.1: Hydroformylation of an olefin to aldehydes	1
Figure 1.2: BINAP and XANTPHOS ligands used in the linear-selective hydroformylation of 1-decene	2
Figure 1.3: The (R, R)-Ph-BPE ligand used in the asymmetric transfer hydroformylation of vinylarenes	3
Figure 1.4: Cyclometallated Ir-Imino complexes developed by Xiao and co-workers for the hydrogenation of ketimines and N-benzylimine	4
Figure 1.5: Achiral Cp [*] -Ir diamine complex used for the enantioselective hydrogenation of ketimines	5
Figure 1.6: Robust cyclometallated Ir-Imino complex used in the hydrogenation of N-benzylimine	5
Figure 1.7: Spiro phosphoramidite ligand used in the enantioselective hydrogenation of N, N-dialkyl enamines.....	6
Figure 1.8: Hydrogenation of enamines vs cyclic imines	6
Figure 1.9: Phosphoramidite ligand used in the synthesis of diarylmethylamines.....	7
Figure 1.10: Hybrid P, N-Ligated Ir complex used in the hydrogenation of N-benzylideneaniline	7
Figure 1.11: A phosphine-oxazoline Ir complex used in the hydrogenation of N-aryl arylmethylimines	8
Figure 1.12: P, N – Ir complex used in the synthesis of dialkylaryl tertiary amines.....	8
Figure 1.13: Ligand used by Zhou in the hydrogenation of exocyclic enamines.....	8
Figure 1.14: The (S, S)-f-Binaphane ligand used in enantioselective hydrogenation	9
Figure 1.15: Ru(II)-thiolate complex and P-ligand used in the enantioselective hydrosilylation of imines	9
Figure 1.16: Ru complex used for the preparation of γ -secondary aminoalcohols	10
Figure 1.17: Chiral Ru complexes used in the hydrogenation of cyclic imines.....	11
Figure 1.18: Ligands used in the hydrogenation of N-aryl ketimines	12
Figure 1.19: Ferrocenyl-based ligand used by the Merck group.....	12
Figure 1.20: Enamine substrate used by the Merck group	13
Figure 1.21: Chiral bis-phosphine ligand	13
Figure 1.22: (R, R)-QuinoxP [*] ligand and the enamine substrate	13
Figure 1.23: Bis-phosphine ligand with an incorporated thiourea moiety	14
Figure 1.24: Unactivated enamine and PPh ₃ and its more electron-deficient counterpart	14
Figure 1.25: Ligands used in the hydrogenation of prochiral enamines	15
Figure 1.26: Cpd and dcpd and the corresponding diamine of dcpd.....	20
Figure 1.27: Orthogonal tandem amination reaction.....	20
Figure 1.28: Xantphenoxaphos ligand and 2-phosphino-substituted imidazole ligand.....	21
Figure 1.29: Rh-carbene catalyst and the ligand used by Abu-Reziq and co-workers.....	22

Figure 1.30: Rh-diphosphine complex with additional binding site	23
Figure 1.31: Tetrabi-phosphorous ligand used in isomerization-hydroaminomethylation	23
Figure 1.32: Pyrrole-based tetraphosphorous ligand used in linear selective hydroaminomethylation	24
Figure 1.33: Yanphos (top) and the synthesis of chiral pyrrolidinones and pyrrolidines.....	24
Figure 1.34: Chiral phosphoric acid derivative	25
Figure 1.35: Rh(I) P, N-ligated complex used in the hydroaminomethylation of styrene in the presence of morpholine	26
Figure 1.36: Product obtained from HAM of di-allyl silanes and benzylamine (top) and HAM of diallyl amines and benzylamine (bottom)	28
Figure 1.37: Pyrazole-based Rh(I) dicarbonyl complex used in the hydroaminomethylation of 1-octene with diethylamine.....	28
Figure 1.38: Synthesis of an azamacroheterocyclic ring.....	29
Figure 1.39: Pharmacologically active amines.....	29
Figure 1.40: Fluspirilene and difenidol drugs	30
Figure 1.41: Synthesis of quinazolinones.....	30
Figure 1.42: 1,2,3,4-tetrahydroquinolines and the two ionic diamine rhodium complexes	31
Figure 1.43: Fenpiprane, diisoproamine and prozapine	31
Figure 1.44: Amine containing steroid derivatives	32
Figure 1.45: Synthesis of Ibutilide	32
Figure 1.46: Hydroaminomethylation of limonene with amines.....	33
Figure 1.47: Hydroaminomethylation of oleic acid ethyl ester	33
Figure 1.48: Synthesis of branched polyamide monomer	34
Figure 1.49: Synthesis of aminohydroxytriglycerides via hydroaminomethylation and hydrogenation of aldehyde moieties.....	34

Chapter 2: Synthesis and Characterization of Novel Iminopyridyl Rh(I) and Ru(II) Complexes

Figure 2.1: Synthesis of functionalized N-Phenyl-2-pyridylmethanimine ligands	42
Figure 2.2: ¹ H NMR spectrum of L5	43
Figure 2.3: Synthesis of functionalized N-Phenyl-2-pyridylmethanimine Rh(I) complexes (C1-C5) ..	44
Figure 2.4: Numbering of C5 for ¹ H NMR analysis	45
Figure 2.5: ¹ H NMR spectrum of C5 ran in Acetone-d ₆	45
Figure 2.6: Synthesis of mono- and bifunctional iminopyridyl ligands	47
Figure 2.7: ¹ H NMR spectrum of L8 ran in CDCl ₃	47
Figure 2.8: Synthesis of C6-C8	48
Figure 2.9: Numbering of C8 for ¹ H NMR analysis	49
Figure 2.10: ¹ H NMR spectrum of C8 ran in acetone-d ₆	50
Figure 2.11: ESI-MS spectrum of C8	50
Figure 2.12: Base peak in the ESI-MS spectrum of C8	51

Chapter 3: Hydroformylation of 1-Octene by Iminopyridyl Rh(I) Complexes

Figure 3.1: Mechanism of the hydroformylation reaction.....	58
Figure 3.2: A phosphite ligand used by Hofmann and co-workers	59
Figure 3.3: Bulky phosphine and phosphite ligands	59
Figure 3.4: Ionic Rh(I) imidazolium based phosphine complex bearing amino substituents	60
Figure 3.5: Rh(I) iminopyridyl catalyst precursors (C1-C4)	61
Figure 3.6: Hydroformylation of 1-octene	61
Figure 3.7: Hydroformylation of 1-octene using Rh(I) iminopyridyl complexes.	62
Figure 3.8: Regioselectivity of C1-C4	63
Figure 3.9: Effect of time	63
Figure 3.10: Effect of time on the regioselectivity.....	64
Figure 3.11: Hydroformylation of 2-octene	64
Figure 3.12: Regioselectivity of the hydroformylation of 2-octene	65
Figure 3.13: Effect of pressure	66
Figure 3.14: Effect of pressure on regioselectivity	66
Figure 3.15: Effect of temperature on conversion and chemoselectivity.	67
Figure 3.16: Effect of temperature on regioselectivity.....	68
Figure 3.17: Effect of time at 65°C	68
Figure 3.18: Effect of time at 65°C on regioselectivity	69
Figure 3.19: Comparing C1 and C2	70
Figure 3.20: Comparing C1 and C2	70
Figure 3.21: Mechanism of the decarbonylation of aldehydes.....	71
Figure 3.22: Aldehyde formation from olefin and formaldehyde	72
Figure 3.23: Attempted hydroformylation of 1-Octene.....	72
Figure 3.24: Hydroformylation with formaldehyde and M-H ₂ formation.....	73

Chapter 4: Hydroaminomethylation of Olefins with Primary and Secondary Amines

Figure 4.1: A general hydroaminomethylation reaction.....	78
Figure 4.2: Catalyst precursors used in the hydroaminomethylation reaction	79
Figure 4.3: Hydroaminomethylation of 1-octene with piperidine.....	79
Figure 4.4: The aldehyde and enamine intermediates in the hydroaminomethylation of 1-Octene and Piperidine	80
Figure 4.5: Influence of catalyst loading using C4	80
Figure 4.6: Influence of reaction time on the hydroaminomethylation of 1-Octene and Piperidine.....	81
Figure 4.7: Evaluating different catalysts in the hydroaminomethylation of 1-octene and piperidine .	83
Figure 4.8: Influence of the 1-octene:piperidine ratio on their hydroaminomethylation	84

Figure 4.9: Influence of pressure on hydroaminomethylation of 1-octene and piperidine	85
Figure 4.10: Influence of temperature on hydroaminomethylation of 1-octene and piperidine.....	86
Figure 4.11: Extending the reaction time to 2 h	87
Figure 4.12: Hydroaminomethylation of 1-octene and aniline.....	88
Figure 4.13: Effect of temperature on the yield of <i>N</i> -alkylated anilines	89
Figure 4.14: Influence of catalyst concentration on the yield of <i>N</i> -alkylated anilines	90
Figure 4.15: Influence of the CO:H ₂ partial pressure on the yield of <i>N</i> -alkylated anilines.....	91
Figure 4.16: Influence of total pressure on the yield of <i>N</i> -alkylated anilines.	92
Figure 4.17: Influence of time on the yield of <i>N</i> -alkylated anilines.....	94
Figure 4.18: Influence of olefin:amine ratio on the yield of secondary <i>N</i> -alkylated anilines.	95
Figure 4.19: Hydroaminomethylation of aniline vs benzylamine	96
Figure 4.20: Ru(II) complexes evaluated in the hydroaminomethylation of 1-octene with benzylamine	97
Figure 4.21: Hydroaminomethylation of 1-octene and benzylamine catalyzed by Ru(II) complexes..	98
Figure 4.22: Influence of temperature on the hydroaminomethylation of 1-octene with benzylamine.	98
Figure 4.23: Comparing different Ru(II) catalysts in the hydroaminomethylatio of 1-octene with benzylamine	99
Figure 4.24: Influence of time of the hydroaminomethylation of 1-octene with benzylamine catalyzed by Ru(II) complex	100
Figure 4.25: Possible mechanism of the Ru(II)-catalyzed hydrogenation of imines	102
 <i>Chapter 5: The synthesis of primary amines, polymer precursors and surfactants via hydroaminomethylation</i>	
Figure 5.1: Synthesis of fatty amines via hydroaminomethylation and Pd-catalyzed debenzylation .	108
Figure 5.2: GC-FID spectrum of the C13 amines	109
Figure 5.3: Regio-isomeric C13 benzylamines obtained after hydroaminomethylation of 1-dodecene and benzylamine	110
Figure 5.4: IR spectra of C13 <i>N</i> -alkylated benzylamines (Top) and C13 fatty amines (bottom)	111
Figure 5.5: ¹ H NMR spectrum of C13 <i>N</i> -alkyl benzylamines (Top) and C13 fatty amines (bottom) ran in CDCl ₃	111
Figure 5.6: Synthesis of Dopamine-analogues (DA2) via hydroaminomethylation and Pd-catalyzed debenzylation	112
Figure 5.7: ¹ H NMR spectra of eugenol (top), hydroaminomethylation product (middle) and dopamine-analogues (bottom).....	113
Figure 5.8: Hydroformylation of 10-methyl undecenoate.....	114
Figure 5.9: IR spectra of methyl 10-undecenoate (top spectrum) and the hydroformylation product (bottom).....	114

Figure 5.10: ^1H NMR spectra of methyl 10-undecenoate (top spectrum) and the hydroformylation product (bottom) in CDCl_3	115
Figure 5.11: ESI-MS (direct injection) spectrum of methyl 12-oxododecanoate and its branched isomers	116
Figure 5.12: L-proline methyl ester and methyl piperidine-4-carboxylate amines for hydroaminomethylation of methyl 10-undecenoate.....	116
Figure 5.13: Hydroaminomethylation of methyl 10-undecenoate with L-proline methyl ester.....	117
Figure 5.14: ^1H NMR spectra of methyl 10-undecenoate (top spectrum) and the diester obtained from hydroaminomethylation (bottom spectrum).....	118
Figure 5.15: ESI-MS spectrum (direct injection, positive mode) of the diester (DE1).....	118
Figure 5.16: Preparation of dicarboxylic acid from diester via base-mediated hydrolysis	119
Figure 5.17: IR spectrum of DE1 (top), potassium carboxylate salt (middle) and DC1 (bottom).....	119
Figure 5.18: ^1H NMR spectra of DE1 (top) and DC1 (bottom).....	120
Figure 5.19: ESI-MS (direct injection, positive mode) spectrum of DC1	120
Figure 5.20: Synthesis of DC2 via hydroaminomethylation and KOH-mediated ester hydrolysis	121
Figure 5.21: <i>N</i> -alkylated piperidine 4-carboxylic acid and L-proline	122
Figure 5.22: ^1H NMR spectra of BS1 (top) and BS2 (bottom) ester precursors in CDCl_3	125
Figure 5.23: IR spectra of BS1 ester precursor (top), BS1 (middle) and BS2 (bottom)	125
Figure 5.24: ^1H NMR spectra of BS1 ester precursor (Top), BS1 (middle) and BS2 (bottom).....	126
Figure 5.25: ESI-MS spectrum (direct injection, positive mode) of BS2	127
Figure 5.26: Conductivity vs Concentration graph for SDS	128
Figure 5.27: Biosurfactants (BS1 , BS3 and BS4) synthesized via reductive amination	128
Figure 5.28: Mixture of piperidine-4-carboxylate-based biosurfactants (BS2) synthesized via hydroaminomethylation.....	129
Figure 5.29: Mixture of proline-based biosurfactants (BS5) synthesized via hydroaminomethylation	129
Figure 5.30: Conductivity vs Concentration for BS1	129
Figure 5.31: Conductivity vs Concentration for BS3	130

List of Tables***Chapter 1: Literature Review of Olefin Hydroformylation and Hydroaminomethylation***

Table 1.1: Hydroaminomethylation using an Aqueous-organic biphasic approach.....	17
--	----

Chapter 2: Synthesis and Characterization of Novel Iminopyridyl Rh(I) and Ru(II) Complexes

Table 2.1: ESI-MS, EA and melting point data for L5	44
Table 2.2: Characterization data for C1-C5	46
Table 2.3: Characterization data for C6-C8	51

Chapter 3: Hydroformylation of 1-Octene by Iminopyridyl Rh(I) Complexes

Table 3.1: Attempted hydroformylation using HRhCO(PPh ₃) ₃	73
---	----

Chapter 4: Hydroaminomethylation of Olefins with Primary and Secondary Amines

Table 4.1: Influence of catalyst loading on the regioselectivity and TON	81
Table 4.2: Regioselectivity and TON at different reaction times	82
Table 4.3: Influence of different catalysts on the regioselectivity and TON.....	83
Table 4.4: Influence of olefin:amine ratio on regioselectivity and TON	85
Table 4.5: Influence of pressure on the regioselectivity and TON.....	86
Table 4.6: Influence of temperature on the regioselectivity and TON	87
Table 4.7: Extending the reaction to 2 h.....	88
Table 4.8: Effect of temperature on the regioselectivity of <i>N</i> -alkylated anilines and TON	90
Table 4.9: Influence of catalyst concentration on the regioselectivity and TON	91
Table 4.10: Influence of the CO:H ₂ partial pressure on the regioselectivity and TON	92
Table 4.11: Influence of total pressure on regioselectivity and TON	93
Table 4.12: Influence on time on the regioselectivity and TON	94
Table 4.13: Influence of olefin:amine ratio on the regioselectivity and TON.....	95
Table 4.14: Regioselectivity and TON of the hydroaminomethylation of aniline and benzylamine	96
Table 4.15: Influence of temperature on regioselectivity and TON.....	99
Table 4.16: Regioselectivity and TON of three different Ru(II) catalysts	100
Table 4.17: Influence of time of the regioselectivity and TON.....	101

Chapter 5: The synthesis of primary amines, polymer precursors and surfactants via hydroaminomethylation

Table 5.1: The CMC's of the biosurfactants (BS1-BS5)	130
---	-----

List of Schemes

Scheme 5.1: Synthesis of biosurfactants (BS1-BS5).....	124
---	-----

Abbreviations and Symbols**Units**

Å	angstrom
J	coupling constant
°C/min	degrees celsius per minute
Hz	hertz
m/z	mass to charge ratio
MHz	megahertz
mg/ml	milligram per millitre
ml/min	millilitre per minute
mmol	millimole
nm	nanometre
ppm	parts per million
cm ⁻¹	wavenumber

Chemicals

BINAP	2,2'-bis(diphenylphosphino)-1,1'-binaphthyl
BArf	tetrakis[3,5-bis(trifluoromethyl)phenyl]borate
Bmim	1-butyl-3-methylimidazolium
COD	cyclooctadiene
CTAB	ctrimonium bromide
DMSO- <i>d</i> ₆	deuterated dimethyl sulfoxide
DCM	dichloromethane
DMSO	dimethyl sulfoxide
DMF	dimethyl formamide
Dppe	1,2-bis(diphenylphosphino)ethane
Emim	1-ethyl-3-methylimidazolium
EtOH	ethanol
MeCN	acetonitrile
MeOH	methanol
NTf ₂	bis(trifluoromethanesulfonyl)imide
OAc	acetate

OTf	trifluoromethanesulfonate
PEG	polyethylene glycol
(R,R)-Ph-BPE	1,2-bis[(2S, 5S)-2,5-diphenylphospholano]ethane
TFA	trifluoroacetic acid
TFE	trifluoroethanol
TPPMS	monosulfonated triphenylphosphine
THF	tetrahydrofuran
TPPTS	trisulfonated triphenylphosphine

Instrumentation

ATR	attenuated total reflectance
ESI-MS	electrospray ionisation mass spectrometry
EA	elemental analysis
FTIR	fourier transform infrared
GC-FID	gas chromatography flame ionization detector
HPLC	high pressure liquid chromatography
ICP-OES	inductively coupled plasma optical emission spectroscopy
NMR	nuclear magnetic resonance
SCD	single crystal diffraction

NMR spectra peak description

bs	broad singlet
comp	complex
d	doublet
dd	doublet of doublets
dt	doublet of triplets
m	multiplet
s	singlet
t	triplet

Other

ATHF	asymmetric transfer hydroformylation
HAM	hydroaminomethylation
% ee	enantiomeric excess
exp	experimental
TOF	turnover frequency
TON	turnover number
CMC	critical micelle concentration

Chapter 1: Literature Review of Olefin Hydroformylation and Hydroaminomethylation

that needs to be taken when handling these gases, the economic implications also needs to be taken in consideration. These factors thus limits the application of hydroformylation in conventional synthetic organic chemistry. A possible solution to this problem is the use of formaldehyde, a so-called syngas surrogate. Formaldehyde can undergo decomposition to CO and H₂ mediated by appropriate catalysts. In this regard, both paraformaldehyde and formalin can be used which is not only economic, but also regarded as a much safer option.

Rosales and co-workers⁵ studied the hydroformylation of 1-hexene using paraformaldehyde with [Rh(dppe)₂]acac (dppe = 1,2-bis(diphenylphosphino)ethane) as the catalyst. The best activity was obtained in 1,4-dioxane as solvent followed by tetrahydrofuran, while poor activity was observed in more polar solvents such as acetonitrile and 2-methoxyethanol. It was further found that superior activities are obtained with formaldehyde compared to a corresponding experiment using 3 bar of CO:H₂ (1:1). Moreover, when 3 bar of H₂ or CO were added to formaldehyde, it led to a drop in the hydroformylation activity. The addition of H₂ and CO to formaldehyde thus led to the retardation of the reaction. The authors reasoned that this is consistent with a mechanism which does not involve decomposition of formaldehyde to CO and H₂. Instead, formaldehyde oxidatively adds to the metal centre forming a M-H and M-CHO species. This is followed by alkene coordination and subsequent insertion into the M-H bond. The alkyl and formyl group then reductively eliminates to form the aldehyde. However, in an earlier study by Börner and co-workers⁶, they found that the addition of 10 bar H₂ actually improves the hydroformylation reaction of 1-octene using 37 % Formalin. Here, [RhCl(COD)]₂ was used as the catalyst precursor and BINAP (2,2'-bis(diphenylphosphino)-1,1'-binaphthyl), which is shown in Figure 1.2, as the ligand. In addition to the improvement in the aldehyde yield, better regioselectivities were also obtained in the presence of additional H₂ (n:iso ratio 1.8:1 (absence of H₂) vs 3.9:1 (presence of H₂)) and this was also accompanied with no significant influence on either the isomerization and hydrogenation side reactions. The authors concluded that the H₂ probably accelerates the hydrogenolysis of the Rh-acyl complex, promoting the reductive elimination of the aldehydes.

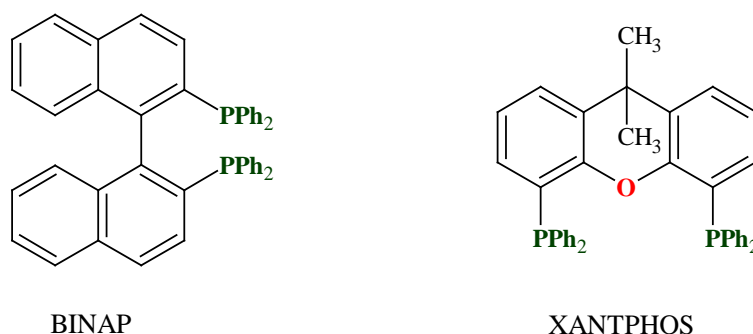
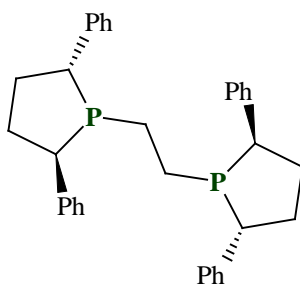


Figure 1.2: BINAP and XANTPHOS ligands used in the linear-selective hydroformylation of 1-decene⁷

Chapter 1: Literature Review of Olefin Hydroformylation and Hydroaminomethylation

The highly linear-selective hydroformylation of 1-decene was reported by Morimoto and co-workers.⁷ Their strategy entailed the simultaneous use of two different phosphine ligands, where one is responsible for the decarbonylation of formaldehyde (BINAP, Figure 1.2) and the other for the hydroformylation reaction (XANTPHOS, Figure 1.2). They used $[\text{RhCl}(\text{COD})]_2$ as the metal precursor. This resulted in a very efficient catalyst system registering high conversions of the alkene (98 %) while also proceeding with high regioselectivity towards the linear aldehyde (n:iso of 98:2). They further demonstrated that using the ligands individually, decreases the efficiency of the whole process especially in the case of the XANTPHOS ligand. Inspired by this, Taddei and co-workers⁸ decided to utilize this same system for the microwave-assisted hydroformylation of olefins using formaldehyde as syngas surrogate. They were specifically interested in shortening the reaction time from the reported 20 h⁷ to 0.5 h. They successfully demonstrated the hydroformylation of 1-octene using 37 % formalin with an aldehyde yield of 90 % and a n:iso ratio of 98:2 under microwave dielectric heating at short reaction times.

A further example of the use of microwave dielectric heating in hydroformylation is published by Clarke and co-workers.⁹ They were interested in the asymmetric transfer hydroformylation (ATHF) of vinylarenes, specifically cis-stilbenes, catalyzed by $[\text{Rh}(\text{acac})(\text{CO})_2]$ and various phosphine ligands. The best activity and enantioselectivity were obtained using (*R,R*)-Ph-BPE (Figure 1.3). They obtained an aldehyde yield of 80 % and ee of 95 % (selective towards the R isomer). These results were found to be superior to conventional asymmetric hydroformylation both in terms of TONs/TOFs and enantiomeric purities. The authors attributed this to the conditions of hydroformylation generated by the surrogate which ought to be beneficial to the process. A further use of this ligand is reported by Morimoto and co-workers¹⁰ which involved the asymmetric hydroformylation of styrene under conventional heating. Under their conditions, they also observed excellent aldehyde yields (99 %) and an enantiomeric excess of 90 % (towards the R isomer).



1,2-bis[(2*S*, 5*S*)-2,5-diphenylphospholano]ethane or (*R,R*)-Ph-BPE

Figure 1.3: The (*R,R*)-Ph-BPE ligand used in the asymmetric transfer hydroformylation of vinylarenes⁹

Chapter 1: Literature Review of Olefin Hydroformylation and Hydroaminomethylation

From the above literature sources it is clear that formaldehyde is a viable alternative to syngas. Further optimization of the process is however still necessary, especially in terms of catalyst loading and catalyst recovery.

1.3 Indirect Reductive Amination of Imine/Enamines catalyzed by Ir, Ru and Rh Metal Complexes

Reductive amination represents an important route towards the synthesis of amines. This reaction can be categorized into either direct or indirect reductive aminations. In direct reductive amination reactions one starts with the aldehyde and amine whereas in the indirect route one first isolates the imine and then subject it to hydrogenation.¹¹ This reaction is atom-economical since only water is formed as a by-product. The most common catalysts for this transformation is based on Ir, Ru and Rh catalysts, however, there are a few reports based on other metals.¹² Since the hydroaminomethylation reaction consists of an imine/enamine hydrogenation step, the hydrogenation of these compounds will be reviewed here in isolation. Hydroaminomethylation will be discussed in more detail later on.

1.3.1 Iridium catalyzed imine/enamine hydrogenation

Xiao and co-workers¹³ developed cyclometallated iridium-imino complexes, bearing different electron withdrawing and donating groups, for the hydrogenation of aliphatic and aromatic ketimines as well as *N*-benzylimines (Figure 1.4).

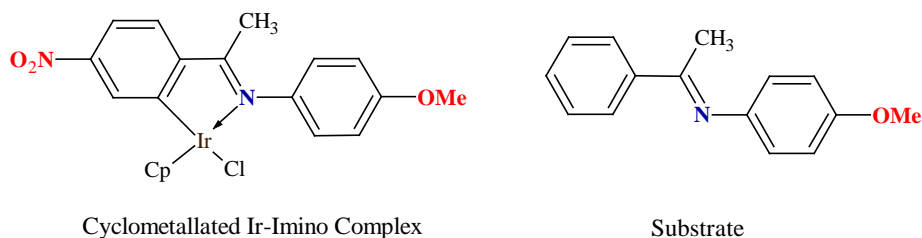


Figure 1.4: Cyclometallated Ir-Imino complexes developed by Xiao and co-workers for the hydrogenation of ketimines and *N*-benzylimine¹³

Various solvents were screened with only trifluoroethanol (TFE) registering acceptable conversions, while no activity was observed in highly polar solvents such as DMF and DMSO. The authors ascribed this observation to the acidic, high polarity and low nucleophilic nature of TFE. A pressure of 20 bar, 75 °C and 0.05 mol % catalyst loading for 30 min were found to be the optimum conditions. In terms of the catalyst design, the highest activity was obtained with a catalyst containing an electron withdrawing group. The catalysts tolerate various electron withdrawing and donating groups on the substrate. More importantly, the catalysts are chemoselective towards the imine bond, while no hydrogenation of other reducible groups occurred (alkene, nitro and nitrile groups). In another paper, the authors also studied the enantioselective hydrogenation of the same substrate using an achiral Cp*-Iridium diamine complex, shown in Figure 1.5, in the presence of a chiral phosphoric acid.¹⁴

Chapter 1: Literature Review of Olefin Hydroformylation and Hydroaminomethylation

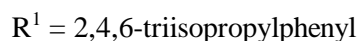
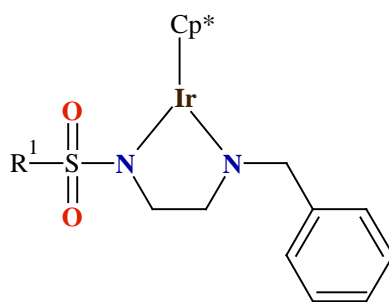


Figure 1.5: Achiral Cp^* -Ir diamine complex used for the enantioselective hydrogenation of ketimines¹⁴

This achiral-chiral metal-organo cooperative catalyst delivered highly enantioselective hydrogenation of both aryl and aliphatic ketimines (ee of 81-98 %). During the catalytic cycle, the phosphoric acid protonates the amine at the amido nitrogen. The presence of the phosphate does lower the rate of the reaction, however, due to the existence of H-bonding between the phosphate, the metal catalyst and the substrate, high enantioselectivities are induced. Furthermore, the catalyst system was also found to be highly tolerant towards other reducible groups (alkene, nitro and nitrile groups) while it was also found that bulky R groups further improves the enantioselectivity. A more robust cyclometallated iridium-imino complex was also prepared (Figure 1.6) and was found to be highly active for the hydrogenation of the imine shown in Figure 1.4, producing a yield of 86 % of the amine at 20 bar H_2 , 85 °C for 1 h in TFE as solvent.¹⁵

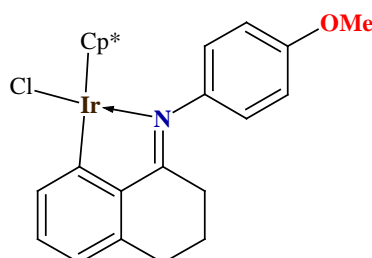


Figure 1.6: Robust cyclometallated Ir-imino complex used in the hydrogenation of *N*-benzylimine¹⁵

Zhou and co-workers¹⁶ studied the enantioselective hydrogenation of cyclic *N*, *N*-dialkyl enamines using a chiral iridium complex $[Ir(COD)Cl]_2$ bearing the spiro phosphoramidite ligand shown in Figure 1.7. This catalyst system is highly efficient under very mild conditions (1 bar H_2) producing 100 % conversion of the substrate to the corresponding chiral amine with an ee of 94 %. The presence of I_2 as an additive is a prerequisite, without which the activity and enantioselectivity is very low. The authors presume that the role of the I_2 is to oxidatively add to the Ir(I) centre producing an Ir(III) species which is responsible for the high activity and enantioselectivity. The authors further demonstrated the successful synthesis of crispine A in high yield (97 %) and ee (90 %) via an enantioselective hydrogenation. Due to the effectiveness of this spiro phosphoramidite ligand in controlling the

Chapter 1: Literature Review of Olefin Hydroformylation and Hydroaminomethylation

proved to be very challenging in terms of stereocontrol with the highest ee of 70 % achieved using a combination of a chiral:achiral ligand (Phosphoramidite:PPh₃) in a 2:1 ratio.

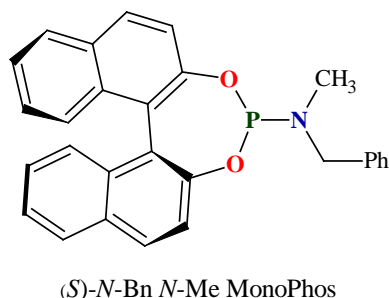


Figure 1.9: Phosphoramidite ligand used in the synthesis of diarylmethylamines²⁰

Diarylmethylamines are an important class of compounds due to its presence in a variety of pharmaceutical compounds. Using [Ir(COD)Cl]₂ and the phosphoramidite ligand shown in Figure 1.9, various diarylmethylamines were produced in high yields (80-96 %) with low to excellent ee's (31-98 %).²⁰ Hou and co-workers further demonstrated the hydrogenation of *N*-substituted diarylmethanimines to the corresponding chiral diarylmethylamines using the chiral (*R,R*)-f-spiroPhos ligand, while this catalyst system was also used to produce optically active cyclic amines.²¹⁻²²

A chiral hybrid *P,N*-bidentate ligand, based on a spiro skeleton, was developed by Ding and co-workers.²³ The corresponding Ir(I) complex, shown in Figure 1.10, was used for the asymmetric hydrogenation of *N*-benzylideneaniline. Full conversion of this substrate was achieved at room temperature, 50 bar H₂ and a catalyst loading of 1 mol%, however, it proceeded with low enantioselectivity (58 % ee).

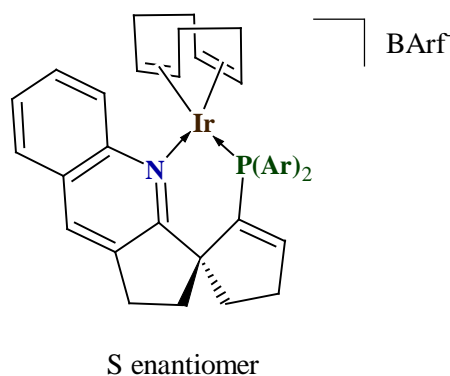


Figure 1.10: Hybrid *P,N*-Ligated Ir complex used in the hydrogenation of *N*-benzylideneaniline²³

Phosphine-oxazolines based ligands are also common *P,N*-bidentate ligands used in the hydrogenation of imines. Lu *et al.* utilized a diphosphinobenzylloxazoline ligand (Figure 1.11) for the hydrogenation of *N*-aryl arylmethylimines (similar as those shown in Figure 1.4), affording the corresponding chiral amines in high yields (86-99 %) and ee's (≥ 75 %).²⁴

Chapter 1: Literature Review of Olefin Hydroformylation and Hydroaminomethylation

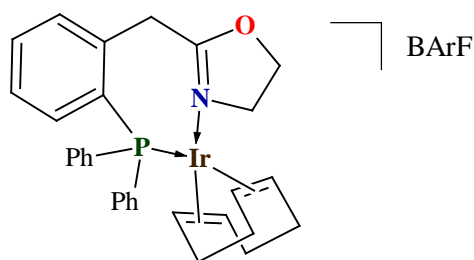


Figure 1.11: A phosphine-oxazoline Ir complex used in the hydrogenation of *N*Oaryl arylmethymines²⁴

Trialkyl and dialkylaryl tertiary amines are a class of compounds important in natural products. The phosphine-oxazoline base complex shown in Figure 1.12 was used in the asymmetric hydrogenation of α -(diethylamino)styrene to α -(diethylamino)ethylbenzene, affording the amine in quantitative yield with an ee of 84 % (R enantiomer).²⁵

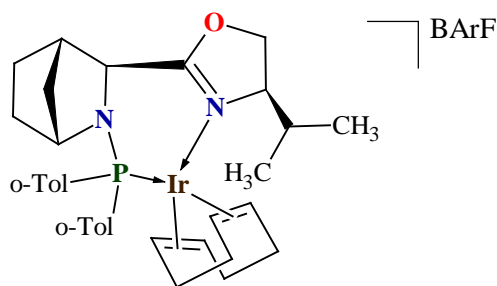


Figure 1.12: P, N – Ir complex used in the synthesis of dialkylaryl tertiary amines²⁵

Cationic Iridium complexes bearing chiral oxazoline- or pyridine-based *P,N* ligands were developed by Pfaltz and Baeza.²⁶⁻²⁷ These complexes were used as catalysts in the asymmetric hydrogenation of unfunctionalized enamines, 1,2-disubstituted enamines as well as acetophenone *N*-arylimines producing the corresponding amines in high yields at low catalyst loadings, low temperatures and moderate hydrogen pressure.²⁶⁻²⁷

The asymmetric hydrogenation of exocyclic enamines produce chiral tetrahydroquinolines.²⁸ [Ir(COD)Cl]₂/(*S*)-MeO-BiPhep/I₂ was found to be a highly efficient catalyst, registering excellent yields and high ee's (96 %).

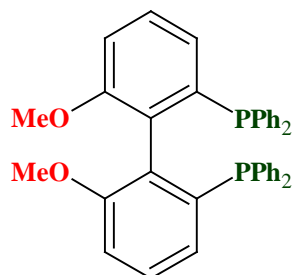


Figure 1.13: Ligand used by Zhou in the hydrogenation of exocyclic enamines²⁸

Chapter 1: Literature Review of Olefin Hydroformylation and Hydroaminomethylation

Similarly, benzodiazepinones and benzodiazepines can be synthesized via the asymmetric hydrogenation of the imine moiety.²⁹ Benzodiazepinones-type compounds find application as antitumor antibiotics while aptazepine are a benzodiazepine compound with antidepressant activity. Due to the relative rigidity and space-demanding features of the seven-membered ring, the hydrogenation is challenging. However, various benzodiazepinones and benzodiazepines derivatives were successfully prepared using an iridium diphosphine catalyst in the presence of morpholine-TFA.²⁹ The antihistaminic drug, mequitazine, which is sold as a racemate, was synthesized in 85 % yield and 47 % ee using a iridium complex and an phosphoramidite ligand in the presence of I₂.³⁰

[Ir(COD)Cl]₂(*S,S*)-f-Binaphane catalyst system (Figure 1.14) catalyzes the enantioselective hydrogenation of various 2-phenyl-1-pyrroline derivatives to the corresponding chiral amines in quantitative yields.³¹ The authors used this same catalyst system to produce enantiomerically enriched β-amino acids in high yields and excellent enantioselectivities with up to 97 % ee.³²

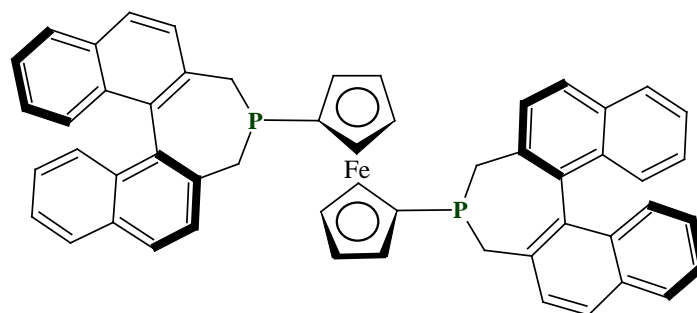


Figure 1.14: The (*S,S*)-f-Binaphane ligand used in enantioselective hydrogenation³¹

Iridium based catalysts are thus highly efficient in the production of various amines via the hydrogenation of imine/enamines intermediates delivering high enantioselectivities in the presence of suitable ligands.

1.3.2 Ruthenium catalyzed imine/enamine hydrogenation

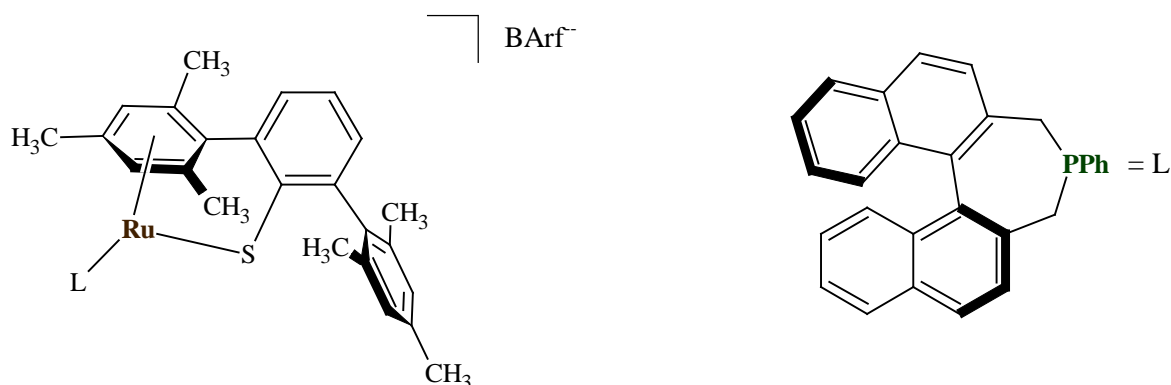


Figure 1.15: Ru(II)-thiolate complex and P-ligand used in the enantioselective hydrosilylation of imines³³

Chapter 1: Literature Review of Olefin Hydroformylation and Hydroaminomethylation

A ruthenium thiolate complex, shown in Figure 1.15, bearing a chiral monodentate phosphine ligand was used by Oestreich and Bähr for the enantioselective hydrosilylation of enolizable imines (acetophenone *N*-arylimines) using Me₂PhSiH.³³ The corresponding amines were isolated after the hydrolysis of the *N*-Si bond in 96 % yield, however, in moderate ee's (54 %).

The hydrogenation of β -*N*-protected enaminoesters provides an important gateway towards the synthesis of β -*N*-protected aminoesters. These types of compounds are precursors toward the preparation of β -lactams, β -peptides and other antibiotics. In this regard, Bruneau and co-workers investigated the hydrogenation of 3-*N*-benzylaminobut-2-enoate in the presence of an acidic medium.³⁴ The authors envisaged that in the presence of acid, the β -*N*-protected enaminoesters could undergo isomerization and protonation to the corresponding iminium salt followed by its subsequent hydrogenation. For this purpose, four different 4-coordinate Ru(II) complexes were synthesized ([CpRu(PPh₃)₂H], [CpRu(PPh₃)₂Cl], [CpRu(PPh₃)₂(MeCN)], [CpRu(PPh₃)₂THF]). Of these complexes, [CpRu(PPh₃)₂Cl] was found to be the most active catalyst, producing a conversion of 80 % in MeOH in 2 h at 20 bar H₂ pressure. Further reaction optimization revealed that RuCl₂(PPh₃)(*p*-cymene) is a far better catalyst precursor, while this system could also be applied in the hydrogenation of a range of other β -*N*-protected aminoesters.³⁴ However, in a paper by Matsumura and co-workers, they demonstrated the direct synthesis of *N*-unprotected β aminoesters via a ruthenium catalyzed enantioselective hydrogenation which also required the presence of an acidic medium.³⁵

Another class of precursor compounds important in medicine, is the chiral γ -secondary aminoalcohols. A series of unprotected β -ketoenamines were successfully hydrogenated by the ruthenium complex

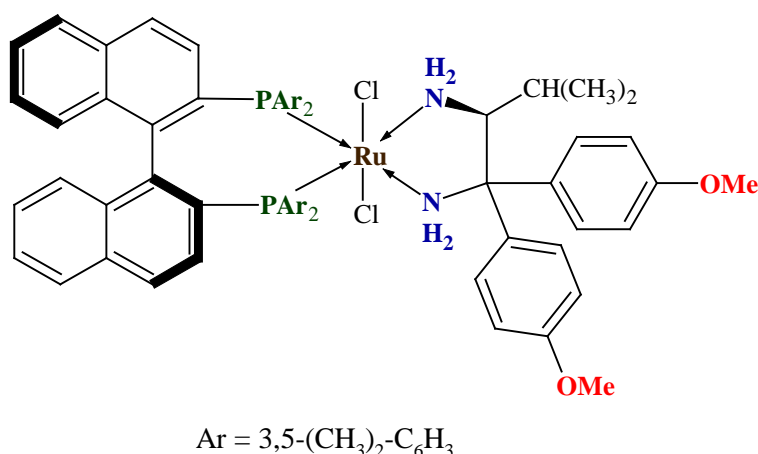


Figure 1.16: Ru complex used for the preparation of γ -secondary aminoalcohols³⁶

shown in Figure 1.16.³⁶ This catalyst delivered a range of chiral γ -secondary aminoalcohols under mild conditions (1 bar H₂ at room temperature) in quantitative yields (>99 %) and high enantioselectivity (ee >99 %). Furthermore, 2-propanol was found to be the best solvent for this transformation which comes

Chapter 1: Literature Review of Olefin Hydroformylation and Hydroaminomethylation

as no surprise due to the effectiveness of this solvent as a source of hydrogen in the transfer hydrogenation of ketones.³⁶

[Ru(OAc)₂(CO)₂(PⁿBu₃)(PPh₃)] was used in the hydrogenation of *N*-benzylideneaniline to the corresponding secondary amines.³⁷ Reaction optimization revealed that higher activities are observed in alcoholic solvents (MeOH and 2,2,2-trifluoroethanol) compared to toluene and THF. Of all these solvents, 2,2,2-trifluoroethanol was found to be the best solvent affording the amines in high conversions (>90 %) under relatively mild conditions (50 °C, 25 bar and 3 h).³⁷

The importance of the order of addition of reagents is underlined by Kačer and co-workers in their investigation into the enantioselective hydrogenation of cyclic imines using a ruthenium diamine complex (Figure 1.17, left).³⁸

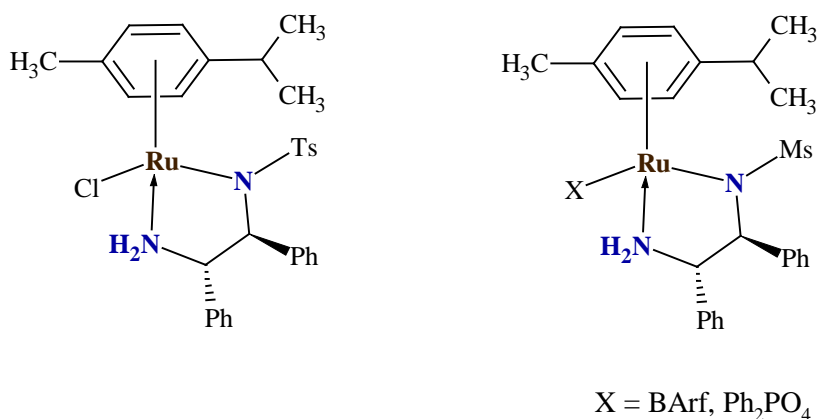


Figure 1.17: Chiral Ru complexes used in the hydrogenation of cyclic imines³⁸

The authors studied the asymmetric hydrogenation of 6,7-dimethoxy-1-methyl-3,4-dihydroisoquinoline. Trifluoroacetic acid is necessary in order to activate the imine by polarizing the C=N bond. However, full conversion of the substrate could only be achieved by changing the order of addition from imine-solvent-catalyst-acid to imine-solvent-acid-catalyst. A range of cyclic imines were subsequently hydrogenated in good-to-excellent yields and enantioselectivities. Fan and co-workers used a variation of this complex (Figure 1.17, right), Ru(η⁶-p-cymene)(MsDPEN)(BARf) (MsDPEN = *N*-(methanesulfonyl)-1,2-diphenylethylenediamine), to hydrogenate a range of cyclic *N*-alkyl imines (2-phenyl-1-pyrroline derivatives) in high yields and up to 98 % ee.³⁹ More recently, the authors also used this same complex, together with its Ph₂PO₄⁻ derivative, for the asymmetric hydrogenation of cyclic imines of benzazepines and benzodiazepines.⁴⁰ Most notably, the authors showed that the enantioselectivity can be reversed by simply changing the counterion (BARf⁻ vs Ph₂PO₄⁻).

Pizzano and co-workers⁴¹ studied the enantioselective hydrogenation of *N*-aryl ketimines to the corresponding amines using [RuCl₂(P-OP)(DPEN)] as catalyst (Figure 1.18) in the presence of *t*BuOK. Various *N*-aryl ketimines bearing electron withdrawing and donating groups were successfully

Chapter 1: Literature Review of Olefin Hydroformylation and Hydroaminomethylation

hydrogenated to their corresponding amines in high yields (>99 %) and ee's (91-96 %) under mild conditions (4-20 bar H₂ at room temperature). Furthermore, the authors also developed lutidine-derived CNC pincer complexes for the hydrogenation of similar imines.⁴²

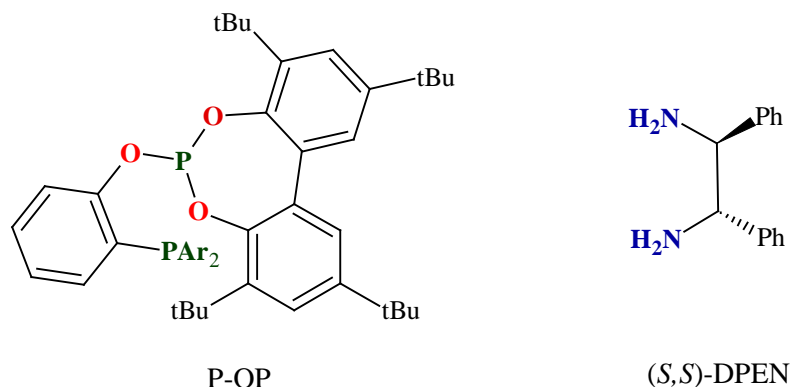


Figure 1.18: Ligands used in the hydrogenation of *N*-aryl ketimines⁴¹

1.3.3 Rhodium catalyzed imine/enamine hydrogenation

Aside from β -alanine, β -amino acids are not found naturally. Therefore, the incorporation of β -amino acids into β -peptide-based antibiotics are investigated as a means of potentially overcoming antibiotic resistance. β -amino acids and their derivatives can be synthesized via the hydrogenation of β -enamine amides and esters. In this regard, the Merck group reported on the highly efficient synthesis of β -amino acid derivatives via the asymmetric hydrogenation of unprotected enamines using [RhCl(COD)]₂ and a ferrocenyl based ligand as shown in Figure 1.19.⁴³

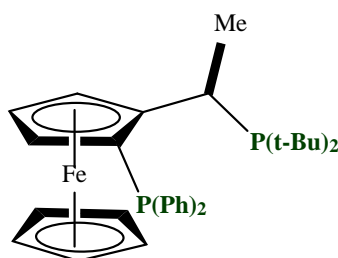


Figure 1.19: Ferrocenyl-based ligand used by the Merck group⁴³

In 2005, authors in the same laboratory also reported on the use of this catalyst system for the hydrogenation of 3-amino-2-butenanilide as well as for the compound shown in Figure 1.20.⁴⁴⁻⁴⁵ The authors found that the hydrogenation of these substrates is inhibited by the amine group. This inhibition can be alleviated via *in situ* protection by Boc₂O, allowing the reaction to proceed under mild reaction conditions.

Chapter 1: Literature Review of Olefin Hydroformylation and Hydroaminomethylation

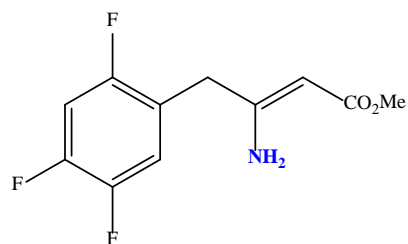


Figure 1.20: Enamine substrate used by the Merck group

Lee and co-workers demonstrated the asymmetric hydrogenation of homoproline derivatives to the corresponding cyclic β -amino acids making use of chiral bisphosphine ligands (Figure 1.21) and $[\text{Rh}(\text{COD})_2]\text{BF}_4$ as metal precursor.⁴⁶

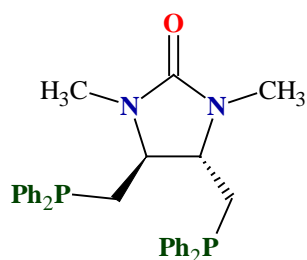


Figure 1.21: Chiral bis-phosphine ligand⁴⁶

The hydrogenation of β -keto- γ -acetal enamides to the corresponding α -acetal- β^{γ} -amino ketones were investigated by Ratovelomanana-Vidal and co-workers.⁴⁷ Excellent yield and enantioselectivities were obtained using $[\text{Rh}(\text{COD})_2]\text{BF}_4$ and QuinoxP* (Figure 1.22) as ligand, however, the reaction proceeded under high catalyst loadings of 10 mol%. Further reaction parameter optimization revealed that the catalyst loading can be decreased to 2 mol%, with the catalyst system producing quantitative yields of the product with ee's around 95 % under mild reaction conditions (40 °C, 1 bar H_2). The reaction was also found to be efficient with both electron-donating and electron-withdrawing groups.

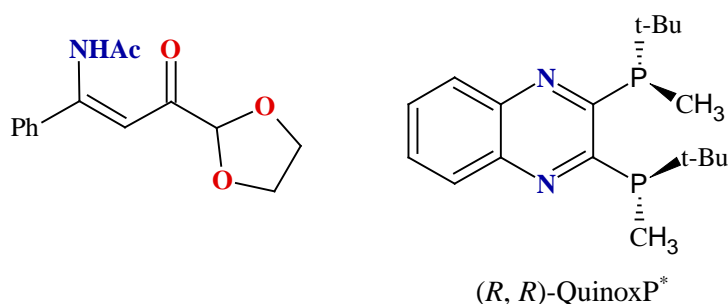


Figure 1.22: (R, R)-QuinoxP* ligand and the enamine substrate⁴⁷

However, β -amino acids derivatives can also be obtained via the hydrogenation of N-aryl β -enamino esters and β -enamino phosphonates, as shown by Zhang and co-workers.⁴⁸⁻⁴⁹ Another area of research these authors are interested in, is the hydrogenation of unprotected NH iminium chloride salts using a Rh-bisphosphine ligand.⁵⁰ A bisphosphine ligand containing a thiourea moiety was found to be

Chapter 1: Literature Review of Olefin Hydroformylation and Hydroaminomethylation

important as a hydrogen bonding donor, providing chiral amines in up to 97 % yield. This same thiourea-bisphosphine ligand was further used to provide access to chiral seven-membered cyclic amines via the hydrogenation of azepine/oxazepine-type seven-membered cyclic imines in up to 99 % conversion.⁵¹

Clarke and co-workers studied the influence of ligand electronic effects in rhodium catalyzed hydrogenation of enamines (4-(2-phenylprop-1-enyl)morpholine) encountered in hydroaminomethylation.⁵²

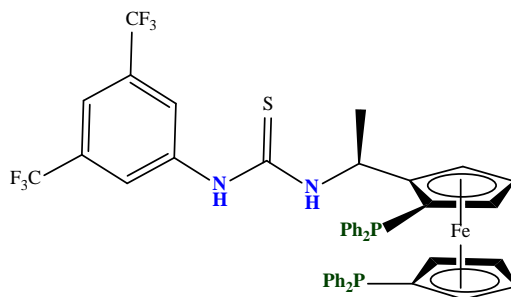


Figure 1.23: Bis-phosphine ligand with an incorporated thiourea moiety⁵²

The authors found that electron-deficient phosphine ligands, as those shown in Figure 1.23, produces more active hydrogenation catalysts compared to those derived from more electron-rich phosphines such as PPh₃. From DFT calculations, the authors concluded that electron-withdrawing ligands accelerates the reductive elimination step. This catalyst system was then further expanded to also investigate the hydrogenation of unactivated enamines (Figure 1.24).⁵³ The catalyst system was also found to be highly efficient for these substrates, proceeding at low catalyst loadings down to 0.01 mol %, however, this required extended reaction times (66 h). The reaction also proceeded at 5 bar H₂ pressure, registering full conversion of the substrate.⁵³

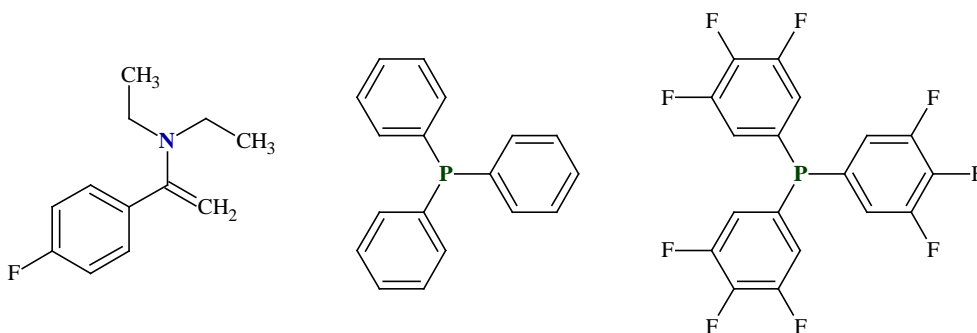


Figure 1.24: Unactivated enamine and PPh₃ and its more electron-deficient counterpart⁵³

The catalyst system utilized above are achiral and therefore produce a racemic mixture of the amine products. Using (*R,R*)-Et-DUPHOS or (*R,R*)-Et-BPE as ligands, produced chiral catalysts. Low hydrogenation activity was observed for these catalysts at room temperature in toluene and 60 bar H₂.⁵⁴ However, the activity could be improved by performing the reaction in chlorobenzene. This did not

Chapter 1: Literature Review of Olefin Hydroformylation and Hydroaminomethylation

only improve the activity, but also the enantioselectivity. In order to improve the enantioselectivity further, the authors investigated the use of I_2 as co-catalyst. Instead of observing an increase in the enantioselectivity, the authors were surprised to find a complete switch in enantioselectivity (from R to S).⁵⁴

In a study by Zhou and co-workers⁵⁵ on the hydrogenation of *N,N*-dialkyl enamines to 1,2-diarylethanamines using chiral monodentate spiro phosphonite ligands, they observed that I_2 had the desired positive effect on the enantioselectivity of the reaction. They also investigated the use of acetic acid as an additive in order to accelerate the reaction. In the presence of acetic acid alone, very low conversions were obtained, however, when I_2 and acetic acid was present together, the reaction rate increased considerably (reaction time decreased from 48 h to 12 h) while further allowing the reaction to proceed under milder reaction conditions (100 bar to 10 bar).⁵⁵

Börner and co-workers studied the asymmetric hydrogenation of pro-chiral electron-rich enamines using Rh(I) diphosphine and diphosphinite catalysts.⁵⁶ The authors studied the hydrogenation of 2-*N*-piperidinyl styrene to the corresponding chiral amine. All catalyst ligand combinations gave quantitative conversion at either 1 or 50 bar of H_2 , however, the ligand shown in Figure 1.25 (left) registered the highest enantioselectivity (53 %, R). When this catalyst system was applied in the hydrogenation of 2,3,3-trimethyl-3*H*-indole, no activity was observed. Upon converting this substrate to the corresponding *N*-methyl or *N*-benzyl enamine, the hydrogenation took place smoothly proceeding at 1 mol % catalyst loading, 1 bar H_2 for 4 h. By increasing the pressure to 50 bar, the hydrogenation could be performed at lower catalyst loading of 0.2 mol% for 30 min.⁵⁶

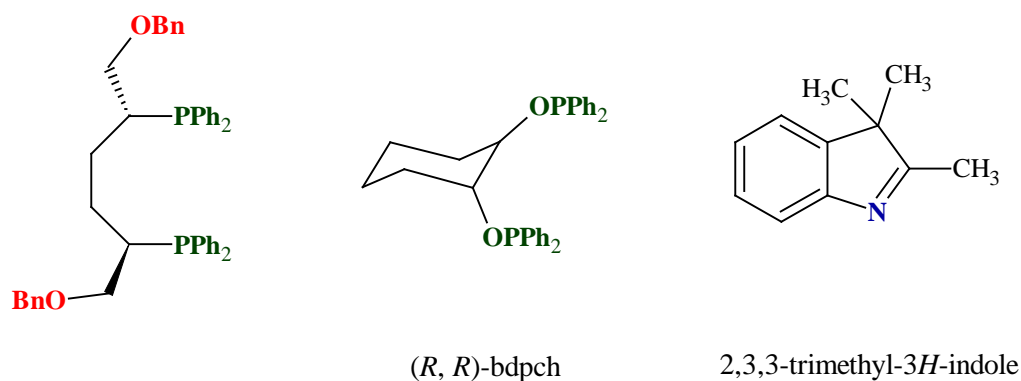


Figure 1.25: Ligands used in the hydrogenation of prochiral enamines⁵⁶

Another way to improve the enantioselectivity of transition metal catalysts is by employing the combinatorial asymmetric approach. This approach entails the utilization of a mixture of chiral ligands (hetero-combination) in order to obtain a combination which is more active and enantioselective than when these ligands are used individually. Reetz and co-workers successfully demonstrated this using mixtures of BINOL-derived chiral monodentate phosphites, phosphonites and phosphine ligands for the hydrogenation of *N*-acyl enamines. The origin of this enhancement was not disclosed.⁵⁷

Chapter 1: Literature Review of Olefin Hydroformylation and Hydroaminomethylation

Kayaki and co-workers⁵⁸ utilized cationic half-sandwich C-N chelating Rh complexes for the hydrogenation of *N*-(1-phenylethylidene)benzylamine. Low hydrogenation activities were observed, producing only 29 % yield of the product at 30 bar H₂ and 1 mol% catalyst loading in 2-propanol. The hydrogenation was performed in the presence of AgSbF₆, a Lewis acid, which activates the imine. These complexes were also found to be active in the hydrogenation of benzonitrile producing dibenzylamine as major product.

The complex, [Rh(PPh₃)₃COD]PF₆, is also able to catalyze the hydrogenation of imines.⁵⁹⁻⁶⁰ This complex was used in the hydrogenation of *N*-(β-naphthylmethylene)aniline to naphthalene-2-ylmethylphenylamine in 87 % yield at 25 °C and 13.8 bar. However, this proceeded at a catalyst loading of 1 mol% and reaction time of 18 h.⁵⁹ Complete reduction of PhCH₂N=CHPh to dibenzylamine was observed in ~30 min by James and co-workers.⁶⁰

1.4 Hydroaminomethylation

Hydroaminomethylation of alkenes were discovered by Reppe at BASF and consists of the initial hydroformylation of the alkene to aldehydes, which then condenses with an amine, forming an imine (in the case of a primary amine) or an enamine (in the case of a secondary amine).⁶¹ These imine/enamine intermediates then undergo hydrogenation catalyzed by the same catalyst, forming the amines. Conventional methods of amine synthesis involves nucleophilic substitution of organic halides by amines, azides or cyanides, requiring multistep synthetic routes and purification steps. Hydroaminomethylation is a one-pot domino process, proceeds with excellent atom economy and only forms water as a by-product.

The group of Behr is quite active in this field, having published a number of papers on this subject.⁶¹ In 2010 they developed a highly efficient method for the hydroaminomethylation of primary and secondary amines under aqueous biphasic conditions. They used the inorganic and organic salts (eg Cl⁻ and OAc⁻) of these amines by adding the appropriate concentrated acid. The authors proposed that in the presence of the concentrated acid, a cationic Rh species forms as a result of the dissociation of a CO ligand. The subsequent cationic rhodium hydride complex are then a much more active hydrogenation catalyst. This allowed them to obtain quantitative conversion of the substrate, 1-octene, with high chemoselectivities towards the saturated amine. The recyclability of the catalyst was not reported.⁶¹

The hydroaminomethylation of 1-dodecene and *N,N*-dimethylamine was investigated by Li and co-workers⁶² also employing an aqueous-organic two phase system. The authors did not utilize any organic solvents. The authors found that in the presence of the surfactant, CTAB, a 20 % increase in the conversion of the substrate is observed. This was attributed to the ability of the surfactant to form micelles which expand the interfacial area between the aqueous and the organic phase. The surfactant also brings Rh species closer to the interfacial area thereby facilitating the catalysis. An increase in

Chapter 1: Literature Review of Olefin Hydroformylation and Hydroaminomethylation

reaction temperature produced an increase in both conversion, amine chemoselectivity (~50 %) and regioselectivity towards the linear amine (7.50:1), however, above 130 °C, the amine selectivity decreased due to an increase in side reactions (isomerization and alkene hydrogenation). Higher pressure was also beneficial for the reactivity and chemoselectivity (amines) of the catalysts, however, at 40 bar, side reactions became more favourable while it also decreased the regioselectivity towards the linear amine. The influence of the Rh:P ratio was also investigated which revealed an increase in the regioselectivity towards the linear amine by suppressing the side reactions (isomerization and alkene hydrogenation). Other alkenes were also well tolerated, however, it was found that as the chain length increased, the amine selectivity decreased due to limited water solubility of the alkenes.⁶²

Table 1.1: Hydroaminomethylation using an aqueous-organic biphasic approach

Substrates	Catalyst System	Optimum Reaction Conditions	Reference
1-Octene, Salts of 1° and 2° Amines	[Rh(COD)Cl] ₂ and TPPTS	0.42 mol % Rh, Rh:P (1:64), Amine:Olefin (2:1), 60 bar CO:H ₂ (1:1), 130 °C, 4 h	61
1-Dodecene and <i>N,N</i> -dimethylamine	RhCl(CO)(TPPTS) ₂	[Rh] = 1.8x10 ⁻³ mol/l, Rh:P (1:32), Amine:Olefin (8:1), 30 bar CO:H ₂ (1:1), 130 °C, 4 h and CTAB	62
1-Octene and di- <i>N</i> -propylamine	Rh nanoparticles stabilized by Ph ₂ P(CH ₂ CH ₂ O) _n CH ₃ (n=16)	0.1 mol % Rh, Rh:P (1:2), Amine:Olefin (1.5:1), 60 bar CO:H ₂ (1:1), 120 °C, 4 h	63

Wang and co-workers⁶³ made use of the thermoregulated phase-transfer catalysis (TRPTC) approach to investigate the hydroaminomethylation of 1-octene and di-*n*-propylamine using Rh nanoparticles in an aqueous/1-butanol biphasic system. The Rh nanoparticles were stabilized by the thermoregulated phosphine ligand Ph₂P(CH₂CH₂O)_nCH₃ (n=16). The influence of various reaction parameters on the reactivity and selectivity of the Rh nanoparticles were investigated. In all cases, full conversion of the substrate was observed. However, increasing both the temperature (90-120 °C) and pressure (20-60 bar) produced an increase in the chemoselectivity towards amines (97 % at 60 bar and 120 °C). This lowered the regioselectivity towards the linear amine, with a L:B ratio of 80:20 obtained at 60 bar and 120 °C. Higher 1-octene:Rh molar ratio led to a decrease in the amine chemoselectivity. When a mercury poisoning test was performed, the reductive amination step was significantly inhibited (19 % amines) but this had no effect on the conversion of the substrate while 78 % aldehydes was observed. This led the authors to conclude that the hydroformylation is catalyzed by a homogeneous Rh complex, and that the Rh nanoparticles act as a reservoir for the catalytic species. Recycling and reusability of the catalyst was also demonstrated which had no effect on the substrate conversion, however, the amine selectivity drops from 97 % in the first run to 85 % in the sixth run. This was subsequently attributed to loss of Rh into the organic phase as confirmed by ICP-OES.⁶³

Chapter 1: Literature Review of Olefin Hydroformylation and Hydroaminomethylation

Weberskirch and co-workers⁶⁴ utilized mono (Rh) – and bimetallic (Rh/Ir) micellar catalyst to study the hydroaminomethylation of 1-octene and *N,N*-dimethylamine. Amphiphilic PPh₃ functionalized poly(2-oxazolines) block co-polymers were used as a macro-ligand. The monometallic Rh catalyst system displayed poor hydroaminomethylation activity (2 % amine yield) at 100 °C and 50 bar of CO:H₂, with the hydrogenation step particularly slow. This low activity was subsequently attributed to deactivation of the catalyst by the amine (*N,N*-dimethylamine) via coordination to the metal. An increase in temperature to 150 °C improved the yield of the amines (22 %), however, a temperature of 170 °C favoured other side reactions. Generally, the *n*-aldehydes is much more reactive in hydroaminomethylation compared to the iso-aldehydes. In order to further improve the hydrogenation step, a bimetallic Rh/Ir system was used in a 1:2 ratio. This improved the yield of the amines to 38 %, however, the hydrogenation of 1-octene to octane also occurred (31 % yield). Performing the reaction at lower temperatures prevented the hydrogenation of the substrate (1 %), however, a lower amine yield was also observed (24 %).⁶⁴

Another approach to efficiently recycle catalysts is by employing ionic liquids in a biphasic approach. In this regard, Luo and co-workers⁶⁵ investigated the biphasic hydroaminomethylation of 1-dodecene and morpholine using Rh-BISBIS catalyst system. Initial investigation using [Bmim][BF₄] as solvent produced good activities and selectivities, however, the recycling of the catalyst was not as efficient. Using a greener ionic liquid, [Bmim][p-CH₃C₆H₄SO₃], allowed the authors to use their catalyst in 6 successive runs. However, this was accompanied with a drop in amine selectivity as well as a drop in the regioselectivity towards the linear amine which was attributed to partial oxidation of the phosphine moieties of the ligand.⁶⁵ The authors further used this same system to study the hydroaminomethylation of 1-dodecene and various secondary amines in an aqueous/organic two-phase system in presence of CTAB.⁶⁶ This system produced excellent conversions around ~97 %, ~80 % chemoselectivity towards the amines and regioselective towards the linear product (L:B of 84:1). This was achieved at a [BISBIS][Rh] ratio of 10:1, 30 bar CO:H₂ (1:1), 130 °C for 5 h. Other alkenes (C₆-C₁₄ terminal alkenes) could also successfully be hydroaminomethylated, while maintaining the chemoselectivity towards the amines (~80 %), however, for C₁₄ it dropped to ~70 %. It was further found that with an increase in the alkyl length, the regioselectivity towards the linear amine increases. Generally it was found that in the presence of more basic and nucleophilic amines (dimethylamine vs morpholine) the chemoselectivity towards amines is higher.⁶⁶

The catalyst system, Rh/Sulfoxantphos, is also able to catalyze the hydroaminomethylation of piperidine and terminal alkenes in an ionic liquid biphasic system using [PMIM][BF₄].⁶⁷ Comparable conversions and chemoselectivities were obtained in [PMIM][BF₄] and Toluene:MeOH (1:1), however, superior regioselectivities were obtained using organic solvents. This system was also fully recyclable maintaining catalytic activity and chemoselectivity. However, a significant drop in the regioselectivity was observed, which is attributed to partial oxidation of the ligand. The activity and chemoselectivity

Chapter 1: Literature Review of Olefin Hydroformylation and Hydroaminomethylation

was maintained due to no Rh and phosphine-ligand leaching as confirmed by ICP-OES. The influence of the reaction conditions was also investigated. It was found that larger substrate/Rh ratios resulted in no decrease in conversion, chemoselectivity towards amine or the regioselectivity towards the linear amine. Generally, at lower temperatures higher regioselectivities towards the linear amine was obtained due to less isomerization.⁶⁷

Behr and co-workers⁶⁸ utilized a temperature-dependant solvent system (TMS systems) to successfully perform the hydroaminomethylation of 1-octene and morpholine using $[\text{Rh}(\text{COD})\text{Cl}]_2$ as catalyst with no added ligand. Propylene carbonate/n-hexane/1,4-dioxane was used as solvent in a 1:0.55:1.3 ratio which produced almost full conversion of the alkene and 96 % chemoselectivity towards amines.⁶⁸

Symmetric dialkylpiperazines can also be prepared via the rhodium catalyzed bis-hydroaminomethylation of piperazine and linear aliphatic alkenes as shown by Seidensticker *et al.*⁶⁹ Under their optimized reaction conditions (40 bar H_2/CO (1.35/1), 120 °C, 16 h) they achieved a yield of 80 % for the amines proceeding at a linear regioselectivity of 77 %. The yield and linear regioselectivity was particular sensitive to the ratio of H_2/CO , with higher ratios leading to by-product formation, especially saturated hydrocarbons. The total pressure of H_2/CO also impacted the amine yield and regioselectivity. The authors further investigated the scope of the reaction employing various olefins ranging from linear terminal and internal olefins, cyclic olefins, styrene as well ester and alcohol containing olefins. These substrates proceeded with moderate to excellent yields and linearities.⁶⁹

The first hydroaminomethylation of cyclopentadiene (cpd) was reported by Behr and co-workers in 2015 (Figure 1.26).⁷⁰ One of the main side reactions of cyclopentadiene is its dimerization to dicyclopentadiene (dcpd) which can be further converted in HAM. Therefore, if the amines of cpd is desired, the dimerization of cpd needs to be suppressed. Hence, various Rh precursors, $\text{CO}:\text{H}_2$ ratios, solvents and additives (phosphine ligands and bases) were screened, which showed that the hydroaminomethylation of cpd and pyrrolidine proceeded smoothly in the presence of only Rh(II) octanoate dimer in the absence of any ligand or other additives towards the monoamine species. The selectivity towards 1-(cyclopentylmethyl)pyrrolidine was 77 %. Closer monitoring of the reaction revealed that in the initial part of the reaction, cpd is hydrogenated to cyclopentene which then undergoes hydroformylation to cyclopentane carbaldehyde which then enters the reductive amination part of hydroaminomethylation. Furthermore, no cyclopentane carbaldehyde nor any enamine was detected, which led the authors to believe that the initial hydrogenation of cpd to cyclopentene is the rate-determining step. Moreover, the reaction could also be expanded to include other amines such as piperidine, morpholine, methyl 4-piperidinecarboxylate, diethylamine and others. All these amines proceeded with moderate to high conversions (56-100 %) and selectivities towards the monoamine species (45-86 %).⁷⁰

Chapter 1: Literature Review of Olefin Hydroformylation and Hydroaminomethylation

Following the successful hydroaminomethylation of cpd, the system was expanded to specifically focus on the hydroaminomethylation of dcpd to TCD-diamines monomers using *n*-butyl amine (Figure 1.26).⁷¹

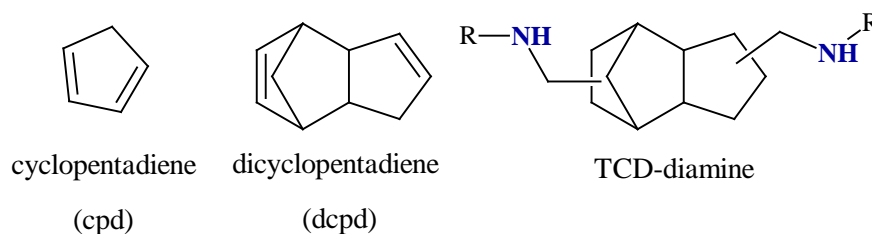


Figure 1.26: Cpd and dcpd and the corresponding diamine of dcpd⁷⁰⁻⁷¹

A chemoselectivity of 88 % towards TCD-diamine could be achieved after the optimization of the reaction conditions (0.5 mol % Rh(II) octanoate dimer, 60 bar CO:H₂ (1:1), 3 h, 120 °C). In order to limit the occurrence of side reactions such as the hydrogenation of C=C double bond and aldol condensation reactions, experiments were carried out using a DCPD:amine ratio of 1:6. Higher activities were obtained in the presence of non-polar solvents. A kinetic investigation was also performed. In these experiments, only the TCD-mono(butyl)imine, TCD-mono(butyl)amine and the target TCD-diamine was observed, possibly revealing that the hydrogenation of TCD-mono(butyl)imine to TCD-mono(butyl)amine is the rate-limiting step. Furthermore, the authors found that the addition of ligands impacted the reaction negatively while the catalytic activity can be improved by raising the temperature, however, this led to catalyst deactivation.⁷¹

Recently, the authors developed a method to synthesize the primary amines of TCD-diamines (Figure 1.27). An orthogonal tandem amination reaction was employed which combines the hydroaminomethylation of dcpd and *n*-butylamine to the corresponding TCD-diamine (secondary amine).⁷² This is then followed by the splitting of the amine using Shvo-catalyst and ammonia. This new multi-step orthogonal approach allowed for the synthesis of the target primary amine in 29 % yield.⁷²

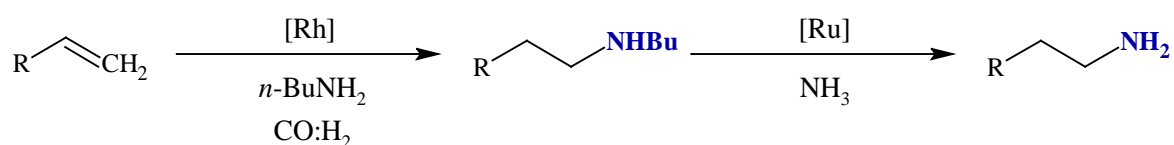


Figure 1.27: Orthogonal tandem amination reaction⁷²

Pharmaceutical important amphetamines can be prepared via the hydroaminomethylation of arylethylenes and anilines.⁷³ Cationic Rh precursors ([Rh(COD)₂BF₄] vs [Rh(acac)(CO)₂], in combination with dppf in the presence of HBF₄, is far more efficient in catalysing the process, achieving

Chapter 1: Literature Review of Olefin Hydroformylation and Hydroaminomethylation

an amine yield of 96 % (iso:n of 88:12). The role of the HBF_4 is presumably to protonate the imines to form iminium ions which are more easily reduced.⁷³

The use of NH_3 in hydroaminomethylation to synthesize primary amines is normally difficult due to issues with selectivity. It usually produces a mixture of primary, secondary and tertiary amines. This can be partially overcome by employing large excesses of ammonia relative to the alkene, although this can lead to catalyst deactivation. However, in a study reported by Beller and co-workers⁷⁴, they demonstrated the highly selective hydroaminomethylation of alkenes and ammonia. The high selectivities were obtained utilizing a dual metal catalyst (Rh/Ir/TPPTS catalyst system) to ensure the rapid hydrogenation of the imines to the amines. Furthermore, the selectivity was further controlled by utilizing a two-phase aqueous/organic phase in order to extract the amine product into the organic phase. This removes it from the catalyst containing aqueous phase, improving the selectivity. This allowed them to produce primary amines in up to 90 % selectivity.⁷⁴ In 2007, they attempted this reaction in the presence of supercritical ammonia.⁷⁵ A bimetallic Rh-Ir catalyst system was again used, where they found that the presence of phosphine ligands such as PPh_3 and Xantphos inhibits the formation of primary amines. Therefore, in the absence of any ligands and using $\text{Rh}(\text{acac})(\text{CO})_2$ and $[\text{IrCl}(\text{cod})]_2$, the highest yield obtained was 60 % (of the primary nonyl amine).⁷⁵

Linear amines can also be obtained via the isomerization-hydroaminomethylation of internal alkenes.⁷⁶ Beller and co-workers⁷⁶ investigated the use of a series of wide-bite-angle ligands. These ligands control the transformation of internal alkenes to linear amines, where it was found that the ligands with wider bite angles produce better regioselectivity towards the linear amine. In this regard, the best catalyst system was found to be a Xantphenoxaphos ligand (Figure 1.28) in combination with $[\text{Rh}(\text{COD})_2]\text{BF}_4$ which produced 96 % regioselectivity towards the linear amine (from 2-pentene and piperidine). In a further report in 2016, $\text{Ru}_3(\text{CO})_{12}$ and a 2-phosphino-substituted imidazole ligand (Figure 1.28, right) was used to study the hydroaminomethylation of 2-octene and piperidine.⁷⁷ The process entailed a domino Water-Gas Shift/Hydroaminomethylation sequence. Again, high yields of the amines were obtained (95 % yield) with an 87 % selectivity towards the linear amine. The authors further demonstrated the use of various other internal olefins (linear internal, cyclic and aromatic olefins) as well as the use of other amines (morpholine and 1-phenylpiperazine).⁷⁷

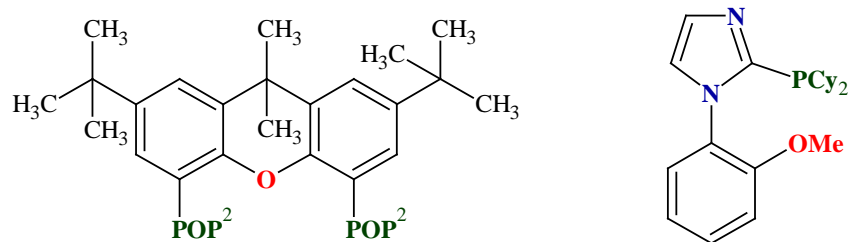


Figure 1.28: Xantphenoxaphos ligand⁷⁶ and 2-phosphino-substituted imidazole ligand⁷⁷

Chapter 1: Literature Review of Olefin Hydroformylation and Hydroaminomethylation

All the systems reported on so far involved the use of phosphine-based ligands. In a study reported by Seayad *et al.*, a rhodium carbene catalyst was used for the hydroaminomethylation (Figure 1.29).⁷⁸ They studied the hydroaminomethylation of 1-pentene and piperidine as a model reaction. Generally, high conversion and amine yields were observed using either Toluene, THF or MeOH, however, better hydrogenation activities was obtained with THF. The hydrogenation of the enamine proceeded smoothly when using higher partial pressures of H₂ relative to CO (CO:H₂ of 1:5 vs 1:1 at 60 bar total pressure) and when employing higher temperatures (85 vs 95 °C). Solvent, temperature and CO:H₂ partial pressure had no significant influence on the regioselectivity (1:b of ~ 63:37). This method could be expanded to include other olefins (1-octene, cyclohexene, cyclooctene, styrene) and amines (morpholine, dimethylamine and *n*-hexylamine) and in most cases excellent amine yields was obtained.⁷⁸ In 2015, another report on the use of magnetically retrievable bis-*N*-heterocyclic carbene Rh(I) based catalysts were published by Abu-Reziq and co-workers (Figure 1.29).⁷⁹ As a model reaction, they studied the hydroaminomethylation of styrene and morpholine. The ligand shown in Figure 1.29 (right) produced the best results in terms of conversion (92 %), amine selectivity (92 %) and regioselectivity (1:b of 1:11). The conversion was high at 80, 100 and 150 °C, however, the reaction at 80 °C was better in terms of chemo- and regioselectivity. In terms of pressure, the reaction proceeded smoothly when employing a H₂:CO ratio of 27.6:6.9. Higher CO partial pressures (while keeping the P_{total} constant) produced lower amine selectivities.⁷⁹

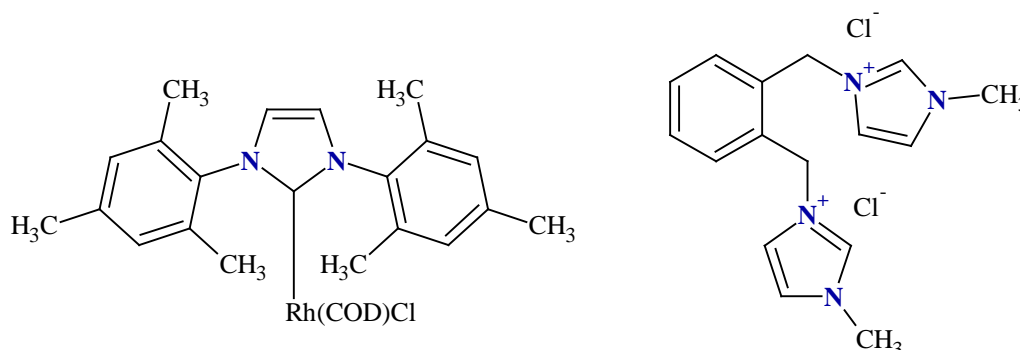


Figure 1.29: Rh-carbene catalyst⁷⁸ and the ligand used by Abu-Reziq and co-workers⁷⁹

Careful control of reaction conditions as well as the choice of ligand can influence the eventual outcome of the hydroaminomethylation reaction. In a report by Ahmed *et al.*, enamines could selectively be synthesized via the so-called hydroaminomethylenation.⁸⁰ Performing the reaction at mild temperatures (65 °C) and pressures (CO:H₂, 1:1, 10 bar), allowed them to prepare the linear enamine almost exclusively (99 % regioselectivity) from 1-pentene and piperidine using [Rh(acac)(CO)₂] and Naphos as ligand.⁸⁰

Thiel and co-workers⁸¹ developed the novel Rh(I) complex shown in Figure 1.30 in order to study the hydroaminomethylation of 1-pentene and piperidine. These ligands contain an additional binding site in their backbone, specifically for the binding of Lewis acids such as KPF₆. In the presence of KPF₆,

Chapter 1: Literature Review of Olefin Hydroformylation and Hydroaminomethylation

improved amine selectivities (80 % in the absence to 94 % in the presence) was observed which were attributed to secondary interactions between the ligands and KPF_6 . Generally better hydrogenation activities were observed at lower CO partial pressures (10 vs 5 bar, at 50 bar H_2).⁸¹

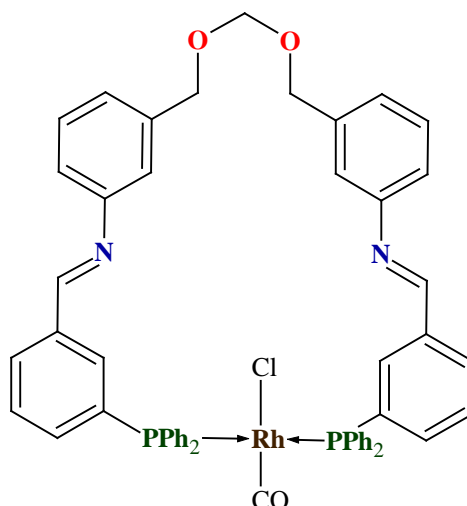


Figure 1.30: Rh-diphosphine complex with additional binding site⁸¹

Gülak *et al.* showed that the hydroaminomethylation reaction can be performed regioselectively in the absence of any phosphine ligand.⁸² They investigated the hydroaminomethylation of 1-octene and piperidine via a water-gas-shift reaction followed by hydroaminomethylation catalyzed by $Ru_3(CO)_{12}$. This method is also applicable to other secondary (such as morpholine and 1-phenylpiperazine) and primary (cyclohexylamine and aniline) amines.⁸²

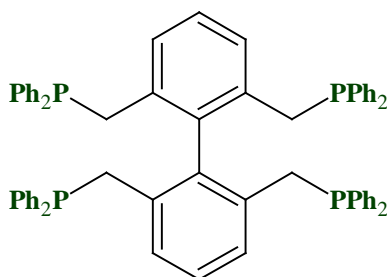
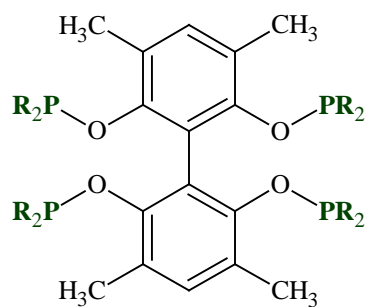


Figure 1.31: Tetrabi-phosphorous ligand used in isomerization-hydroaminomethylation⁸³

The effectiveness of the tetrabi-type ligands (Figure 1.31) to facilitate the isomerization-hydroaminomethylation of internal alkenes to linear amines was demonstrated by Liu *et al.*⁸³ In combination with $Rh(acac)(CO)_2$, this catalyst system delivered high amine chemo- (84-95 %) and regioselectivities (>90 %) towards the linear amine (2-octene and piperidine) in mixtures of 2-propanol and ethanol, ethanol and toluene and methanol and toluene. This catalyst operated under quite low pressures of $CO:H_2$ (5:5 bar) at 125-135 °C. 2-Pentene and 2-hexene could also regioselectively be transformed to their corresponding linear amines in >99 % n-selectivity.⁸³

Chapter 1: Literature Review of Olefin Hydroformylation and Hydroaminomethylation



R = Pyrrole

Figure 1.32: Pyrrole-based tetraphosphorous ligand used in linear selective hydroaminomethylation⁸⁴

The focus was then shifted to the linear selective hydroaminomethylation of styrene and piperidine using a pyrrole-based tetraphosphorus ligand as shown in Figure 1.32.⁸⁴ The authors envisioned that due to the multiple chelating ability, steric interactions as well as the improved local ligand concentration, will facilitate high regioselectivities towards the linear amine. After successful reaction condition optimization in terms of solvent (tert-amyl alcohol), pressure (40:10 bar CO:H₂) and source of Rh ([Rh(nbd)₂]SbF₆), the hydroaminomethylation of styrene and piperidine could successfully be performed proceeding at high amine chemoselectivity (92 %) and linear regioselectivity (93 %).⁸⁴ This ligand could also successfully be applied in the linear selective hydroaminomethylation of 1-pentene and 1-hexene with piperidine producing excellent amine chemo- (>98 %) and regioselectivities (97-99 %).⁸⁵

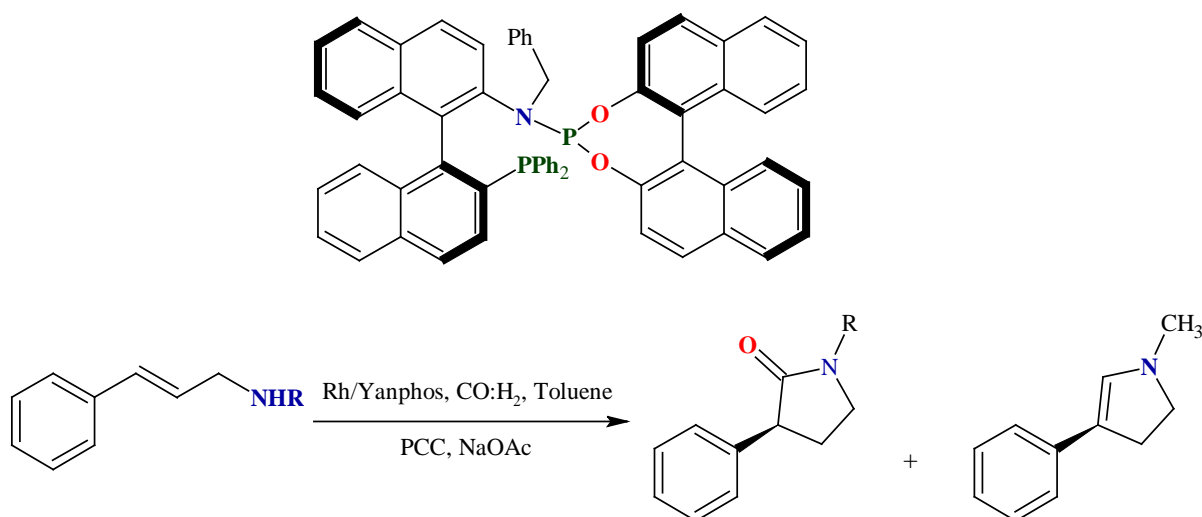


Figure 1.33: Yanphos (top) and the synthesis of chiral pyrrolidinones and pyrrolidines⁸⁶

Chiral pyrrolidinones and pyrrolidines can be synthesized via the interrupted asymmetric hydroaminomethylation of trans-1,2-disubstituted alkenes such as *N*-benzyl-3-phenylprop-2-en-1-amine catalyzed by the Rh/Yanphos catalyst system (Figure 1.33).⁸⁶

Chapter 1: Literature Review of Olefin Hydroformylation and Hydroaminomethylation

Interrupting the reaction via stabilization of the chiral hemiacetal intermediate allowed them to successfully synthesize the chiral amides and amines after either oxidation or reduction.⁸⁶

The hydroaminomethylation of 1-nonene and aqueous dimethylamine was studied by Karakhanov *et al.* using $\text{Rh}(\text{acac})(\text{CO})_2$ and an excess PPh_3 .⁸⁷ Hydrogenation activities below 5 % was observed at 80 °C, which significantly increased at elevated temperatures (at 130 °C and 40 bar $\text{CO}:\text{H}_2$ (1:1) the amine yield was 73 %). To further boost the hydrogenation activity, a 1:2 ratio of $\text{CO}:\text{H}_2$ (at 40 bar) was used producing an amine yield of 80 % while in the presence of Ru (as $\text{Ru}_3(\text{CO})_{12}$) the yield of amines increased to 92 %. The low solubility of aqueous dimethylamine in non-polar media can be overcome by using DMF as the source of amine.⁸⁷

The concept of SILP (Supported Ionic Liquid Phase) catalysts was also applied to hydroaminomethylation.⁸⁸ The hydroaminomethylation of ethylene and diethylamine was studied to produce diethylpropylamine (DEPA). Various IL coatings, immobilized on Silica 100, were screened ($[\text{EMIM}][\text{OAc}]$, $[\text{EMIM}][\text{OTf}]$, $[\text{MMMIM}][\text{NTf}_2]$ and $[\text{OMIM}][\text{NTf}_2]$), of which $[\text{MMMIM}][\text{NTf}_2]$ produced the highest yield of amine (35 %) using $\text{Rh}(\text{acac})(\text{CO})_2$ and Xantphos. This IL coating represents the least basic anion and least lipophilic cation. In the absence of IL coating, only 2 % amine was produced with the major side reaction yielding the aldol condensation product. Therefore, in the presence of IL, side reactions are inhibited. The yield of amine could be increased to 70 % by changing the support material from Silica 100 to PBSAC (polymer-based spherical activated carbon). Using this system, the authors further showed the long-term stability of this catalyst system by performing the continuous gas-phase hydroaminomethylation for more than 18 days time-on-stream.⁸⁸

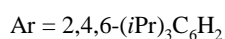
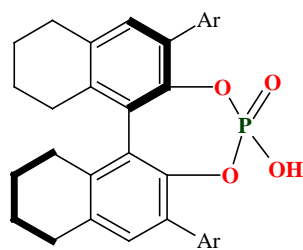


Figure 1.34: Chiral phosphoric acid derivative⁸⁹

Amines can be synthesized enantioselectively by employing a metal/organo relay catalytic strategy.⁸⁹ Han and co-workers⁸⁹ performed the enantioselective hydroaminomethylation of styrene and aniline derivatives under very mild reaction conditions (1-2 bar $\text{CO}:\text{H}_2$ (1:1), 25-50 °C, 16-72 h). In this approach, $\text{Rh}(\text{acac})(\text{CO})_2$ and (*R,R*)-Ph-BPE catalyzes the branched selective hydroformylation of styrene which is followed by imine formation. A chiral Bronsted acid catalyst, shown in Figure 1.34, then catalyses the dynamic kinetic reduction of imines to chiral amines. Using this approach,

Chapter 1: Literature Review of Olefin Hydroformylation and Hydroaminomethylation

enantiomeric ratios of up to 97:3 could be achieved. Aliphatic alkenes and vinyl esters could also be used, however, with moderate yields and enantioselectivities.⁸⁹

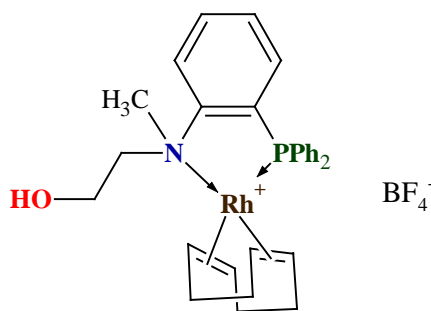


Figure 1.35: Rh(I) *P, N*-ligated complex used in the hydroaminomethylation of styrene in the presence of morpholine⁹⁰

The cationic Rh(I) [*P, N*] complex shown in Figure 1.35 also catalyses the hydroaminomethylation of styrene and morpholine.⁹⁰ This reaction proceeded under a high pressure of syngas (100 bar CO:H₂, 1:1) which at 100 °C, produce amines chemoselectively (99 %) with a 86 % regioselectivity towards the branched amine.⁹⁰

Aqueous methylformate in DMF can produce CO and H₂, while the DMF can be a source of dimethylamine for the subsequent hydroaminomethylation reaction. Both Ru and Rh can catalyse this process, as shown by Karakhanov and co-workers.⁹¹ They used Ru₃(CO)₁₂ or Rh(acac)(CO)₂ in the presence of PPh₃ to study the hydroaminomethylation of 1-nonene and dimethylamine. The Rh system produced higher amine yields (92 % amines) compared to the Ru system (61 %) at 170 °C. However, higher regioselectivities were observed towards the linear amine in the case of Ru (66 % vs 15 % in the case of Rh). Combining the Ru and Rh complexes, thus forming a Ru/Rh bimetallic catalyst system, produced a more active catalyst which could also be used to study the hydroaminomethylation of other higher alkenes.⁹¹

Bhange and co-workers⁹² utilized a PEG-anchored Rh polyether complex to study the hydroaminomethylation of cyclopentene and morpholine. This reaction proceeded smoothly in toluene producing 100 % amine yield at 28 bar and 100 °C while the activity was low in *n*-hexane or PEG-600 as solvent. Other amines (such as piperidine, piperazine, cyclohexylamine, benzyl amine, aniline) and alkenes (such as cyclohexene, styrene, 1-hexene) could also successfully be transformed to the corresponding amines in high yields while the authors also showed that the catalyst can be recycled up to five times without a significant drop in amine yield.⁹² In a separate report, the authors also studied the hydroaminomethylation of 1-hexene and piperidine using a Rh-phosphinite complex.⁹³ Reaction condition optimization revealed that the reaction proceed smoothly using a CO:H₂ ratio of ~1:2, benefitting the hydrogenation step. Therefore, using 7/23 bar CO:H₂, full conversion of 1-hexene is observed, 99 % amine selectivity and 66 % regioselectivity towards the linear amine at 80 °C and 8 h in THF. If the temperature is increased, the activity and amine chemoselectivity is maintained, however, the regioselectivity towards the linear amine drops to 51 %. The catalyst loading could also successfully

Chapter 1: Literature Review of Olefin Hydroformylation and Hydroaminomethylation

be reduced from Rh:substrate ratio of 1:1000 to 1:3333, with only a 6 % drop in conversion to 94 % while maintaining high amine chemoselectivities and regioselectivities. Toluene and MeOH produced lower activities and selectivities. The authors further studied the hydroaminomethylation of various aliphatic, cyclic and aromatic olefins, all proceeding with excellent conversions and amine selectivities.⁹³

Blum and co-workers⁹⁴ showed that the regioselectivity in the hydroaminomethylation reaction of vinylarenes and aniline derivatives can be determined by the hydrophobicity of the catalyst support. They prepared a rhodium catalyst ($[\text{Rh}(\text{COD})\text{Cl}]_2$) immobilized on hydrophobized sol-gel ceramic supports. The Rh complexed to covalently bonded 2-(diphenylphosphino)-ethyltriethoxysilane. By varying the length of the hydrophobic moiety, the authors showed that superior regioselectivities towards the branched amines are obtained (95 % using an octyl moiety) which is further amplified by performing the reaction at mild temperatures (60 °C) and a 3:1 H_2 :CO ratio. Furthermore, the authors showed that anilines could be prepared *in situ* from their corresponding nitroarenes. The hydroaminomethylation reaction took place in an aqueous micro-emulsion which therefore required the presence of a surfactant (CTAB) to solubilize the substrate. Moreover, due to the strong coordination of Rh to the phosphine moieties, no significant leaching of the catalyst was observed.⁹⁴

Eilbracht and Srivastava⁹⁵ studied the ruthenium catalyzed hydroaminomethylation of cyclopentene and morpholine using CO_2 via the initial reverse-water-gas-shift (RWGS) reaction followed by hydroaminomethylation. Under their initial reaction conditions (30/50 bar CO_2/H_2 , 160 °C, Toluene, LiCl and $\text{Ru}_3(\text{CO})_{12}$), a 50/50 split in yield between cyclopentane and *N*-cyclopentylmethyl-morpholine was obtained. The role of the LiCl is as a promotor to $\text{Ru}_3(\text{CO})_{12}$ to assist in the RWGS reaction to produce CO from CO_2 . However, due to its low solubility in toluene, not enough CO is available for hydroformylation and therefore significant hydrogenation of cyclopentene to cyclopentane is observed. Using a phase transfer catalyst (BTAC, benzyl triethyl ammonium chloride) improved the solubility of LiCl and by using 20/60 bar CO_2/H_2 , the amine could be synthesized selectively in 98 % yield. Following the successful optimization of the reaction conditions, the RWGS-HAM of other cyclic olefins (cyclohexene, cyclooctene), styrene, α -methylstyrene and 1-octene with morpholine was also studied.⁹⁵

Earlier, Eilbracht and co-workers showed that hydroaminomethylation can be used for the synthesis of diamines (Figure 1.36) and triamines from diallyl ethers, silanes and amines via the Rh(I) catalyzed hydroaminomethylation in almost quantitative yield.⁹⁶ However, in the case of diallylamines, the authors observed the formation of γ -lactams due to a hydrocarboxylation/hydroaminomethylation sequence (only the linear product is shown in Figure 1.36).⁹⁶

Chapter 1: Literature Review of Olefin Hydroformylation and Hydroaminomethylation

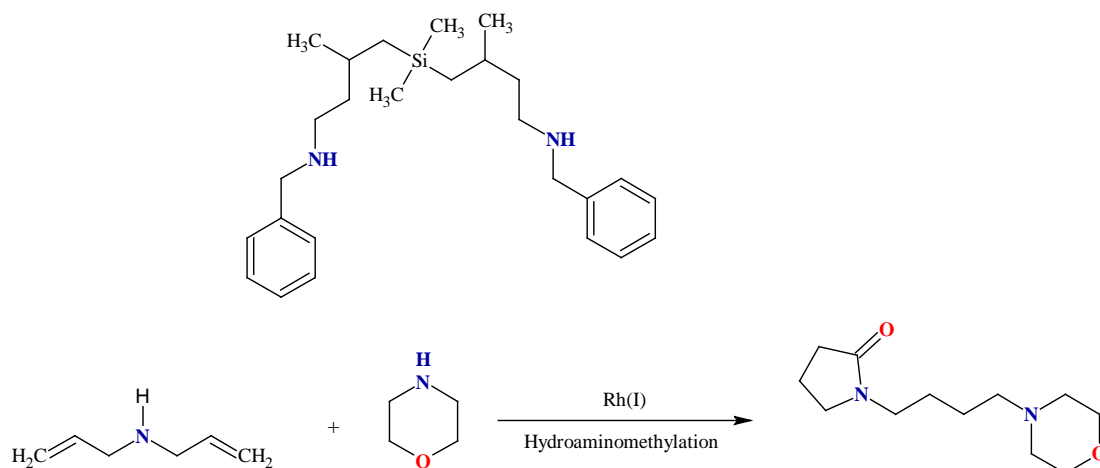


Figure 1.36: Product obtained from HAM of di-allyl silanes and benzylamine (top) and HAM of di-allyl amines and benzylamine⁹⁶

The pyrazole-based Rh(I) catalyst shown in Figure 1.37 was used in the hydroaminomethylation of 1-octene and diethylamine.⁹⁷ Another derivative of this complex was also synthesized by replacing one of the CO ligands with a PPh₃ ligand. Comparing the activities of these two complexes in the hydroaminomethylation reaction revealed that the PPh₃ containing catalyst produces much higher conversions of the olefin (95 % vs 67 % for the di-carbonyl complex), however, the di-carbonyl complex hydrogenate the enamines far more efficiently (85 % amine yield compared to 37 % for the PPh₃ containing catalyst). The activity differences was not further explained. However, in our opinion, the presence of the PPh₃ ligand probably creates a steric environment which hinders the coordination of the enamine and its subsequent hydrogenation.⁹⁷

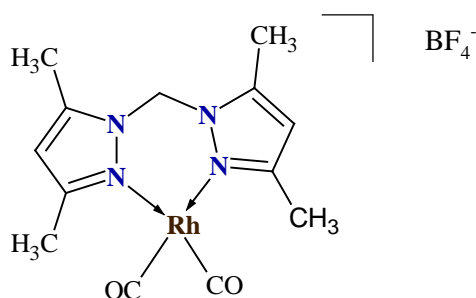


Figure 1.37: Pyrazole-based Rh(I) dicarbonyl complex used in the hydroaminomethylation of 1-octene with diethylamine⁹⁷

Alper and co-workers⁹⁸ used the zwitterionic Rh(I) complex, [Rh(COD)(η⁶-PhBPh₃)], to study the hydroaminomethylation of various vinyl arenes and aliphatic, cyclic and aromatic amines. Generally, the corresponding branched amine was regioselectively prepared in most cases, if the temperature is kept below 100 °C, with a yield of 91 % obtained for styrene and isopropylamine.⁹⁸

Chapter 1: Literature Review of Olefin Hydroformylation and Hydroaminomethylation

1.4.1 Synthesis of medicinal compounds via hydroaminomethylation

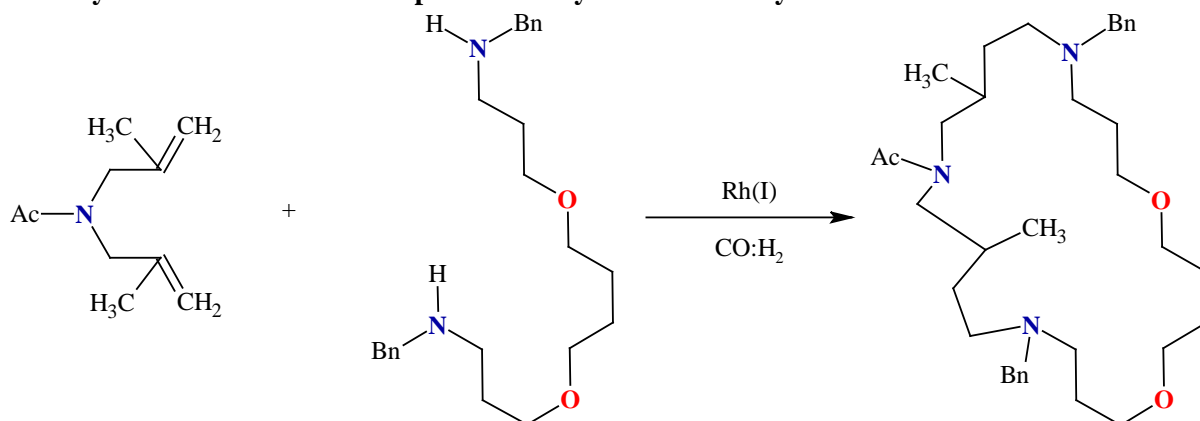


Figure 1.38: Synthesis of an azamacroheterocyclic ring⁹⁹

Hydroaminomethylation can be used to synthesize azamacroheterocyclic rings via the Rh(I)-catalysed hydroaminomethylation of dienes and α,ω -diamines as shown by Eilbracht and co-workers (Figure 1.38).⁹⁹ These azamacroheterocyclic rings have the ability to coordinate cations, anions or neutral compounds and as result are highly applicable in medicine. Using either $[\text{Rh}(\text{COD})\text{Cl}]_2$ or $[\text{Rh}(\text{acac})(\text{CO})_2]$ in the absence of additional ligands, azamacroheterocyclic compounds with rings ranging from 13-36 members were synthesized in low to moderate yields (19-51 %). Mixing equimolar of either LiBr, KI, CsI or RbI with the azamacroheterocycle shown in Figure 1.38, revealed selectivity towards Rb^+ as confirmed by ^{13}C and ^{87}Rb NMR spectroscopy.⁹⁹ Cleavage of the benzyl groups using Pd/C in the presence of H_2 , generate a debenzylated macroheterocyclic system containing secondary amines. Further ring-closing hydroaminomethylation of a diene with this secondary amine provides access to cryptands.¹⁰⁰

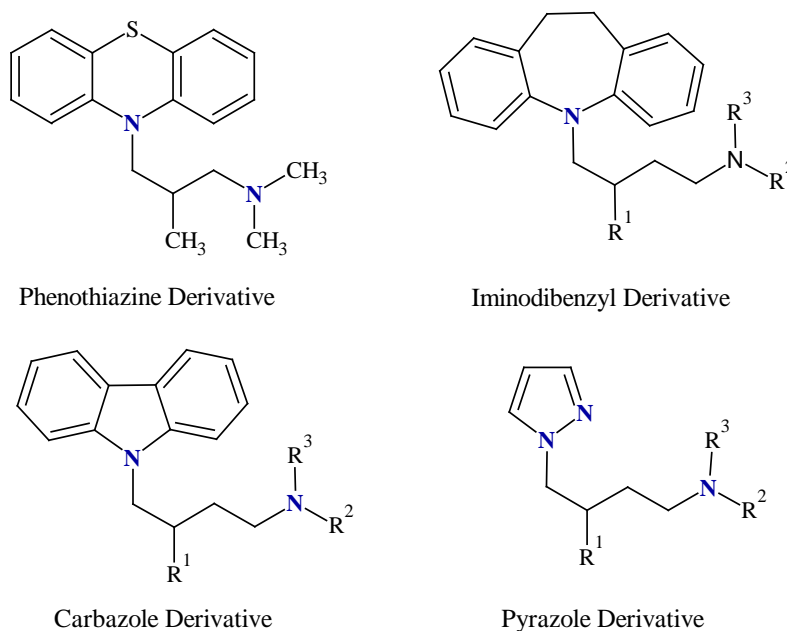


Figure 1.39: Pharmacologically active amines¹⁰¹

Chapter 1: Literature Review of Olefin Hydroformylation and Hydroaminomethylation

Similarly, pharmacologically active derivatives of phenothiazine, iminodibenzyl, carbazole and pyrazole can be synthesized via the Rh(I)-catalysed hydroaminomethylation of *N*-allylic or *N*-methallylic compounds with either primary or secondary amines (Figure 1.39). The authors showed that the reaction is well tolerated towards both aromatic and aliphatic amines.¹⁰¹

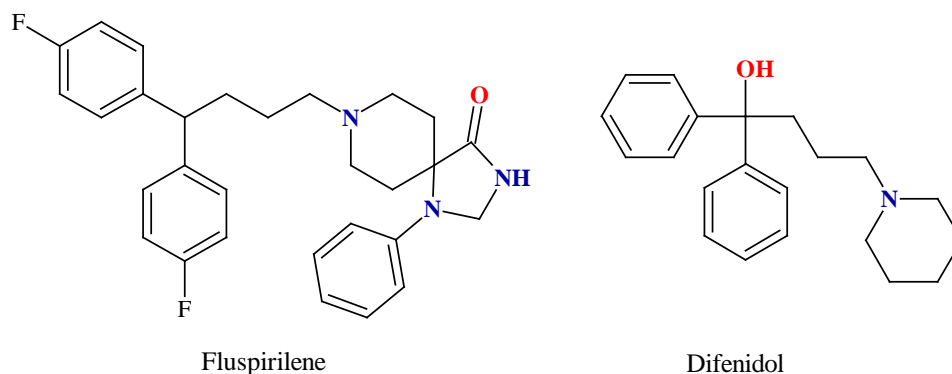


Figure 1.40: Fluspirilene and difenidol¹⁰²

The antihistaminic drug difenidol (Figure 1.40) and the antipsychotic drug fluspirilene (Figure 1.40) can be prepared in a facile manner by employing a Rh(I)-catalysed hydroaminomethylation reaction.¹⁰² The synthesis of these drugs normally entails substitution reactions between the amine and the corresponding diaryl-halide derivatives. The synthesis of these drugs commence with a Grignard reaction between either substituted (in the case of fluspirilene) or unsubstituted diaryl ketones and vinyl magnesium chloride to produce 1,1-diaryl-2-propen-1-ol which then undergoes hydroaminomethylation with the appropriate amine (piperidine in the case of difenidol and 1-phenyl-1,3,8-triazaspiro[4,5]decan-4-one in the case of fluspirilene). Removal of the OH group under acidic and hydrogenating conditions allows for the quantitative preparation of fluspirilene in four steps from commercially available starting materials.¹⁰²

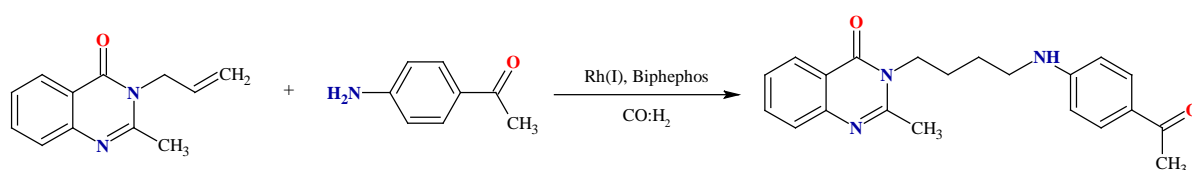


Figure 1.41: Synthesis of quinazolinones¹⁰³

The hydroaminomethylation of 3-allyl-2-methylquinazolin-4(3*H*)-one and amines such as 4-aminoacetophenone produces 3-substituted quinazolinones which serves as precursors towards the preparation of compounds containing chalcones and pyrazole moieties (Figure 1.41).¹⁰³ The reaction of these chalcones with hydrazine produces pyrazoloquinazolinones with important biological and pharmaceutical activities.¹⁰³

Alper and co-workers demonstrated the synthesis of 1,2,3,4-tetrahydroquinolines (Figure 1.42) from 2-isopropenylanilines derivatives via Rh(I)-catalyzed hydroaminomethylation.¹⁰⁴ They later expanded

Chapter 1: Literature Review of Olefin Hydroformylation and Hydroaminomethylation

this procedure to the synthesis of 1- and 2-benzazepines using the two ionic diamine rhodium complexes shown in Figure 1.42.¹⁰⁵⁻¹⁰⁶

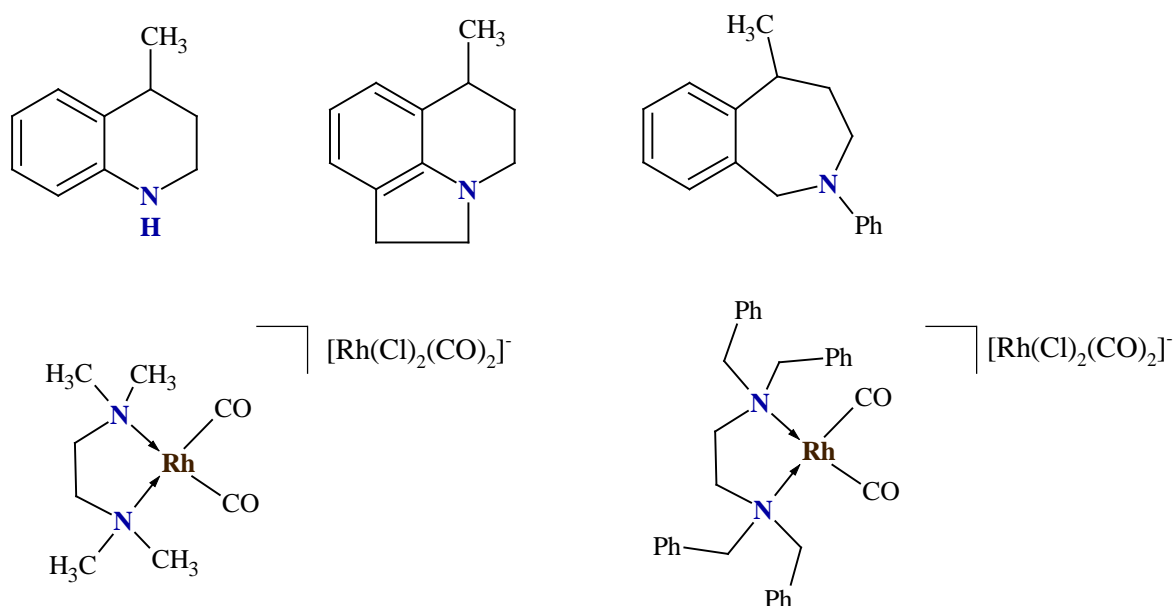


Figure 1.42: 1,2,3,4-tetrahydroquinolines and the two ionic diamine rhodium complexes¹⁰⁵⁻¹⁰⁶

The hydroaminomethylation of 1,1-diphenylethene and secondary amines can lead to a variety of interesting pharmacologically active drugs (Figure 1.43). In combination with piperidine, fenpiprane can be prepared which is a drug used for the treatment of functional gastrointestinal disorders. Reaction with diisopropylamine and azepane produces diisoproamine and prozapine respectively (choleric agents).¹⁰⁷⁻¹⁰⁸

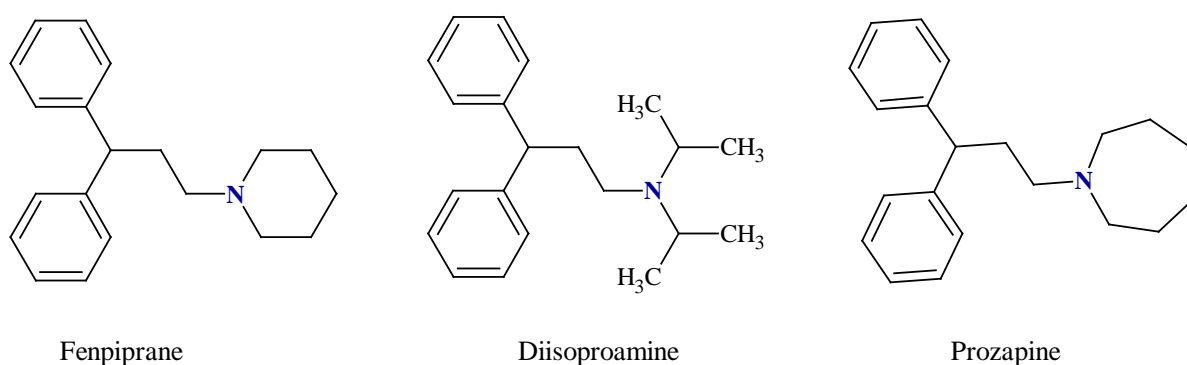


Figure 1.43: Fenpiprane, diisoproamine and prozapine¹⁰⁷⁻¹⁰⁸

Zhang and co-workers also studied the intramolecular hydroaminomethylation of (E)-*N*-benzylcinnamylamine, however, this produced 4-aryl-2,3-dihydropyrroles.¹⁰⁹

In their quest to perform the total synthesis of the lycopodium alkaloid, lycoplamine H, Weinreb and Sacher made use of an intramolecular hydroaminomethylation reaction in order to perform the

Chapter 1: Literature Review of Olefin Hydroformylation and Hydroaminomethylation

annulation of the azocane moiety from the bicyclo[2.2.2]octane scaffold. They managed to perform this reaction in 75 % yield after initial reaction optimization.¹¹⁰

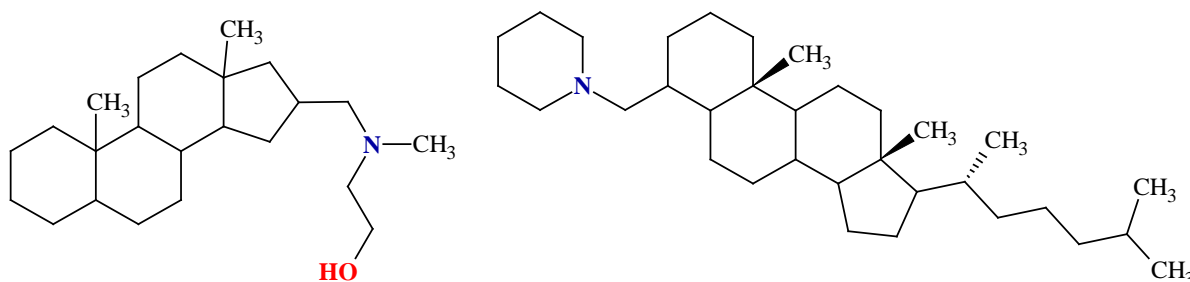


Figure 1.44: Amine containing steroid derivatives¹¹¹⁻¹¹²

The hydroaminomethylation of steroids with aminoalcohols can produce interesting amino containing steroid derivatives.¹¹¹⁻¹¹² Törös and co-workers¹¹¹ were specifically interested in studying the hydroaminomethylation of 3 β -hydroxy-5 α -androst-16-ene and various aminoalcohols, such as 2-(methylamino)ethanol, obtaining a yield of 78 % towards the target amine shown in Figure 1.44 (left). Various other aminoalcohols (4-aminophenol, 3-aminopropanol and 2-(propylamino)ethanol) could be studied, all proceeding with excellent yields (81-92 %) to the target amines.¹¹¹ In a study by Pereira and co-workers,¹¹² they prepared tertiary amines containing piperidyl and morpholyl moieties (Figure 1.44, right) due to the biological relevance of these molecules. Both these amines could be prepared in 59 and 51 % isolated yields.

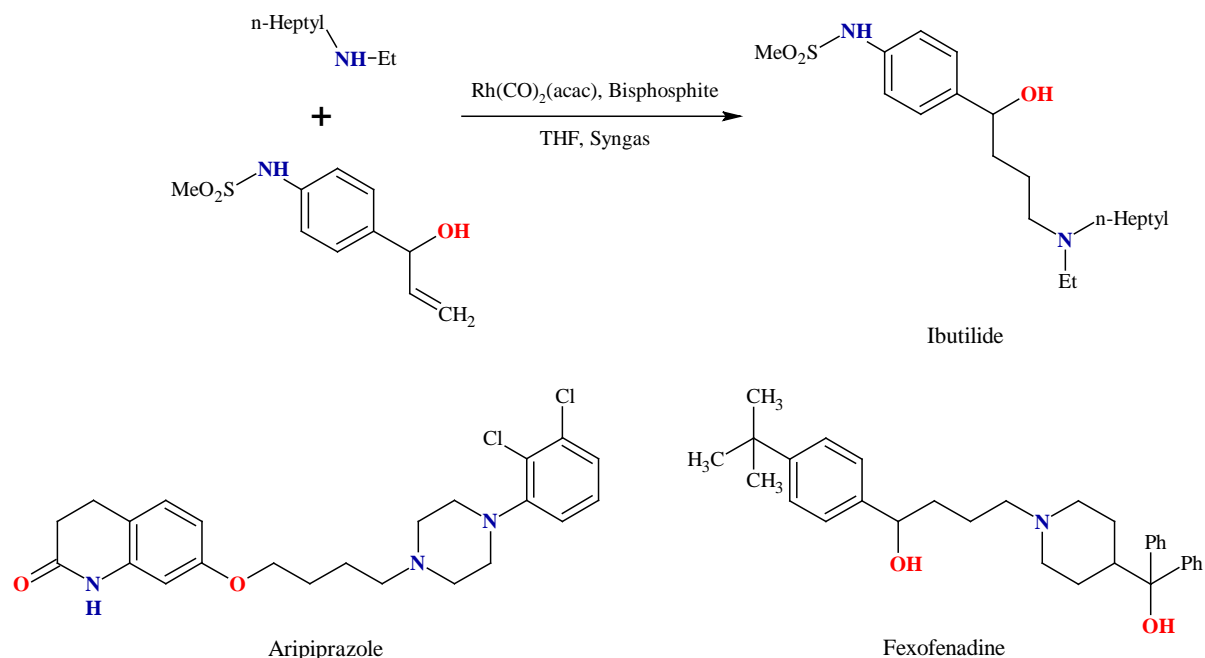


Figure 1.45: Synthesis of Ibutilide¹¹³

The synthesis of ibutilide, an anti-arrhythmia drug, was described by Whiteker and co-workers (Figure 1.45). This drug was isolated in 55 % yield using 1 mol% catalyst loading. This reaction

Chapter 1: Literature Review of Olefin Hydroformylation and Hydroaminomethylation

required the presence of a bisphosphite ligand to ensure high linear regioselectivity. Employing this same methodology, the antidepressant, aripiprazole, was isolated in 67 % yield from its corresponding precursors.¹¹³ Similarly, the antihistamine, fexofenadine, can also be synthesized via hydroaminomethylation using this same catalyst system.¹¹⁴

1.4.2 Synthesis of polymers and surfactants via hydroaminomethylation

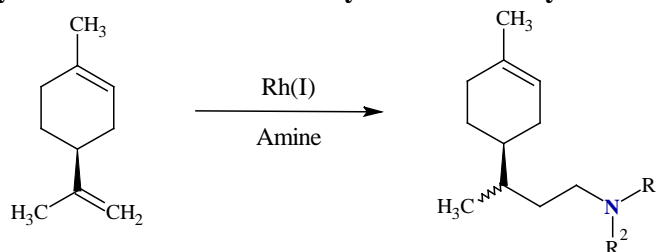


Figure 1.46: Hydroaminomethylation of limonene with amines¹¹⁵⁻¹¹⁶

The hydroaminomethylation of terpenes, such as limonene, can provide access to products important in the natural product and polymer industry (Figure 1.46). Da Rosa and co-workers¹¹⁵ studied the hydroaminomethylation of R(+)-limonene and various primary and secondary amines. R(+)-limonene has two double bonds which can potentially be transformed, however, due to the low reactivity of the cyclic double bond, transformation exclusively occurs at the aliphatic double bond. Furthermore, due to the steric hindrance of the isopropenyl moiety, only *n*-products were formed.¹¹⁵ In 2015, Behr and Wintzer studied the hydroaminomethylation of limonene with ammonia for the synthesis of primary amines which are intermediates in the synthesis of polyisocyanates. The latter are precursors to polyurethane polymers.¹¹⁶

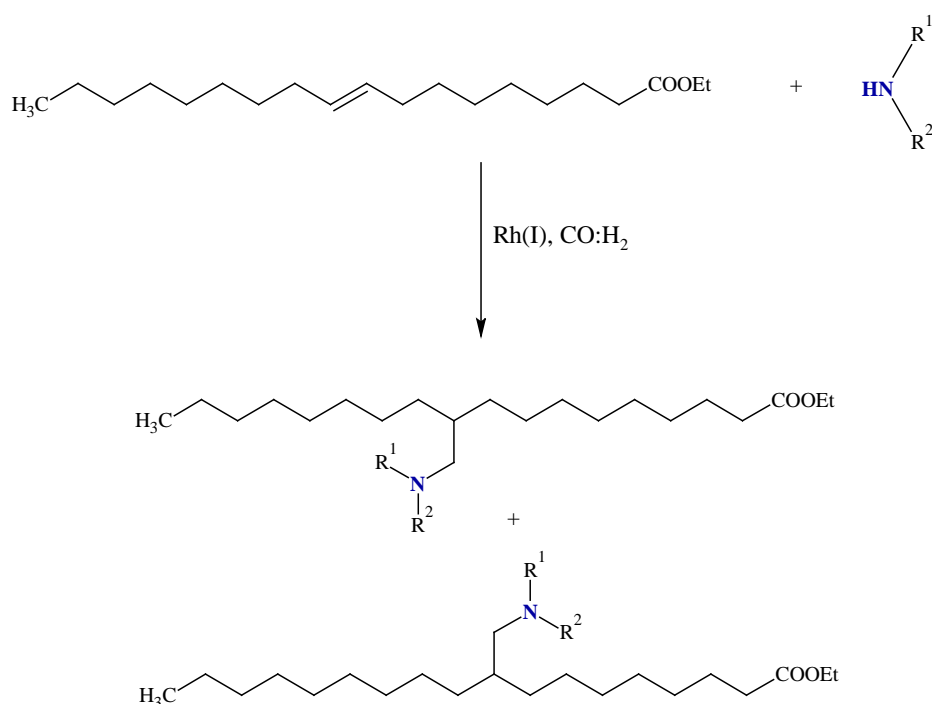


Figure 1.47: Hydroaminomethylation of oleic acid ethyl ester¹¹⁷

Chapter 1: Literature Review of Olefin Hydroformylation and Hydroaminomethylation

The hydroaminomethylation of oleochemicals and amines (1° or 2°) produces branched fatty acid derivatives with many industrial applications, especially in the surfactant industry (Figure 1.47). In this regard, Behr *et al.* was specifically interested in the hydroaminomethylation of oleic acid ethyl esters with a range of primary (hexylamine, benzylamine, aspartic acid ethyl ester and valinol) and secondary (morpholine) amines.¹¹⁷ The use of primary amines allowed them to link two molecules of oleic acid, with the amine as a bridge. These authors have also employed L-proline as an amine source. This produced di-ester monomers which is precursors towards biopolymers.¹¹⁸

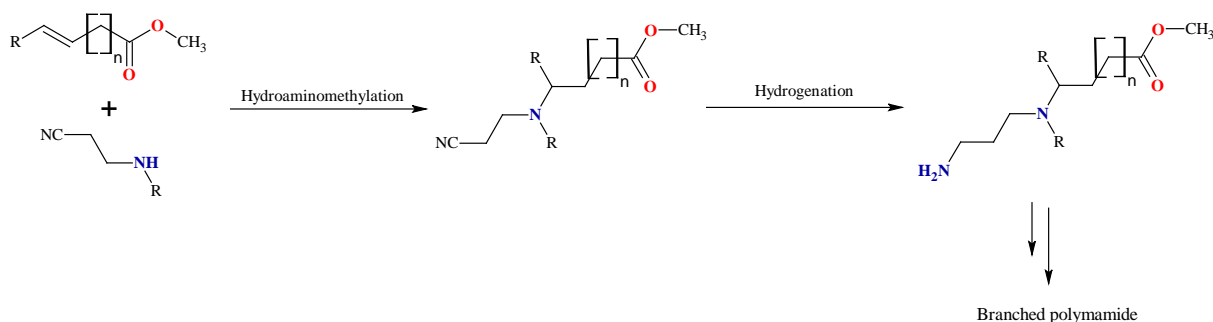


Figure 1.48: Synthesis of branched polyamide monomer¹¹⁹

Recently, they shifted their attention towards the preparation of branched polyamide polymers, with the monomer shown in Figure 1.48.¹¹⁹ For this purpose, they used functionalized amino-nitrile together with methyl oleate as starting materials.

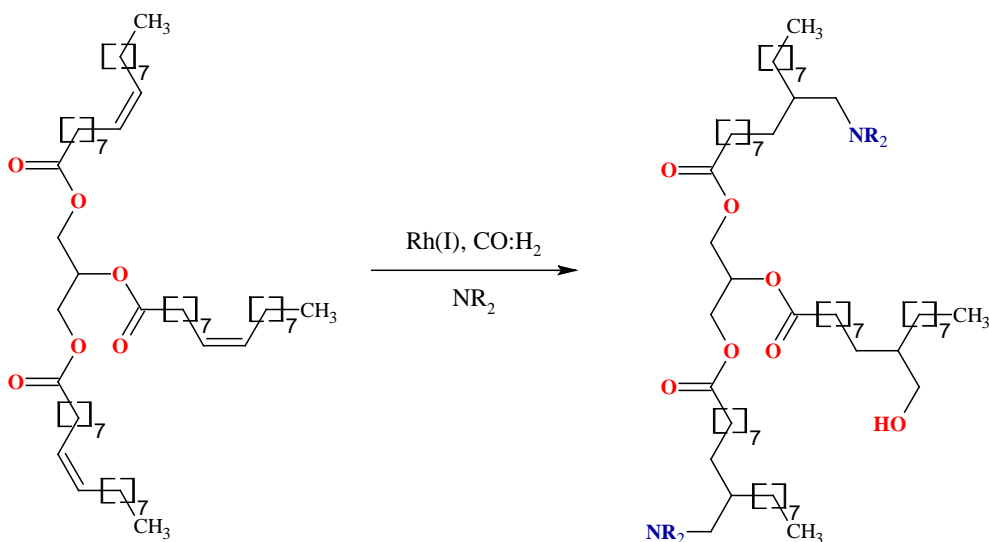


Figure 1.49: Synthesis of aminohydroxytriglycerides via hydroaminomethylation and hydrogenation of aldehyde moieties¹²⁰

Hapiot and co-workers¹²⁰ combined HAM with hydrohydroxymethylation in order to synthesize aminohydroxytriglycerides where they found that by careful control of the reaction conditions, they can control the proportion of aminomethyl and hydroxymethyl groups which is grafted on the triglyceride fatty chains (Figure 1.49). These aminohydroxyglycerides are also precursors to polymers.¹²⁰

Chapter 1: Literature Review of Olefin Hydroformylation and Hydroaminomethylation

1.5 Concluding Remarks and Project Objectives

Amines are useful compounds for various applications. These applications include pharmaceuticals, cosmetics and polymers, to name a few. Via reductive amination and hydroaminomethylation, amines can be synthesized in a facile manner in high yields. Since only water is formed in this process, isolation of the amines is relatively easy.

Reductive amination are in most cases mediated by either Ir, Ru and Rh catalysts. However, Ir and Ru are not as efficient in mediating the hydroaminomethylation reaction compared to Rh-based catalysts. All of the examples that were discussed above involved Rh-based catalysts, attesting to its high activity in this process.

Phosphine-based rhodium catalysts dominate in mediating this reaction. This is as a result of their ability to control the chemo- and regioselectivity of the initial hydroformylation reaction. However, some phosphine ligands are prone to oxidation in air which limits their recycling and reusability. Therefore, alternative ligand systems are still been investigated even though phosphine-based rhodium catalysts are so successful in mediating this process.

The use of non-phosphine based rhodium catalysts in the hydroaminomethylation reaction is fairly scarce. Therefore, we have decided to synthesize a few rhodium iminopyridine complexes and evaluate them as catalyst precursors in the hydroaminomethylation of olefins and amines. To the best of our knowledge, rhodium iminopyridine complexes have not been evaluated in this transformation before. Thus, the objectives of this project entails:

- 1) The synthesis and characterization of iminopyridine ligands followed by their complexation to Rh(I) and Ru(II).
- 2) Evaluation of the Rh(I) complexes in the hydroformylation of 1-octene. Investigating the influence of temperature, pressure and reaction time on the conversion of the substrate as well as the chemo- and regioselectivity.
- 3) Evaluate the Rh(I) and Ru(II) complexes in the hydroaminomethylation of 1-octene with both primary (aniline and benzylamine) and secondary amines (piperidine). Investigating the influence of temperature, pressure (total as well as partial pressure of CO and H₂) and reaction time on the conversion of the substrate as well as the chemo- and regioselectivity.
- 4) The synthesis of surfactants, polymer precursors and primary amines via hydroaminomethylation.

Chapter 1: Literature Review of Olefin Hydroformylation and Hydroaminomethylation

1.6 Overview of thesis

Chapter 2 contains the synthesis and characterization of the Rh(I) and the Ru(II) complexes. These complexes were fully characterized using a range of analytical techniques, including IR and NMR (^1H and ^{13}C) spectroscopy, mass spectrometry, elemental analysis and melting point.

In **Chapter 3**, the hydroformylation of 1-octene using the Rh(I) complexes is discussed. The influence of temperature, pressure and reaction time is investigated. We further evaluated the potential of formaldehyde as a syngas surrogate and the results are discussed.

In **Chapter 4**, the hydroaminomethylation of 1-octene with piperidine, aniline and benzylamine are discussed. We evaluated different catalysts and compared the activity to $\text{HRhCO}(\text{PPh}_3)_3$. The influence of temperature, reaction time, olefin:amine ratio and pressure were also investigated. Comparison between aniline and benzylamine are also discussed. The Ru(II) complexes were also tested in the hydroaminomethylation of 1-octene and benzylamine and the activity compared to the rhodium-based catalysts.

Chapter 5 deals with the synthesis of surfactants, polymer precursors and primary amines. The hydroaminomethylation of 1-octene and amino acids methyl esters (proline and piperidine-carboxylic acid) are performed. Base-mediated saponification provides access to the surfactants. The Critical Micelle Concentrations (CMCs) of these surfactants are also discussed. Furthermore, di-carboxylic acid compounds are also synthesized via hydroaminomethylation and ester hydrolysis (from methyl 10-undecenoate and the amino acid methyl esters mentioned above). Moreover, the synthesis of primary amines via hydroaminomethylation and palladium catalyzed debenzoylation are also discussed.

1.7 References

1. J. Pospech, I. Fleischer, R. Franke, S. Buchholz and M. Beller, *Angew. Chem. Int. Ed.*, 2013, **52**, 2852-2872.
2. M. Beller, B. Cornils, C. D. Frohning and C. W. Kohlpaintner, *J. Mol. Catal. A: Chem.*, 1995, **104**, 17-85.
3. L. H. Slaugh and R. D. Mullineaux, *J. Organomet. Chem.*, 1968, **13**, 469-477.
4. (a) F. H. Jardine, J. A. Osborn, G. Wilkinson and J. F. Young, *Chem. and Ind. (London)*, 1965, 560. (b) D. Evans, J. A. Osborn and G. Wilkinson. *J. Chem. Soc. A.*, 1968, 3133.
5. M. Rosales, H. Pérez, F. Arrieta, R. Izquierdo, C. Moratinos and P. J. Baricelli, *J. Mol. Catal. A: Chem.*, 2016, **421**, 122-130.
6. M. Uhlemann, S. Doerfelt and A. Börner, *Tetrahedron Lett.*, 2013, **54**, 2209-2211.
7. G. Makado, T. Morimoto, Y. Sugimoto, K. Tsutsumi, N. Kagawa and K. Kakiuchi, *Adv. Synth. Catal.*, 2010, **352**, 299-304.
8. E. Cini, E. Airiau, N. Girard, A. Mann, J. Salvadori and M. Taddei, *Synlett.*, 2011, **2**, 199-202.

Chapter 1: Literature Review of Olefin Hydroformylation and Hydroaminomethylation

9. J. A. Fuentes, R. Pittaway and M. L. Clarke, *Chem. Eur. J.*, 2015, **21**, 10645-10649.
10. T. Morimoto, T. Fujii, K. Miyoshi, G. Makado, H. Tanimoto, Y. Nishiyama and K. Kakiuchi, *Org. Biomol. Chem.*, 2015, **13**, 4632-4636.
11. A. F. Abdel-Magid, K. G. Carson, B. D. Harris, C. A. Maryanoff and R. D. Shah, *J. Org. Chem.*, 1996, **61**, 3849-3862.
12. R. Ma, L. He, Q. Song, Y. Zhou and K. Liu, *RSC Adv.*, 2014, **4**, 11867-11871.
13. B. Villa-Marcos, W. Tang, X. Wu and J. Xiao, *Org. Biomol. Chem.*, 2013, **11**, 6934-6939.
14. W. Tang, S. Johnston, C. Li, J. A. Iggo, J. Bacsa and J. Xiao, *Chem. Eur. J.*, 2013, **19**, 14187-14193.
15. W. Tang, C. Lau, X. Wu and J. Xiao, *Synlett.*, 2014, **25**, 81-84.
16. G. Hou, J. Xie, P. Yan and Q. Zhou, *J. Am. Chem. Soc.*, 2009, **131**, 1366-1367.
17. P. Yan, J. Xie, G. Hou, L. Wang and Q. Zhou, *Adv. Synth. Catal.*, 2009, **351**, 3243-3250.
18. J. Xie, P. Yan, Q. Zhang, K. Yuan and Q. Zhou, *ACS Catal.*, 2012, **2**, 561-564.
19. N. Mršić, L. Panella, A. J. Minnaard, B. L. Feringa and J. G. de Vries, *Tetrahedron: Asymmetry*, 2011, **22**, 36-39.
20. G. Hou, R. Tao, Y. Sun, Z. Zhang and F. Gosselin, *J. Am. Chem. Soc.*, 2010, **132**, 2124-2125.
21. D. Kong, M. Li, G. Zi, G. Hou and Y. He, *J. Org. Chem.*, 2016, **81**, 6640-6648.
22. Y. Zhang, D. Kong, R. Wang and G. Hou, *Org. Biomol. Chem.*, 2017, **15**, 3006-3012.
23. Z. Han, Z. Wang, X. Zhang and K. Ding, *Tetrahedron: Asymmetry*, 2010, **21**, 1529-1533.
24. W. Lu, Y. Chen and X. Hou, *Adv. Synth. Catal.*, 2010, **352**, 103-107.
25. P. Cheruku, T. L. Church, A. Trifonova, T. Wartmann and P. G. Andersson, *Tetrahedron Lett.*, 2008, **49**, 7290-7293.
26. A. Baeza and A. Pfaltz, *Chem. Eur. J.*, 2009, **15**, 2266-2269.
27. A. Baeza and A. Pfaltz, *Chem. Eur. J.*, 2010, **16**, 4003-4009.
28. X. Wang, D. Wang, S. Lu, C. Yu and Y. Zhou, *Tetrahedron: Asymmetry*, 2009, **29**, 1040-1045.
29. K. Gao, B. Wu, C. Yu, Q. Chen, Z. Ye and Y. Zhou, *Org. Lett.*, 2012, **14**, 3890-3893.
30. S. Gauthier, L. Larquetoux, M. Nicolas, T. Ayad, P. Maillos and V. Ratovelomanana-Vidal, *Synlett.*, 2014, **25**, 1606-1610.
31. M. Chang, W. Li, G. Hou and X. Zhang, *Adv. Synth. Catal.*, 2010, **352**, 3121-3125.
32. G. Hou, W. Li, M. Ma, X. Zhang and X. Zhang, *J. Am. Chem. Soc.*, 2010, **132**, 12844-12846.
33. S. Bähr and M. Oestreich, *Organometallics*, 2017, **36**, 935-943.
34. H. Hebbache, T. Jerphagnon, Z. Hank, C. Bruneau and J. Renaud, *J. Organomet. Chem.*, 2010, **695**, 870-874.
35. K. Matsumura, X. Zhang, K. Hori, T. Murayama, T. Ohmiya, H. Shimizu, T. Saito and N. Sayo, *Org. Process Res. Dev.*, 2011, **15**, 1130-1137.
36. H. Geng, X. Zhang, M. Chang, L. Zhou, W. Wu and X. Zhang, *Adv. Synth. Catal.*, 2011, **353**, 3039-3043.

Chapter 1: Literature Review of Olefin Hydroformylation and Hydroaminomethylation

37. I. Scodeller, A. Salvini, G. Manca, A. Ienco, L. Luconi and W. Oberhauser, *Inorg. Chim. Acta*, 2015, **431**, 242-247.
38. B. Vilhanová, J. Václavík, P. Šot, J. Pecháček, J. Zápál, R. Pažout, J. Maixner, M. Kuzma and P. Kačer, *Chem. Commun.*, 2016, **52**, 362-365.
39. F. Chen, Z. Ding, J. Qin, T. Wang, Y. He and Q. Fan, *Org. Lett.*, 2011, **13**, 4348-4351.
40. Z. Yang, Z. Ding, F. Chen, Y. He, N. Yang and Q. Fan, *Eur. J. Org. Chem.*, 2017, 1973-1977.
41. M. Vaquero, A. Suárez, S. Vargas, G. Bottari, E. Álvarez and A. Pizzano, *Chem. Eur. J.*, 2012, **18**, 15586-15591.
42. M. Hernández-Juárez, M. Vaquero, E. Álvarez, V. Salazar and A. Suárez, *Dalton Trans.*, 2013, **42**, 351-354.
43. Y. Hsiao, N. R. Rivera, T. Rosner, S. W. Krska, E. Njolito, F. Wang, Y. Sun, J. D. Armstrong, E. J. J. Grabowski, R. D. Tillyer, F. Spindler and C. Malan, *J. Am. Chem. Soc.*, 2004, **126**, 9918-9919.
44. K. B. Hansen, T. Rosner, M. Kubryk, P. G. Dormer and J. D. Armstrong, *Org. Lett.*, 2005, **7**, 4935-4938.
45. M. Kubryk and K. B. Hansen, *Tetrahedron: Asymmetry*, 2006, **17**, 205-209.
46. Y. J. Zhang, J. H. Park and S. Lee, *Tetrahedron: Asymmetry*, 2004, **15**, 2209-2212.
47. Q. Llopis, G. Guillamot, P. Phansavath and V. Ratovelomanana-Vidal, *Org. Lett.*, 2017, **19**, 6428-6431.
48. Q. Dai, W. Yang and X. Zhang, *Org. Lett.*, 2005, **7**, 5343-5345.
49. M. Zhou, Z. Xue, M. Cao, X. Dong and X. Zhang, *Org. Biomol. Chem.*, 2016, **14**, 4582-4584.
50. Q. Zhao, J. Wen, R. Tan, K. Huang, P. Metola, R. Wang, E. V. Anslyn and X. Zhang, *Angew. Chem. Int. Ed.*, 2014, **53**, 8467-8470.
51. P. Li, Y. Huang, X. Hu, X. Dong and X. Zhang, *Org. Lett.*, 2017, **19**, 3855-3858.
52. J. A. Fuentes, P. Wawrzyniak, G. J. Roff, M. Bühl and M. L. Clarke, *Catal. Sci. Technol.*, 2011, **1**, 431-436.
53. S. Tin, T. Fanjul and M. L. Clarke, *Beilstein J. Org. Chem.*, 2015, **11**, 622-627.
54. S. Tin, T. Fanjul and M. L. Clarke, *Catal. Sci. Technol.*, 2016, **6**, 677-680.
55. G. Hou, J. Xie, L. Wang and Q. Zhou, *J. Am. Chem. Soc.*, 2006, **128**, 11774-11775.
56. V. I. Tararov, R. Kadyrov, T. H. Riermeier, J. Holz and A. Börner, *Tetrahedron Lett.*, 2000, **41**, 2351-2355.
57. M. T. Reetz, G. Mehler and A. Meiswinkel, *Tetrahedron: Asymmetry*, 2004, **15**, 2165-2167.
58. Y. Sato, Y. Kayaki and T. Ikariya, *Organometallics*, 2016, **35**, 1257-1264.
59. V. R. Landaeta, B. K. Muñoz, M. Peruzzini, V. Herrera, C. Bianchini and R. A. Sánchez-Delgado, *Organometallics*, 2006, **25**, 403-409.
60. P. Marcazzan, C. Abu-Gnim, K. N. Seneviratne and B. R. James, *Inorg. Chem.*, 2004, **43**, 4820-4824.

Chapter 1: Literature Review of Olefin Hydroformylation and Hydroaminomethylation

61. A. Behr, M. Becker and S. Reyer, *Tetrahedron Lett.*, 2010, **51**, 2438-2441.
62. Y. Y. Wang, M. M. Luo, Y. Z. Li, H. Chen and X. J. Li, *Appl. Catal., A.*, 2004, **272**, 151-155.
63. K. Li, Y. Wang, Y. Xu, W. Li, M. Niu, J. Jiang and Z. Jin, *Catal. Commun.*, 2013, **34**, 73-77.
64. B. Gall, M. Bortenschlager, O. Nuyken and R. Weberskirch, *Macromol. Chem. Phys.*, 2008, **209**, 1152-1159.
65. Y. Wang, M. Luo, Q. Lin, H. Chen and X. Li, *Green Chem.*, 2006, **8**, 545-548.
66. Y. Wang, J. Chen, M. Luo, H. Chen and X. Li, *Catal. Commun.*, 2006, **7**, 979-981.
67. B. Hamers, P. S. Bäuerlein, C. Müller and D. Vogt, *Adv. Synth. Catal.*, 2008, **350**, 332-342.
68. A. Behr and R. Roll, *J. Mol. Catal. A: Chem.*, 2005, **239**, 180-184.
69. T. Seidensticker, J. M. Vosberg, K. A. Ostrowski and A. J. Vorholt, *Adv. Synth. Catal.*, 2016, **358**, 610-612.
70. A. Behr, D. Levikov and E. Nürenberg, *RSC Adv.*, 2015, **5**, 60667-60673.
71. S. Fuchs, M. Steffen, A. Dobrowolski, T. Rösler, L. Johnen, G. Meier, H. Strutz, A. Behr and A. J. Vorholt, *Catal. Sci. Technol.*, 2017, **7**, 5120-5127.
72. S. Fuchs, T. Rösler, B. Grabe, A. Kampwerth, G. Meier, H. Strutz, A. Behr and A. J. Vorholt, *Appl. Catal., A.*, 2018, **550**, 198-205.
73. L. Routaboul, C. Buch, H. Klein, R. Jackstell and M. Beller, *Tetrahedron Lett.*, 2005, **46**, 7401-7405.
74. B. Zimmermann, J. Herwig and M. Beller, *Angew. Chem. Int. Ed.*, 1999, **38**, 2372-2375.
75. H. Klein, R. Jackstell, M. Kant, A. Martin and M. Beller, *Chem. Eng. Technol.*, 2007, **30**, 721-725.
76. M. Ahmed, R. P. J. Bronger, R. Jackstell, P. C. J. Kamer, P. W. N. M. van Leeuwen and M. Beller, *Chem. Eur. J.*, 2006, **12**, 8979-8988.
77. J. Liu, C. Kubis, R. Franke, R. Jackstell and M. Beller, *ACS Catal.*, 2016, **6**, 907-912.
78. A. M. Seayad, K. Selvakumar, M. Ahmed and M. Beller, *Tetrahedron Lett.*, 2003, **44**, 1679-1683.
79. B. Dutta, R. Schwarz, S. Omar, S. Natour and R. Abu-Reziq, *Eur. J. Org. Chem.*, 2015, 1961-1969.
80. M. Ahmed, A. M. Seayad, R. Jackstell and M. Beller, *Angew. Chem. Int. Ed.*, 2003, **42**, 5615-5619.
81. Y. Sun, M. Ahmed, R. Jackstell, M. Beller and W. R. Thiel, *Organometallics*, 2004, **23**, 5260-5267.
82. S. Gülak, L. Wu, Q. Liu, R. Franke, R. Jackstell and M. Beller, *Angew. Chem. Int. Ed.*, 2014, **53**, 7320-7323.
83. G. Liu, K. Huang, B. Cao, M. Chang, S. Li, S. Yu, L. Zhou, W. Wu and X. Zhang, *Org. Lett.*, 2012, **14**, 102-105.
84. S. Li, K. Huang, J. Zhang, W. Wu and X. Zhang, *Org. Lett.*, 2013, **15**, 3078-3081.

Chapter 1: Literature Review of Olefin Hydroformylation and Hydroaminomethylation

85. G. Liu, Z. Li, H. Geng and X. Zhang, *Catal. Sci. Technol.*, 2014, **4**, 917-921.
86. C. Chen, S. Jin, Z. Zhang, B. Wei, H. Wang, K. Zhang, H. Lv, X. Dong and X. Zhang, *J. Am. Chem. Soc.*, 2016, **138**, 9017-9020.
87. E. A. Karakhanov, E. A. Runova, Y. S. Kardasheva, D. V. Losev, A. L. Maksimov and M. V. Terenina, *Petrol. Chem.*, 2012, **52**, 204-210.
88. M. J. Schneider, M. Lijewski, R. Woelfel, M. Haumann and P. Wasserscheid, *Angew. Chem. Int. Ed.*, 2013, **52**, 6996-6999.
89. J. Meng, X. Li and Z. Han, *Org. Lett.*, 2017, **19**, 1076-1079.
90. I. D. Kostas, *J. Chem. Research*, 1999, 630-631.
91. E. Karakhanov, A. Maksimov, Y. Kardasheva, E. Runova, R. Zakharov, M. Terenina, C. Kenneally and V. Arredondo, *Catal. Sci. Technol.*, 2014, **4**, 540-547.
92. S. R. Khan, M. V. Khedkar, Z. S. Qureshi, D. B. Bagal and B. M. Bhanage, *Catal. Commun.*, 2011, **5**, 141-145.
93. S. Khan and B. M. Bhanage, *Appl. Organometal. Chem.*, 2013, **27**, 711-715.
94. Z. Nairoukh and J. Blum, *J. Org. Chem.*, 2014, **79**, 2397-2403.
95. V. K. Srivastava and P. Eilbracht, *Catal. Commun.*, 2009, **10**, 1791-1795.
96. P. Eilbracht, C. L. Kranemann and L. Bärfacker, *Eur. J. Org. Chem.*, 1999, 1907-1914.
97. E. Teuma, M. Loy, C. Le Berre, M. Etienne, J. Daran and P. Kalck, *Organometallics*, 2003, **22**, 5261-5267.
98. Y. Lin, B. E. Ali and H. Alper, *Tetrahedron Lett.*, 2001, **42**, 2423-2425.
99. C. L. Kranemann, B. Costisella and P. Eilbracht, *Tetrahedron Lett.*, 1999, **40**, 7773-7776.
100. C. L. Kranemann and P. Eilbracht, *Eur. J. Org. Chem.*, 2000, 2367-2377.
101. T. Rische, K. Müller and P. Eilbracht, *Tetrahedron*, 1999, **55**, 9801-9816.
102. A. Schmidt, M. Marchetti and P. Eilbracht, *Tetrahedron*, 2004, **60**, 11487-11492.
103. Y. A. El-Badry, A. F. El-Faragy and P. Eilbracht, *Helv. Chim. Acta*, 2013, **96**, 1782-1792.
104. T. O. Vieira and H. Alper, *Chem. Commun.*, 2007, 2710-2711.
105. T. O. Vieira and H. Alper, *Org. Lett.*, 2008, **10**, 485-487.
106. K. Okuro and H. Alper, *Tetrahedron Lett.*, 2010, **51**, 4959-4961.
107. M. Ahmed, C. Buch, L. Routaboul, R. Jackstell, H. Klein, A. Spannenberg and M. Beller, *Chem. Eur. J.*, 2007, **13**, 1594-1601.
108. S. Li, K. Huang, J. Zhang, W. Wu and X. Zhang, *Org. Lett.*, 2013, **15**, 1036-1039.
109. Z. Zheng, B. Cao and X. Zhang, *Tetrahedron Lett.*, 2014, **55**, 4489-4491.
110. J. R. Sacher and S. M. Weinreb, *Org. Lett.*, 2012, **14**, 2172-2175.
111. E. Nagy, B. Heil and S. Töros, *J. Organomet. Chem.*, 1999, **586**, 101-105.
112. A. R. Almeida, R. M. B. Carrilho, A. F. Peixoto, A. R. Abreu, A. Silva and M. M. Pereira, *Tetrahedron*, 2017, **73**, 2389-2395.

Chapter 1: Literature Review of Olefin Hydroformylation and Hydroaminomethylation

113. J. R. Briggs, J. Klosin and G. T. Whiteker, *Org. Lett.*, 2005, **7**, 4795-4798.
114. G. T. Whiteker, *Top. Catal.*, 2010, **53**, 1025-1030.
115. C. S. Graebin, V. L. Eifler-Lima and R. G. da Rosa, *Catal. Commun.*, 2008, **9**, 1066-1070.
116. A. Behr and A. Wintzer, *Chem. Eng. Technol.*, 2015, **38**, 2299-2304.
117. A. Behr, M. Fiene, C. Buß and P. Eilbracht, *Eur. J. Lipid Sci. Technol.*, 2000, **102**, 467-471.
118. A. Behr, T. Seidensticker and A. J. Vorholt, *Eur. J. Lipid Sci. Technol.*, 2014, **116**, 477-485.
119. A. J. Vorholt, S. Immohr, K. A. Ostrowski, S. Fuchs and A. Behr, *Eur. J. Lipid Sci. Technol.*, 2017, **119**, 1600211.
120. T. Vanbésien, E. Monflier and F. Hapiot, *Green Chem.*, 2017, **19**, 1940-1948.

Chapter 2: Synthesis and Characterization of Novel Iminopyridyl Rh(I) and Ru(II) Complexes

2.1 Introduction

The condensation of aldehydes or ketones with amines in the Schiff base condensation reaction produces an imine moiety. This reaction is particularly popular in coordination chemistry due to the ability of these compounds to coordinate to metal ions.¹⁻³ Incorporation of a pyridyl moiety into the imine ligand architecture produces bidentate ligands which has the ability to potentially form more stable complexes than their monodentate counterparts. In this regard, a number of iminopyridyl ligands have been synthesized and subsequently complexed to various metal ions, including Rh and Ru.^{1,4} Stable complexes with Rh and Ru were formed, as previously shown by us.⁵⁻⁶ These complexes are particular useful in catalysis, while some of the Ru complexes have also been shown to exhibit anticancer properties.⁷⁻⁹ When these ligands are coordinated to Rh(III) $[\text{Rh}(\text{Cp}^*)(\text{Cl})_2]_2$ and Ru(II) $(\text{Ru}(\text{p-cymene})(\text{Cl})_2)_2$, complexes containing stereogenic metal centres are formed with potential applications in enantioselective catalysis.¹⁰

2.2 Synthesis and characterization of Rh(I) complexes

2.2.1 Synthesis of iminopyridyl ligands (L1-L5)

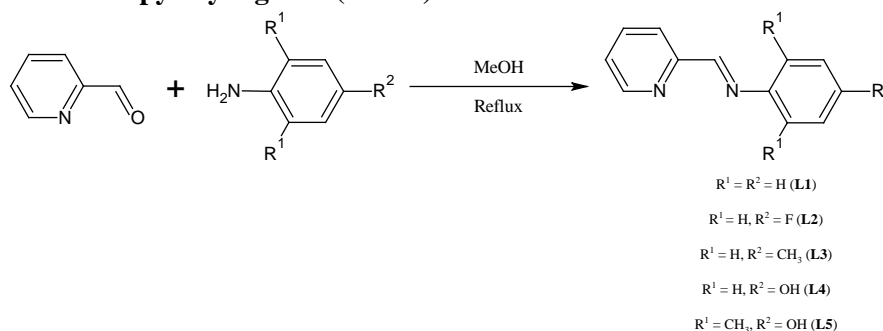


Figure 2.1: Synthesis of functionalized N-Phenyl-2-pyridylmethanimine ligands

L1-L4 are known ligands which were synthesized according to previously reported literature methods.¹¹⁻¹³ Adopting these literature methods allowed us to synthesize the novel ligand **L5**. **L5** was isolated as a yellow-brown solid in 84 % yield after recrystallization from hot EtOH. This ligand was found to be stable at room temperature and could be stored at room temperature for extended periods of time. It exhibits solubility in DMSO, acetone and MeOH while it is partially soluble in EtOH, MeCN and diethyl ether. **L5** was fully characterized using a range of analytical techniques including IR and NMR (¹H and ¹³C) spectroscopy, mass spectrometry, elemental analysis and melting point determination. Successful Schiff base condensation was confirmed via monitoring the disappearance of

Chapter 2: Synthesis and Characterization of Novel Iminopyridyl Rh(I) and Ru(II) Complexes

the carbonyl (C=O) moiety of the aldehyde and the appearance of a new imine (C=N) moiety in the ligand. In this regard, the absorbance at $\sim 1710\text{ cm}^{-1}$ disappeared with the formation of a new band at 1637 cm^{-1} due to the newly formed C=N bond.

In the ^1H NMR spectrum, shown in Figure 2.2, the newly formed H-C=N- proton resonated at 8.34 ppm, while the spectrum contained no aldehydic proton, further confirming the successful condensation of the aldehyde and the amine. The proton bonded to the carbon next to the pyridyl nitrogen is situated at 8.71 ppm, while the rest of the pyridyl protons can be observed between 7.42-8.30 ppm. The relatively large singlet at 6.55 ppm can be assigned to the protons of the phenyl group while the broad singlet at 6.75 ppm belongs to the OH group. Lastly, the singlet at 2.10 ppm is due to the methyl groups, integrating for 6 protons.

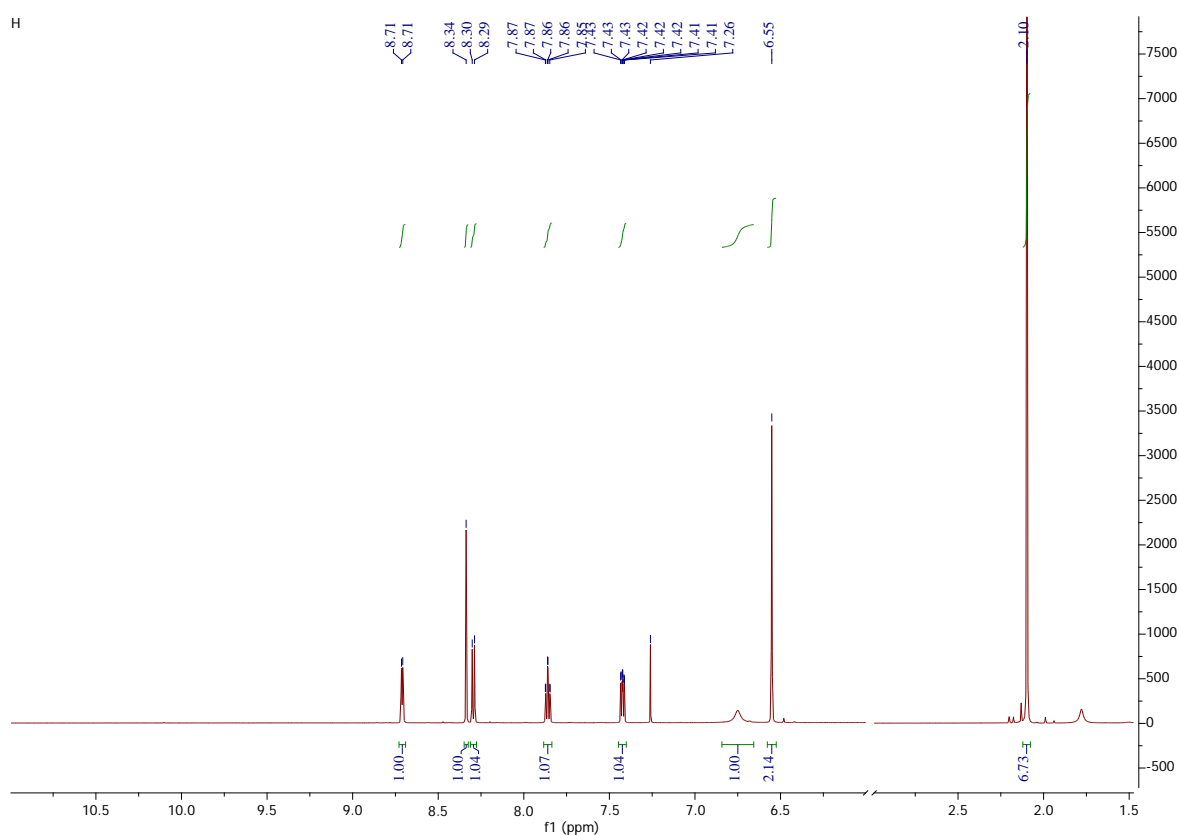


Figure 2.2: ^1H NMR spectrum of **L5**

^{13}C NMR spectroscopy further confirm the successful synthesis of **L5**. The signal for the imine carbon (H-C=N-) is located at 154.3 ppm. Eight other resonances are observed between 115.2-163.3 ppm assigned to the rest of the phenyl and pyridyl carbons while the resonance at 18.5 ppm is due to the methyl groups. In the ESI-MS spectrum of **L5**, the base peak appeared at m/z 227.12 which can be assigned to the molecular ion, $[\text{M}+\text{H}]^+$. Additionally, a sodium adduct ($[\text{M}+\text{Na}]^+$) was also observed at m/z 249.10. **L5** was further characterized via elemental analysis and melting point determination, with the results shown in Table 2.1.

Chapter 2: Synthesis and Characterization of Novel Iminopyridyl Rh(I) and Ru(II) Complexes

Table 2.1: ESI-MS, EA and melting point data for L5

Analytical technique	Characterization Data
ESI-MS	m/z 227.12 [M+H] ⁺ m/z 249.10 [M+Na] ⁺
EA Analysis	C ₁₄ H ₁₄ N ₂ O:0.2EtOH Theoretical C(73.45 %), H (6.51 %), N (11.90 %) Found C(73.37 %), H (6.49 %), N (12.35 %)
Melting point	179-181 °C

2.2.2 Synthesis of novel iminopyridyl Rh(I) complexes (C1-C5)

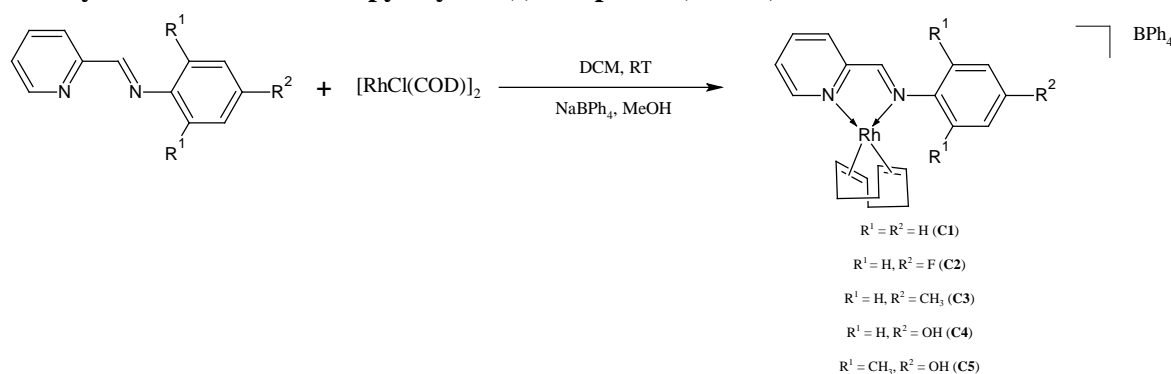


Figure 2.3: Synthesis of functionalized N-Phenyl-2-pyridylmethanimine Rh(I) complexes (C1-C5)

L1-L5 were then complexed to rhodium using the [Rh(COD)Cl]₂ dimer, prepared according to a literature procedure¹⁴, to produce five novel Rh(I) complexes. For the complexation, we employed a procedure we published previously.⁵ The ligands cleave the Rh-chloro bridges (-Rh-Cl-Rh-), of the dimeric precursor, producing a cationic complex with a chloride as counter-ion, which is subsequently exchanged for the larger tetraphenylborate anion [BPh₄]⁻ which is able to stabilise the complex more effectively. The synthesis of these complexes entails stirring the dimer in a DCM solution. Upon addition of the ligands, the yellow solution immediately turns black. This black solution is stirred for 1 h at room temperature, however, in the case of **C5**, a brown precipitate formed. The solvent was then removed, while in the case of **C5**, the precipitate was recovered via filtration. The residues were then dissolved in MeOH followed by the addition of NaBPh₄ as a solid, which immediately induce precipitation of the complexes. **C1-C5** were isolated in fair to high yields (65-85 %) as black (**C1-C2**) and brown solids (**C3-C5**). Stabilization of these complexes with the tetraphenylborate anion [BPh₄]⁻ ensured their air and moisture stability. In addition, the complexes could also be stored in the solid state for extended periods of time. All complexes are soluble in acetone, acetonitrile and dimethyl sulfoxide, while **C1**, **C3** and **C5** exhibits additional solubility in dichloromethane, chloroform and tetrahydrofuran. Since the characterization data (IR and NMR) are fairly similar for all the complexes, the discussion will be limited to **C5**.

Chapter 2: Synthesis and Characterization of Novel Iminopyridyl Rh(I) and Ru(II) Complexes

In order to confirm successful complexation of the ligands to the Rh(I) metal centre, changes in the C=N moieties (imine and pyridyl C=N) were monitored using IR and NMR (^1H and ^{13}C) spectroscopy. In the ligand (**L5**), the imine and pyridyl C=N moieties were observed at 1638 and 1586 cm^{-1} respectively. Upon complexation, the imine shifted to 1614 cm^{-1} while the pyridyl moiety shifted to slightly higher wavenumbers (1590 cm^{-1}) confirming coordination to the Rh(I) metal centre.

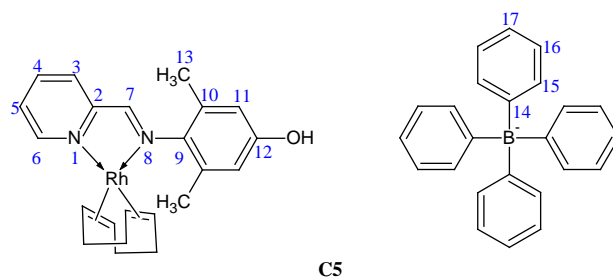


Figure 2.4: Numbering of **C5** for ^1H NMR analysis

In the ^1H NMR spectrum of **C5**, which is shown in Figure 2.5, the imine proton (H-C=N-) resonated at 8.47 ppm compared to 8.34 ppm in the ligand while the proton bonded to carbon-6 shifted from 8.71 ppm in the ligand to 8.09 ppm in **C5**. Furthermore, the spectrum of **C5** also shows the presence of the $[\text{BPh}_4]^-$ anion which shows resonances at 6.81, 6.94 and 7.36 ppm, integrating for a sum of 20 protons. The olefinic protons of the 1,5-cyclooctadiene ring are situated at 4.25 ppm while the aliphatic protons are at 2.53 and 2.90 ppm.

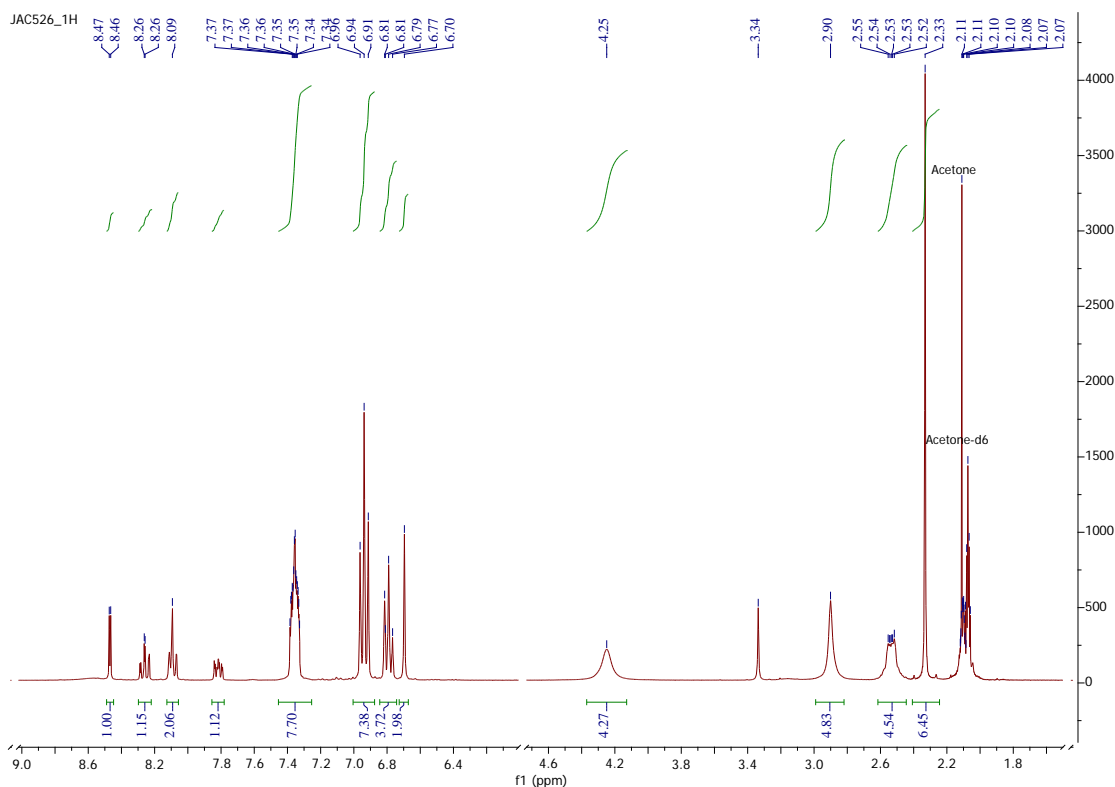


Figure 2.5: ^1H NMR spectrum of **C5** ran in Acetone- d_6

Chapter 2: Synthesis and Characterization of Novel Iminopyridyl Rh(I) and Ru(II) Complexes

Similarly, in the ^{13}C NMR spectrum of **C5**, the imine carbon (H-C=N-) shifted from 154.3 ppm in **L5** to 175.3 ppm in **C5**, while carbon-6 resonated at 154.8 ppm compared to 152.7 ppm in the ligand. Eight other resonances are observed between 114.9-156.4 ppm. These resonances belong to the phenyl moiety and the remaining pyridyl carbons. The olefinic carbons of the 1,5-cyclooctadiene ring shows two resonances at 87.14 and 87.31 ppm while the aliphatic carbons resonate at 30.1 ppm. A resonance at 17.7 ppm is observed which is due to the methyl groups.

In the ESI-MS spectrum of **C5**, the parent ion of the cation is observed at m/z 437.11. This peak is also the base peak in the spectrum. Further peaks are observed at m/z 211, 252.03 and 293.05 which are assigned to $[\text{Rh}(\text{COD})]^+$, $[\text{Rh}(\text{COD})(\text{MeCN})]^+$ and $[\text{Rh}(\text{COD})(\text{MeCN})_2]^+$ respectively. The peak at m/z 252.03 has a higher intensity than the other two peaks.

Table 2.2 shows the ESI-MS, elemental analysis and melting point data for all the complexes (**C1-C5**), confirming the successful preparation and characterization of these complexes.

Table 2.2: Characterization data for **C1-C5**

Complex	ESI-MS	EA	Melting point
C1	m/z 392.03 $[\text{M}]^+$	$\text{C}_{44}\text{H}_{42}\text{BN}_2\text{Rh}:0.5\text{DCM}$ Theoretical C(70.79 %), H (5.74 %), N (3.71 %) Found C(70.59 %), H (6.06 %), N (3.51 %)	Decomposition without melting at 172-174 °C
C2	m/z 410.02 $[\text{M}]^+$	$\text{C}_{44}\text{H}_{41}\text{BFN}_2\text{Rh}:0.25\text{DCM}$ Theoretical C(70.70 %), H (5.56 %), N (3.73 %) Found C(70.65 %), H (6.19 %), N (3.76 %)	167-169 °C
C3	m/z 406.09 $[\text{M}]^+$	$\text{C}_{45}\text{H}_{44}\text{BN}_2\text{Rh}$ Theoretical C(74.39 %), H (6.10 %), N (3.86 %) Found C(73.68 %), H (6.51 %), N (3.79 %)	121-123 °C
C4	m/z 409.10 $[\text{M}]^+$	$\text{C}_{44}\text{H}_{42}\text{BN}_2\text{ORh}$ Theoretical C(72.54 %), H (5.81 %), N (3.85 %) Found C(72.39 %), H (4.65 %), N (3.44 %)	146-148 °C
C5	m/z 437.11 $[\text{M}]^+$	$\text{C}_{46}\text{H}_{46}\text{BN}_2\text{ORh}:0.25\text{DCM}$ Theoretical C(71.42 %), H (6.03 %), N (3.60 %) Found C(71.31 %), H (6.67 %), N (3.54 %)	Decomposition without melting at 139-141 °C

Chapter 2: Synthesis and Characterization of Novel Iminopyridyl Rh(I) and Ru(II) Complexes

2.3 Synthesis and characterization of Ru(II) complexes

2.3.1 Synthesis of iminopyridyl ligands (L6-L8)

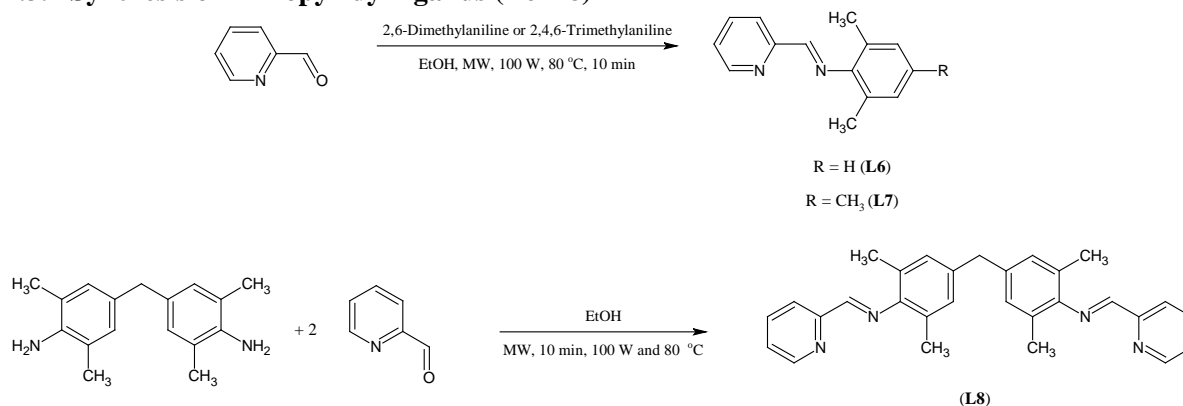
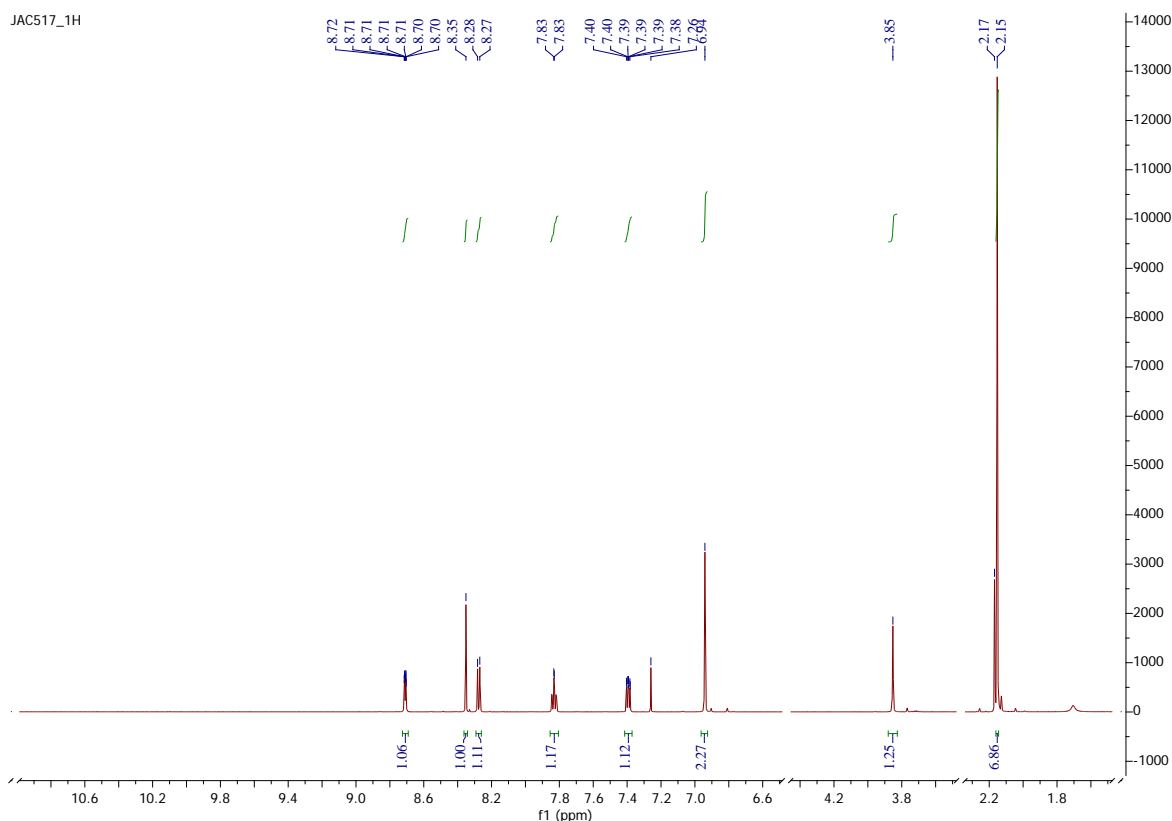


Figure 2.6: Synthesis of mono- and bifunctional iminopyridyl ligands

L6-L8 are known iminopyridyl ligands, however, the Ru(II) complex of **L8** is not known while **L6** and **L7** have been complexed to Ru(II) before, but were isolated as their PF₆⁻ salts.^{4,15} The reaction times for the preparation of these ligands using conventional methods are normally quite long.¹⁶⁻¹⁸ Therefore, here we present the facile synthesis of these ligands in 10 minutes using microwave dielectric heating.

Figure 2.7: ¹H NMR spectrum of **L8** ran in CDCl₃

L6 and **L7** were isolated as brown oils in 82-92 % yield after purification via vacuum distillation. **L8** was isolated as a mustard yellow solid in 82 % yield after recrystallization from EtOH. Characterization

Chapter 2: Synthesis and Characterization of Novel Iminopyridyl Rh(I) and Ru(II) Complexes

of **L6-L8** were performed using IR and NMR (^1H and ^{13}C) spectroscopy. **L8** will be discussed as a representative example.

Similarly as for the other iminopyridyl ligands discussed earlier, the aldehyde absorbance at $\sim 1710\text{ cm}^{-1}$ disappeared with the appearance of a new band at 1639 cm^{-1} due to the newly formed imine bond. In the ^1H NMR spectrum, shown in Figure 2.7, the imine proton resonated at 8.35 ppm with the absence of the aldehyde proton. The protons bonded to the pyridyl ring resonated between 7.39-8.71 ppm while the benzylidene protons are observed at 6.94 ppm. The protons due to the methylene group was observed at 3.85 ppm and those of the methyl groups at 2.15 ppm. ^{13}C NMR spectroscopy was used to further confirm the preparation of the ligands with all the data consistent with the literature.¹⁶⁻¹⁸

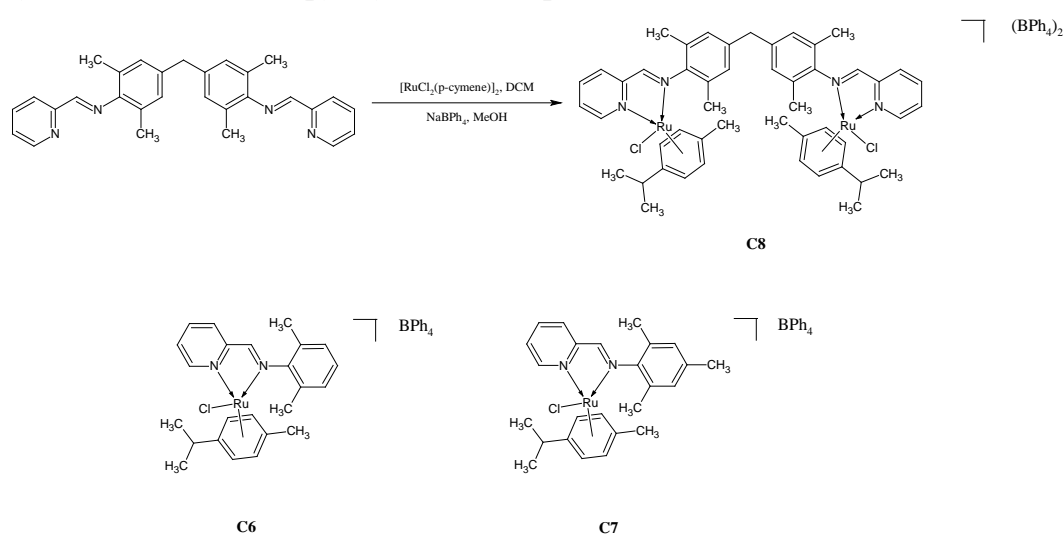
2.3.2 Synthesis of novel iminopyridyl Ru(II) complexes (**C6-C8**)

Figure 2.8: Synthesis of **C6-C8**

C6-C8 was synthesized using a similar procedure as for **C1-C5**, the only modification is that the ligands (**L6-L8**) were added as solutions due to their solubility in DCM. Therefore, $[\text{RuCl}_2(\text{p-cymene})]_2$ was dissolved in DCM forming a red-orange solution. Yellow solutions of the ligands (**L6-L8**) were then added and the resulting solutions stirred at room temperature for 1 h with no apparent colour changes occurring. After the allotted time, the solvent was removed and the red-orange residues dissolved in MeOH. Addition of NaBPh_4 as a solid produce immediate yellow precipitates for **C6-C8**. **C6** and **C8** were recrystallized from DCM:Hexane and DCM:Diethyl ether solutions respectively. In the case of **C6**, it was isolated as yellow-orange crystals in 84 % yield while **C7** and **C8** were isolated as yellow amorphous solids in 86 and 90 % yields respectively. The presence of the tetraphenylborate anion ensured their air and moisture stability of the complexes while they could also be stored for extended periods of time on the shelf. **C6** and **C8** were found to be soluble in DCM, acetone, THF, MeCN and DMSO while **C7** is only completely soluble in DMSO and partially soluble in the other aforementioned

Chapter 2: Synthesis and Characterization of Novel Iminopyridyl Rh(I) and Ru(II) Complexes

solvents. **C6-C7** were found to be temperature stable with the complexes only decomposing above 200 °C while **C8** decomposed between 169-171 °C.

The characterization of **C8** will be discussed as a representative example. **C6-C8** were fully characterized using a range of analytical techniques which includes IR and NMR (¹H and ¹³C) spectrometry, mass spectrometry, elemental analysis and melting point determinations. Similar trends in terms of the shift in the imine and the pyridyl C=N moieties were observed compared to the Rh(I) complexes discussed above. For the imine moiety, the band shifted from 1639 cm⁻¹ in the ligand to 1612 cm⁻¹ in the complex due to a change in the double-bond character of the imine upon coordination. The pyridyl C=N moiety shifted to 1598 cm⁻¹ from 1584 cm⁻¹ in the complex.

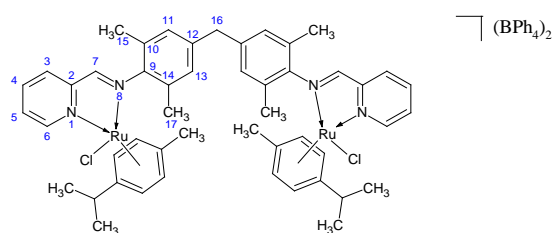


Figure 2.9: Numbering of **C8** for ¹H NMR analysis

Characterization via ¹H NMR spectroscopy, with the spectrum shown in Figure 2.10, revealed that **H6** resonated at 9.57 ppm. This proton is thus showing a significant shift upon complexation since it resonated at 8.71 ppm in the ligand (**L8**). **H7** shows a slight shift from 8.35 ppm in **L8** to 8.12 ppm in **C8**. The rest of the pyridyl protons (**H3-H5**) resonated between 7.84-8.18 ppm while the protons due to the BPh₄⁻ anion are found between 6.74-7.28 ppm. The protons of the p-cymene ring resonated between 5.27-5.79 ppm. Furthermore, due to chiral Ru(II) centre, the methyl groups shows two resonances situated at ~2.19 and 2.37 ppm.

The ¹³C NMR spectrum further confirmed the successful synthesis of **C8**. Seven resonances are observed between 18.7-41.4 ppm. All the methyl and methine carbons of the p-cymene ring as well as the methyl and the benzyl carbons bonded to the aromatic ring are inequivalent as a result of the stereogenic Ru(II) centre.¹⁰ As a result of this, the aromatic carbons of the p-cymene ring are also inequivalent, resonating between 86.3-108.3 ppm. The imine carbon was found to resonate at 173.4 ppm.

ESI-MS analysis were performed in the positive mode by directly injecting the complex into the mass spectrometer. The molar mass of the di-cation is 974 g/mol. The [M]²⁺ ion was observed at m/z 487.0931, as shown in Figure 2.11, with the experimental pattern (insert in Figure 2.11) corresponding to the theoretical isotopic pattern. However, this peak was not the base peak in the spectrum. The base peak occurred at m/z 614.1877, as shown in Figure 2.12. This peak corresponds to a species which forms as a result of the hydrolysis of one of the imine bonds of the parent species. As a result of this hydrolysis,

Chapter 2: Synthesis and Characterization of Novel Iminopyridyl Rh(I) and Ru(II) Complexes

only one Ru(II) centre remained coordinated. Similarly, the experimental pattern and the theoretical isotopic pattern (insert in Figure 2.12) shows good correlation.

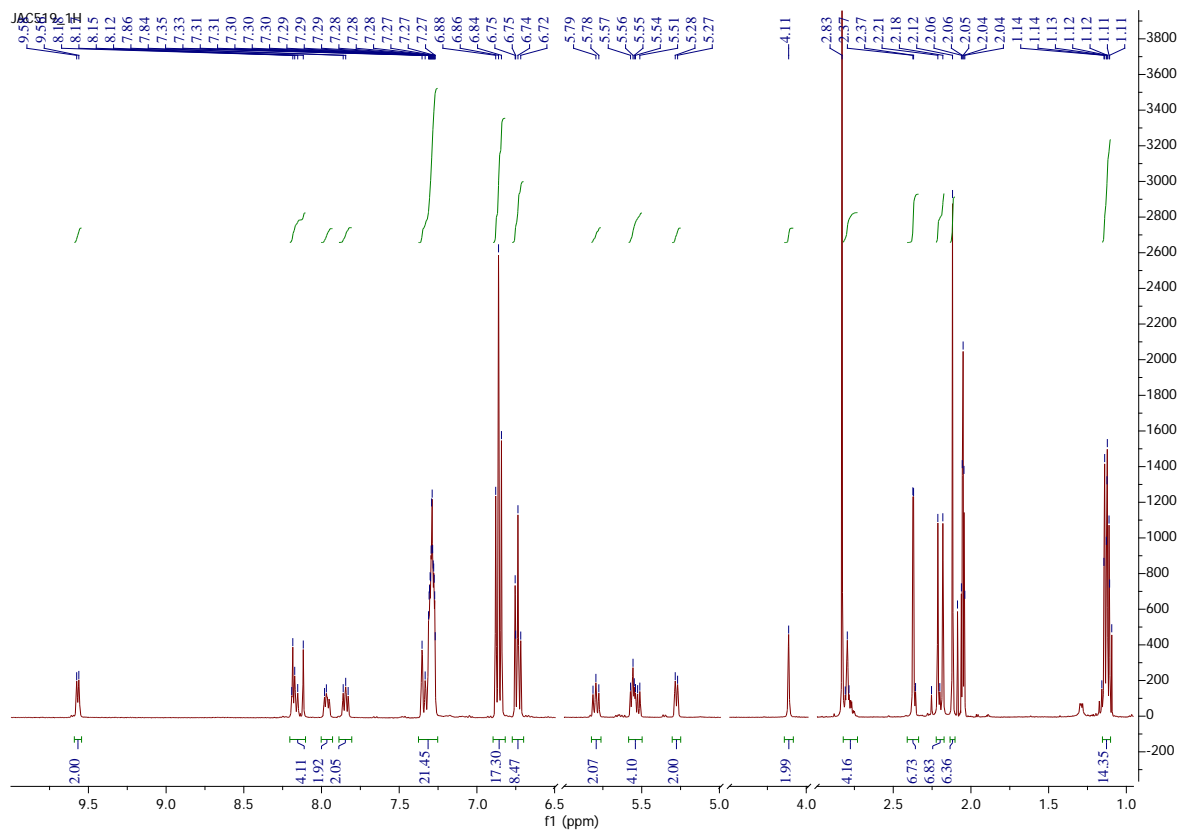


Figure 2.10: ^1H NMR spectrum of C8 ran in acetone- d_6

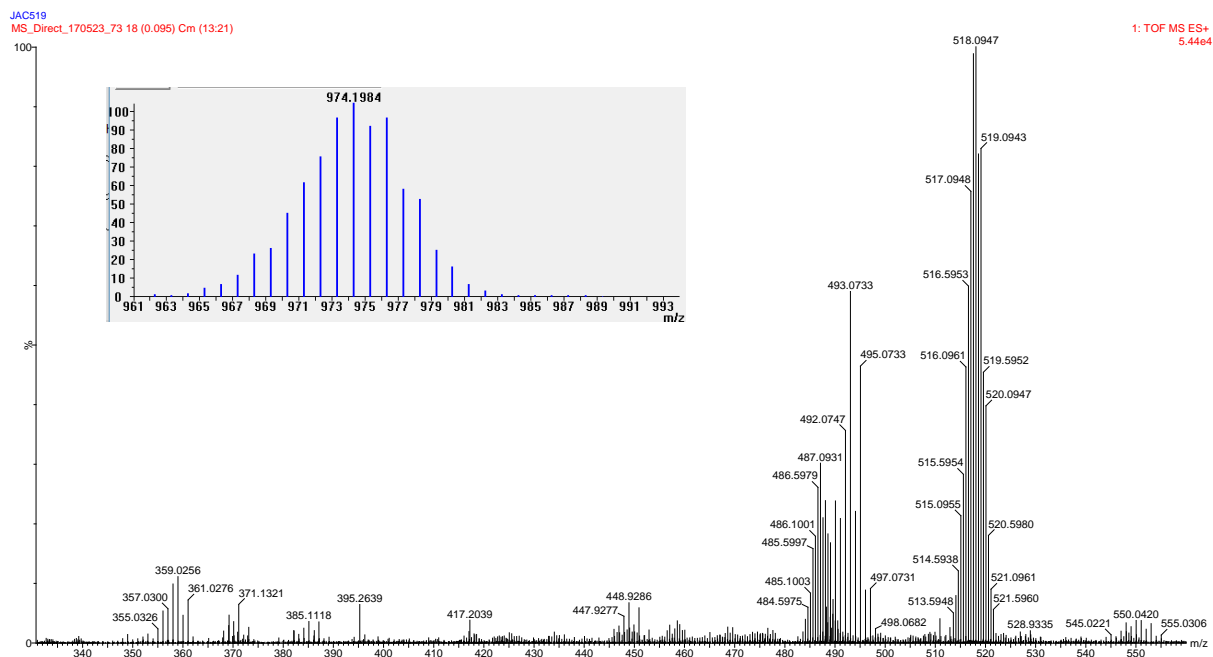


Figure 2.11: ESI-MS spectrum of C8

Chapter 2: Synthesis and Characterization of Novel Iminopyridyl Rh(I) and Ru(II) Complexes

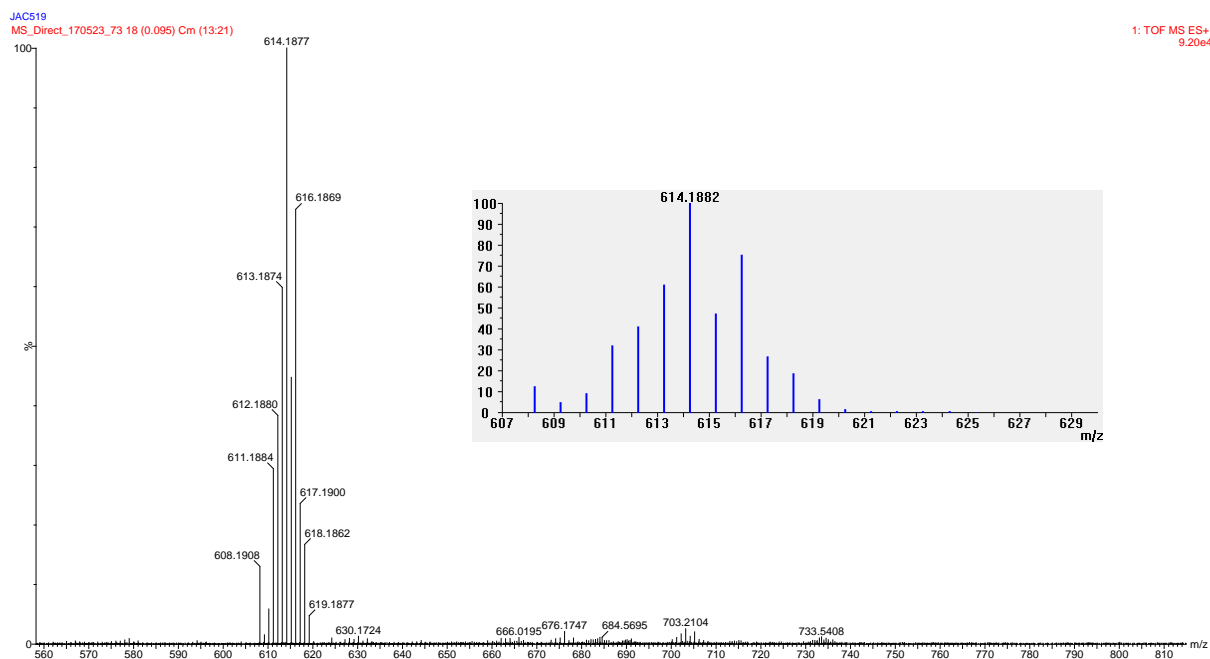


Figure 2.12: Base peak in the ESI-MS spectrum of C8

Table 2.3 shows the ESI-MS, elemental analysis and melting point data for all the complexes (C6-C8), confirming the successful preparation and characterization of these complexes.

Table 2.3: Characterization data for C6-C8

Complex	ESI-MS	EA	Melting point
C6	m/z 481.0990 [M] ⁺	C ₄₈ H ₄₈ BClN ₂ Ru Theoretical C(72.04 %), H (6.05 %), N (3.50 %) Found C(71.87 %), H (6.21 %), N (3.58 %)	Decomposition without melting at 208-209 °C
C7	m/z 495.1139 [M] ⁺	C ₄₉ H ₅₀ BClN ₂ Ru:0.5MeOH Theoretical C(71.61 %), H (6.31 %), N (3.37 %) Found C(71.38 %), H (6.38 %), N (3.45 %)	Decomposition without melting at 231-233 °C
C8	m/z 487.0931 [M] ²⁺	C ₉₇ H ₉₆ B ₂ Cl ₂ N ₄ Ru ₂ :Diethyl ether Theoretical C(71.92 %), H (6.33 %), N (3.32 %) Found C(71.08 %), H (6.28 %), N (3.55 %)	Decomposition without melting at 169-171 °C

2.4 Conclusion

Five novel Rh(I) and three novel Ru(II) complexes were successfully synthesized and fully characterized using a range of analytical techniques. The Rh(I) complexes were isolated in moderate to high yields (65-85 %) while the Ru(II) complexes were isolated in high yields (84-90 %).

Chapter 2: Synthesis and Characterization of Novel Iminopyridyl Rh(I) and Ru(II) Complexes

2.5 Experimental

General Methods and Materials

All of the reagents were purchased from either Merck or Sigma Aldrich and were used without further purification. Solvents were purchased from Merck or Kimix, and were dried by distillation, solvent purifiers or over molecular sieves (acetone, dichloromethane, diethylether, chloroform and methanol).

All reactions were performed using standard Schlenk techniques under a stream of N₂ gas.

FTIR spectra were recorded on a Thermo Nicolet Avatar 330 FTIR Spectrometer equipped with a Smart performer (Zn/Se) ATR attachment. NMR spectra were recorded on a Varian Unity Inova NMR Spectrometer (300, 400 and 600 MHz). Mass Spectra were obtained by analysis on a Waters Synapt G2 Spectrometer. Vario EL cube elemental analysis instrument from Elementar was used for the elemental analysis. A Stuart Scientific melting point apparatus SMP3 was used for determining melting points.

Synthesis of 3,5-dimethyl-4-[(pyridin-2-ylmethylidene)amino]phenol (L5)

Pyridine-2-carbaldehyde (0.234 g, 2.19 mmol) and 4-amino-3,5-dimethylphenol (0.30 g, 2.19 mmol) were dissolved in MeOH (20 ml) forming a brown solution. The resulting brown solution was stirred under reflux for 4 h. After the allotted 4 h, the solvent was removed and the resulting solid was recrystallized from EtOH. The product was then isolated via filtration as a brown crystalline solid (0.410 g, 84 %). IR (ATR) ν (C=N) 1637, 1585 cm⁻¹ (pyridyl). ¹H NMR (600 MHz, CDCl₃) δ_{H} : 2.11 (s, 6 H, Ar-(CH₃)₂), 6.56 (s, 2 H, Ar-H), 6.76 (s, 1 H, Ar-OH), 7.43 (m, 1 H, pyr-H), 7.87 (m, 1 H, pyr-H), 8.30 (d, J = 7.9 Hz, 1 H, pyr-H), 8.35 (s, 1 H, CH=N), 8.72 (d, J = 4.6 Hz, 1 H, pyr-H). ¹³C NMR (151 MHz, CDCl₃) δ_{C} : 18.45, 115.2, 121.3, 125.4, 128.9, 137.0, 143.2, 149.3, 152.7, 154.3, 163.3 ppm. HRMS (ESI+ mode, m/z): Calcd for [M+H]⁺ 227.1184, found 227.1181, Calcd for [M+Na]⁺ 249.1004, found 249.1000. Anal. Calcd (%) for C₁₄H₁₄N₂O.EtOH (5:1): C, 73.45; H, 6.51; N, 11.90; found: C, 73.37; H, 6.49; N, 12.35. Melting point: 179-181 °C.

Synthesis of C1

[Rh(COD)Cl]₂ (48 mg, 0.097 mmol) was dissolved in dichloromethane (4 ml) forming a bright yellow solution. A solution of *N*-phenyl-1-(pyridin-2-yl)methanimine (34 mg, 0.20 mmol) in dichloromethane (1 ml) was then added dropwise to the stirring solution of the dimer forming a black solution and this solution was stirred for 1 h at room temperature. After 1 h, the solvent was removed and the resulting dark-brown residue dissolved in MeOH (5 ml). Sodium tetraphenylborate (67 mg, 0.20 mmol) was then added as a solid, with the immediate precipitation of a dark-brown solid. The mixture was stirred for 15 min at 0 °C. The precipitate was isolated via filtration and washed extensively with MeOH. Recrystallization from dichloromethane:hexane afforded the complex as a black crystalline solid (0.099 g, 71 %). IR (ATR) ν (C=N) 1587 cm⁻¹ (pyridyl C=N). ¹H NMR (400 MHz, DMSO-*d*₆) δ_{H} : 1.94 (m, 4

Chapter 2: Synthesis and Characterization of Novel Iminopyridyl Rh(I) and Ru(II) Complexes

H, COD), 2.43 (m, 4 H, COD), 4.25 (broad s, 4 H, COD), 6.79 (m, 4 H, BPh₄), 6.93 (m, 8 H, BPh₄), 7.19 (m, 8 H, BPh₄), 7.32 (m, 2 H, Ar-**H**), 7.41 (m, 1 H, Ar-**H**), 7.50 (m, 2 H, Ar-**H**), 7.83 (m, 1 H, pyr-**H**), 8.14 (comp, 2 H, pyr, **CH=N**, pyr-**H**), 8.30 (m, 1 H, pyr-**H**), 8.71 (s, 1 H, **CH=N**). ¹³C NMR (151 MHz, DMSO-d₆) δ_C : 29.9, 84.6, 84.7, 121.5, 121.6, 125.3, 128.1, 129.2, 129.4, 129.8, 135.5, 141.3, 147.2, 150.1, 154.6, 157.4, 163.3, 172.6 ppm. HRMS (ESI+ mode, m/z): Calcd for [M]⁺ 392.0760, found 392.0281. Anal. Calcd (%) for C₄₄H₄₂BN₂Rh.0.5Dichloromethane: C, 70.79; H, 5.74; N, 3.71; found: C, 70.59; H, 6.06; N, 3.51. Decomposed with melting: 172-174 °C.

Synthesis of C2

Prepared using the same procedure as **C1** from [Rh(COD)Cl]₂ (28 mg, 0.057 mmol) and *N*-(4-fluorophenyl)-1-(pyridin-2-yl)methanimine (23 mg, 0.11 mmol) and recrystallized from Dichloromethane:Diethyl Ether and isolated in 65 % (54 mg) yield. IR (ATR) ν (C=N) 1614, 1589 cm⁻¹. ¹H NMR (300 MHz, DMSO-d₆) δ_H : 1.93 (m, 4 H, COD), 2.42 (m, 4 H, COD), 4.24 (broad s, 4 H, COD), 6.79 (m, 4 H, BPh₄), 6.93 (m, 8 H, BPh₄), 7.19 (m, 8 H, BPh₄), 7.34 (m, 2 H, Ar-**H**), 7.40 (m, 2 H, Ar-**H**), 7.84 (m, 1 H, pyr-**H**), 8.16 (comp, 2 H, pyr, **CH=N**, pyr-**H**), 8.31 (m, 1 H, pyr-**H**), 8.72 (s, **CH=N**). ¹³C NMR (151 MHz, DMSO-d₆) δ_C : 29.9, 84.5, 84.6, 116.1, 121.5, 123.9, 125.3, 129.7, 135.5, 141.4, 143.6, 150.1, 154.5, 160.4, 162.0, 173.0 ppm. HRMS (ESI+ mode, m/z): Calcd for [M]⁺ 410.0666, found 410.0185. Anal. Calcd (%) for C₄₄H₄₁BFN₂Rh.0.25Dichloromethane: C, 70.70; H, 5.56; N, 3.73; found: C, 70.65; H, 6.19; N, 3.76. Melting point: 167-169 °C.

Synthesis of C3

[Rh(COD)Cl]₂ (49 mg, 0.10 mmol) was dissolved in dichloromethane (5 ml) forming a bright yellow solution. *N*-(4-methylphenyl)-1-(pyridin-2-yl)methanimine (39 mg, 0.20 mmol) was then added as a solid to the stirring solution of the dimer, leading to an immediate colour change from bright yellow to black. This was allowed to stir for 1 h at room temperature. After 1 h, the solvent was removed and the resulting dark-brown residue dissolved in MeOH (5 ml). Sodium tetraphenylborate (68 mg, 0.20 mmol) was then added as a solid, with the immediate precipitation of a brown solid. The reaction mixture were stirred for 15 min at 0 °C. The precipitate was isolated via filtration and washed extensively with MeOH resulting in a brown solid (0.098 g, 67 %). IR (ATR) ν (C=N) 1618, 1588 cm⁻¹. ¹H NMR (400 MHz, DMSO-d₆) δ_H : 1.92 (m, 4 H, COD), 2.34 (s, 3 H, Ar-**CH**₃), 2.41 (m, 4 H, COD), 4.24 (broad s, 4 H, COD), 6.79 (m, 4 H, BPh₄), 6.92 (m, 8 H, BPh₄), 7.18 (comp, 10 H, Ar-**H**, BPh₄), 7.30 (d, *J* = 8.2 Hz, 2 H, Ar-**H**), 7.83 (m, 1 H, pyr-**H**), 8.14 (comp, 2 H, pyr, **CH=N**, pyr-**H**), 8.31 (m, 1 H, pyr-**H**), 8.68 (d, *J* = 1.2 Hz, 1 H, **CH=N**). ¹³C NMR (151 MHz, DMSO-d₆) δ_C : 20.6, 29.9, 84.6, 84.7, 121.4, 121.5, 122.4, 125.3, 129.3, 129.6, 135.5, 137.7, 141.3, 144.9, 150.1, 154.6, 163.5, 172.2 ppm. HRMS (ESI+ mode, m/z): Calcd for [M]⁺ 407.0995, found 406.0916. Anal. Calcd (%) for C₄₅H₄₄BN₂Rh: C, 74.39; H, 6.10; N, 3.86; found: C, 73.68; H, 6.51; N, 3.79. Melting point: 121-123 °C.

Chapter 2: Synthesis and Characterization of Novel Iminopyridyl Rh(I) and Ru(II) Complexes

Synthesis of C4

Prepared using the same procedure as **C3** from [Rh(COD)Cl]₂ dimer (50 mg, 0.10 mmol) and 4-[[pyridin-2-ylmethylidene]amino]phenol (40 mg, 0.20 mmol) and isolated in 85 % (125 mg) yield. IR (ATR) ν (C=N) 1614, 1593 cm⁻¹. ¹H NMR (300 MHz, DMSO-d₆) δ_{H} : 1.93 (m, 4 H, COD), 2.42 (m, 4 H, COD), 4.25 (broad s, 4 H, COD), 6.84 (comp, 6 H, Ar-**H**, BPh₄), 6.94 (m, 8 H, BPh₄), 7.18 (comp, 10 H, Ar-**H**, BPh₄), 7.80 (m, 1 H, pyr-**H**), 8.12 (comp, 2 H, pyr, **CH=N**, pyr-**H**), 8.29 (m, 1 H, pyr-**H**), 8.63 (d, $J = 1.5$ Hz, 1 H, **CH=N**). ¹³C NMR (151 MHz, DMSO-d₆) δ_{C} : 29.9, 84.5, 84.6, 115.5, 121.5, 122.9, 125.3, 129.1, 129.5, 135.5, 139.3, 141.2, 149.9, 154.7, 157.4, 163.8, 171.4 ppm. MS (ESI+ mode, m/z): Calcd for [Rh(COD)]⁺ 211.0, found 211.0, Calcd for [Rh(COD)(MeCN)]⁺ 252.0, found 252.0, Calcd for [Rh(COD)(MeCN)₂]⁺ 293.1, found 293.1. Anal. Calcd (%) for C₄₄H₄₂BN₂ORh: C, 72.54; H, 5.81; N, 3.85; found: C, 72.39; H, 4.65; N, 3.44. Melting point: 146-148 °C.

Synthesis of C5

[Rh(COD)Cl]₂ (50 mg, 0.10 mmol) was dissolved in dichloromethane (5 ml) forming a bright yellow solution. 3,5-dimethyl-4-[(pyridin-2-ylmethylidene)amino]phenol (46 mg, 0.20 mmol) was then added as a solid to the stirring solution of the dimer forming a black solution immediately, with the formation of a brown precipitate after a few minutes. This mixture was stirred for 1 h at room temperature. A solution of NaBPh₄ (69 mg, 0.20 mmol) in MeOH (3 ml) was then added dropwise, forming a black solution. This was stirred for an additional 1 h at room temperature. After the allotted time the solvent was removed followed by the addition of another portion of MeOH (5 ml). The product was then isolated via filtration and washed with MeOH (10 ml) (119 mg, 77 %). IR (ATR) ν (C=N) 1614, 1590 cm⁻¹. ¹H NMR (300 MHz, Acetone-d₆) δ_{H} : 2.31 (s, 6 H, Ar-(**CH**₃)₂), 2.51 (m, 4 H, COD), 2.88 (broad s, 4 H, COD), 4.23 (broad s, 4 H, COD), 6.67 (s, 2 H, Ar-**H**), 6.77 (m, 4 H, BPh₄), 6.91 (m, 8 H, BPh₄), 7.33 (m, 8 H, BPh₄), 7.80 (m, 1 H, pyr-**H**), 8.06 (comp, 2 H, pyr, **CH=N**, pyr-**H**), 8.22 (m, 1 H, pyr-**H**), 8.45 (d, $J = 2.9$ Hz, 1 H, **CH=N**). ¹³C NMR (75 MHz, Acetone-d₆) δ_{C} : 17.7, 30.1, 87.1, 87.3, 114.9, 121.4, 125.1, 129.3, 130.2, 130.3, 136.2, 136.8, 141.7, 150.4, 154.8, 156.4, 163.7, 175.3 ppm. HRMS (ESI+ mode, m/z): Calcd for [M]⁺ 437.1100, found 437.1099. Anal. Calcd (%) for C₄₆H₄₆BN₂ORh.0.25Dichloromethane: C, 71.42; H, 6.03; N, 3.60; found: C, 71.31; H, 6.67; N, 3.54. Decomposed without melting: 139-141 °C.

Synthesis of *N*-(2,6-dimethylphenyl)-1-(pyridin-2-yl)methanimine (L6)

Pyridine-2-carbaldehyde (0.435 g, 4.06 mmol) and 2,6-dimethylaniline (0.492 g, 4.06 mmol) were added to EtOH (2 ml) forming a brown solution in a 10 ml microwave reaction vessel. This was allowed to react in a microwave reactor at 100 W for 10 min while keeping the temperature constant at 80 °C. After the allotted time, the solvent was removed producing a brown oil which was purified using

Chapter 2: Synthesis and Characterization of Novel Iminopyridyl Rh(I) and Ru(II) Complexes

vacuum distillation (0.810 g, 95 %). IR (ATR) ν (C=N) 1640, 1584 cm^{-1} (pyridyl). ^1H NMR (400 MHz, CDCl_3) δ_{H} : 2.18 (s, 6 H, Ar-(CH_3)₂), 6.99 (m, 1 H, Ar-**H**), 7.10 (m, 2 H, Ar-**H**), 7.41 (m, 1 H, pyr-**H**), 7.85 (m, 1 H, pyr-**H**), 8.30 (m, 1 H, pyr-**H**), 8.36 (s, 1 H, $\text{CH}=\text{N}$), 8.73 (m, 1 H, pyr-**H**). ^{13}C NMR (151 MHz, CDCl_3) δ_{C} : 18.2, 121.2, 125.3, 126.8, 128.1, 136.7, 137.0, 149.6, 150.2, 154.4, 163.4 ppm.

Synthesis of 1-(pyridin-2-yl)-*N*-(2,4,6-trimethylphenyl)methanimine (L7)

Prepared using the same procedure as **L6** from Pyridine-2-carbaldehyde (0.435 g, 4.06 mmol) and 2,4,6-trimethylaniline (0.549 g, 4.06 mmol) and isolated in (0.750 g, 82 %). IR (ATR) ν (C=N) 1639, 1585 cm^{-1} (pyridyl). ^1H NMR (400 MHz, CDCl_3) δ_{H} : 2.16 (s, 6 H, Ar-(CH_3)₂), 2.31 (s, 3 H, Ar- CH_3), 6.92 (s, 2 H, Ar-**H**), 7.40 (m, 1 H, pyr-**H**), 7.84 (m, 1 H, pyr-**H**), 8.29 (m, 1 H, pyr-**H**), 8.36 (s, 1 H, $\text{CH}=\text{N}$), 8.72 (m, 1 H, pyr-**H**). ^{13}C NMR (151 MHz, CDCl_3) δ_{C} : 18.2, 20.7, 121.1, 125.2, 126.8, 128.8, 133.4, 136.6, 149.5, 150.2, 154.5, 163.4 ppm.

Synthesis of L8

Prepared using the same procedure as **L6** from Pyridine-2-carbaldehyde (84 mg, 0.78 mmol) and 4,4'-Methylenebis(2,6-dimethylaniline) (100 mg, 0.39 mmol). Recrystallized from EtOH (0.139 g, 82 %). IR (ATR) ν (C=N) 1639, 1584 cm^{-1} (pyridyl). ^1H NMR (600 MHz, CDCl_3) δ_{H} : 2.16 (s, 12 H, Ar-(CH_3)₂), 3.86 (s, 2 H, Ar- CH_2 -Ar), 6.95 (s, 4 H, Ar-**H**), 7.40 (m, 2 H, pyr-**H**), 7.84 (m, 2 H, pyr-**H**), 8.29 (d, $J = 8.2$ Hz, 2 H, pyr-**H**), 8.36 (s, 2 H, $\text{CH}=\text{N}$), 8.72 (d, $J = 4.7$ Hz, 2 H, pyr-**H**). ^{13}C NMR (151 MHz, CDCl_3) δ_{C} : 18.3, 40.8, 121.1, 125.2, 127.0, 128.7, 136.6, 137.1, 148.3, 149.6, 154.5, 163.4 ppm.

Synthesis of C6

$[\text{RuCl}_2(\text{p-cymene})]_2$ (50 mg, 0.082 mmol) was dissolved in dichloromethane (3 ml) forming a red-orange solution. A solution of *N*-(2,6-dimethylphenyl)-1-(pyridin-2-yl)methanimine (34 mg, 0.16 mmol) in dichloromethane (2 ml) was then added dropwise to the stirring solution of the dimer and stirred for 1 h at room temperature. After 1 h, the solvent was removed and the resulting red-orange residue dissolved in MeOH (5 ml). Sodium tetraphenylborate (56 mg, 0.16 mmol) was then added as a solid, with the immediate precipitation of a yellow solid. This was stirred for 15 min at 0 °C. The yellow solid was recovered via filtration and washed extensively with MeOH. Recrystallization from Dichloromethane:Hexane afforded the complex as red-orange crystals (110 mg, 84 %). IR (ATR) ν (C=N) 1612. ^1H NMR (400 MHz, Acetone- d_6) δ_{H} : 1.17 (d, $J = 3.9$ Hz, 3 H, p-cy, CH_3 -CH- CH_3), 1.19 (d, $J = 4.3$ Hz, 3 H, p-cy, CH_3 -CH- CH_3), 2.24 (s, 3 H, p-cy, Ar- CH_3), 2.34 (s, 3 H, Ar- CH_3), 2.41 (s, 3 H, Ar- CH_3), 2.86 (m, 1 H, p-cy, CH_3 -CH- CH_3), 5.41 (d, $J = 6.6$ Hz, 1 H, p-cy), 5.70 (m, 2 H, p-cy), 5.88 (d, $J = 6.2$ Hz, 1 H, p-cy), 6.77 (m, 4 H, BPh₄), 6.91 (m, 8 H, BPh₄), 7.33 (comp, 11 H, Ar-**H**, BPh₄), 7.93 (m, 1 H, pyr-**H**), 8.31 (comp, 2 H, pyr-**H**), 8.81 (s, 1 H, $\text{CH}=\text{N}$), 9.66 (d, $J = 5.5$ Hz, 1 H, pyr-**H**, $\text{CH}=\text{N}$). ^{13}C NMR (75 MHz, Acetone- d_6) δ_{C} : 17.7, 18.0, 19.6, 21.5, 21.7, 31.1, 85.6, 86.0, 87.0, 87.8, 101.0, 107.5, 121.3, 125.1, 128.4, 128.7, 128.9, 129.3, 129.6, 130.0, 131.6, 136.1, 140.0, 151.1,

Chapter 2: Synthesis and Characterization of Novel Iminopyridyl Rh(I) and Ru(II) Complexes

154.6, 155.9, 164.0, 172.5 ppm. HRMS (ESI+ mode, m/z): Calcd for [M]⁺ 481.0988, found 481.0990. Anal. Calcd (%) for C₄₈H₄₈BClN₂Ru: C, 72.04; H, 6.05; N, 3.50; found: C, 71.87; H, 6.21; N, 3.58. Decomposed without melting: 208-209 °C.

Synthesis of C7

Prepared using the same procedure as **C6** from [RuCl₂(p-cymene)]₂ (50 mg, 0.082 mmol), 1-(pyridin-2-yl)-N-(2,4,6-trimethylphenyl)methanimine (37 mg, 0.16 mmol) and sodium tetraphenylborate (56 mg, 0.16 mmol). **C7** isolated as a yellow solid (115 mg, 86 %). IR (ATR) ν (C=N) 1612. ¹H NMR (600 MHz, DMSO-d₆) δ_{H} : 1.05 (comp, 6 H, p-cy, CH₃-CH-CH₃), 2.10 (s, 3 H, p-cy, Ar-CH₃), 2.16 (s, 3 H, Ar-CH₃), 2.30 (s, 3 H, Ar-CH₃), 2.36 (s, 3 H, Ar-CH₃), 2.67 (spt, *J* = 6.9 Hz, 1 H, p-cy, CH₃-CH-CH₃), 5.31 (d, *J* = 5.9 Hz, 1 H, p-cy), 5.59 (d, *J* = 6.4 Hz, 1 H, p-cy), 5.62 (d, *J* = 6.4 Hz, 1 H, p-cy), 5.94 (d, *J* = 6.4 Hz, 1 H, p-cy), 6.79 (m, 4 H, BPh₄), 6.92 (m, 8 H, BPh₄), 7.11 (s, 1 H, Ar-H), 7.17 (comp, 9 H, Ar-H, BPh₄), 7.92 (m, 1 H, pyr-H), 8.20 (d, *J* = 7.6 Hz, 1 H, pyr-H), 8.29 (m, 1 H, pyr-H), 8.83 (s, 1 H, CH=N), 9.63 (d, *J* = 5.3 Hz, 1 H, pyr-H, CH=N). ¹³C NMR (151 MHz, DMSO-d₆) δ_{C} : 17.9, 18.1, 19.6, 20.4, 21.6, 22.0, 30.6, 84.6, 85.7, 86.7, 87.2, 100.4, 106.4, 121.5, 125.3, 128.3, 129.2, 129.8, 130.9, 135.5, 137.3, 140.0, 148.6, 154.0, 156.0, 163.5, 173.2 ppm. HRMS (ESI+ mode, m/z): Calcd for [M]⁺ 495.1145, found 495.1139. Anal. Calcd (%) for C₄₉H₅₀BClN₂Ru:0.5MeOH: C, 71.61; H, 6.31; N, 3.37; found: C, 71.38; H, 6.38; N, 3.45. Decomposed without melting: 231-233 °C.

Synthesis of C8

Prepared using the same procedure as **C6** from [RuCl₂(p-cymene)]₂ (40 mg, 0.065 mmol), **L8** (28 mg, 0.065 mmol) and sodium tetraphenylborate (45 mg, 0.13 mmol). **C7** isolated as a yellow solid (94 mg, 90 %). IR (ATR) ν (C=N) 1612, 1598 cm⁻¹ (pyridyl C=N). ¹H NMR (400 MHz, Acetone-d₆) δ_{H} : 1.12 (comp, 12 H, p-cy, CH₃-CH-CH₃), 2.12 (s, 6 H, p-cy, Ar-CH₃), 2.18 (s, 3 H, Ar-CH₃), 2.21 (s, 3 H, Ar-CH₃), 2.37 (comp, 6 H, Ar-CH₃), 2.80 (m, 3 H, p-cy, CH₃-CH-CH₃), 4.11 (s, 2 H, Ar-CH₂-Ar), 5.28 (m, 2 H, p-cy), 5.54 (comp, 4 H, p-cy), 5.79 (m, 2 H, p-cy), 6.74 (m, 8 H, BPh₄), 6.86 (m, 16 H, BPh₄), 7.30 (comp, 20 H, Ar-H, BPh₄), 7.84 (m, 2 H, pyr-H), 7.97 (m, 2 H, pyr-H), 8.12 (s, 2 H, CH=N), 8.17 (m, 2 H, pyr-H), 9.57 (m, 2 H, pyr-H, CH=N). ¹³C NMR (75 MHz, Acetone-d₆) δ_{C} : 18.7, 19.1, 20.7, 22.6, 22.7, 32.1, 41.4, 86.3, 86.4, 86.8, 86.9, 87.9, 88.1, 88.6, 88.7, 101.7, 102.0, 108.2, 108.3, 122.4, 126.2, 130.0, 130.3, 130.9, 131.0, 132.8, 137.1, 140.9, 150.5, 155.3, 156.8, 165.9, 173.4 ppm. HRMS (ESI+ mode, m/z): Calcd for [M]²⁺ 487.0992, found 487.0931. Anal. Calcd (%) for C₉₇H₉₆B₂Cl₂N₄Ru₂:Diethyl Ether: C, 71.92; H, 6.33; N, 3.32; found: C, 71.08; H, 6.28; N, 3.55. Decomposed without melting: 169-171 °C.

2.6 References

1. C. Alonso-Moreno, F. Carrillo-Hermosilla, J. Romero-Fernández, A. M. Rodríguez, A. Otero and A. Antinolo, *Adv. Synth. Catal.*, 2009, **351**, 881-890.
2. S. Dai, X. Sui and C. Chen, *Chem. Commun.*, 2016, **52**, 9113-9116.

Chapter 2: Synthesis and Characterization of Novel Iminopyridyl Rh(I) and Ru(II) Complexes

3. J. Li, L. Guo, Z. Tian, M. Tian, S. Zhang, K. Xu, Y. Qian and Z. Liu, *Dalton Trans.*, 2017, **46**, 15520-15534.
4. J. M. Gichumbi, H. B. Friedrich and B. Ormondi, *J. Mol. Catal. A: Chem.*, 2016, **416**, 29-38.
5. J. October and S. F. Mapolie, *J. Organomet. Chem.*, 2017, **840**, 1-10.
6. H. Kotzé and S. F. Mapolie, *Appl. Organometal. Chem.*, 2017, 31:e3643.
7. M. Maroto-Díaz, B. T. Elie, P. Gómez-Sal, J. Pérez-Serrano, R. Gómez, M. Contel and F. J. de la Mata, *Dalton Trans.*, 2016, **45**, 7049-7066.
8. M. J. Chow, C. Licon, D. Y. Q. Wong, G. Pastorin, C. Gaiddon and W. H. Ang, *J. Med. Chem.*, 2014, **57**, 6043-6059.
9. G. R. Jadhav, S. Sinha, M. Chhabra and P. Paira, *Bioorg. Med. Chem. Lett.*, 2016, **26**, 2695-2700.
10. D. Carmona, C. Vega, F. J. Lahoz, S. Elipe, L. A. Oro, M. P. Lamata, F. Viguri, R. García-Correas, C. Cativiela and M. P. López-Ram de Vú, *Organometallics*, 1999, **18**, 3364-3371.
11. Y. Gao, Y. Zhang, C. Qiu and J. Zhao, *Appl. Organometal. Chem.*, 2011, **25**, 54-60.
12. Y. Dong, R. Fan, W. Chen, H. Zhang, Y. Song, X. Du, P. Wang, L. Wei and Y. Yang, *Dalton Trans.*, 2017, **46**, 1266-1276.
13. Q. Zhang, H. Su, J. Luo and Y. Wei, *Tetrahedron*, 2013, **69**, 447-454.
14. G. Giordano and R. H. Crabtree, *Inorg. Synth.* **1979**, 19, 218-220.
15. J. M. Gichumbi, H. B. Friedrich and B. Ormondi, *Inorganica Chim. Acta*, 2017, **456**, 55-63.
16. J. Li, L. Guo, Z. Tian, M. Tian, S. Zhang, K. Xu, Y. Qian and Z. Liu, *Dalton Trans.*, 2017, **46**, 15520-15534.
17. S. Jie, D. Zhang, T. Zhang, W. Sun, J. Chen, Q. Ren, D. Liu, G. Zheng and W. Chen, *J. Organomet. Chem.*, 2005, **690**, 1739-1749.
18. Y. Dong, R. Fan, X. Wang, P. Wang, H. Zhang, L. Wei, Y. Song, X. Du, W. Chen and Y. Yang, *Eur. J. Inorg. Chem.*, 2016, 3598-3610.

Chapter 3: Hydroformylation of 1-Octene by Iminopyridyl Rh(I) Complexes

3.1 Introduction

Hydroformylation is an atom-economical production of aldehydes via the addition of CO and H₂ over a C=C double bond, producing either linear or branched aldehydes.¹ This reaction thus represents an important industrial process due to the usefulness of the resulting aldehydes as precursors to other value-added materials. The linear aldehydes are specifically used as precursors to alcohols, plasticizers and in the cosmetic industry while the branched aldehydes are important in the pharmaceutical industry.¹⁻³

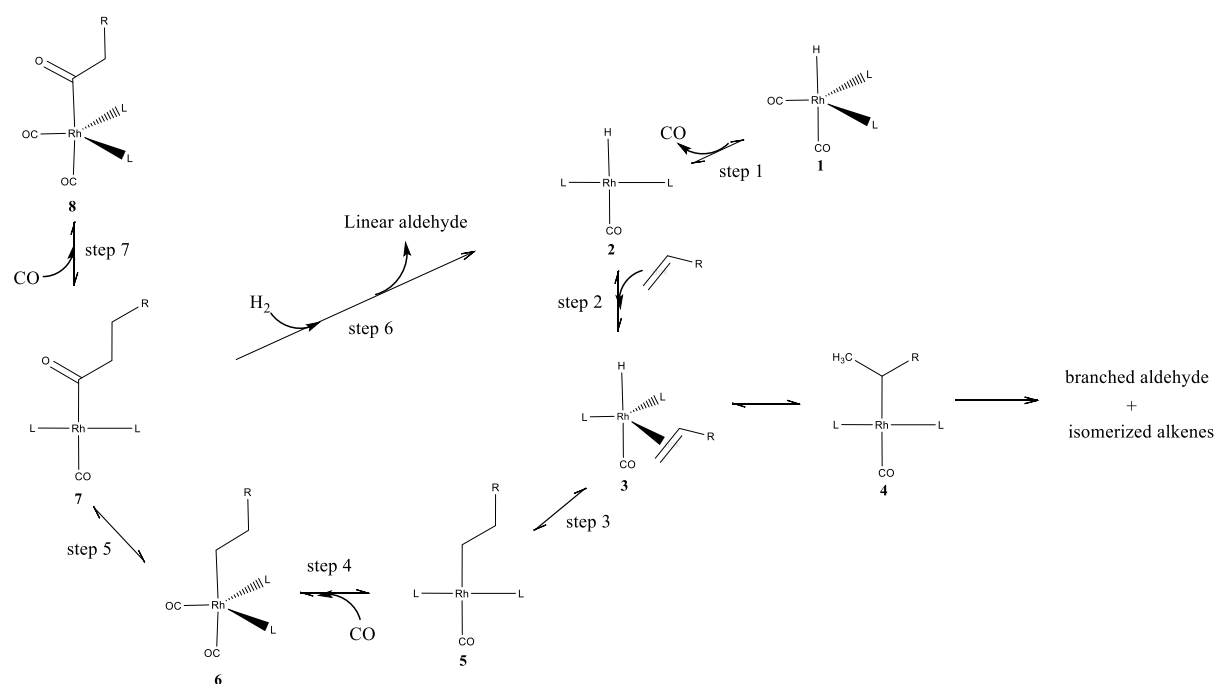


Figure 3.1: Mechanism of the hydroformylation reaction⁴

The general mechanism of the hydroformylation reaction is shown in Figure 3.1. The first step in the reaction is the dissociation of CO from the pre-catalyst (1), producing a four-coordinate species (2). Coordination of the olefin substrate then occurs producing a π-complex (3). Depending on whether Markovnikov or anti-Markovnikov addition occurs, either a linear (5) or a branched metal alkyl species (4) can form. CO coordination then occurs followed by migration of the alkyl group onto a CO ligand (carbonylation) producing a metal acyl species (7). If an additional CO ligand coordinates, a di-carbonyl metal acyl species forms (8). This species is off cycle and are therefore catalytically inactive. Oxidative addition of H₂ to the four-coordinate metal acyl species will form a di-hydride species after which

Chapter 3: Hydroformylation of 1-Octene by Iminopyridyl Rh(I) Complexes

reductive elimination of the adjacent acyl and hydride ligands occurs to produce the aldehyde, regenerating the active species. All of these steps are in equilibrium, except for the reductive elimination step. In the case of the branched metal alkyl species (4), when it is involved in the aforementioned steps, it will produce branched aldehydes. However, a major side reaction in competition with the hydroformylation process is the isomerization of the olefin. This can occur upon β -hydride elimination from the branched metal alkyl species producing a M-H species and the internal olefin. All of these steps can be influenced by the total pressure, partial pressures of CO and H₂, temperature and the nature of the catalyst.

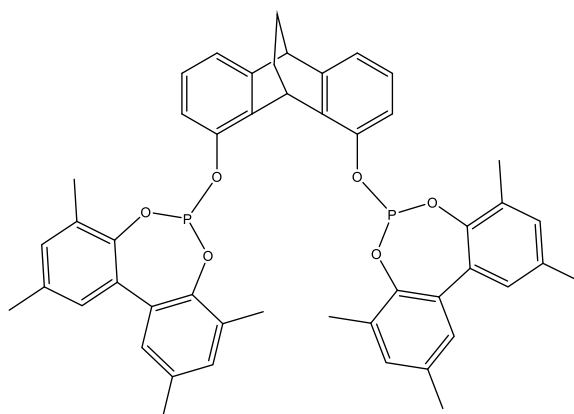


Figure 3.2: A phosphite ligand used by Hofmann and co-workers⁸

In general, phosphine-based rhodium catalysts dominate in mediating this process.⁵⁻⁷ Rhodium-based catalysts have been found to be far more efficient than other catalysts based on other metals such as Ru, Co and Fe.⁸ Phosphine ligands are normally capable of elegantly controlling the chemo- and regioselectivity of this process.⁹⁻¹⁰ An example of this is demonstrated in a report by Hofmann and co-workers⁹ where they targeted adipic aldehyde via the hydroformylation of 4-pentenal. Various ligand structures were screened where they found that the phosphite ligand shown in Figure 3.2 can produce the target aldehyde in 96 % selectivity.

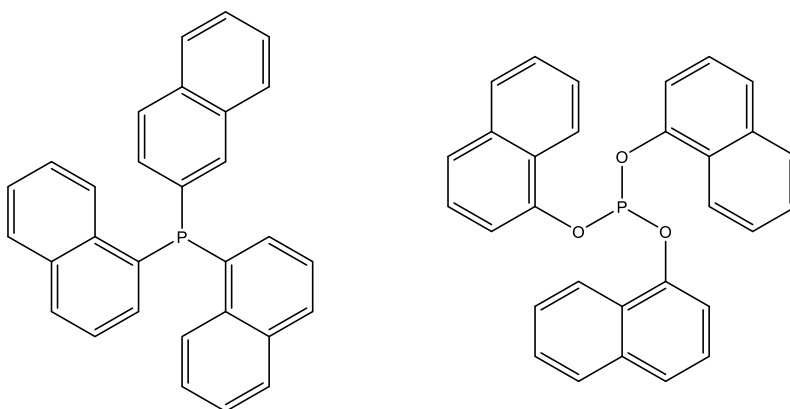


Figure 3.3: Bulky phosphine and phosphite ligands¹⁰

Chapter 3: Hydroformylation of 1-Octene by Iminopyridyl Rh(I) Complexes

Bajaj and co-workers¹⁰ used modified bulky phosphine and phosphite ligands (shown in Figure 3.3) to study the hydroformylation of 1-hexene to the branched aldehydes. Slightly elevated temperatures (110-120 °C) as well as a high syngas pressure (40 bar CO:H₂, 1:1) allowed them to produce branched aldehydes in 83 % selectivity. This high branched regioselectivity was attributed to the initial isomerization of 1-hexene followed by the hydroformylation of these internal alkenes to the corresponding branched aldehydes.

The most well-known industrial processes involving hydroformylation is the Ruhrchemie/Rhone-Poulenc, BASF-oxo, Exxon and the Shell processes. Only the Ruhrchemie/Rhone-Poulenc process rely on rhodium, with the process occurring in an aqueous biphasic system using the water soluble TPPTS ligand, while the other processes are based on cobalt phosphine catalysts. Due to the lower hydroformylation activity of cobalt, these processes are normally carried out at high temperatures around 150-190 °C.^{2,11}

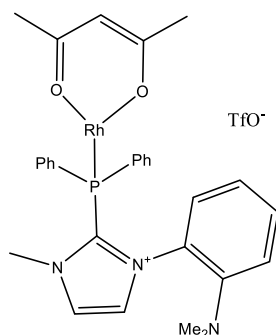


Figure 3.4: Ionic Rh(I) imidazolium based phosphine complex bearing amino substituents¹⁴

However, phosphine ligands are prone to oxidation in air, which can lead to catalyst deactivation.¹²⁻¹³ This is especially undesirable when catalyst recycling and reusability are required. In light of the above, other donor atoms, such as nitrogen, can be introduced into the ligand architecture, in addition to phosphorous, to produce *N, P* hybrid ligands.¹⁴⁻¹⁵ This provides the possibility of hemilability, where the weakly coordinating group (the relatively hard N-donor) can dissociate during catalysis, thus creating a vacant site on the metal allowing the substrate to bind. After the reaction is complete, the N-donor coordinates again, stabilizing the catalyst. In this regard, Liu and co-workers¹⁴ showed that the ionic Rh(I) imidazolium based hybrid *N, P* systems (Figure 3.4) are far better catalysts compared to Rh(acac)(CO)(PPh₃). The higher activity was attributed to weaker Rh-CO bonds, as confirmed by IR spectroscopy and SCD analysis. This facilitates the dissociation and re-insertion of CO into Rh-alkyl species, with subsequent production of the aldehydes. The authors further found that these *N, P* hybrid systems stabilize the Rh-H species better when compared to the Rh(acac)(CO)(PPh₃) catalyst by preventing the formation of inactive CO-bridged Rh-dimers. Furthermore, Kostas and Screttas previously showed that amino-phosphine ligands can also successfully be used to facilitate the hydroformylation of styrene.¹⁵ Moreover, it is also possible to utilize systems based on N-donor atoms

Chapter 3: Hydroformylation of 1-Octene by Iminopyridyl Rh(I) Complexes

alone. As shown by us and others, this produces highly efficient catalysts for the hydroformylation of 1-octene. However, this proceeds at lower chemo- and regioselectivities compared to phosphine-based systems.¹⁶⁻¹⁸

In view of the above, we synthesized four cationic iminopyridyl Rh(I) complexes bearing electron withdrawing (F) and electron donating (OH and CH₃) groups in order to study the effect of these on the catalytic activity.

3.2 Hydroformylation of 1-octene

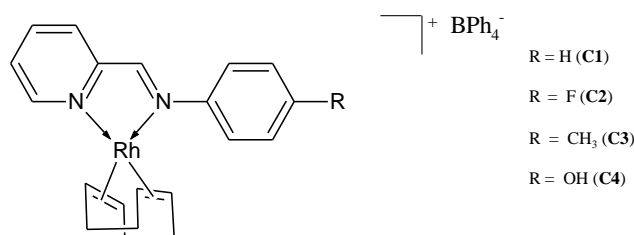


Figure 3.5: Rh(I) iminopyridyl catalyst precursors (C1-C4)

The catalyst precursors evaluated in the hydroformylation of 1-octene are shown in Figure 3.5. The hydroformylation of 1-octene was studied under the same reaction conditions we reported previously.¹⁶ These conditions are 30 bar CO:H₂ (1:1), 75 °C and 0.05 mol % catalyst loading (catalyst:substrate ratio of 1:2000).

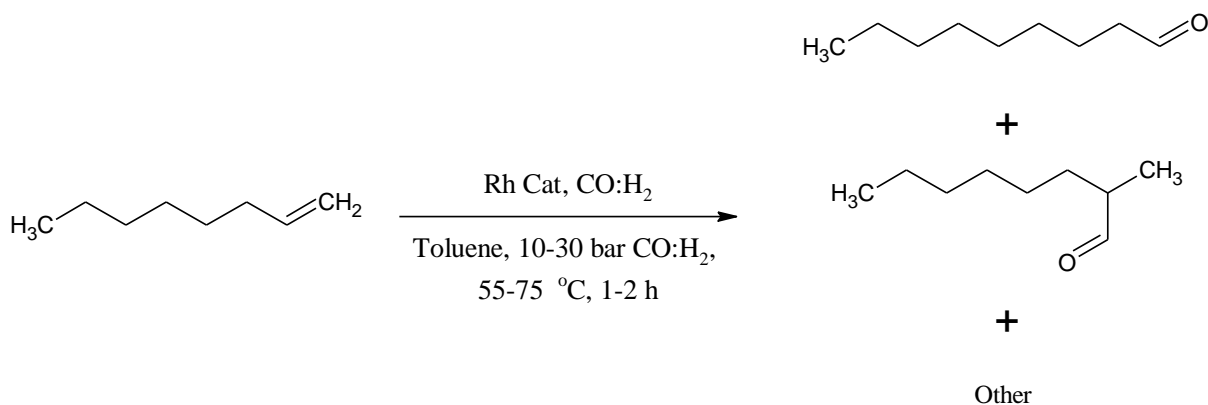


Figure 3.6: Hydroformylation of 1-octene

3.2.1 Hydroformylation of 1-octene using four different Rh(I) iminopyridyl complexes

All four catalyst precursors gave full conversion of the substrate after 2 h. It was therefore not possible to elucidate the effect of the substituent on the catalytic activity under these conditions. What we can conclude from these experiments is that the substituent (R) has no effect on the chemoselectivity of the catalytic reaction under investigation, since relatively similar product distributions are obtained. The chemoselectivities obtained with these catalyst precursors are moderate since there are almost an even distribution between internal octenes and aldehydes. This chemoselectivity is far lower than what is

Chapter 3: Hydroformylation of 1-Octene by Iminopyridyl Rh(I) Complexes

normally obtained using phosphine-based catalysts.¹⁹ Hydroformylation with phosphine ligands are normally performed in the presence of excess ligand.¹⁹ The role of the excess ligand is to inhibit isomerization of the terminal olefin by occupying vacant sites on the metal, thus preventing β -hydride elimination. β -Hydride elimination requires a vacant site on the metal to accommodate the incoming hydride. Secondly, due to their bulky nature, they can further inhibit the formation of branched metal-alkyl species which further inhibits isomerization.²⁰ This directly influences both the chemo- and regioselectivity (linear:branched) of the aldehydes.²⁰ As a result of the lack in bulkiness of our ligands, the isomerization of the terminal olefin is a significant side reaction leading to poor chemoselectivities.

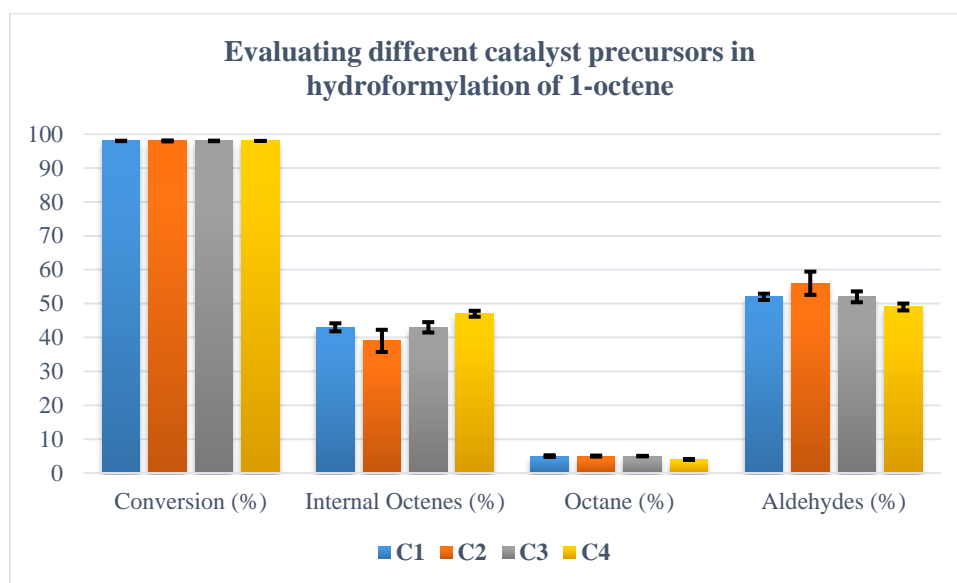


Figure 3.7: Hydroformylation of 1-octene using Rh(I) iminopyridyl complexes. 1-Octene (6.37 mmol), 30 bar CO:H₂ (1:1), 75 °C, 0.05 mol %, 2 h.

The hydrogenation of the olefin to the alkane is a minor side reaction (~5 %). The route leading to the aldehydes and internal olefins are most likely more favourable under these conditions.

The regioselectivity of **C1-C4** is shown in Figure 3.8. Similar regioselectivities are obtained for all four catalyst precursors. Under these conditions, the regioselectivity is slightly in favour of the linear aldehyde. The linear aldehyde is produced from a linear Rh-alkyl species while the branched aldehydes are produced from a branched Rh-alkyl species. In addition to undergoing carbonylation to produce the aldehydes, the branched Rh-alkyl species are also prone to β -hydride elimination producing the internal olefins. Additionally, Lazzaroni and co-workers²¹ showed that at high temperatures, β -hydride elimination occurs to a greater extent in branched metal-alkyl species compared to linear metal-alkyl species. As a result of this, more linear aldehyde are produced, accounting for the observed regioselectivities.

Chapter 3: Hydroformylation of 1-Octene by Iminopyridyl Rh(I) Complexes

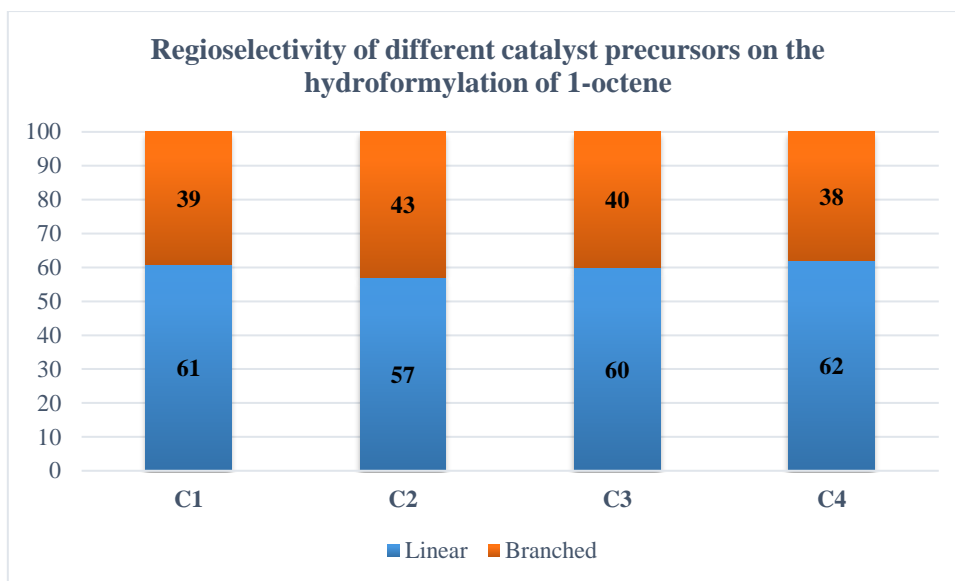


Figure 3.8: Regioselectivity of C1-C4. 1-Octene (6.37 mmol), 30 bar CO:H₂ (1:1), 75 °C, 0.05 mol % (Catalyst:substrate 1:2000), 2 h.

3.2.2 Effect of time on the hydroformylation of 1-octene

The hydroformylation of 1-octene was then also evaluated for 1 h using C2 (Figure 3.9) in order to monitor the progress of the reaction.

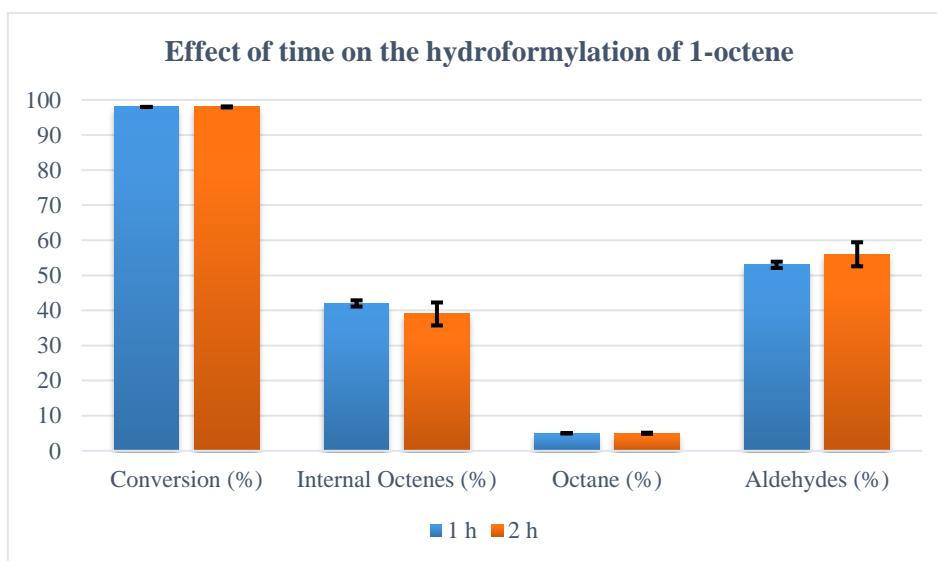


Figure 3.9: Effect of time. 1-Octene (6.37 mmol), 30 bar CO:H₂ (1:1), 75 °C and 0.05 mol % of C2 (Catalyst:substrate 1:2000).

It was found that shortening the reaction time to 1 h had no significant effect on the conversion, the product distribution or the regioselectivity (Figure 3.9-3.10). The internal olefins showed a slight decrease while the aldehydes showed a slight increase, however, this is within experimental error. After 1 h, the 1-octene are almost completely consumed while almost no internal octenes are converted to aldehydes to a significant extent between 1-2 h under these reaction conditions. This lack of conversion

Chapter 3: Hydroformylation of 1-Octene by Iminopyridyl Rh(I) Complexes

of the internal octenes are due to their lower reactivity in comparison to the terminal olefin and for this reason the regioselectivity also remained the same over the period 1-2 h (Figure 3.10).

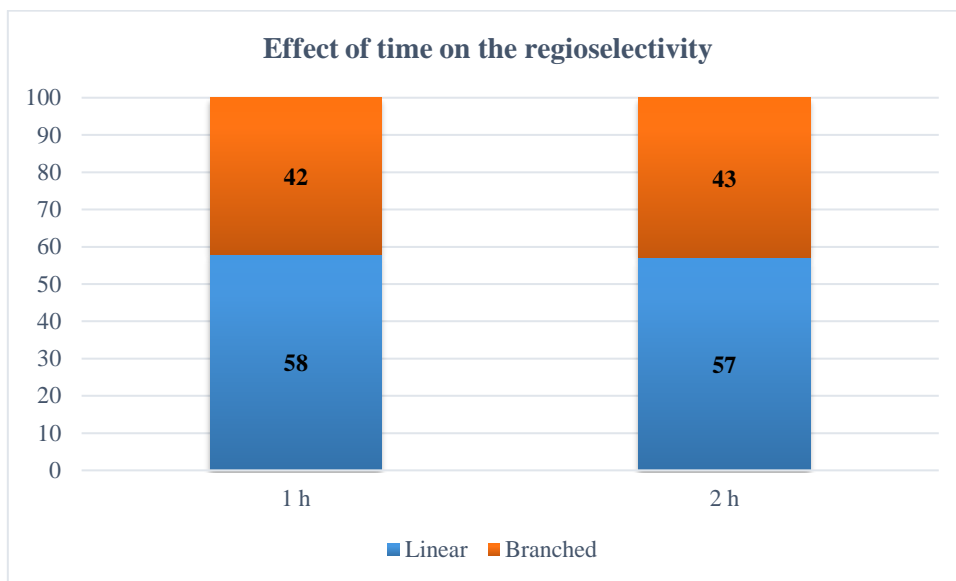


Figure 3.10: Effect of time on the regioselectivity. 1-Octene (6.37 mmol), 30 bar CO:H₂ (1:1), 75 °C and 0.05 mol % of C2 (Catalyst:substrate 1:2000).

Therefore, we investigated the hydroformylation of an internal olefin in order to determine whether the hydroformylation of internal olefins is indeed slower than their terminal counterparts (Figure 3.11-3.12).

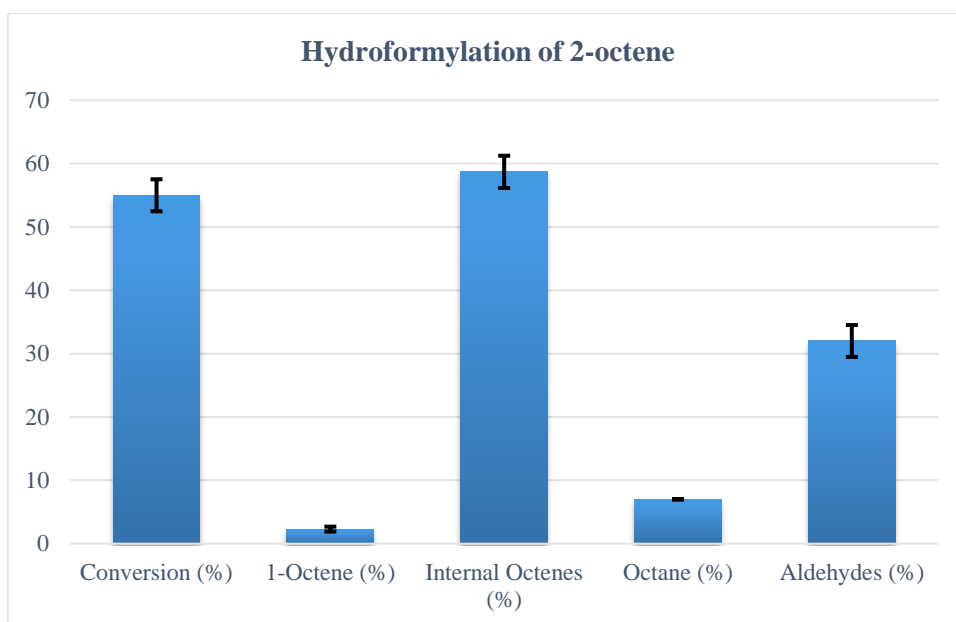


Figure 3.11: Hydroformylation of 2-octene. 2-Octene (6.37 mmol), 30 bar CO:H₂ (1:1), 75 °C and 0.05 mol % of C2 (Catalyst:substrate 1:2000), 2 h.

The hydroformylation of 2-octene was studied under the same conditions as for 1-octene, with the reaction performed for 2 h. Under these conditions, 55 % of the 2-octene was converted during which the major products were found to be other internal octenes (3- and 4-octene) and only ~32 % aldehydes.

Chapter 3: Hydroformylation of 1-Octene by Iminopyridyl Rh(I) Complexes

The amount of aldehydes is much more than what was obtained when using 1-octene (Figure 3.9) as substrate and extending the reaction from 1 to 2 h. This is as a result of the fact that in the reaction where 2-octene was used as a substrate (Figure 3.11), the internal olefin was already present at a much higher concentration than compared to after 1 h in Figure 3.9. Furthermore, as shown in Figure 3.9, a mixture of 2-, 3-, and 4-octene is present in the reaction mixture. However, what this experiment is demonstrating is that the hydroformylation of internal olefins is indeed slower than their terminal analogues.

The regioselectivity obtained from the hydroformylation of 2-octene is shown in Figure 3.12.

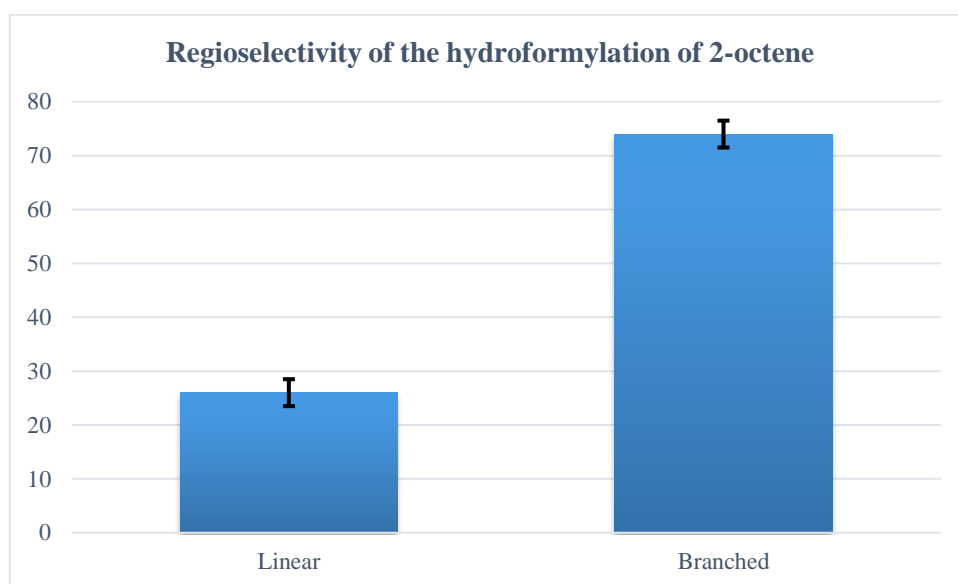


Figure 3.12: Regioselectivity of the hydroformylation of 2-octene. 2-Octene (6.37 mmol), 30 bar CO:H₂ (1:1), 75 °C and 0.05 mol% of C2 (Catalyst:substrate 1:2000), 2 h.

Interestingly, this shows that linear aldehydes is also formed. Linear aldehydes can only form from terminal olefins. Therefore, linear aldehydes form in a two-step process involving initial alkene isomerization followed by hydroformylation.²² Thus, the 2-octene undergoes isomerization to 1-octene which is then subsequently hydroformylated to the linear aldehyde. Figure 3.11 shows that 1-octene is indeed formed.

3.2.3 Effect of pressure on the hydroformylation of 1-octene

Next, the influence of the total pressure on catalytic activity, chemo- and regioselectivity was investigated (Figures 3.13 and 3.14).

Although pressure had no significant effect on the conversion of the substrate, it did influence the chemoselectivity. With an increase in pressure, there is a decrease in isomerization of 1-octene to internal octenes with a concomitant increase in the amount of aldehydes. This is consistent with literature and can be explained in terms of the accepted mechanism of the hydroformylation reaction (Figure 3.1).²²⁻²⁴ Once the metal-alkyl species (linear or branched) forms, it can either undergo

Chapter 3: Hydroformylation of 1-Octene by Iminopyridyl Rh(I) Complexes

carbonylation producing the aldehydes or β -hydride elimination leading to the isomerization of the olefin. With an increase in pressure, the concentration of CO increases and this therefore favours the carbonylation reaction leading to more aldehydes at higher pressures. The pressure had no significant influence on the hydrogenation of the olefin to alkane (octane).

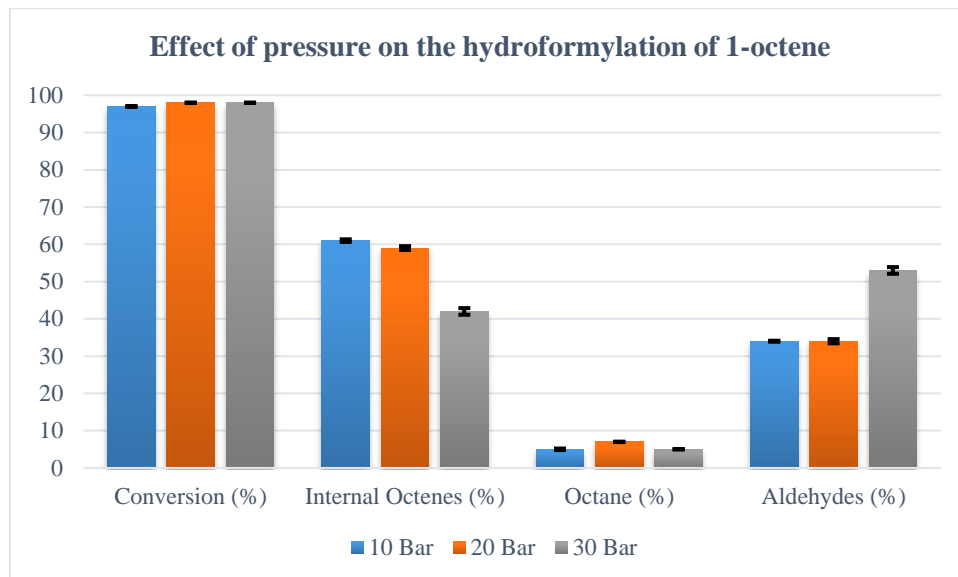


Figure 3.13: Effect of pressure. 1-Octene (6.37 mmol), CO:H₂ (1:1), 1 h, 75 °C and 0.05 mol % of C2 (Catalyst:substrate 1:2000).

The influence of the pressure on the regioselectivity is shown in Figure 3.14.

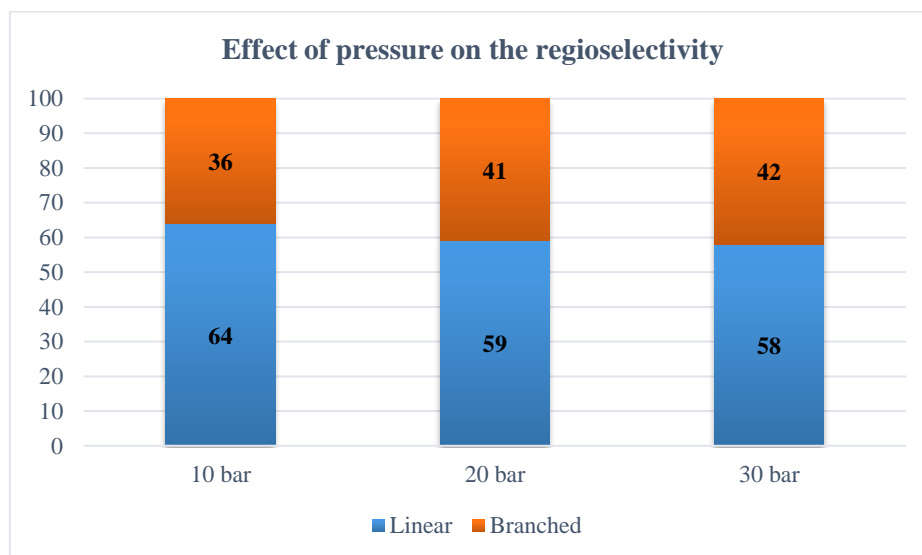


Figure 3.14: Effect of pressure on regioselectivity. 1-Octene (6.37 mmol), CO:H₂ (1:1), 1 h, 75 °C and 0.05 mol% of C2 (Catalyst:substrate 1:2000).

As the total pressure is increased, more branched aldehydes are produced relative to the linear aldehyde. This is as a result of higher CO partial pressures, favouring the carbonylation reaction relative to the β -hydride elimination reaction. Therefore, the branched rhodium-alkyl species is more likely to undergo carbonylation (producing the branched aldehydes) than to undergo β -hydride elimination (producing

Chapter 3: Hydroformylation of 1-Octene by Iminopyridyl Rh(I) Complexes

isomerized olefins). This is thus consistent with the effect of pressure on the chemoselectivity (Figure 3.13).²²⁻²⁴ Furthermore, 2-octene can also give rise to linear aldehyde via alkene isomerization-hydroformylation, which could possibly explain why there is not a significant increase in the branched aldehydes (Figure 3.11-3.12).²²

3.2.4 Effect of temperature on the hydroformylation of 1-octene

Lower conversions are obtained at lower temperatures (55 °C), however, at 65 °C full conversion of the substrate is obtained (Figure 3.15). Temperature also had a significant effect on the chemoselectivity of the reaction. As the temperature is increased, isomerization of 1-octene increased, in accordance with literature.²⁵ The isomerization process has a higher activation energy compared to hydroformylation and therefore is facilitated when experiments are conducted at higher temperatures.²⁶

This also holds true for the hydrogenation of olefins to alkanes since a marginal increase in the amount of octane occurred upon increasing the temperature. As a result, higher chemoselectivities towards aldehydes are obtained at lower temperature.

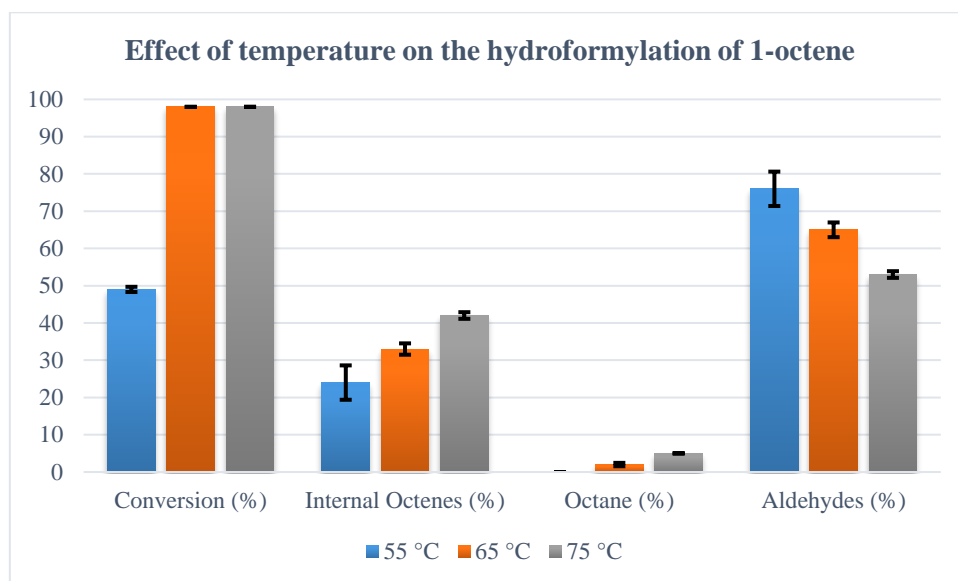


Figure 3.15: Effect of temperature on conversion and chemoselectivity. 1-Octene (6.37 mmol), 30 bar CO:H₂ (1:1), 1 h and 0.05 mol % of **C2** (Catalyst:substrate 1:2000).

In terms of the regioselectivity, the linear aldehyde predominates at lower temperatures as can be seen in Figure 3.16. As mentioned previously, the linear aldehyde is derived from a linear rhodium-alkyl species. The branched rhodium-alkyl species is thermodynamically more stable and thus becoming more prevalent at higher temperatures.²⁷ As a result, more branched aldehydes are produced at higher temperatures.²⁵

Chapter 3: Hydroformylation of 1-Octene by Iminopyridyl Rh(I) Complexes

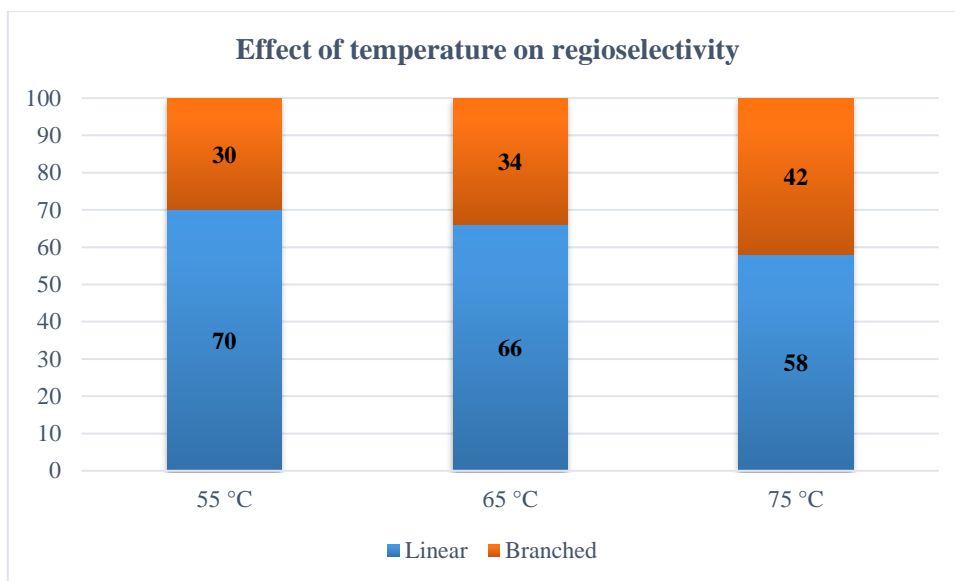


Figure 3.16: Effect of temperature on regioselectivity. 1-Octene (6.37 mmol), 30 bar CO:H₂ (1:1), 1 h and 0.05 mol % of C2 (Catalyst:substrate 1:2000).

3.2.5 Effect of time on the hydroformylation of 1-octene at 65 °C

Performing the hydroformylation reaction for 30 min resulted in a much lower conversion of ~62%. After 30 min, ~60% aldehydes are obtained which increases to ~65% after an hour while the level of internal octenes display a decrease. This seems to indicate that between 30-60 min, full conversion of 1-octene is achieved after which the catalyst starts converting internal octenes slowly. As a result of this, more branched aldehydes are formed after 60 min, as can be seen in Figure 3.18. Since the internal octenes are less reactive than the terminal octenes, they are converted at a much slower rate.

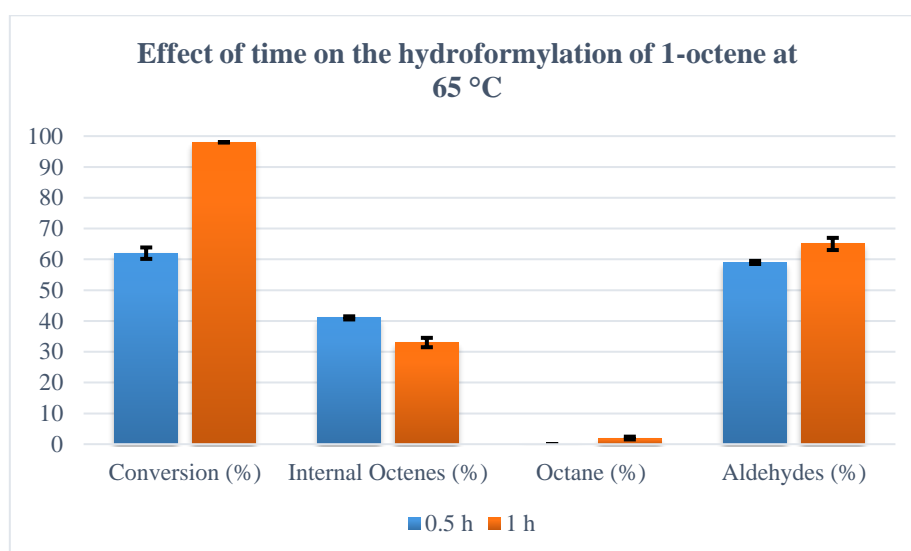


Figure 3.17: Effect of time at 65°C. 1-Octene (6.37 mmol), 30 bar CO:H₂ (1:1), 65 °C and 0.05 mol % of C2 (Catalyst:substrate 1:2000).

Chapter 3: Hydroformylation of 1-Octene by Iminopyridyl Rh(I) Complexes

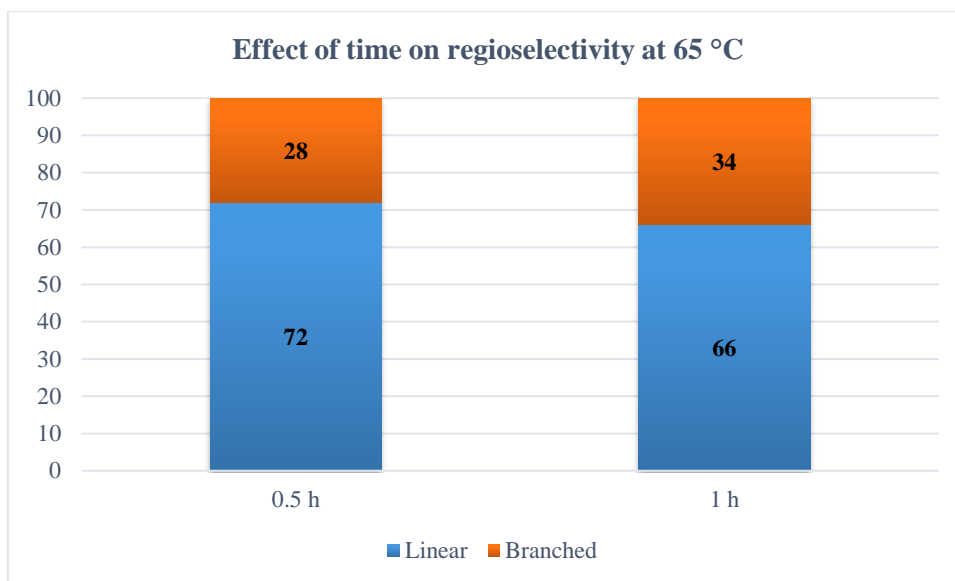


Figure 3.18: Effect of time at 65°C on regioselectivity. 1-Octene (6.37 mmol), 30 bar CO:H₂ (1:1), 65 °C and 0.05 mol % of **C2** (Catalyst:substrate 1:2000).

3.2.6 Comparing the catalytic activity of **C1** with that of **C2**

Since moderate catalytic activity was obtained for **C2** at 65 °C and performing the reaction for 30 min, another catalyst precursor was also evaluated under these conditions in order to determine whether the fluorine substituent has an effect on the catalytic activity. We have previously investigated the effect of the substituents (F, OH and CH₃, **section 3.2.1**), however, since we obtained full conversion of the substrate, we were unable to determine the effect of the substituents. Therefore, we evaluated **C1** as a catalyst precursor in the hydroformylation of 1-octene under 30 bar CO:H₂ (1:1), 65 °C, 0.5 h and 0.05 mol%. The catalytic activity was then compared to the catalytic activity obtained using **C2** (Figure 3.19-3.20).

Catalyst precursors **C1** and **C2** were compared under the following conditions (30 bar CO:H₂, 65 °C, 30 min and 0.05 mol% catalyst loading) to determine if the ligand exerts any effect on the catalytic activity. This was investigated previously under **section 3.2.1**, but due to the fact that all catalysts registered full conversion of the substrate, we were unable to draw any conclusions from this. However, under these conditions, moderate conversion of the substrate is obtained (~60 %). From Figures 3.19-3.20 we can conclude that the ligand essentially has no effect on the catalytic activity even though **C2** bears an electron withdrawing fluorine substituent on the phenyl group attached to the imine nitrogen.

Chapter 3: Hydroformylation of 1-Octene by Iminopyridyl Rh(I) Complexes

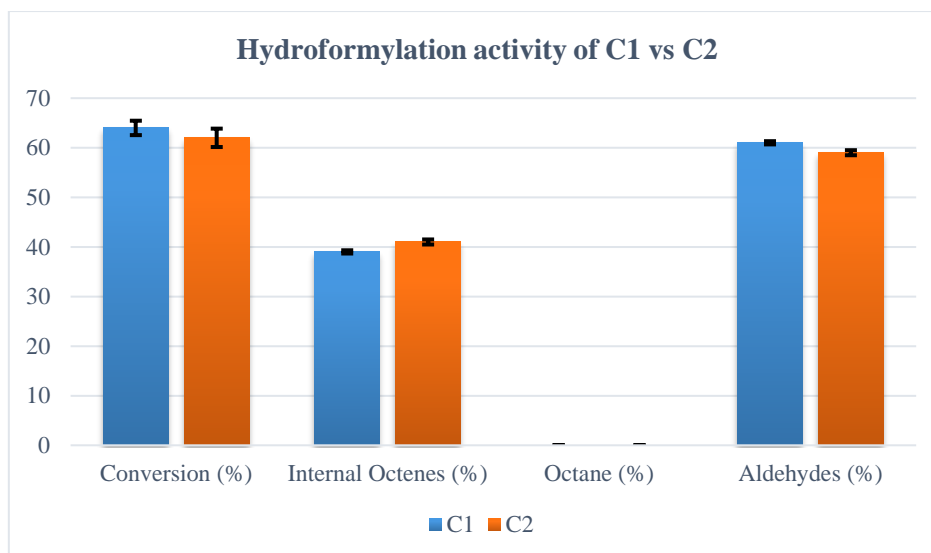


Figure 3.19: Comparing **C1** and **C2**. 1-Octene (6.37 mmol), 30 bar CO:H₂ (1:1), 65 °C, 30 min and 0.05 mol % (Catalyst:substrate 1:2000).

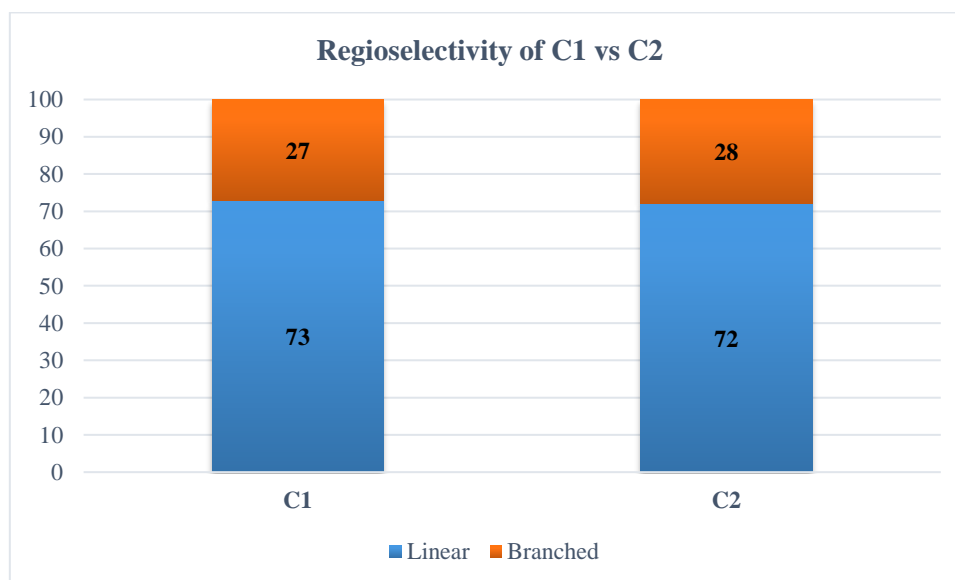


Figure 3.20: Comparing **C1** and **C2**. 1-Octene (6.37 mmol), 30 bar CO:H₂ (1:1), 65 °C, 30 min and 0.05 mol % (Catalyst:substrate 1:2000).

3.3 Hydroformylation using paraformaldehyde as syngas surrogate

The use of syngas surrogates have previously been investigated as a potential alternative to CO and H₂ as a result of the toxicity, safety and economic implications associated with the use of syngas. A number of syngas surrogates for use in carbonylations have been investigated previously. These include the use of formic acid, methanol, a methyl formate-water mixture and paraformaldehyde/formalin.²⁸⁻²⁹ Formic acid, in particular, is an attractive surrogate since it is a potential bio-renewable resource, however, this process normally requires elevated temperatures. Similarly, MeOH and methyl formate also requires high temperatures while in the case of methyl formate, water is needed for the WGS (water-gas-shift) reaction. Formaldehyde is thus a much more viable option to use in hydroformylation since no

Chapter 3: Hydroformylation of 1-Octene by Iminopyridyl Rh(I) Complexes

additional additives (such as LiCl salts) are required and the reactions are normally carried out around 100 °C.²⁹

Aldehydes, such as formaldehyde, can oxidatively add to a Rh-metal centre. This led to the discovery by Tsuji and Ohno that aldehydes can be decarbonylated by the Wilkinson's catalyst, $\text{RhCl}(\text{PPh}_3)_3$.³⁰⁻³¹ This mostly produces paraffins, however, both terminal and internal olefins (as a result of β -hydride elimination of the Rh-alkyl) can also form. Madsen and co-workers³² combined experiments with theory in order to elucidate the mechanism of the aldehyde decarbonylation reaction, which is shown in Figure 3.21. The first step in this reaction is the coordination of the aldehyde, via a CO substitution reaction. Oxidative addition of the aldehyde then occurs producing a Rh-H and a Rh-acyl species. This is followed by migratory extrusion of a CO ligand and reductive elimination of benzene, regenerating the active species.³²

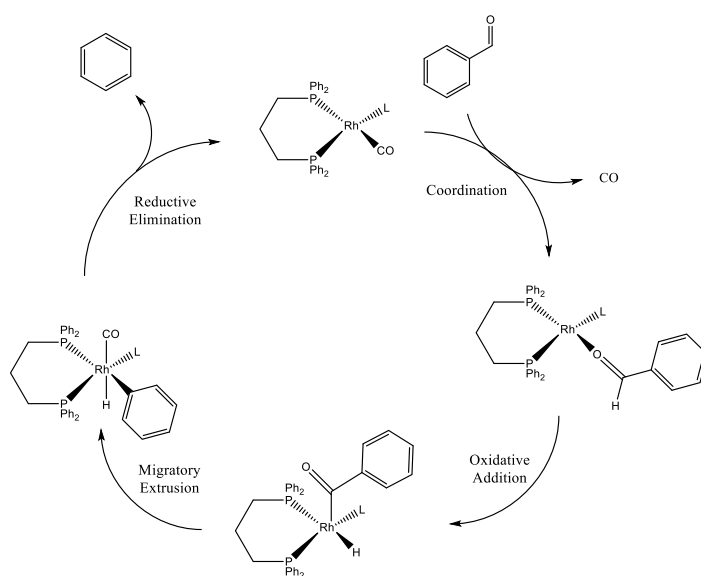


Figure 3.21: Mechanism of the decarbonylation of aldehydes³²

Chapter 3: Hydroformylation of 1-Octene by Iminopyridyl Rh(I) Complexes

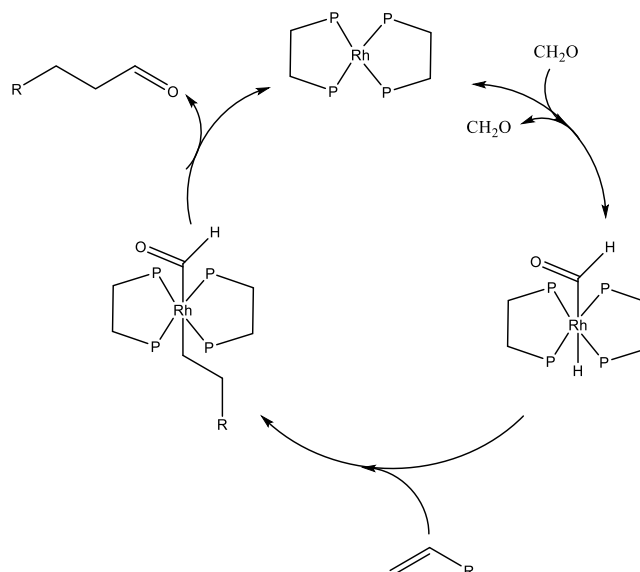


Figure 3.22: Aldehyde formation from olefin and formaldehyde³⁴

Similarly, formaldehyde can also undergo decarbonylation, thus producing CO and H₂ which can be used in the hydroformylation reaction. Two pathways are possible for the hydroformylation of olefins with formaldehyde. The CO and H₂ produced during the catalytic decomposition of formaldehyde can be used in the conventional hydroformylation mechanism shown earlier in Figure 3.1. However, work conducted by Meng³³ and Rosales³⁴ showed that aldehydes can also be produced without the formation of free CO, as shown in Figure 3.22. Instead, coordination of formaldehyde occurs followed by oxidative addition to form a Rh-H and a Rh-formyl species. Subsequent coordination of the olefin then occurs followed by its insertion into the Rh-H bond to form a Rh-alkyl species. The aldehyde is then produced after reductive elimination of the alkyl and the formyl moieties.³⁴

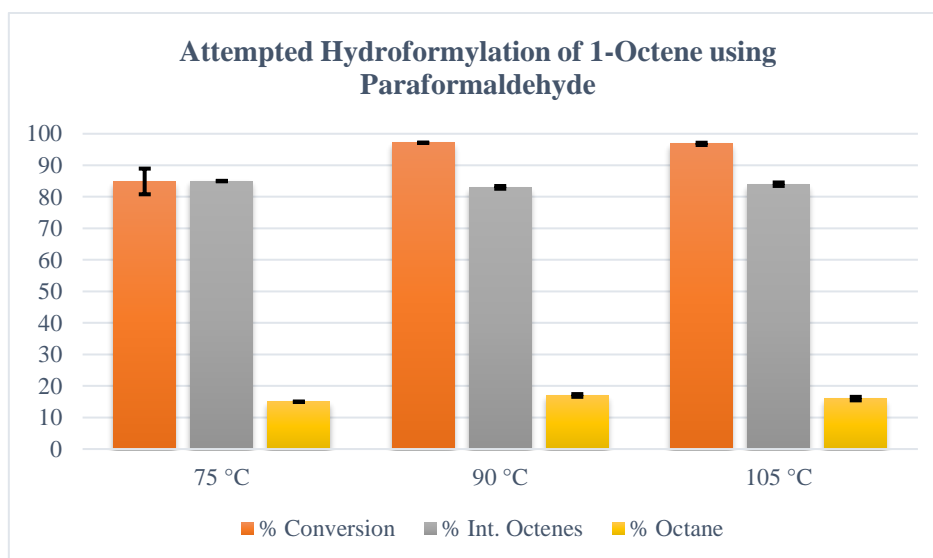


Figure 3.23: Attempted hydroformylation of 1-Octene. 1-Octene (1.4 mmol), CI (0.5 mol%), Paraformaldehyde (5 eq), Toluene (3 ml), 6 h

Chapter 3: Hydroformylation of 1-Octene by Iminopyridyl Rh(I) Complexes

In view of this, we evaluated **C1** as a potential catalyst precursor for the hydroformylation of 1-octene using paraformaldehyde (Figure 3.23). We evaluated **C1** at three different temperatures, however in all instances no aldehyde products were obtained. Instead, 1-octene underwent isomerization (~80 %) to its internal counterparts (2-, 3- and 4-octene) and hydrogenation to octane (~20 %). The presence of these products seems to indicate that during the course of the reaction, a Rh-H species was formed since this is required for isomerization and hydrogenation activity.

HRhCO(PPh₃)₃ was then also evaluated as catalyst since it has been shown previously³⁵ to be able to catalyze this process (Table 3.1), however, similar results in terms of the product distribution (internal olefins and paraffins) was obtained even in the presence of excess triphenylphosphine ligand. A blank experiment, in the absence of the catalyst, was also performed. No activity was obtained in the absence of catalyst, confirming that the catalyst is necessary for the isomerization and hydrogenation reactions.

Table 3.1: Attempted hydroformylation using HRhCO(PPh₃)₃

Entry	Catalyst	Temperature (°C)	PPh ₃ (eq)	Conversion (%)	Internal Octenes (%)	Octane (%)
1	Blank	65	~	~	~	~
2	HRhCO(PPh ₃) ₃	65	~	47	86	14
3	HRhCO(PPh ₃) ₃	65	5	44	87	13
4	HRhCO(PPh ₃) ₃	100	5	82	90	10

1-Octene (1.4 mmol), HRhCO(PPh₃)₃ (6.4 mg, 0.007 mmol), PPh₃ (9.2 mg, 0.035 mmol), Paraformaldehyde (5 eq relative to substrate), THF (3 ml), 6 h.

Rosales and co-workers³⁴ showed that it is possible to form di-hydride metal complexes from formaldehyde with the release of a CO ligand (Figure 3.24).

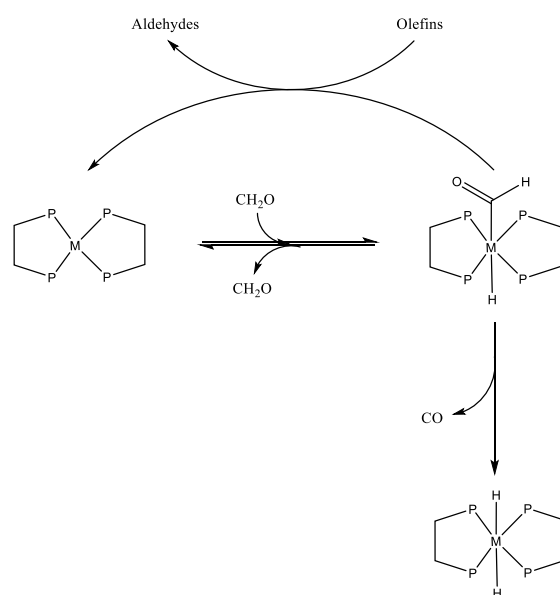


Figure 3.24: Hydroformylation with formaldehyde and M-H₂ formation³⁴

Chapter 3: Hydroformylation of 1-Octene by Iminopyridyl Rh(I) Complexes

Therefore, we believe that this is also likely for **C1** which could account for the observed isomerization and hydrogenation activity. Therefore, we can potentially conclude that in our case the formaldehyde is rather a source of H₂, with the complex unable to use the CO as a result of the low pressure generated upon release of CO.

3.4 Conclusion

We evaluated four catalyst precursors (**C1-C4**) in the hydroformylation of 1-octene. We found that the substituents (F, OH and CH₃) has minimal effect on the catalytic activity, chemoselectivity and regioselectivity. The effect of pressure and temperature was also investigated. At low pressure (10 bar), isomerization of the olefin predominates and as a result, higher regioselectivities towards the linear aldehyde are obtained. As the temperature was increased, the conversion of the substrate increases. Comparing the product distributions at 65 °C with that obtained at 75 °C, superior chemoselectivity towards the aldehyde are obtained at the lower temperature since at the higher temperature isomerization of the olefin is much more competitive. As a result of this, slightly better regioselectivities towards the linear aldehyde are obtained at the lower temperature. Lastly, we can conclude that the optimum conditions for this reaction is 30 bar CO:H₂ (1:1), 65 °C, 0.5-1 h and 0.05 mol%.

The hydroformylation of 1-octene was also attempted using formaldehyde as a syngas surrogate. Complete conversion of the substrate was obtained, however, only internal octenes (~80 %) and octane (~20 %) was obtained. This was subsequently attributed to the low pressure of syngas generated during the decomposition of formaldehyde as well as the potential formation of a Rh di-hydride complex.

3.5 Experimental Section

General Methods and Materials

All of the reagents and standards were purchased from either Merck or Sigma Aldrich and were used without further purification. Solvents were purchased from Merck or Kimix, and were purified by a Pure SolvTM Micro solvent purifier equipped with activated alumina columns.

Syngas (CO:H₂, 1:1) was purchased from Afrox and used as is.

Instrumentation

Catalytic reactions were performed in a 50 ml Amar reactor equipped with a Teflon liner. Catalytic reactions were monitored using a Varian 3800 Gas Chromatograph containing a Petrocol DH 50.2 (50 m x 0.2 mm x 0.5 μm) column equipped with a FID detector. Temperature program: 80 °C (6 min hold), 100 °C (10 °C/min), 100 °C (10 min hold), 220 °C (20 °C/min), 220 °C (10 min hold), with total run time of 34 min. Helium was used as carrier gas at constant flow with a 1.1 ml/min flowrate. P-Xylene was used as the internal standard.

Chapter 3: Hydroformylation of 1-Octene by Iminopyridyl Rh(I) Complexes

Catalytic Procedure and Analysis

The following procedure describes a representative example of a typical hydroformylation reaction and its analysis using GC-FID. All experiments were performed in duplicate:

The reactor was charged with toluene (5 ml) and the appropriate amount of the catalyst precursor to yield a suspended mixture containing a total amount of 0.0032 mmol of rhodium. 1-Octene (6.37 mmol, 1 ml) was added resulting in a Rh:substrate ratio of 1:2000. The reactor was purged with 10 bar syngas three times after which the reactor was pressurized up to the required pressure and time and the heating started. At the conclusion of the reaction, the reactor was cooled in an ice-water bath for 30 min. After quenching, the reactor was degassed and the reaction mixture filtered using a syringe filter. 0.15 ml of the reaction mixture, 0.05 ml p-xylene (internal standard) and 0.8 ml Toluene were transferred to a GC vial and submitted for analysis. Substrate conversion, product distributions and chemo – and regioselectivities were calculated relative to the internal standard.

The following procedure describes a representative example of a typical reaction with formaldehyde as syngas surrogate and its analysis using GC-FID. All experiments were performed in duplicate:

The reactor was charged with toluene (3 ml) and the appropriate amount of the catalyst precursor to yield a suspended mixture containing a total amount of 0.007 mmol of rhodium. 0.22 ml 1-octene (1.4 mmol) was added resulting in a Rh:substrate ratio of 1:200. The reactor was then heated to the appropriate temperature and the reaction continued for the appropriate time. At the conclusion of the reaction, the reactor was cooled in an ice-water bath for 30 min. After quenching, the reaction mixture was filtered using a syringe filter. 0.15 ml of the reaction mixture, 0.05 ml p-xylene (internal standard) and 0.8 ml Toluene were transferred to a GC vial and submitted for analysis. Substrate conversion, product distributions and chemo – and regioselectivities were calculated relative to the internal standard.

3.6 References

1. G. M. Torres, R. Frauenlob, R. Franke and A. Börner, *Catal. Sci. Technol.*, 2015, **5**, 34-54.
2. R. Franke, D. Selent and A. Börner, *Chem. Rev.*, 2012, **112**, 5675-5732.
3. G. T. Whiteker and C. J. Cobley, *Top. Organomet. Chem.*, 2012, **42**, 35-46.
4. P. C. J. Kamer, A. van Rooy, G. C. Schoemaker and P. W. N. M. van Leeuwen, *Coord. Chem. Rev.*, 2004, **248**, 2409-2424.
5. Z. Xie, G. R. Akien, B. R. Sarkar, B. Subramaniam and R. V. Chaudhari, *Ind. Eng. Chem. Res.*, 2015, **54**, 10656-10660.
6. A. Schmied, A. Straube, T. Grell, S. Jähnigen and E. Hey-Hawkins, *Dalton Trans.*, 2015, **44**, 18760-18768.
7. Z. Yu, M. S. Eno, A. H. Annis and J. P. Morken, *Org. Lett.*, 2015, **17**, 3264-3267.

Chapter 3: Hydroformylation of 1-Octene by Iminopyridyl Rh(I) Complexes

8. J. Pospech, I. Fleischer, R. Franke, S. Buchholz and M. Beller, *Angew. Chem. Int. Ed.*, 2013, **52**, 2852-2872.
9. J. Mormul, M. Mulzer, T. Rosendahl, F. Rominger, M. Limbach and P. Hofmann, *Organometallics*, 2015, **34**, 4102-4108.
10. A. A. Dabbawala, R. V. Jasra and H. C. Bajaj, *Catal. Commun.*, 2011, **12**, 403-407.
11. C. W. Kohlpaintner, R. W. Fischer and B. Cornils, *Appl. Catal., A*, 2001, **221**, 219-225.
12. T. E. Kunene, P. B. Webb and D. J. Cole-Hamilton, *Green Chem.*, 2011, **13**, 1476-1481.
13. M. Haumann, M. Jakuttis, S. Werner and P. Wasserscheid, *J. Catal.*, 2009, **263**, 321-327.
14. S. Chen, Y. Li, Y. Wang, Z. Zhao, Y. Liu, *J. Mol. Catal. Chem.*, 2015, **396**, 68-76.
15. I. D. Kostas and C. G. Screttas, *J. Organomet. Chem.*, 1999, **585**, 1-6.
16. J. October and S. F. Mapolie, *J. Organomet. Chem.*, 2017, **840**, 1-10.
17. S. Siangwata, N. Baartzes, B. C. E. Makhubela and G. S. Smith, *J. Organomet. Chem.*, 2015, **796**, 26-32.
18. B. C. E. Makhubela, A. M. Jardine, G. Westman and G. S. Smith, *Dalton Trans.*, 2012, **41**, 10715-10723.
19. W. Alsalahi and A. M. Trzeciak, *J. Mol. Catal. Chem.*, 2015, **408**, 147-151.
20. P. C. J. Kamer, P. W. N. M. van Leeuwen and J. N. H. Reek, *Acc. Chem. Res.*, 2001, **34**, 895-904.
21. R. Lazzaroni, G. Uccello-Barretta and M. Benetti, *Organometallics*, 1989, **9**, 2323-2327.
22. L. Zhang, C. Li, X. Zheng, H. Fu, H. Chen and R. Li, *Catal. Lett.*, 2014, **144**, 1074-1079.
23. F. Zhou, L. Zhang, Q. Wu, F. Guo, S. Tang, B. Xu, M. Yuan, H. Fu, R. Li, Z. Zheng and H. Chen, *Appl. Organometal. Chem.*, 2019, **33**, 1-10.
24. C. Williams, M. Ferreira, E. Monflier, S. F. Mapolie and G. S. Smith, *Dalton Trans.*, 2018, **47**, 9418-9429.
25. W. Han, S. Qin, X. Shu, Q. Wu, B. Xu, R. Li, Z. Zheng and H. Chen, *RSC Adv.*, 2016, **6**, 53012-53016.
26. C. A. Tolman and J. W. Faller, *Mechanistic Studies of Catalytic Reactions Using Spectroscopic and Kinetic Techniques*, Plenum Press, New York, 1983.
27. L. Routaboul, C. Buch, H. Klein, R. Jackstell and M. Beller, *Tetrahedron Lett.*, 2005, **46**, 7401-7405.
28. G. Jenner, E. M. Nahmed and S/ Libs-Konrath, *J. Mol. Catal.*, 1991, **64**, 337-347.
29. L. Wu, Q. Liu, R. Jackstell and M. Beller, *Angew. Chem. Int. Ed.*, 2014, **53**, 6310-6320.
30. J. Tsuji and K. Ohno, *Tetrahedron Lett.*, 1965, **6**, 3969-3971.
31. K. Ohno and J. Tsuji, *J. Am. Chem. Soc.*, 1968, **90**, 99-107.
32. P. Fristrup, M. Kreis, A. Palmelund, P. Norrby and R. Madsen, *J. Am. Chem. Soc.*, 2008, **130**, 5206-5215.
33. F. Wang, Q. Meng and M. Li, *Int. J. Quantum Chem.*, 2010, **110**, 850-859.

Chapter 3: Hydroformylation of 1-Octene by Iminopyridyl Rh(I) Complexes

34. M. Rosales, H. Pérez, F. Arrieta, R. Izquierdo, C. Moratinos and P. J. Baricelli, *J. Mol. Catal. A: Chem.*, 2016, **421**, 122-130.
35. H. S. Ahn, S. H. Han, S. J. Uhm, W. K. Seok, H. N. Lee and G. A. Korneeva, *J. Mol. Catal. A: Chem.*, 1999, **144**, 295-306.

Chapter 4: Hydroaminomethylation of Olefins with Primary and Secondary Amines

4.1 Introduction

The synthesis of nitrogen-containing compounds is important since these types of compounds find application in various fields ranging from pharmaceuticals, cosmetics and other fine-chemicals. Various methods of amine synthesis are known, including the reduction of unsaturated nitrogen-containing compounds, alkylation of ammonia as well as primary and secondary amines, Gabriel synthesis, Beckman rearrangement of oximes and Schmidt degradation of acyl azides obtained from carboxylic acids.¹⁻⁵ Most of these methods involve the use of corrosive acids and bases (HCl, H₂SO₄ and KOH) and strong reducing agents (LiAlH₄). Some procedures are also associated with the production of corrosive by-products. As a result of this, more environmentally friendly processes are constantly being sought. A few processes which can be regarded as being environmentally more friendly include catalytic nucleophilic substitution reactions of alcohols using N-containing nucleophiles, reductive amination of carbonyls, hydroamination and hydroaminomethylation.⁶⁻⁹ Of these processes, we were particularly interested in the hydroaminomethylation reaction due to our prior work on hydroformylation with analogous Rh complexes.

Hydroaminomethylation was discovered by Reppe at BASF.⁹ It is a tandem, one-pot reaction consisting of the initial hydroformylation of olefins to aldehydes, followed by the condensation of the aldehydes with primary/secondary amines to produce imine/enamine intermediates. These imine/enamine intermediates are then reduced to amines by the same catalyst responsible for the initial hydroformylation reaction.⁹ A general hydroaminomethylation scheme is shown in Figure 4.1.

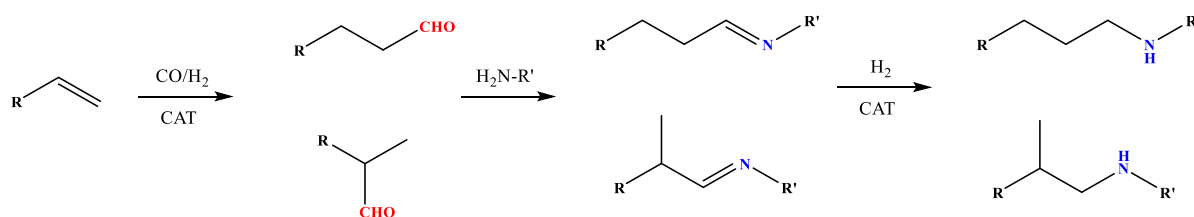


Figure 4.1: A general hydroaminomethylation reaction

Hydroaminomethylation is an attractive alternative for the synthesis of amines as a result of its atom-efficiency, producing only water as a by-product.⁹ One of the main requirements for hydroaminomethylation is that the catalyst needs to be active for both the hydroformylation reaction while it should also selectively reduce the imine/enamine intermediates in the presence of other reducible compounds such as the olefins and aldehydes. The reaction is further complicated by the fact

Chapter 4: Hydroaminomethylation of Olefins with Primary and Secondary Amines

that in some instances the hydroformylation and the hydrogenation reactions require different reaction conditions (especially as far as temperature is concerned) and therefore careful optimization of reaction conditions are required in order to limit competing reactions.

In the last decade or so, a few reports have appeared in which hydroaminomethylation was used to produce compounds useful as polymer precursors, surfactants and pharmaceuticals. This highlights the potential of this reaction for the production of value-added chemicals.¹⁰⁻¹² In light of this, we decided to study the hydroaminomethylation of 1-octene in the presence of both secondary (piperidine) and primary amines (aniline and benzylamine).

4.2 Hydroaminomethylation of 1-octene and piperidine catalyzed by Rh(I) catalyst precursors

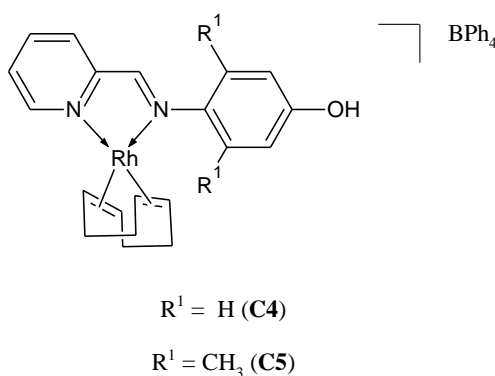


Figure 4.2: Catalyst precursors used in the hydroaminomethylation reaction

The hydroaminomethylation of 1-octene and piperidine, shown in Figure 4.3, was studied using the catalyst precursors shown in Figure 4.2. The initial reaction conditions were 30 bar CO:H_2 (1:1), 75 °C, 0.1 mol% catalyst loading and reaction times varying between 1 and 2 hours.

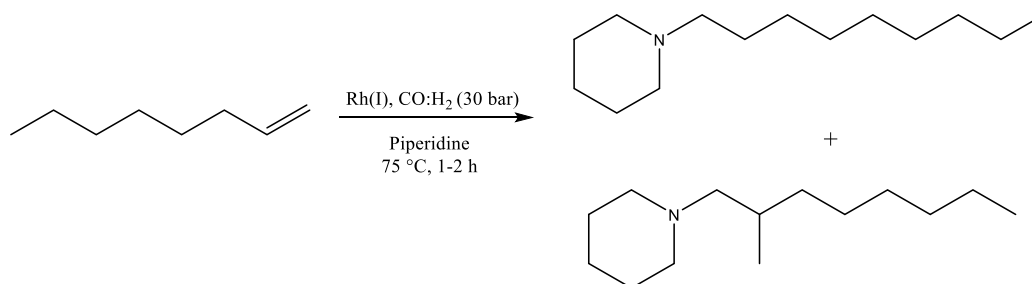


Figure 4.3: Hydroaminomethylation of 1-octene with piperidine

In Figure 4.4, the major aldehydes and enamine intermediates which form in the hydroaminomethylation of 1-octene and piperidine are shown. Additionally, the 1-octene is also prone to isomerization to form internal octenes as well as hydrogenation to octane. Furthermore, the possibility also exists that the aldehydes can be reduced to alcohols.

Chapter 4: Hydroaminomethylation of Olefins with Primary and Secondary Amines

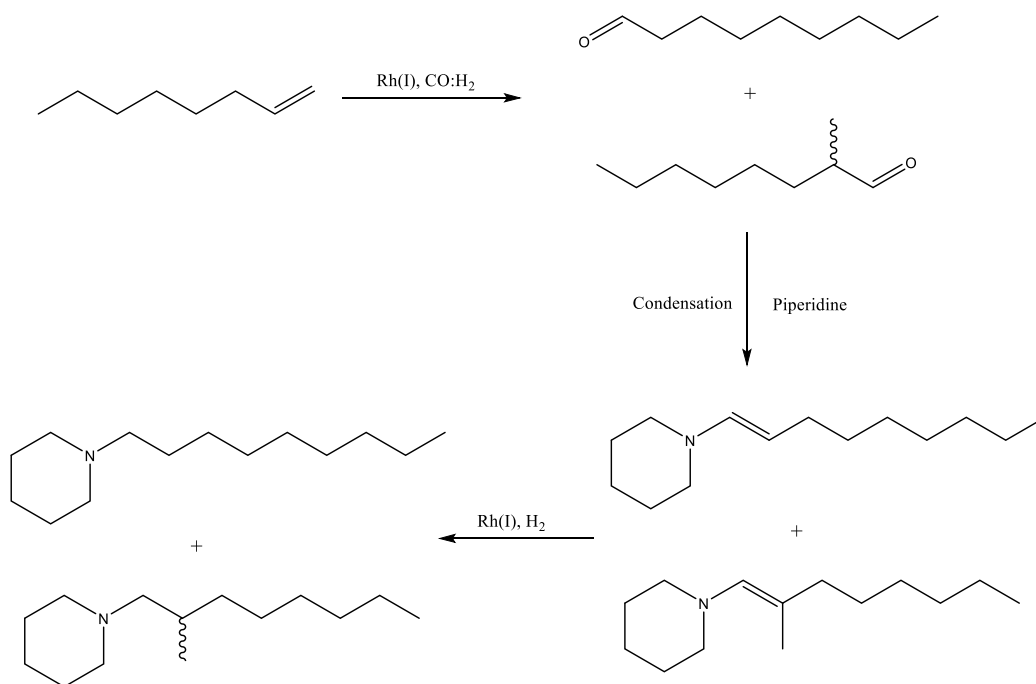


Figure 4.4: The aldehyde and enamine intermediates in the hydroaminomethylation of 1-Octene and Piperidine

4.2.1 Influence of catalyst loading on catalytic activity

As a point of departure, we evaluated the influence of the catalyst amount on the hydroaminomethylation of 1-octene in the presence of piperidine, with the results shown in Figure 4.5 and Table 4.1.

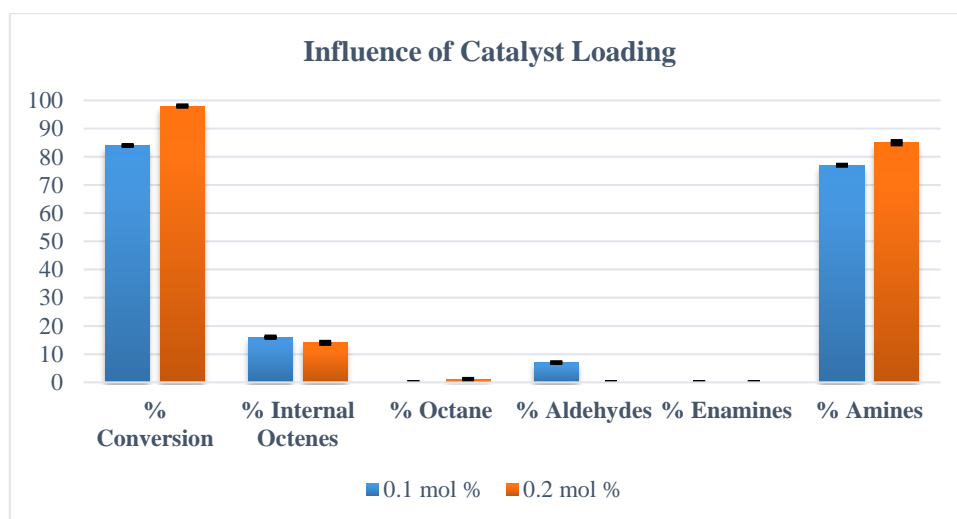


Figure 4.5: Influence of catalyst loading using C4. 1-Octene (1.6 mmol), Piperidine (1.6 mmol), Toluene (5 ml), 30 bar CO:H₂ (1:1), 75 °C, 2 h.

With an increase in the catalyst loading from 0.1 to 0.2 mol%, the conversion of 1-octene as well as the yield of amines increased, as can be seen in Figure 4.5. This is attributed to the higher concentration of the catalyst, thus facilitating faster consumption of the olefin as well as faster generation of the target amines. However, based on the TON's, which is displayed in Table 4.1, hydroaminomethylation is

Chapter 4: Hydroaminomethylation of Olefins with Primary and Secondary Amines

more efficient at a catalyst loading of 0.1 mol%, proceeding at a TON of 642 towards the target amines. Although aldehyde intermediates remained when using the 0.1 mol% catalyst loading, this catalyst loading was selected for further reaction condition optimization. It was found that the remaining aldehyde fraction was exclusively branched in nature. This was attributed to the higher reactivity of the linear aldehydes in reductive amination, resulting in these being consumed much faster in comparison to their branched analogues.^{9b} Furthermore, a higher regioselectivity towards the linear amine (1-nonylpiperidine) is obtained at a catalyst loading of 0.1 mol% compared to a loading of 0.2 mol%. At a loading of 0.1 mol%, a fair amount of branched aldehyde was still present and this can subsequently be converted to branched amines. This will increase the regioselectivity to the branched product. At this point, the level of branched product will be similar to what was obtained at 0.2 mol% catalyst loading.

Table 4.1: Influence of catalyst loading on the regioselectivity and TON^a

Cat. Loading (mol %)	Regioselectivity		TON ^d
	L:b (Aldehydes) ^b	L:b (Amines) ^c	
0.1	0:100	75:25	642
0.2	~	65:35	416

^a1-Octene (1.6 mmol), Piperidine (1.6 mmol), Toluene (5 ml), 30 bar CO:H₂ (1:1), 75 °C, 2 h.

^bL:b (aldehydes) (linear aldehydes:branched aldehydes)

^cL:b (amines) (linear amines:branched amines)

^dTON = moles amines/moles Rh(I)

4.2.2 Influence of time on the catalytic activity

The hydroaminomethylation of 1-octene in the presence of piperidine was evaluated at different reaction times (1 to 2 h) in order to monitor the progress of the reaction (Figure 4.6 and Table 4.2).

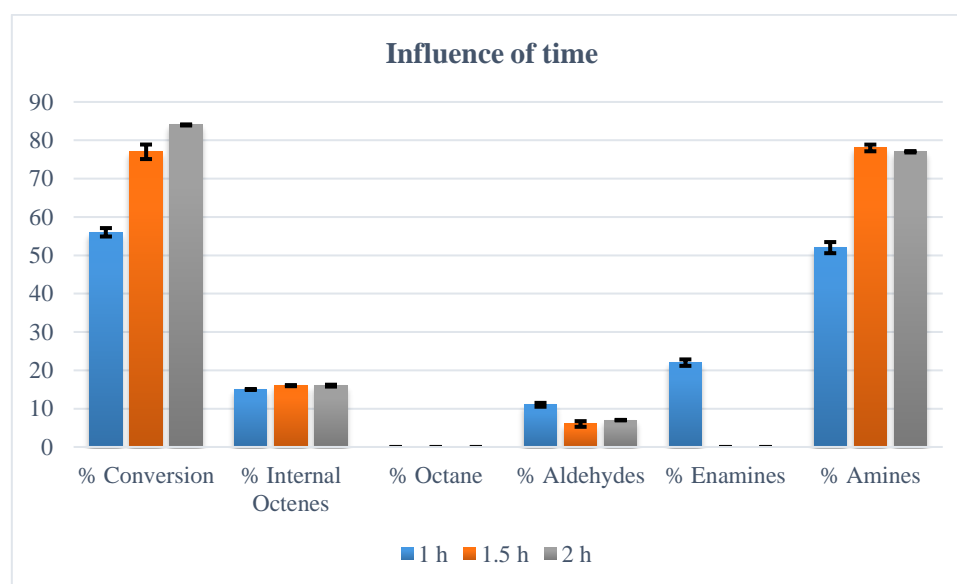


Figure 4.6: Influence of reaction time on the hydroaminomethylation of 1-Octene and Piperidine. 1-Octene (1.6 mmol), Piperidine (1.6 mmol), 0.1 mol% catalyst loading (C4), Toluene (5 ml), 30 bar CO:H₂ (1:1), 75 °C.

Chapter 4: Hydroaminomethylation of Olefins with Primary and Secondary Amines

The catalytic activity increased as the reaction time was extended from 1 to 2 h, as indicated by the conversion of the substrate (Figure 4.6) and the TON's displayed in Table 4.2, as more time was allowed for the substrate to react. It was further found that the amount of internal octenes remained fairly constant (< 20 %) between 1 to 2 h. Since the conversion of internal octenes are far slower than the conversion of terminal octenes, it would seem to indicate that the internal octenes are formed early on in the reaction. It would appear that the catalyst only start converting internal octenes in large amounts once all terminal octenes have been consumed. Furthermore, amines were found to be the major products (~50-80 %) formed between 1 to 2 h, while ~5-10 % aldehyde intermediates still remained after this time. Moreover, enamines were only observed after about an hour into the reaction. These were subsequently completely hydrogenated to the corresponding amines with the process being completed between 1.5 to 2 h. The hydrogenation of 1-octene to octane and the hydrogenation of the aldehydes to the corresponding alcohols were not observed, with the catalyst selectively hydrogenating only the enamines to amines.

Table 4.2: Regioselectivity and TON at different reaction times^a

t (h)	Regioselectivity		TON ^d
	L:b (Aldehydes) ^b	L:b (Amines) ^c	
1	0:100	83:17	291
1.5	0:100	76:24	599
2	0:100	75:25	642

^a1-Octene (1.6 mmol), Piperidine (1.6 mmol), 0.1 mol% catalyst loading (C4), Toluene (5 ml), 30 bar CO:H₂ (1:1), 75 °C.

^bL:b (aldehydes) (linear aldehydes:branched aldehydes)

^cL:b (amines) (linear amines:branched amines)

^dTON = moles amines/moles Rh(I)

In terms of the regioselectivity, only branched aldehydes were once again obtained. As alluded to earlier, this is as a result of their lower reactivity in reductive amination.^{9b} Generally, the reaction is regioselective towards the linear amine (1-nonylpiperidine). Since the linear aldehyde is more reactive than the branched aldehyde, they are converted to the corresponding linear amine at a faster rate and as such higher regioselectivity towards the linear amine is obtained. However, as the reaction progresses, the branched aldehydes are also subsequently converted to the corresponding branched amines with the result that the regioselectivity towards the linear amine decreases.

4.2.3 Evaluating different catalysts in the hydroaminomethylation of 1-octene and piperidine

Different catalysts (C4, C5 and HRhCO(PPh₃)₃) were then evaluated in the hydroaminomethylation of 1-octene in the presence of piperidine (Figure 4.7 and Table 4.3) at a reaction time of 1 h.

Similar activities and selectivities (chemo- and regioselectivity) were obtained for C4 and C5, with the presence of the methyl groups having almost no effect. The superior hydroformylation activity of HRhCO(PPh₃)₃ is underlined by the 98 % conversion of the substrate. This is attributed to the presence of Rh-H and Rh-CO moieties in the catalyst precursor (HRhCO(PPh₃)₃), a prerequisite for an active

Chapter 4: Hydroaminomethylation of Olefins with Primary and Secondary Amines

hydroformylation catalyst. However, this catalyst is far less efficient in the hydrogenation of the enamine intermediates in comparison to **C4** and **C5**, as indicated by the amount of amines in Figure 4.7 and the TON's displayed in Table 4.3. The most notable difference between $\text{HRhCO}(\text{PPh}_3)_3$, **C4** and **C5** is the presence of the bulky and basic PPh_3 ligands. The presence of these ligands increases the steric bulk around the metal centre which can hinder the coordination of the enamine intermediates and their subsequent hydrogenation. Furthermore, hydroaminomethylation reactions using Rh-phosphine catalysts are normally carried out at high temperatures ($>100\text{ }^\circ\text{C}$).¹³⁻¹⁴

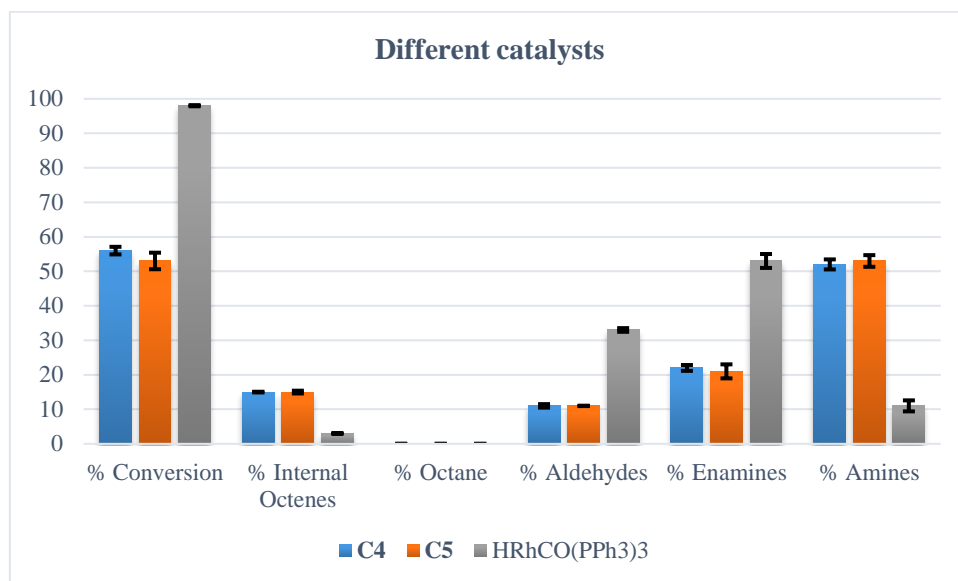


Figure 4.7: Evaluating different catalysts in the hydroaminomethylation of 1-octene and piperidine. 1-Octene (1.6 mmol), Piperidine (1.6 mmol), 0.1 mol% catalyst loading, Toluene (5 ml), 30 bar CO:H_2 (1:1), $75\text{ }^\circ\text{C}$ and 1 h.

The remaining aldehyde fraction was found to be exclusively branched in nature. Higher regioselectivity towards the linear amine was obtained using the $\text{HRhCO}(\text{PPh}_3)_3$ catalyst compared to when **C4** and **C5** were employed (Table 4.3). However, it should be pointed out that since ~35 % branched aldehydes are still present, the initially high linear regioselectivity is expected to decrease if the branched aldehydes are allowed to react further.

Table 4.3: Influence of different catalysts on the regioselectivity and TON^a

Catalysts	Regioselectivity		TON ^d
	L:b (Aldehydes) ^b	L:b (Amines) ^c	
C4	0:100	83:17	291
C5	0:100	81:19	278
$\text{HRhCO}(\text{PPh}_3)_3$	0:100	94:6	104

^a1-Octene (1.6 mmol), Piperidine (1.6 mmol), 0.1 mol% catalyst loading, Toluene (5 ml), 30 bar CO:H_2 (1:1), $75\text{ }^\circ\text{C}$, 1 h.

^bL:b (aldehydes) (linear aldehydes:branched aldehydes)

^cL:b (amines) (linear amines:branched amines)

^dTON = moles amines/moles Rh(I)

Chapter 4: Hydroaminomethylation of Olefins with Primary and Secondary Amines

4.2.4 Influence of olefin:amine ratio on the activity and selectivity of the hydroaminomethylation of 1-octene with piperidine

Next, the influence of the 1-octene:piperidine ratio on the activity and selectivity of the hydroaminomethylation reaction were investigated (Figure 4.8 and Table 4.4).

It was found that as the amount of piperidine increases, the conversion of 1-octene as well as the amount of *N*-alkylated piperidines increased, especially in the presence of an excess of piperidine (1:1.5 olefin:amine ratio). Although not that significant, a slight decrease in the amount of internal octenes were also observed. Therefore, this signifies that piperidine is able to inhibit side reactions, such as the isomerization of the terminal olefin to its corresponding internal olefins.¹⁵ In order for isomerization to occur, a vacant site on the metal is necessary so as to accommodate the hydrogen being transferred during the termination step. It is envisaged that piperidine most likely occupies vacant sites on the metal centre, thereby partially inhibiting the isomerization of the terminal olefins. Furthermore, the amount of aldehyde intermediates also decreases as the concentration of piperidine increases, since the Schiff-base condensation reaction is faster in the presence of a higher piperidine concentration. Therefore, enamine intermediates are produced at a much faster rate and these are subsequently hydrogenated to the corresponding *N*-alkylated piperidines. The ability of piperidine to partially inhibit olefin isomerization together with the faster production of enamine intermediates are responsible for the higher activity (as signified by the TON's displayed in Table 4.4) and chemoselectivity of the catalyst towards the *N*-alkylated piperidines in the presence of an excess of amine.

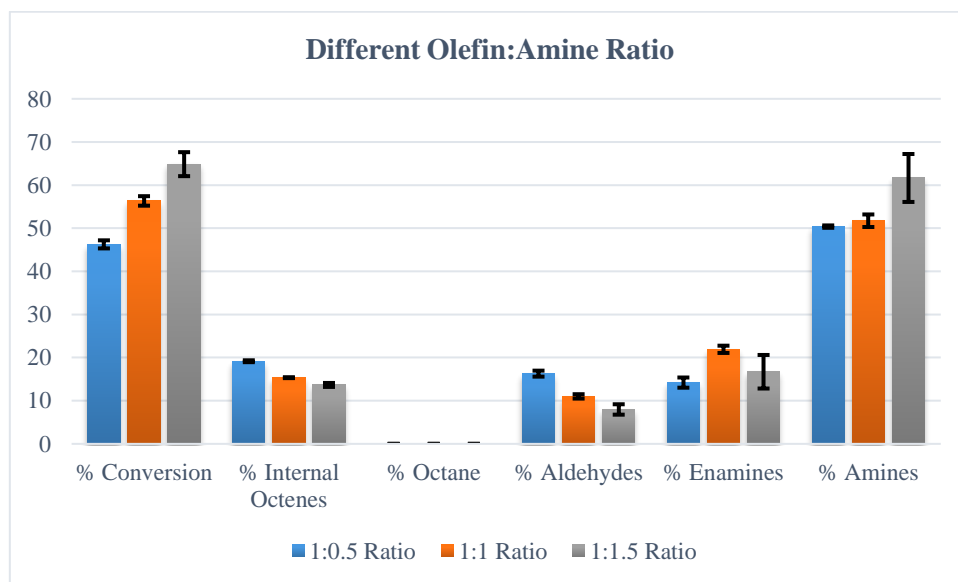


Figure 4.8: Influence of the 1-octene:piperidine ratio on their hydroaminomethylation. 1-Octene (1.6 mmol), Piperidine (0.8-2.4 mmol), 0.1 mol% catalyst loading (C4), Toluene (5 ml), 30 bar CO:H₂ (1:1), 75 °C and 1 h.

The influence of the olefin:amine ratio on the regioselectivity is shown in Table 4.4. As a result of an increase in catalytic activity as the olefin:amine ratio increases, the aldehydes are produced at a much faster rate, since side reactions, such as the isomerization of 1-octene, are inhibited. Comparing

Chapter 4: Hydroaminomethylation of Olefins with Primary and Secondary Amines

reactions conducted at 1:1 and 1:1.5 olefin:amine ratio, in both cases, only branched aldehydes were observed while in the case of reactions conducted at 1:0.5 olefin:amine ratio, some linear aldehyde still remained. Slightly less 2-methyloctanal (branched aldehyde) remained in the case of reactions conducted using amine rich mixtures such as 1:1.5 compared to the other ratios, as shown in Figure 4.8.

As a result of this, more branched *N*-alkylated piperidines are formed in the presence of an excess piperidine (1:1.5 amine ratio) leading to a lower regioselectivity towards the linear *N*-alkylated piperidine in comparison to what is obtained using a 1:0.5 and 1:1 olefin:amine ratio.¹⁵

Table 4.4: Influence of olefin:amine ratio on regioselectivity and TON^a

Olefin:Amine Ratio	Regioselectivity		TON ^d
	L:b (Aldehydes) ^b	L:b (Amines) ^c	
1:0.5	10:90	83:17	232
1:1	0:100	83:17	291
1:1.5	0:100	79:21	399

^a1-Octene (1.6 mmol), Piperidine (0.8-2.4 mmol), 0.1 mol% catalyst loading (C4), Toluene (5 ml), 30 bar CO:H₂ (1:1), 75 °C, 1 h.

^bL:b (aldehydes) (linear aldehydes:branched aldehydes)

^cL:b (amines) (linear amines:branched amines)

^dTON = moles amines/moles Rh(I)

Since superior hydroaminomethylation activity was obtained using a olefin:amine ratio of 1:1.5, this ratio was used for further reaction condition optimization.

4.2.5 Influence of pressure on the activity and selectivity of the hydroaminomethylation of 1-octene and piperidine

Next, we investigated the influence of pressure on the conversion of the substrate as well as the chemoselectivity of the reaction (Figure 4.9) while the regioselectivity is shown in Table 4.5.

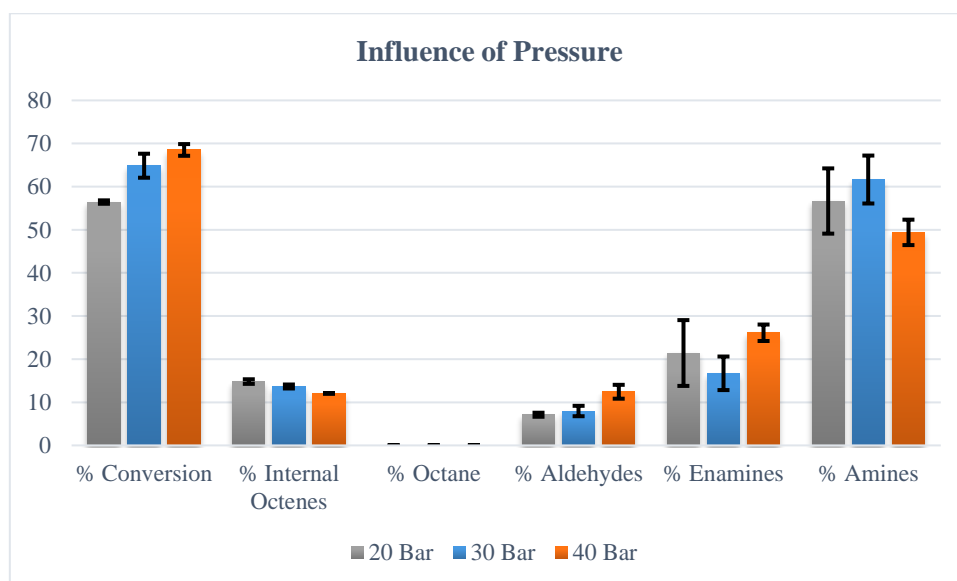


Figure 4.9: Influence of pressure on hydroaminomethylation of 1-octene and piperidine. 1-Octene (1.6 mmol), Piperidine (2.4 mmol), 0.1 mol% catalyst loading (C4), Toluene (5 ml), 20-40 bar CO:H₂ (1:1), 75 °C and 1 h.

Chapter 4: Hydroaminomethylation of Olefins with Primary and Secondary Amines

The conversion of 1-octene increased with an increase in the pressure (20-40 bar CO:H₂, 1:1). Pressure had no significant effect on the isomerization of 1-octene to its internal counterparts. However, the best catalytic activity was obtained utilizing a pressure of 30 bar. Higher chemoselectivities towards the *N*-alkylated piperidines were obtained, as can be seen in Figure 4.9 as well as the TON's displayed in Table 4.5. As the pressure is increased from 20-40 bar, both the CO and H₂ partial pressure increases. We postulate that at 40 bar, Rh species rich in CO ligands can potentially form, which is inactive in hydrogenation reactions, hence, lower TON's is obtained at 40 bar CO:H₂ (1:1).

Pressure had no marked effect on the regioselectivity of the *N*-alkylated piperidines, as can be seen in Table 4.5 below.

Table 4.5: Influence of pressure on the regioselectivity and TON^a

Pressure (bar)	Regioselectivity		TON ^d
	L:b (Aldehydes) ^b	L:b (Amines) ^c	
20	5:95	80:20	319
30	0:100	79:21	399
40	7:93	83:17	339

^a1-Octene (1.6 mmol), Piperidine (2.4 mmol), 0.1 mol% catalyst loading (C4), Toluene (5 ml), 30 bar CO:H₂ (1:1), 75 °C, 1 h.

^bL:b (aldehydes) (linear aldehydes:branched aldehydes)

^cL:b (amines) (linear amines:branched amines)

^dTON = moles amines/moles Rh(I)

We selected 30 bar CO:H₂ (1:1) for further optimization of the yield of the *N*-alkylated piperidines.

4.2.6 Influence of temperature on the activity and selectivity of the hydroaminomethylation of 1-octene and piperidine

The influence of temperature on the substrate conversion, chemo- and regioselectivity is displayed in Figure 4.10 and Table 4.6.

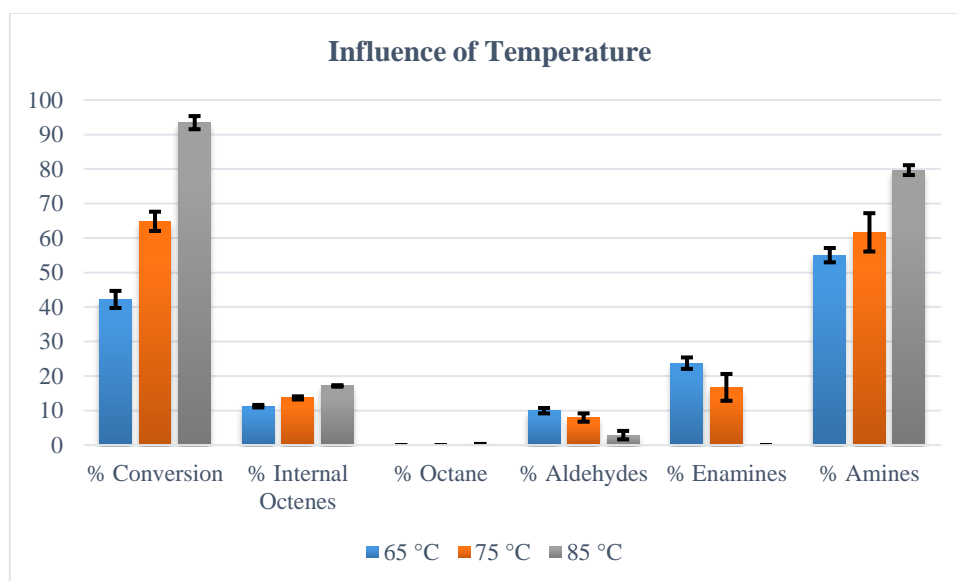


Figure 4.10: Influence of temperature on hydroaminomethylation of 1-octene and piperidine. 1-Octene (1.6 mmol), Piperidine (2.4 mmol), 0.1 mol% catalyst loading (C4), Toluene (5 ml), 30 bar CO:H₂ (1:1), 65-85 °C and 1 h.

Chapter 4: Hydroaminomethylation of Olefins with Primary and Secondary Amines

With an increase in temperature, a significant increase in the conversion of the substrate was observed (Figure 4.10). This coincided with a significant increase in the yield of *N*-alkylated piperidines (Figure 4.10) to ~80 %, proceeding at a TON of 756 (Table 4.6). No enamine intermediates were obtained at 85 °C, while only 3 % branched aldehydes remained. The higher temperature significantly boosted both the hydroformylation and the reductive amination processes.

Table 4.6: Influence of temperature on the regioselectivity and TON^a

Temperature (° C)	Regioselectivity		TON ^d
	L:b (Aldehydes) ^b	L:b (Amines) ^c	
65	0:100	79:21	232
75	0:100	79:21	399
85	0:100	75:25	756

^a1-Octene (1.6 mmol), Piperidine (2.4 mmol), 0.1 mol% catalyst loading (C4), Toluene (5 ml), 30 bar CO:H₂ (1:1), 65-85 °C, 1 h.

^bL:b (aldehydes) (linear aldehydes:branched aldehydes)

^cL:b (amines) (linear amines:branched amines)

^dTON = moles amines/moles Rh(I)

A slight decrease in the regioselectivity towards the linear *N*-alkylated piperidine were observed since the majority of branched aldehydes were subsequently converted to the corresponding branched *N*-alkylated piperidines.

Since the catalytic activity was significantly boosted when a temperature of 85 °C was used, this temperature was chosen after which the reaction time was extended to 2 h (Figure 4.11 and Table 4.7).

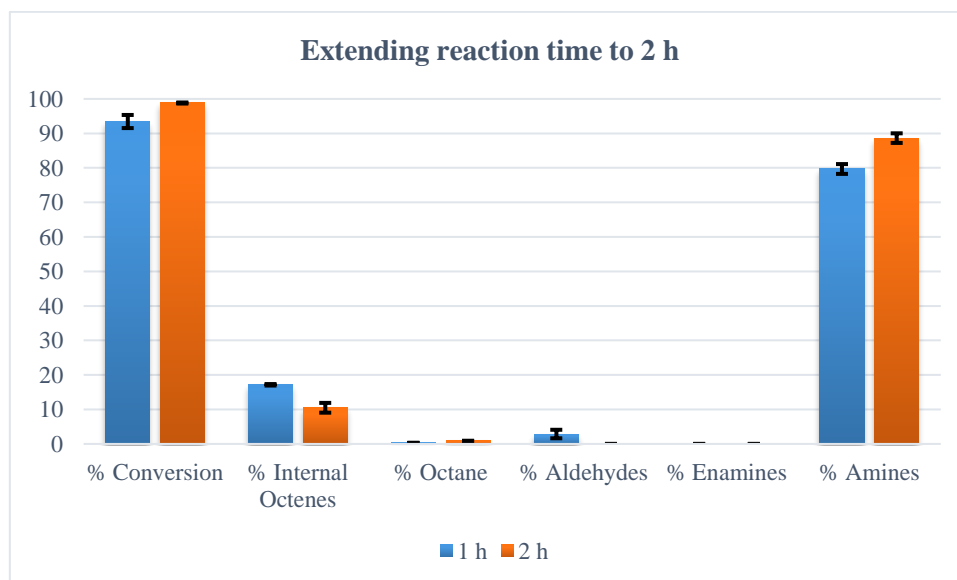


Figure 4.11: Extending the reaction time to 2 h. 1-Octene (1.6 mmol), Piperidine (2.4 mmol), 0.1 mol% catalyst loading (C4), Toluene (5 ml), 30 bar CO:H₂ (1:1), 85 °C.

Extending the reaction from 1 to 2 h allowed for the complete consumption of 1-octene. This further resulted in improvement in the chemoselectivity to *N*-alkylated piperidines with a yield of ~90 % at a TON of 873. Furthermore, roughly 10 % decrease in the amount of internal octenes were observed.

Chapter 4: Hydroaminomethylation of Olefins with Primary and Secondary Amines

These internal octenes were converted to branched aldehydes. After Schiff-base condensation and hydrogenation of the resulting enamines, branched *N*-alkylated piperidines will form. An increase in the amount of branched *N*-alkylated piperidines is responsible for the decrease in the regioselectivity towards the linear *N*-alkylated piperidine as shown in Table 4.7.

Table 4.7: Extending the reaction to 2 h^a

Regioselectivity			
t (h)	L:b (Aldehydes) ^b	L:b (Amines) ^c	TON ^d
1	0:100	75:25	756
2	~	63:37	873

^a1-Octene (1.6 mmol), Piperidine (2.4 mmol), 0.1 mol% catalyst loading (C4), Toluene (5 ml), 30 bar CO:H₂ (1:1), 85 °C.

^bL:b (aldehydes) (linear aldehydes:branched aldehydes)

^cL:b (amines) (linear amines:branched amines)

^dTON = moles amines/moles Rh(I)

4.3 Hydroaminomethylation of 1-octene in the presence of primary amines (Aniline and Benzylamine)

Following the evaluation of C4 as a catalyst precursor in the hydroaminomethylation of 1-octene with the secondary amine, piperidine, we shifted our attention towards the use of primary amines, specifically aniline and benzylamine (Figure 4.12).

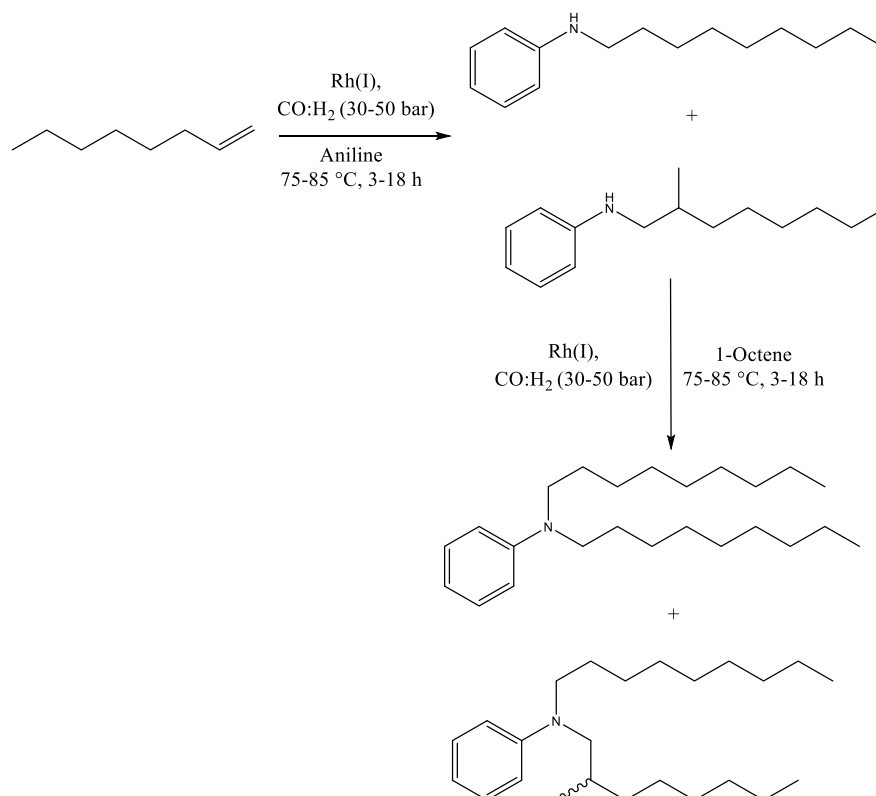


Figure 4.12: Hydroaminomethylation of 1-octene and aniline

The hydroaminomethylation of primary amines produces secondary amines. These secondary amines can further be hydroaminomethylated to tertiary amines. Therefore, as a first point of departure, we

Chapter 4: Hydroaminomethylation of Olefins with Primary and Secondary Amines

evaluated the hydroaminomethylation of 1-octene and aniline using an olefin:amine ratio of 2:1 in order to synthesize these tertiary amines. The rationale behind this is because these tertiary amines serve as interesting precursors for surfactants (after incorporation of a polar head-group).

4.3.1 Effect of temperature and catalyst concentration on the yield of *N*-alkylated anilines

The hydroaminomethylation of 1-octene with aniline was investigated at the optimum conditions that were established for the hydroaminomethylation of 1-octene and piperidine (Figure 4.13 and Table 4.8). Aniline is less basic than piperidine and therefore we expected that the yield of the *N*-alkylated anilines will initially be low. Therefore optimization of the reaction conditions (temperature, catalyst loading, pressure and time) will be necessary.

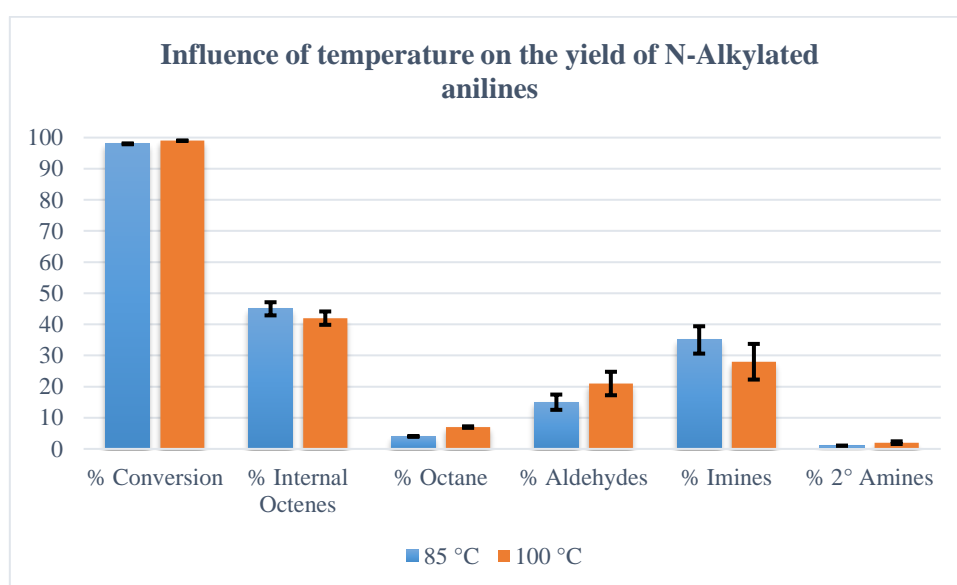


Figure 4.13: Effect of temperature on the yield of *N*-alkylated anilines. 1-Octene (1.6 mmol), Aniline (0.8 mmol), 0.1 mol% catalyst loading (C4), Toluene (5 ml), 30 bar CO:H₂ (1:1), 85 °C, 1 h.

The hydroaminomethylation of 1-octene with aniline was evaluated at 85 and 100 °C, however, at both these temperatures, the yield of the secondary *N*-alkylated anilines was very low (≥ 2 %). Full conversion of the olefin substrate, 1-octene, was obtained which indicates that the hydroformylation reaction proceeds smoothly under these conditions. More stringent reaction conditions are required in order to accelerate the reductive amination process. Furthermore, a wide spectrum of products was obtained, including internal octenes, aldehydes, imines and trace amounts of octane. The isomerization of the 1-octene to its internal counterparts seems to be a quite significant side reaction, even more so than when we evaluated the hydroaminomethylation of 1-octene and piperidine (Section 4.2). We attribute this to the lower basicity of aniline in comparison to piperidine. It is less likely to occupy any vacant sites on the metal in order to inhibit β -hydrogen elimination with the result that more internal octenes forms in comparison to when piperidine is the amine.

Chapter 4: Hydroaminomethylation of Olefins with Primary and Secondary Amines

Similar regioselectivities were obtained at 85 and 100 °C (Table 4.8). In terms of the regioselectivity of the aldehydes, more branched aldehydes are present. As alluded to earlier, linear aldehydes are more reactive in reductive amination than branched aldehydes, and therefore they are consumed at a much faster rate.^{9b}

Table 4.8: Effect of temperature on the regioselectivity of *N*-alkylated anilines and TON^a

Temperature (° C)	Regioselectivity		TON ^d
	L:b (Aldehydes) ^b	L:b (Amines) ^c	
85	35:65	100:0	6
100	36:64	100:0	24

^a1-Octene (1.6 mmol), Aniline (0.8 mmol), 0.1 mol% catalyst loading (C4), Toluene (5 ml), 30 bar CO:H₂ (1:1), 85 °C, 1 h.

^bL:b (aldehydes) (linear aldehydes:branched aldehydes)

^cL:b (amines) (linear amines:branched amines)

^dTON = moles amines/moles Rh(I)

The concentration of the catalyst (C4) was then increased (Figure 4.14 and Table 4.9), while keeping the temperature constant at 85 °C, in order to increase the yield of the *N*-alkylated anilines.

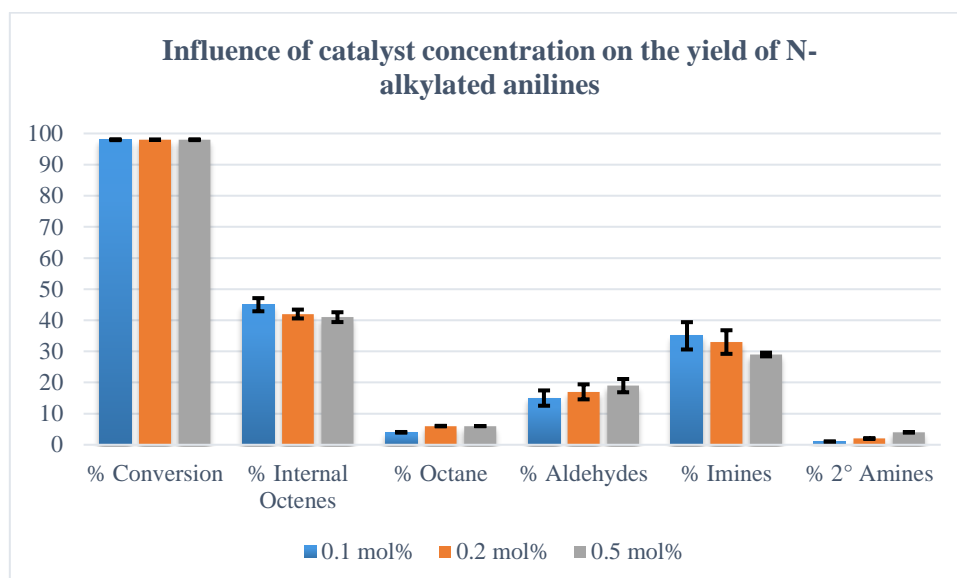


Figure 4.14: Influence of catalyst concentration on the yield of *N*-alkylated anilines. 1-Octene (1.6 mmol), Aniline (0.8 mmol), C4, Toluene (5 ml), 30 bar CO:H₂ (1:1), 85 °C, 1 h.

Even though not that significant, increasing the catalyst loading from 0.1 to 0.5 mol%, a slight decrease in the amount of internal octenes and imines occurred, while the amount of aldehydes and secondary *N*-alkylated anilines increased. However, higher catalyst concentrations had no significant effect on the regioselectivity, as seen in Table 4.9 below.

Since slightly higher activities were obtained using a catalyst loading of 0.5 mol%, further optimization of the reaction conditions were conducted using this catalyst loading.

Chapter 4: Hydroaminomethylation of Olefins with Primary and Secondary Amines

Table 4.9: Influence of catalyst concentration on the regioselectivity and TON^a

Cat. Loading (mol %)	Regioselectivity		TON ^d
	L:b (Aldehydes) ^b	L:b (Amines) ^c	
0.1	35:65	100:0	6
0.2	37:63	100:0	10
0.5	35:65	100:0	7

^a1-Octene (1.6 mmol), Aniline (0.8 mmol), C4, Toluene (5 ml), 30 bar CO:H₂ (1:1), 85 °C, 1 h.

^bL:b (aldehydes) (linear aldehydes:branched aldehydes)

^cL:b (amines) (linear amines:branched amines)

^dTON = moles amines/moles Rh(I)

4.3.2 Influence of pressure (total and partial) on the yield of *N*-alkylated anilines

Only trace amounts of *N*-alkylated anilines were initially obtained, with temperature and catalyst loading having no significant effect on the yield of the target amines. Therefore, we shifted our attention towards the pressure. We set out to explore the effect of the partial pressure of CO:H₂, specifically moving into a more H₂-rich environment since this has been shown previously to be beneficial for the hydrogenation of the imines (Figure 4.15 and Table 4.10).¹⁶

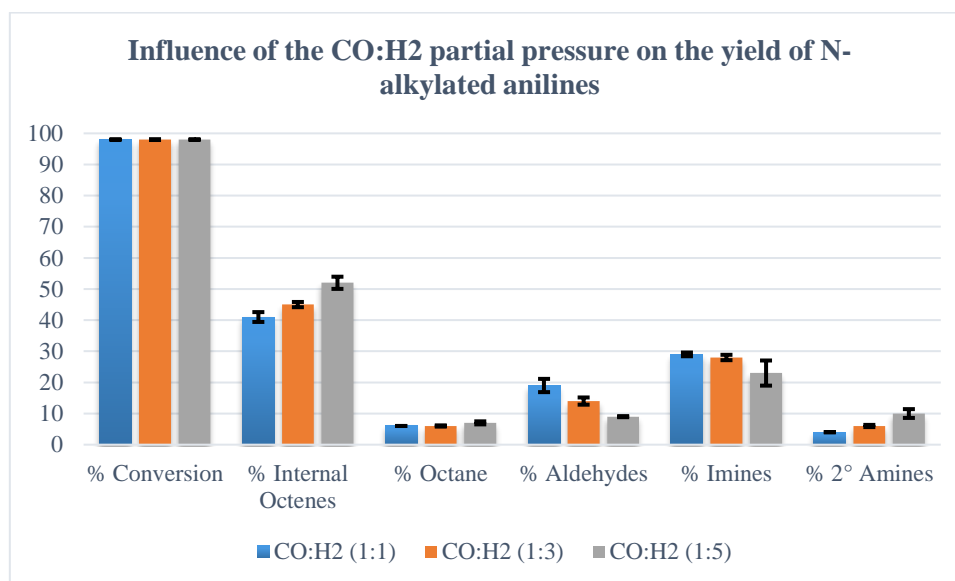


Figure 4.15: Influence of the CO:H₂ partial pressure on the yield of *N*-alkylated anilines. 1-Octene (1.6 mmol), Aniline (0.8 mmol), 0.5 mol% catalyst loading (C4), Toluene (5 ml), 30 bar CO:H₂, 85 °C, 1 h.

The yield of secondary *N*-alkylated anilines could be increased to 10 % upon increasing the partial pressure of H₂. This is also clear from the TON's displayed in Table 4.10. However, the higher H₂ partial pressure favoured the isomerization of the terminal olefin to its internal counterparts, evident by the increase in the amount of internal octenes as shown in Figure 4.15. This observation is consistent with the general mechanism of the hydroformylation reaction. The two major competing processes in hydroformylation is carbonylation of the Rh-alkyl species, which ultimately produces the aldehydes, and β-hydride transfer of the Rh-alkyl species, producing the isomerized olefins. As the H₂ partial

Chapter 4: Hydroaminomethylation of Olefins with Primary and Secondary Amines

pressure is increased, the CO partial pressure concurrently decreased in order to keep the total pressure constant. Thus, the concentration of CO will also be lower and therefore subsequent carbonylations of the Rh-alkyl species will be slower. This favours the β -hydride transfer reactions producing much more internal octenes at higher H₂ partial pressures.

The effect of the H₂ partial pressure on the regioselectivity is shown in Table 4.10. In the presence of a H₂-rich environment, far less aldehydes are produced since isomerization of the terminal olefins is favoured. Since linear aldehydes are more reactive than branched aldehydes, they will be consumed at a much faster rate and therefore as the H₂ partial pressure is increased, the regioselectivity towards the linear aldehyde decrease.

Table 4.10: Influence of the CO:H₂ partial pressure on the regioselectivity and TON^a

CO:H ₂ ratio	Regioselectivity		TON ^d
	L:b (Aldehydes) ^b	L:b (Amines) ^c	
1:1	35:65	100:0	7
1:3	32:68	93:7	12
1:5	28:72	93:7	19

^a1-Octene (1.6 mmol), Aniline (0.8 mmol), 0.5 mol% catalyst loading (C4), Toluene (5 ml), 30 bar CO:H₂, 85 °C, 1 h.

^bL:b (aldehydes) (linear aldehydes:branched aldehydes)

^cL:b (amines) (linear amines:branched amines)

^dTON = moles amines/moles Rh(I)

The total pressure of the reaction was then increased, while keeping the ratio of CO:H₂ constant at 1:3 (Figure 4.16 and Table 4.11).

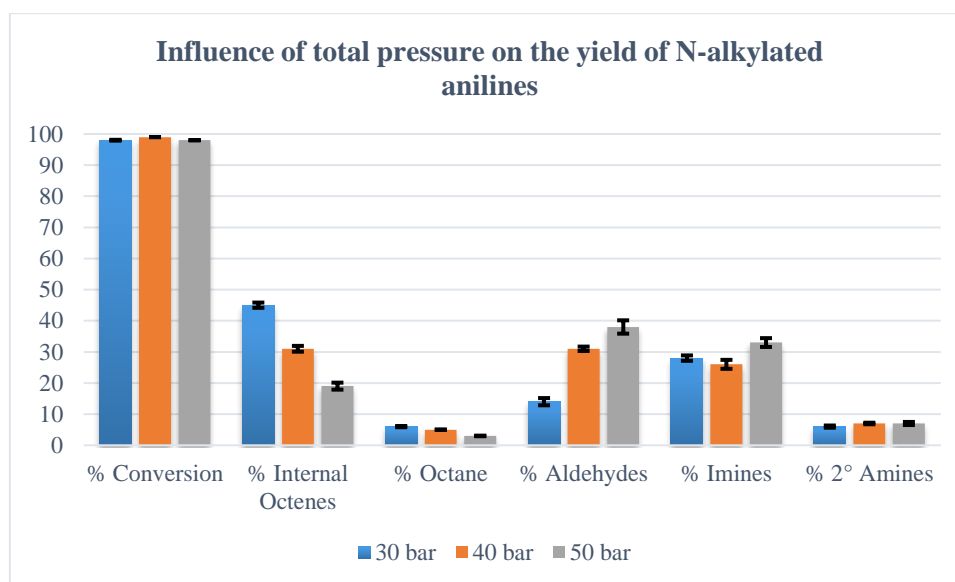


Figure 4.16: Influence of total pressure on the yield of N-alkylated anilines. 1-Octene (1.6 mmol), Aniline (0.8 mmol), 0.5 mol% catalyst loading (C4), Toluene (5 ml), CO:H₂ (1:3), 85 °C, 1 h.

Increasing the total pressure from 30 to 50 bar also had no significant effect on the yield of the N-alkylated anilines, however, it significantly impacted the hydroformylation reaction. With an increase in pressure, the amount of internal octenes that is forming due to isomerization, decreased significantly

Chapter 4: Hydroaminomethylation of Olefins with Primary and Secondary Amines

while the amount of aldehydes increased significantly. Therefore, the increase in pressure had the opposite effect than an increase in the H₂ partial pressure. Once again, this is also consistent with the mechanism of the hydroformylation reaction. As the total pressure is increased, both the partial pressure of CO and H₂ is increased. This translates into a higher concentration of these gases in solution. This accelerates the carbonylation of the Rh-alkyl species, while inhibiting the competing β -hydride transfer reactions. As a result, much more aldehydes are produced at the higher pressure.

Furthermore, since the extent of isomerization of the terminal olefins is less at the higher pressures, less branched aldehydes are formed and therefore an increase in the regioselectivity towards the linear aldehydes are obtained, as can be seen in Table 4.11. This is further consistent with the literature.¹⁷

Table 4.11: Influence of total pressure on regioselectivity and TON^a

Pressure (bar)	Regioselectivity		TON ^d
	L:b (Aldehydes) ^b	L:b (Amines) ^c	
30	32:68	93:7	12
40	40:60	93:7	14
50	42:58	93:7	14

^a1-Octene (1.6 mmol), Aniline (0.8 mmol), 0.5 mol% catalyst loading (C4), Toluene (5 ml), CO:H₂ (1:3), 85 °C, 1 h.

^bL:b (aldehydes) (linear aldehydes:branched aldehydes)

^cL:b (amines) (linear amines:branched amines)

^dTON = moles amines/moles Rh(I)

4.3.3 Influence of time on the yield of *N*-alkylated anilines

Although the temperature, catalyst loading and pressure (partial and total) were varied, this had no significant effect on the yield of the target amines, even though these factors had a significant effect on the hydroformylation reaction. However, it should be pointed out that up until this point, the hydroaminomethylation of 1-octene with aniline had only been evaluated for 1 h only. Therefore, the reaction time was extended in an attempt to increase the yield of the *N*-alkylated anilines (Figure 4.17 and Table 4.12).

Extending the reaction time from 1 to 18 h allowed for the complete consumption of all internal olefins with the subsequent production of branched aldehydes, evident by the increase in the amount of aldehydes (Figure 4.17) and as demonstrated by the l:b ratios displayed in Table 4.12 below. After 3 h reaction time, the amount of aldehyde starts decreasing again as they undergo condensation to form imines. Furthermore, after 18 h, the linear aldehydes are completely consumed as a result of their higher reactivity (Table 4.12).^{9b} Gratifyingly enough, a significant decrease in the amount of imines also occurred, producing secondary *N*-alkylated anilines with up to ~50 % yield. Only after 18 h reaction time were tertiary *N*-alkylated anilines detected. The regioselectivity towards the linear amine (*N*-nonyl aniline) is high at short reaction time, however, this decreases over prolonged reaction time as more branched secondary *N*-alkylated anilines is formed.

Chapter 4: Hydroaminomethylation of Olefins with Primary and Secondary Amines

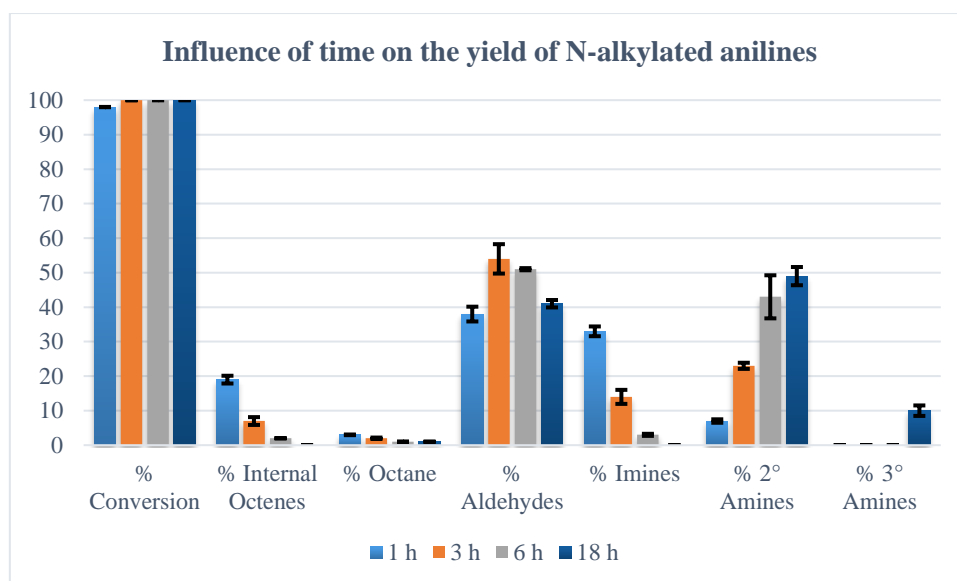


Figure 4.17: Influence of time on the yield of *N*-alkylated anilines. 1-Octene (1.6 mmol), Aniline (0.8 mmol), 0.5 mol% catalyst loading (C4), Toluene (5 ml), 50 bar CO:H₂ (1:3), 85 °C.

Table 4.12: Influence on time on the regioselectivity and TON^a

Regioselectivity			
t (h)	L:b (Aldehydes) ^b	L:b (Amines) ^c	TON ^d
1	42:58	93:7	14
3	39:61	88:12	46
6	25:75	81:19	86
18	0:100	70:30	97

^a1-Octene (1.6 mmol), Aniline (0.8 mmol), 0.5 mol% catalyst loading (C4), Toluene (5 ml), 50 bar CO:H₂ (1:3), 85 °C.

^bL:b (aldehydes) (linear aldehydes:branched aldehydes)

^cL:b (amines) (linear amines:branched amines)

^dTON = moles amines/moles Rh(I)

4.3.4 Influence of the olefin:amine ratio on the yield of secondary *N*-alkylated anilines

From the results above, it would appear as if the formation of the tertiary *N*-alkylated anilines is very slow. We therefore shifted our attention towards the synthesis of the secondary *N*-alkylated anilines. In order to accomplish this, we varied the ratio of the olefin:amine ratio (Figure 4.18 and Table 4.13). The reaction was done over a six hour period.

The hydroaminomethylation of 1-octene with aniline proceeds at a faster rate as the concentration of aniline is increased, with the yield of the targeted amines increasing significantly. This is attributed to the higher concentration of the aniline which accelerates the reductive amination reaction. Far less aldehyde intermediates are obtained when 1:1 and 1:1.5 olefin:amine ratios are used because the formed aldehydes condense rapidly with aniline in to form the corresponding imines. Since the imine intermediates are formed more rapidly, they can subsequently be hydrogenated to the targeted amines. This translates into a highly chemoselective synthesis of secondary *N*-alkylated anilines in 96 % yield, proceeding at a TON of 192, when employing a olefin:amine ratio of 1:1.5.

Chapter 4: Hydroaminomethylation of Olefins with Primary and Secondary Amines

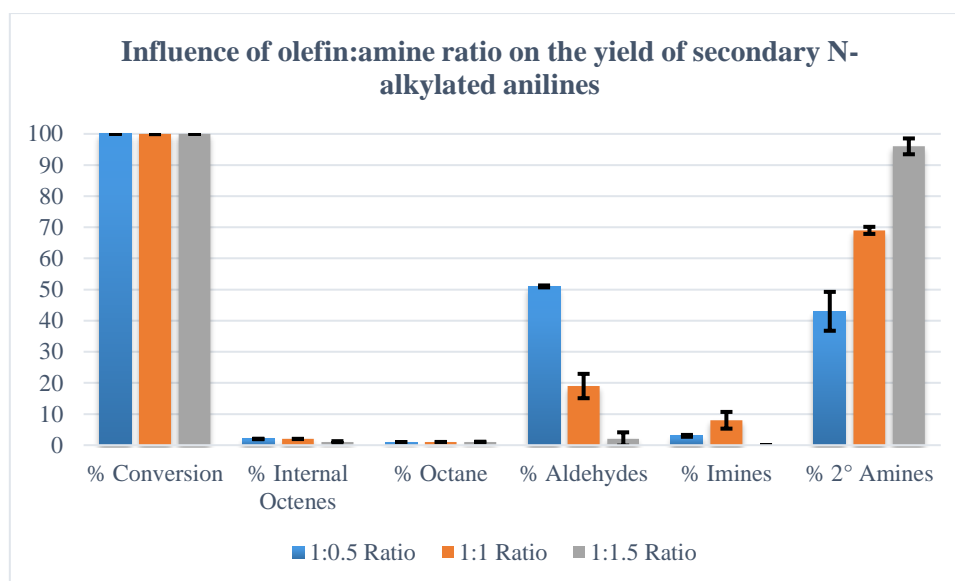


Figure 4.18: Influence of olefin:amine ratio on the yield of secondary N-alkylated anilines. 1-Octene (1.6 mmol), Aniline (0.8-2.4 mmol), 0.5 mol% catalyst loading (C4), Toluene (5 ml), 50 bar CO:H₂ (1:3), 85 °C, 6 h.

The influence of the olefin:amine ratio on the regioselectivity is shown in Table 4.13. Once again, the l:b ratio of the aldehydes shows that the linear aldehydes are consumed much faster as a result of its higher reactivity. However, moderate regioselectivities are obtained for the target amines (l:b of 56:44).

Table 4.13: Influence of olefin:amine ratio on the regioselectivity and TON^a

Olefin:amine ratio	Regioselectivity		TON ^d
	L:b (Aldehydes) ^b	L:b (Amines) ^c	
1:0.5	25:75	81:19	86
1:1	5:95	75:25	138
1:1.5	0:100	56:44	192

^a1-Octene (1.6 mmol), Aniline (0.8-2.4 mmol), 0.5 mol% catalyst loading (C4), Toluene (5 ml), 50 bar CO:H₂ (1:3), 85 °C, 6 h.

^bL:b (aldehydes) (linear aldehydes:branched aldehydes)

^cL:b (amines) (linear amines:branched amines)

^dTON = moles amines/moles Rh(I)

4.3.5 The hydroaminomethylation of aniline vs benzylamine

In order to broaden the scope of the hydroaminomethylation reaction, we also evaluated the hydroaminomethylation of 1-octene in the presence of benzylamine and compared this to the results we obtained with aniline (Figure 4.19 and Table 4.14).

This reaction was performed using a 1:1 ratio of olefin:amine ratio while the reaction was also conducted for 3 h. This was done since we expected that the hydroaminomethylation reaction using benzylamine would be very facile as a result of its higher basicity. Thus, benzylamine is expected to be much more nucleophilic than aniline, which should accelerate the Schiff-base condensation reaction. The earlier during the reaction cycle these imine intermediates are present, the sooner they will be hydrogenated to the corresponding amines. In addition, the imine moiety in the case of benzylamine is

Chapter 4: Hydroaminomethylation of Olefins with Primary and Secondary Amines

not resonance-stabilized by the aromatic moiety as is the case for aniline, which should further lead to a more facile hydrogenation reaction. This was indeed the case, as shown in Figure 4.19. The secondary *N*-alkylated benzylamines were synthesized chemoselectively in 95 % GC yield. Furthermore, a much higher TON was obtained in the case of benzylamine, compared to the TON obtained for the reaction conducted using aniline (Table 4.14). This confirms the acceleration of the hydroaminomethylation reaction in the presence of the more nucleophilic benzylamine.

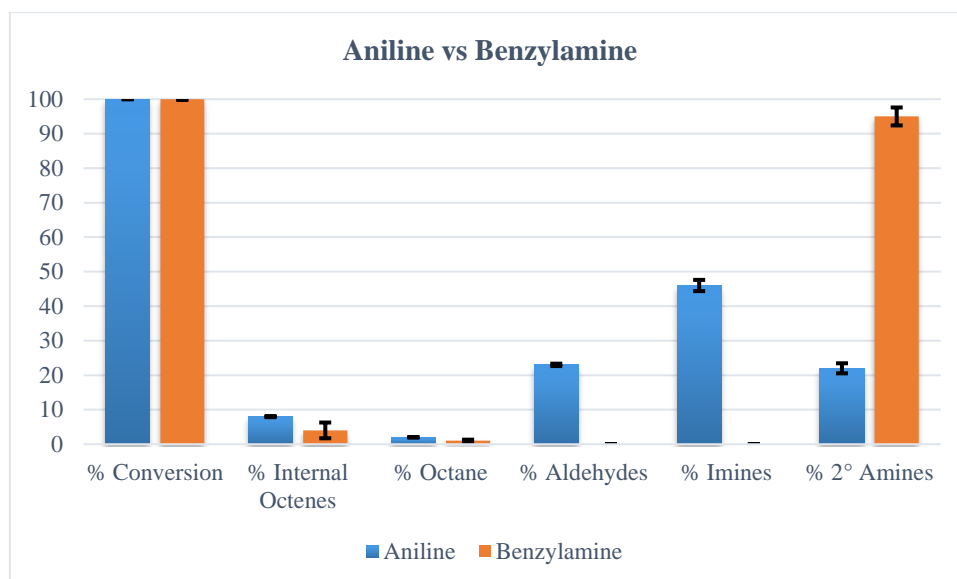


Figure 4.19: Hydroaminomethylation of aniline vs benzylamine. 1-Octene (1.6 mmol), Amine (1.6 mmol), 0.5 mol% catalyst loading (C4), Toluene (5 ml), 50 bar CO:H₂ (1:3), 85 °C, 3 h.

Very moderate regioselectivities towards the secondary *N*-alkylated benzylamines were obtained compared to the selective linear synthesis of the secondary *N*-alkylated anilines (Table 4.14). In the case of the reaction conducted with aniline, ~10 % internal octenes as well as ~25 % aldehydes (predominantly branched in nature) are still present in the reaction mixture. Subsequent conversion of these will deliver branched amines which should lower the regioselectivity of the secondary *N*-alkylated anilines.

Table 4.14: Regioselectivity and TON of the hydroaminomethylation of aniline and benzylamine^a

Amine	Regioselectivity		TON ^d
	L:b (Aldehydes) ^b	L:b (Amines) ^c	
Aniline	20:80	87:13	44
Benzylamine	~	59:41	190

^a1-Octene (1.6 mmol), Amine (1.6 mmol), 0.5 mol% catalyst loading (C4), Toluene (5 ml), 50 bar CO:H₂ (1:3), 85 °C, 3 h.

^bL:b (aldehydes) (linear aldehydes:branched aldehydes)

^cL:b (amines) (linear amines:branched amines)

^dTON = moles amines/moles Rh(I)

Chapter 4: Hydroaminomethylation of Olefins with Primary and Secondary Amines

4.4 Hydroaminomethylation of 1-octene with benzylamine catalyzed by Ru(II) catalyst precursors

Hydroaminomethylation of olefins and amines are efficiently mediated by Rh-based catalysts. Nevertheless, rhodium is very expensive and therefore alternative catalyst systems, making use of cheaper metals, are required. A viable alternative to rhodium is ruthenium. Furthermore, ruthenium is in some instances combined with rhodium, forming a dual-metal catalyst system.¹⁸⁻¹⁹ This is done in order to exploit the excellent hydrogenation ability of ruthenium. However, catalyst systems relying on ruthenium alone to catalyze the hydroaminomethylation reaction are also known, but this is relatively scarce.²⁰⁻²² Beller and co-workers investigated the use of ruthenium in a domino water-gas shift/hydroaminomethylation sequence while Eilbracht and Srivastava made use of a reverse-water-gas-shift/hydroaminomethylation sequence in order to synthesize *N*-alkylated amines.²⁰⁻²²

In light of the above, we embarked on the evaluation of the three Ru(II) complexes shown in Figure 4.20, in the hydroaminomethylation of 1-octene with benzylamine.

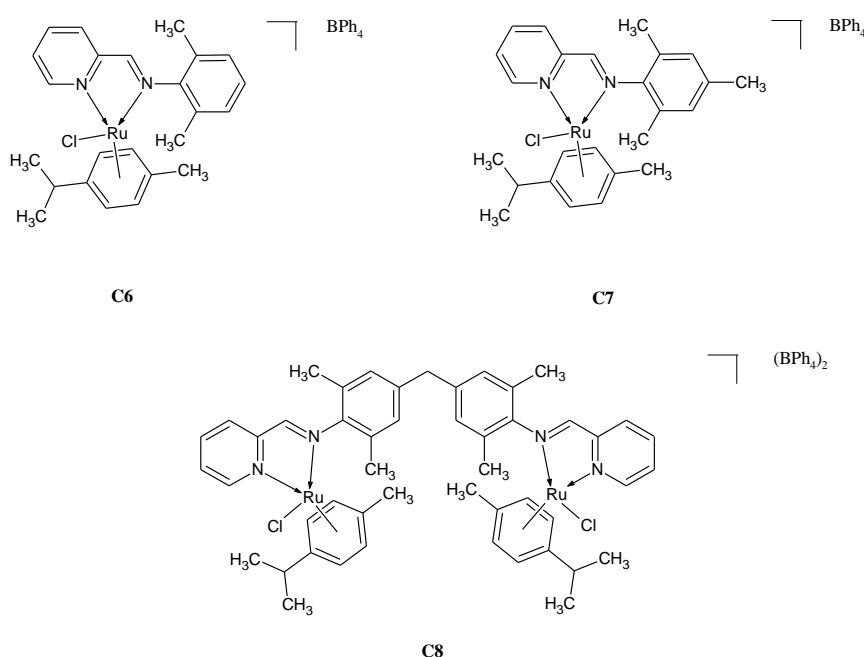


Figure 4.20: Ru(II) complexes evaluated in the hydroaminomethylation of 1-octene with benzylamine

The hydroaminomethylation of 1-octene and benzylamine towards the corresponding secondary *N*-alkyl benzylamines is shown in Figure 4.21. The initial reaction conditions were chosen as 50 bar CO:H₂ (1:3), 85 °C, 0.5 mol% catalyst loading (**C6**), 3 h reaction time employing an olefin:amine ratio of 1:1.

Chapter 4: Hydroaminomethylation of Olefins with Primary and Secondary Amines

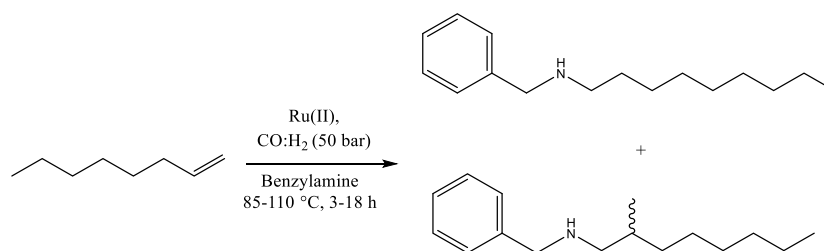


Figure 4.21: Hydroaminomethylation of 1-octene and benzylamine catalyzed by Ru(II) complexes

4.4.1 Influence of temperature on the hydroaminomethylation of 1-octene with benzylamine

C6 was initially evaluated as a catalyst precursor in the hydroaminomethylation of 1-octene and benzylamine under the conditions mentioned above. However, under these conditions, only 10 % of the 1-octene was converted of which the major product was the imine (80 %), with the internal olefins the balance. Therefore, the temperature of the reaction were then increased to 110 °C (Figure 4.22 and Table 4.15).

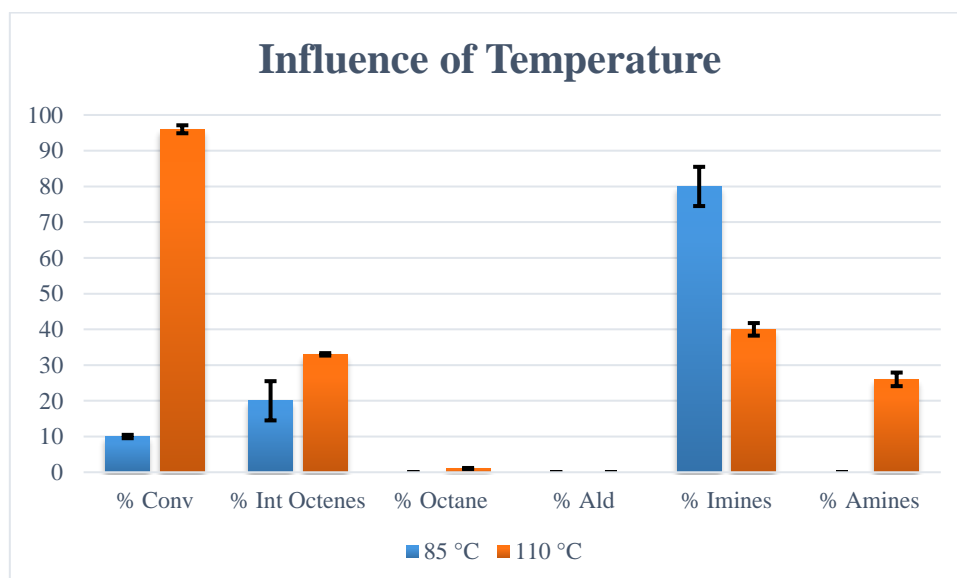


Figure 4.22: Influence of temperature on the hydroaminomethylation of 1-octene with benzylamine. 1-Octene (1.6 mmol), Benzylamine (1.6 mmol), 0.5 mol% catalyst loading (**C6**), Toluene (5 ml), 50 bar CO:H₂ (1:3), 3 h.

Increasing the temperature from 85 to 110 °C allowed for almost complete conversion of the substrate (~95 %). The major products were found to be the imine intermediates while just below 30 % secondary *N*-alkylated benzylamines were also obtained. What was interesting from the product distribution was the absence of any aldehyde intermediates, even though ~40 % olefins (terminal and internal) were still present. This seems to indicate that the aldehyde intermediates are consumed faster in the Schiff-base condensation reaction than at the rate at which they are produced in hydroformylation. This is subsequently attributed to the lower hydroformylation activity of ruthenium compared to the rhodium-based catalysts discussed previously.

Chapter 4: Hydroaminomethylation of Olefins with Primary and Secondary Amines

As shown in Table 4.15, higher regioselectivity towards the linear amine is obtained. The linear aldehyde is produced at a much faster rate. Furthermore, owing to its higher reactivity in reductive amination^{9b}, the linear amine is produced during the early stages of the reaction, hence the higher regioselectivity. This high linear regioselectivity is expected to decrease after conversion of the internal olefins to branched aldehydes, followed by its subsequent conversion to branched amines.

Table 4.15: Influence of temperature on regioselectivity and TON^a

Temperature (°C)	Regioselectivity		TON ^d
	L:b (Aldehydes) ^b	L:b (Amines) ^c	
85	~	~	~
110	~	86:14	51

^a1-Octene (1.6 mmol), Benzylamine (1.6 mmol), 0.5 mol% catalyst loading (C6), Toluene (5 ml), 50 bar CO:H₂ (1:3), 3 h.

^bL:b (aldehydes) (linear aldehydes:branched aldehydes)

^cL:b (amines) (linear amines:branched amines)

^dTON = moles amines/moles Ru(II)

4.4.2 Comparing the activity of different Ru(II) catalysts in the hydroaminomethylation of 1-octene with benzylamine

Since moderate hydroaminomethylation activity was obtained for C6 at 50 bar CO:H₂ (1:3), 110 °C, 0.5 mol% catalyst loading and 3 h reaction time, the activity of C7-C8 were also evaluated under these conditions (Figure 4.23 and Table 4.16). C8 contains two metal centres and therefore when using this complex as a catalyst, the catalyst loading was adjusted in order to ensure that the Ru(II) concentration is comparable to that used for the mononuclear-analogues (C6 and C7).

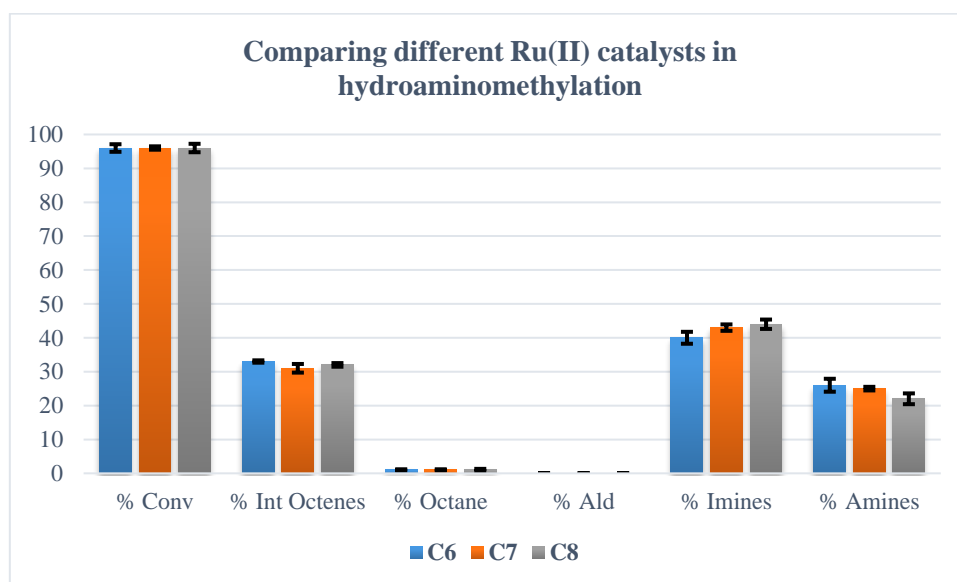


Figure 4.23: Comparing different Ru(II) catalysts in the hydroaminomethylation of 1-octene with benzylamine. 1-Octene (1.6 mmol), Benzylamine (1.6 mmol), 0.5 mol% catalyst loading, Toluene (5 ml), 50 bar CO:H₂ (1:3), 110 °C, 3 h.

The hydroaminomethylation activity obtained for C6-C8 are relatively similar, as can be seen from the product distributions displayed in Figure 4.23 as well as the regioselectivities and TON's showed in Table 4.16.

Chapter 4: Hydroaminomethylation of Olefins with Primary and Secondary Amines

It would therefore appear as if the nuclearity of the complex has no significant effect on the catalytic activity. Instead, the two metal centres in **C8** behave as independent catalytic centres exerting no effect on each other. It was expected that the binuclear nature of **C8** would lead to an enhanced catalytic reaction as is often observed when using multinuclear catalyst precursors such as dendrimers for example.²³

Table 4.16: Regioselectivity and TON of three different Ru(II) catalysts^a

Regioselectivity			
Catalysts	L:b (Aldehydes) ^b	L:b (Amines) ^c	TON ^d
C6	~	86:14	51
C7	~	84:16	48
C8	~	86:14	43

^a1-Octene (1.6 mmol), Benzylamine (1.6 mmol), 0.5 mol% catalyst loading, Toluene (5 ml), 50 bar CO:H₂ (1:3), 110 °C, 3 h.

^bL:b (aldehydes) (linear aldehydes:branched aldehydes)

^cL:b (amines) (linear amines:branched amines)

^dTON = moles amines/moles Ru(II)

4.4.3 Influence of time on the Ru(II) catalyzed hydroaminomethylation of 1-octene with benzylamine

The reaction time was then extended from 3 to 18 h (Figure 4.24 and Table 4.17).

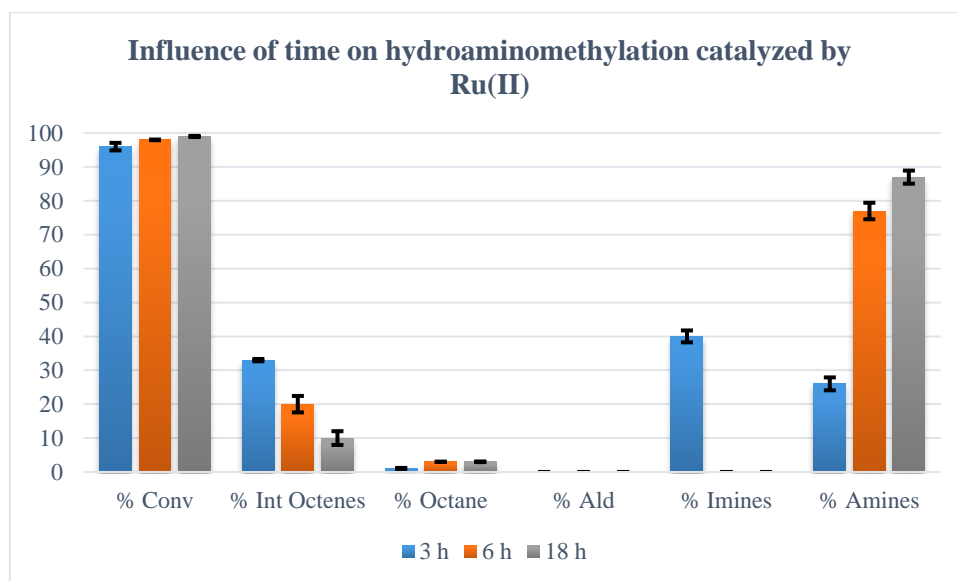


Figure 4.24: Influence of time of the hydroaminomethylation of 1-octene with benzylamine catalyzed by Ru(II) complex. 1-Octene (1.6 mmol), Benzylamine (1.6 mmol), 0.5 mol% catalyst loading (**C6**), Toluene (5 ml), 50 bar CO:H₂ (1:3), 110 °C.

Analysis of the product stream clearly indicates that the GC yield of the secondary *N*-alkylated benzylamines (Figure 4.24) and the TON's (Table 4.17) increased significantly upon extending the reaction time. The extended reaction time allowed the catalyst not only to convert the internal olefins to branched aldehydes, but also to completely hydrogenate the imines to the corresponding amines. The imine intermediates are completely consumed after 6 h, while during this time 20 % internal olefins still remains. Furthermore, the decrease in the internal olefins is much slower than the significant increase

Chapter 4: Hydroaminomethylation of Olefins with Primary and Secondary Amines

in the yield of the amine, especially between reaction times of 3-6 h. Since internal olefins are less reactive in hydroformylation compared to terminal olefins, subsequent conversion of the internal olefins will be slow. This leads to a much slower production of branched aldehydes. Therefore, one would expect that after some time, the rate at which amines are produced will slow down, which is the case as can be seen in Figure 4.24.

Once again, no aldehyde intermediates were detected. As alluded to earlier, this suggests that the hydroformylation of the olefins (terminal and internal) are slower than their subsequent Schiff-base condensation with benzylamine.

In terms of the regioselectivity, it was found that as the reaction time was extended, the regioselectivity towards the linear amine decreased. By extending the reaction time, more of the internal olefins were converted to branched aldehydes. These branched aldehydes subsequently undergo reductive amination with benzylamine to produce branched amines, thus reducing the selectivity to linear isomers.

Table 4.17: Influence of time of the regioselectivity and TON^a

Time (h)	Regioselectivity		TON ^d
	L:b (Aldehydes) ^b	L:b (Amines) ^c	
3	~	86:14	51
6	~	75:25	151
18	~	64:36	172

^a1-Octene (1.6 mmol), Benzylamine (1.6 mmol), 0.5 mol% catalyst loading (C6), Toluene (5 ml), 50 bar CO:H₂ (1:3), 110 °C.

^bL:b (aldehydes) (linear aldehydes:branched aldehydes)

^cL:b (amines) (linear amines:branched amines)

^dTON = moles amines/moles Ru(II)

4.4.4 Possible mechanism for the Ru-catalyzed hydrogenation of imines

A possible mechanism for the ruthenium-catalyzed hydrogenation of *N*-alkyl benzylimines is shown in Figure 4.25. This is based on similar mechanisms previously reported for rhodium and iridium complexes.^{9b, 25}

It is proposed that the first step in this process is most likely the oxidative addition of H₂, producing a Ru-dihydride species (**1**). The next step is reductive elimination of HCl, producing a four-coordinate Ru(II) species (**2**). Coordination of the imine substrate then occurs, producing species **3**. At this point, the first hydride transfer can occur, producing the iminium species (**4**). Oxidative addition of another H₂ occurs, producing another Ru-dihydride species containing the iminium ion (**5**). The amines are then released after a second hydride transfer, regenerating the active species (**2**).

Chapter 4: Hydroaminomethylation of Olefins with Primary and Secondary Amines

Ru(II) complexes (**C6-C8**) were also successfully evaluated as catalyst precursors in the hydroaminomethylation of 1-octene and benzylamine. Although not as active as Rh(I), these complexes also serves as efficient catalysts at slightly elevated temperatures. It was found that for the Ru(II) complexes, the hydroformylation reaction is slower than the Schiff-base condensation of the aldehydes with the amine. However, these complexes performs better as hydrogenation catalysts than hydroformylation catalysts. This possibly creates an avenue for a dual-metal catalyst, in which the Ru(II) systems can possibly be combined with Rh(I). In this way, the superior hydroformylation activity of Rh(I) can be exploited in conjunction with the excellent hydrogenation activity of Ru(II).

Importantly, it was found that the hydrogenation of the olefins to alkanes, as well as the hydrogenation of the aldehydes to alcohols, were not found to be an issue for either the Rh(I) and Ru(II) complexes. These catalysts thus selectively only hydrogenate the imines to the corresponding amines.

Lastly, we have successfully employed rhodium and ruthenium iminopyridine complexes in the hydroaminomethylation of 1-octene with primary (aniline and benzylamine) and secondary amines (piperidine). To the best of our knowledge, this is the first time that iminopyridine complexes of rhodium and ruthenium have been employed in this transformation.

4.6 Experimental

4.6.1 General Considerations

All of the reagents were purchased from either Merck or Sigma Aldrich and were used without further purification. Solvents were purchased from Merck or Kimix, and were dried by conventional distillation, Pure SolvTM micro solvent purifiers fitted with activated alumina columns or simple storing over molecular sieves. The HRhCO(PPh₃)₃ complex was prepared according to literature procedure.²⁴ CO, H₂ and syngas (CO:H₂, 1:1) was purchased from Afrox SA.

4.6.2 Instrumentation

Catalytic reactions were performed in a 50 ml Amar pressure reactor equipped with a Teflon liner. Catalytic reactions were monitored using a Varian 3800 Gas Chromatograph containing a Petrocol DH 50.2 (50 m x 0.2 mm x 0.5 μm) column equipped with a FID detector. For piperidine as amine the following temperature program was used: 80 °C (6 min hold), 100 °C (10 °C/min), 100 °C (10 min hold), 220 °C (20 °C/min), 220 °C (16 min hold), with total run time of 40 min. For aniline and benzylamine as amine the following temperature program was used: 80 °C (6 min hold), 100 °C (10 °C/min), 100 °C (10 min hold), 220 °C (20 °C/min), 220 °C (36 min hold), with total run time of 60 min. Helium was used as carrier gas at constant flow with a 1.1 ml/min flowrate. P-Xylene was used as the internal standard.

Chapter 4: Hydroaminomethylation of Olefins with Primary and Secondary Amines

4.6.3 General method for the hydroaminomethylation reaction**4.6.3.1 Hydroaminomethylation of 1-octene in the presence of piperidine**

The reactor was charged with toluene (5 mL) and the appropriate amount of the catalyst precursor in toluene. 1-Octene (179 mg, 0.25 mL, 1.6 mmol) and piperidine (136 mg, 0.158 mL, 1.6 mmol) was added resulting in a Rh:1-octene:piperidine ratio of 1:1000:1000. The reactor was flushed with syngas three times after which the reactor was pressurised to the required pressure and the heating started. At the conclusion of the reaction, the reactor was cooled and the reactor carefully vented and then opened. The reaction mixture was filtered using a syringe filter and dried over anhydrous MgSO₄. A sample (0.95 mL) of the reaction mixture was transferred to a GC vial containing 0.05 mL p-xylene (internal standard). The mixture was analysed using GC-FID. The components of the reaction mixture were identified using authentic GC standards (where available).

4.6.3.2 Hydroaminomethylation of 1-octene in the presence of aniline

The reactor was charged with toluene (5 mL) and the appropriate amount of the catalyst precursor in toluene. 1-Octene (179 mg, 0.25 mL, 1.6 mmol) and aniline (149 mg, 0.146 mL, 1.6 mmol) was added resulting in a Rh:1-octene:aniline ratio of 1:200:200. The reactor was flushed with syngas three times after which the reactor was pressurised to the required pressure and the heating started. At the conclusion of the reaction, the reactor was cooled and the reactor carefully vented and then opened. The reaction mixture was filtered using a syringe filter and dried over anhydrous MgSO₄. A sample (0.95 mL) of the reaction mixture was transferred to a GC vial containing 0.05 mL p-xylene (internal standard). The mixture was analysed using GC-FID. The components of the reaction mixture were identified using authentic GC standards (where available).

4.6.3.3 Hydroaminomethylation of 1-octene in the presence of benzylamine

The reactor was charged with toluene (5 mL) and the appropriate amount of the catalyst precursor in toluene. 1-Octene (179 mg, 0.25 mL, 1.6 mmol) and benzylamine (171 mg, 0.175 mL, 1.6 mmol) was added resulting in a Rh:1-octene:aniline ratio of 1:200:200. The reactor was flushed with syngas three times after which the reactor was pressurised to the required pressure and the heating started. At the conclusion of the reaction, the reactor was cooled and the reactor carefully vented and then opened. The reaction mixture was filtered using a syringe filter and dried over anhydrous MgSO₄. A sample (0.95 mL) of the reaction mixture was transferred to a GC vial containing 0.05 mL p-xylene (internal standard). The mixture was analysed using GC-FID. The components of the reaction mixture were identified using authentic GC standards (where available).

4.7 References

1. H. Elsen, C. Färber, G. Ballmann and S. Harder, *Angew. Chem. Int. Ed.*, 2018, **57**, 7156-7160.

Chapter 4: Hydroaminomethylation of Olefins with Primary and Secondary Amines

2. K. Shimizu, S. Kanno, K. Kon, S. M. A. H. Siddiki, H. Tanaka and Y. Sakata, *Catal. Today*, 2014, **232**, 134-138.
3. A. K. Yadav and L. D. S. Yadav, *RSC Adv.*, 2014, **4**, 34764-34767.
4. H. Hu, X. Cai, Z. Xu, X. Yan and S. Zhao, *Molecules*, 2018, **23**, 1764-1773.
5. C. Yu, R. Li and P. Gu, *Tetrahedron Lett.*, 2016, **57**, 3568-3570.
6. C. Gunanathan and D. Milstein, *Angew. Chem.*, 2008, **120**, 8789-8792.
7. A. García-Ortiz, J. D. Vidal, M. J. Climent, P. Concepción, A. Corma and S. Iborra, *ACS Sustainable Chem. Eng.*, 2019, **7**, 6243-6250.
8. (a) L. Huang, M. Arndt, K. Gooßen, H. Heydt, L. J. Gooßen, *Chem. Rev.*, 2015, **115**, 2596-2697.
(b) C. Michon, M-A Abadie, F. Medina, *J. Organomet. Chem.*, 2017, **847**, 13-27.
9. (a) C. Chen, X. Dong and X. Zhang, *Org. Chem. Front*, 2016, **3**, 1359-1370.
(b) P. Kalck and M. Urrutigoity, *Chem. Rev.*, 2018, **118**, 3833-3861.
(c) J. Hannedouche and E. Schulz, *Organometallics*, 2018, **37**, 4313-4326.
10. A. J. Vorholt, S. Immohr, K. A. Ostrowski, S. Fuchs and A. Behr, *Eur. J. Lipid Sci. Technol.*, 2017, **119**, 1600211-1600221.
11. A. Behr, M. Fiene, C. Buß and P. Eilbracht, *Eur. J. Lipid Sci. Technol.*, 2000, **102**, 467-471.
12. S. Li, K. Huang, J. Zhang, W. Wu and X. Zhang, *Org. Lett.*, 2013, **15**, 1036-1039.
13. G. Liu, Z. Li, H. Geng and X. Zhang, *Catal. Sci. Technol.*, 2014, **4**, 917-921.
14. K. Li, Y. Wang, Y. Xu, W. Li, M. Niu, J. Jiang and Z. Jin, *Catal. Commun.*, 2013, **34**, 73-77.
15. Y. Y. Wang, M. M. Luo, Y. Z. Li, H. Chen and X. J. Li, *Appl. Catal. A*, 2004, **272**, 151-155.
16. B. Dutta, R. Schwarz, S. Omar, S. Natour and R. Abu-Reziq, *Eur. J. Org. Chem.*, 2015, 1961-1969.
17. K. Li, Y. Wang, Y. Xu, W. Li, M. Niu, J. Jiang and Z. Jin, *Catal. Commun.*, 2013, **34**, 73-77.
18. E. Teuma, M. Loy, C. Le Berre, M. Etienne, J. Daran and P. Kalck, *Organometallics*, 2003, **22**, 5261-5267.
19. E. A. Karakhanov, E. A. Runova, Y. S. Kardasheva, D. V. Losev, A. L. Maksimov and M. V. Terenina, *Petrol. Chem.*, 2012, **52**, 204-210.
20. J. Liu, C. Kubis, R. Franke, R. Jackstell and M. Beller, *ACS Catal.*, 2016, **6**, 907-912.
21. S. Gülak, L. Wu, Q. Liu, R. Franke, R. Jackstell and M. Beller, *Angew. Chem. Int. Ed.*, 2014, **53**, 7320-7323.
22. V. K. Srivastava and P. Eilbracht, *Catal. Commun.*, 2009, **10**, 1791-1795.
23. N. C. Antonels, J. R. Moss and G. S. Smith, *J. Organomet. Chem.*, 2011, **696**, 2003-2007.
24. Y. Diao, J. Li, L. Wang, P. Yang, R. Yan, L. Jiang, H. Zhang and S. Zhang, *Catal. Today*, 2013, **200**, 54-62.
25. A. Fabrello, A. Bachelier, M. Urrutigoity and P. Kalck, *Coord. Chem. Rev.*, 2010, **254**, 273-287.

Chapter 5: The synthesis of primary amines, polymer precursors and surfactants via hydroaminomethylation

5.1 Introduction

Hydroaminomethylation is a powerful route towards the synthesis of amines. The main advantage of this reaction is its atom-efficiency, producing only water as by-product, while amines are synthesized in high yields. Furthermore, isolation of these amines after hydroaminomethylation does not involve laborious purification steps.

Work done by Eilbracht and co-workers in the late 1990's and early 2000's paved the way for an in-depth investigation into the potential application of hydroaminomethylation. They specifically focussed on the synthesis of azamacroheterocycles (including polyazamacroheterocycles), pharmacologically active diamines, cryptands, 4,4-diarylbutylamines such as fluspirilene as well as organic compounds containing the quinazoline scaffold, via hydroaminomethylation.¹⁻⁵ Most of the work reported in these publications involved the use of a Rh-precursor (either $[\text{Rh}(\text{COD})\text{Cl}]_2$ or $[\text{Rh}(\text{acac})(\text{CO})_2]_2$) in the absence of any ligands. The groups of Beller and Zhang investigated the synthesis of 3,3-diarylpropylamines, such as fempiprane (antiallergic agent).⁶⁻⁷ Furthermore, hydroaminomethylation can also be performed intramolecularly. This allowed Alper and co-workers to synthesize 1,2,3,4-tetrahydroquinolines and 2,3,4,5-tetrahydro-1*H*-2-benzazepines.⁸⁻¹⁰ In addition to the synthesis of pharmacologically active amines, hydroaminomethylation can also be used to synthesize polymer and surfactant precursors.¹¹⁻¹⁴

The latter inspired us to explore the use of hydroaminomethylation to synthesize primary amines, biopolymer precursors as well as biosurfactants.

5.2 The synthesis of primary amines via hydroaminomethylation

In synthetic organic chemistry, the Gabriel phthalimide amine synthesis represents an important and historical route towards the synthesis of primary amines. Generally, in this process alkyl halides are used as alkylating agents, after which the free amine is liberated either through acid hydrolysis or via the Ing-Manske procedure using hydrazine.¹⁵⁻¹⁶ Another important route towards primary amines is via the reduction of nitro or nitrile-containing compounds.¹⁷⁻²⁰ These reductions are normally carried out by a metal-catalyzed process.¹⁷⁻¹⁸ However, in a report by Benaglia and co-workers, they developed a metal-free reduction of aliphatic and aromatic nitro derivatives via a continuous-flow process.¹⁹

Chapter 5: The synthesis of primary amines, polymer precursors and surfactants via hydroaminomethylation

Kobayashi and co-workers also synthesized primary amines via a continuous-flow process making use of a polysilane/SiO₂-supported palladium catalyst.²⁰

Additionally, primary amines can be synthesized via the alkylation of ammonia. In this regard, Gunanathan and Milstein developed a ruthenium-catalyzed process for the selective production of primary amines directly from alcohols and ammonia.²¹ This resulted in the atom-economical production of primary amines under mild conditions, with only water as a by-product. Similarly, Shimizu and co-workers also studied the synthesis of primary amines from alcohols and ammonia using a Ni/CaSiO₃ catalyst.²²

Hydroaminomethylation of olefins with ammonia is therefore also a plausible route towards the synthesis of primary amines. Since the olefin is a cheap feedstock, this approach is particularly attractive for the synthesis of valuable primary amines. Examples of hydroaminomethylation employing ammonia as an amine-source are relatively scarce. The primary amines that are obtained from the hydroaminomethylation of olefins and ammonia are themselves more reactive than ammonia in hydroaminomethylation. This results in the production of secondary as well as traces of tertiary amines. Nevertheless, Beller and co-workers reported the first efficient production of primary amines from ammonia.²³ In order to ensure high selectivity towards the primary amine, they employed a dual-metal catalyst system (Rh/Ir) to ensure rapid hydrogenation of the imine, while also performing the reaction in the presence of excess of aqueous ammonia, therefore limiting secondary side reactions. However, employing large excess of aqueous ammonia can lead to catalyst deactivation, while also hampering the Schiff-base condensation reaction. Therefore, the same authors turned their attention towards the use of supercritical ammonia.²⁴ This allowed them to synthesize the primary amines in up to 60 % yield, albeit at very high pressures.

A possible alternative to the use of ammonia is to use ammonia-surrogates. Various ammonia-surrogates are known, however, we opted for benzylamine. In Chapter 4, we demonstrated the chemoselective synthesis of *N*-alkyl benzylamines in high yields under mild conditions. The benzyl group can easily be removed via a Pd-catalyzed debenzylation in the presence of H₂, producing primary amines (Figure 5.1).

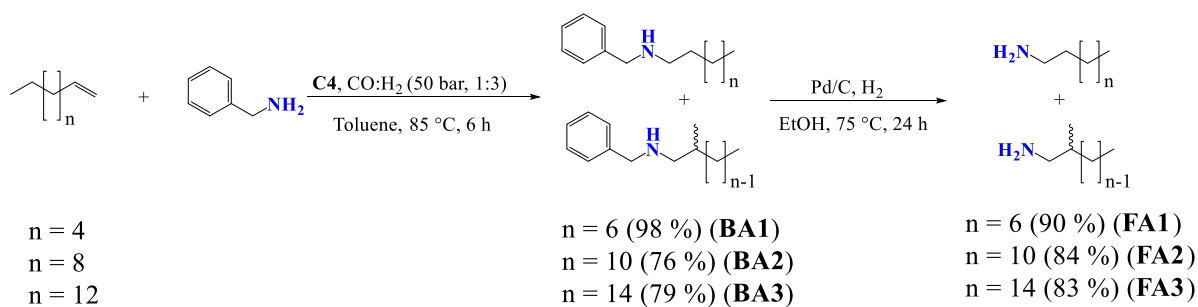


Figure 5.1: Synthesis of fatty amines via hydroaminomethylation and Pd-catalyzed debenzylation

Chapter 5: The synthesis of primary amines, polymer precursors and surfactants via hydroaminomethylation

We investigated the hydroaminomethylation of α -olefins (1-octene, 1-dodecene and 1-hexadecene) with benzylamine, producing *N*-alkyl benzylamines (Figure 5.1, **BA1-BA3**). The *N*-alkyl benzylamines were isolated in high to excellent yields (76-98 %) as light yellow oils. Using Pd/C in the presence of H₂, allowed for the synthesis of fatty amines (**FA1-FA3**) in high to excellent yields (83-90 %) as colorless oils.

In industry, fatty amines are commonly synthesized via the Nitrile process.²⁵ This process entails the reaction of naturally occurring fatty acids with ammonia at high temperatures (>250 °C), in the presence of a metal oxide catalyst, to produce fatty nitriles. These fatty nitriles subsequently undergo hydrogenation by Raney nickel, in the presence of excess ammonia, to the corresponding fatty amines. Excess ammonia is necessary to inhibit the formation of secondary and tertiary amines. Although our strategy involves the use of rhodium-based catalysts, it is still superior to the nitrile process in terms of activity and selectivity. The hydroaminomethylation of the α -olefins in the presence of benzylamine proceeds smoothly under mild conditions giving high yields to the corresponding *N*-alkyl benzylamines. Furthermore, secondary *N*-alkyl benzylamines are selectively obtained even though these compounds can undergo further *N*-alkylation to tertiary amines. Subsequently, these secondary *N*-alkyl benzylamines undergoes hydrogenolysis, producing the fatty amines in high yields as mixtures of regio-isomers (as a result of the isomerization of the α -olefins).

The fatty amines produced were characterized using IR and ¹H NMR spectroscopy, as well as GC-FID analysis. Since the characterization data is similar for all the compounds, the discussion will be limited to **FA2** (the C13 fatty amines).

In our study of the hydroaminomethylation of 1-octene in the presence of benzylamine in Chapter 4, we obtained a GC yield of ~95 % towards the *N*-alkylated benzylamines. Therefore, we extended the reaction time from 3 to 6 h in order to ensure full conversion of the olefins (terminal and internal) to the target amines. GC-FID analysis (Figure 5.2) confirmed complete conversion of all the olefins as well as the aldehyde and imine intermediates to **BA2** (secondary *N*-alkylated benzylamines).

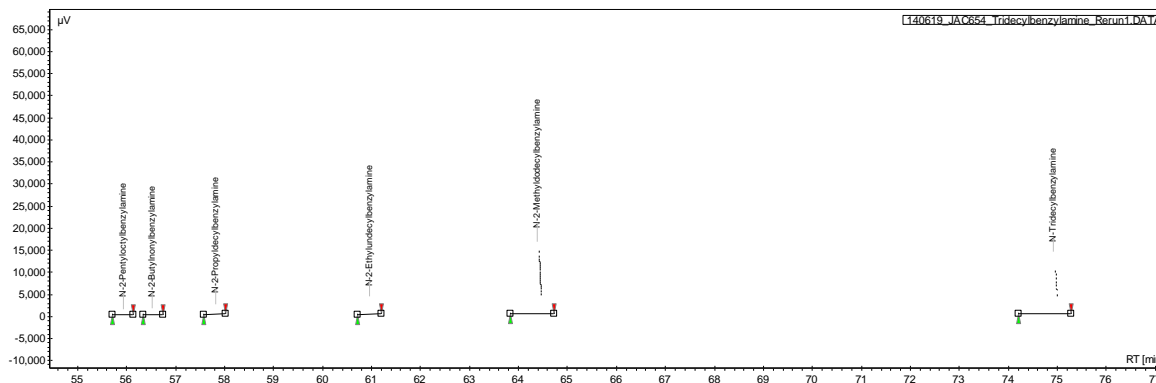
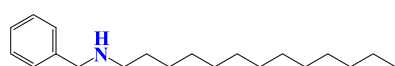


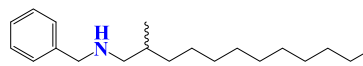
Figure 5.2: GC-FID spectrum of the C13 amines

Chapter 5: The synthesis of primary amines, polymer precursors and surfactants via hydroaminomethylation

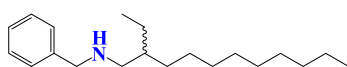
BA2 were isolated as a regio-isomeric mixture of six amines, as can be seen in Figure 5.2. The four minor amines form as a result of the isomerization of the α -olefin to its internal counterparts, followed by their subsequent conversion to the corresponding amines. The two major amines, with peaks in the chromatogram at ~64.5 and 75 min, belongs to *N*-2-methyldodecylbenzylamine and *N*-tridecylbenzylamine (Figure 5.3) respectively.



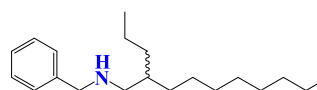
N-tridecylbenzylamine



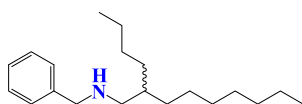
N-2-methyldodecylbenzylamine



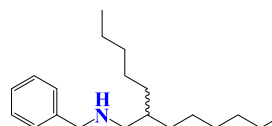
N-2-ethylundecylbenzylamine



N-2-propyldecylbenzylamine



N-2-butylnonylbenzylamine



N-2-pentyldecylbenzylamine

Figure 5.3: Regio-isomeric C13 benzylamines obtained after hydroaminomethylation of 1-dodecene and benzylamine

The IR spectrum of **BA2** is shown in Figure 5.4 (top spectrum) while the bottom spectrum belongs to the C13 fatty amines (**FA2**, after Pd-catalyzed debenzilation). From the top spectrum, the presence of the benzyl group is confirmed by the absorptions at 3028-3085 cm^{-1} , assigned to the =C-H stretches of the aromatic moiety. Furthermore, the out-of-plane bending vibrations is also observed at 696 and 728 cm^{-1} . Additionally, the C=C stretches of the aromatic moiety appeared at 1494 and 1604 cm^{-1} . Furthermore, the very strong C-H stretches of the alkyl chain are observed at 2851-2955 cm^{-1} .

Hydrogenolysis were then carried out on **BA2**. This reaction was carried out using the heterogeneous catalyst, Pd/C, at 75 °C (reaction did not work at room temperature). This produced the free fatty amines (**FA2**). From the bottom spectrum in Figure 5.4, the removal of the benzyl group is confirmed by the disappearance of the C=C aromatic stretches as well as the =C-H stretching and bending vibrations.

Further confirmation was obtained from ^1H NMR spectroscopy (Figure 5.5). The ^1H NMR spectrum of **BA2** is the top spectrum while the bottom spectrum is that of **FA2**. These spectra clearly confirm the successful removal of the benzyl group due to the disappearance of the signals at 3.79 (benzyl protons) and 7.33 ppm (aromatic protons).

Chapter 5: The synthesis of primary amines, polymer precursors and surfactants via hydroaminomethylation

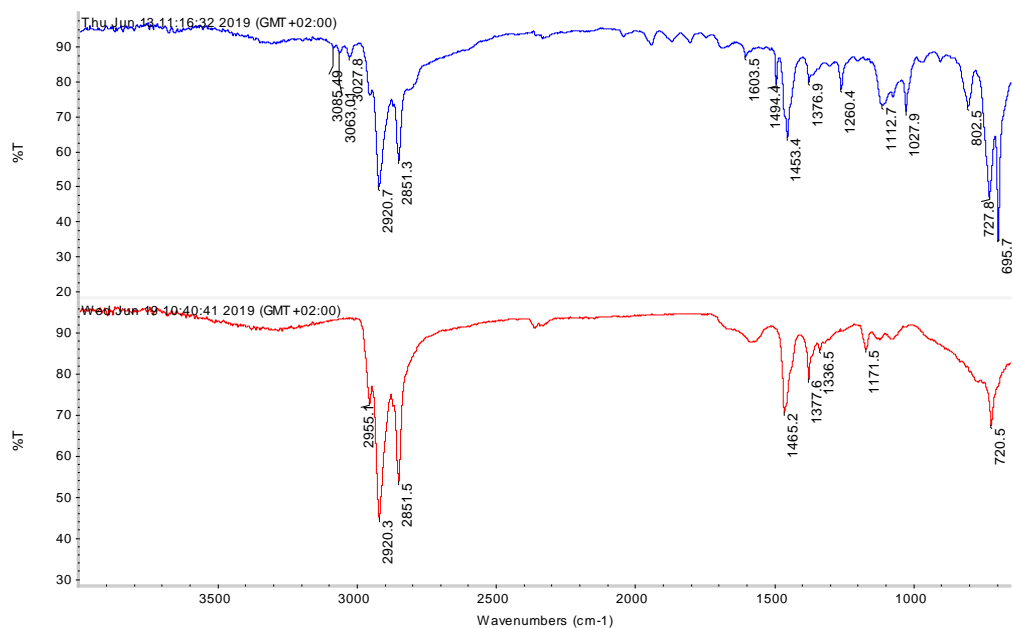


Figure 5.4: IR spectra of C13 N-alkylated benzylamines (Top) and C13 fatty amines (bottom)

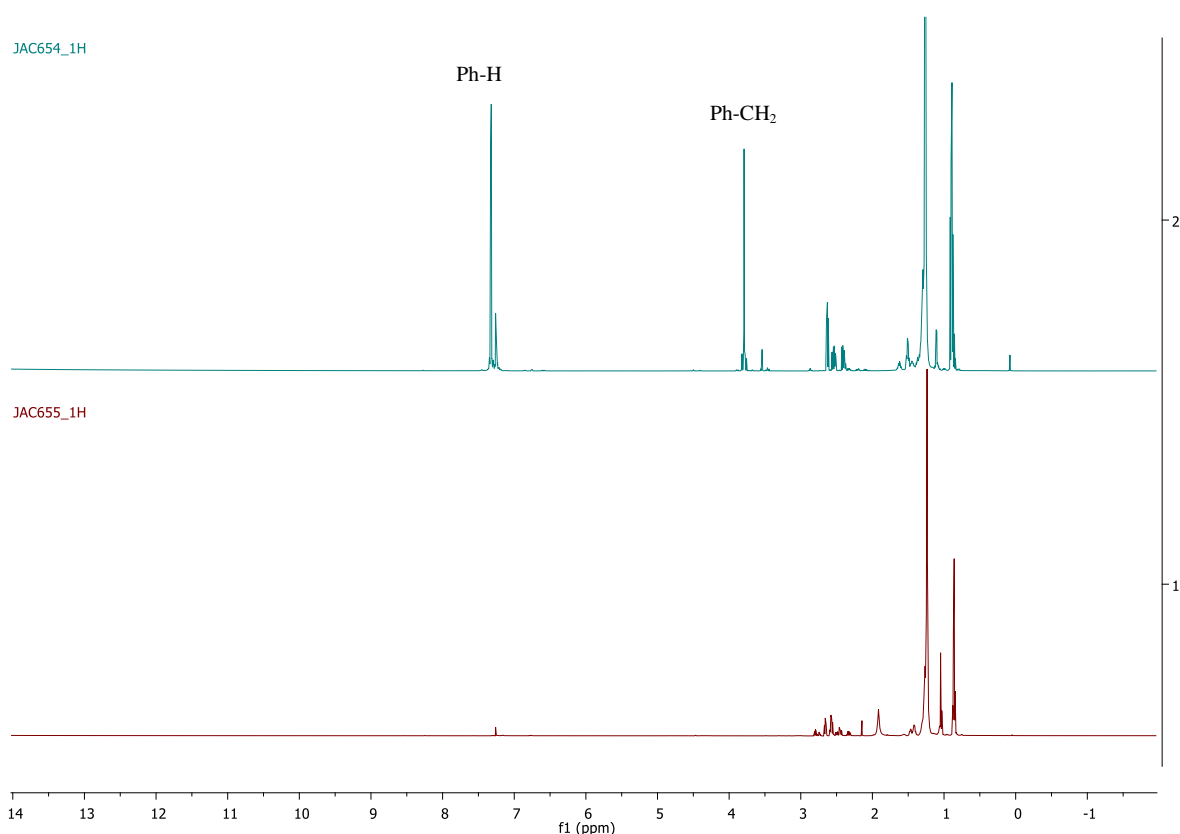


Figure 5.5: ¹H NMR spectrum of C13 N-alkyl benzylamines (Top) and C13 fatty amines (bottom) ran in CDCl₃

We have therefore successfully demonstrated the synthesis of fatty amines from cheap olefin feedstocks via hydroaminomethylation and Pd-catalyzed debenylation. To the best of our knowledge, this is the first time that fatty amines have been synthesized via this route. These fatty amines were isolated as mixtures of regio-isomers which form as a result of the isomerization of the olefins. Fatty amines

Chapter 5: The synthesis of primary amines, polymer precursors and surfactants via hydroaminomethylation

available commercially are mixtures of amines as well (mixture of carbon chains or a specific carbon chain).²⁶

Following the successful synthesis of fatty amines from α -olefins in the presence of benzylamine, we turned our attention towards the study of bio-renewable substrates, more specifically, the synthesis of primary amines via the hydroaminomethylation of eugenol. Eugenol is an aromatic compound which is extracted from essential oils, especially from clove oil.²⁷ Eugenol finds use in the perfume and flavouring industry. The use of eugenol in hydroaminomethylation is not that common with relatively few reports available in the literature.²⁸⁻³⁰ The conversion of bio-renewable substrates to value-added products can help alleviate the strain on fossil fuels. The valorization of eugenol in hydroaminomethylation to form primary amines are particularly interesting because the resulting products are dopamine-analogues and are therefore pharmacologically-active amines (Figure 5.6).

Following the hydroaminomethylation of eugenol in the presence of benzylamine, **DA1** was isolated in 93 % yield as a orange-brown oil. Subjecting **DA1** to Pd-catalyzed hydrogenolysis, produces the corresponding dopamine-analogues (**DA2**) as a light yellow oil (94 % yield).

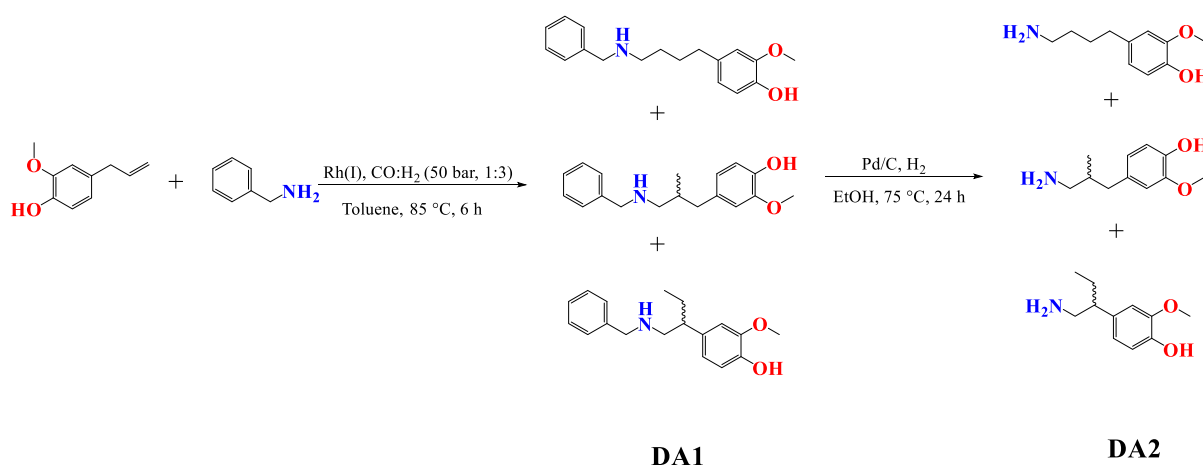


Figure 5.6: Synthesis of Dopamine-analogues (**DA2**) via hydroaminomethylation and Pd-catalyzed debenzylation

The ¹H NMR spectrum of eugenol is shown in Figure 5.7 (top spectrum). In this spectrum, the olefinic protons are observed at 5.12 and 6.02 ppm. Upon successful hydroaminomethylation, these signals disappear (Figure 5.7, middle spectrum), with the appearance of new signals at 3.79 ppm, assigned to the benzylic protons, and at 7.32 ppm, which is assigned to the aromatic protons. Furthermore, various new signals appear between 1-3 ppm, which are due to the new aliphatic protons. As was the case for the fatty amines discussed above, a mixture of regio-isomers was obtained as a result of the isomerization of eugenol. After hydrogenolysis, the signals at 3.79 and 7.32 ppm disappear, confirming the successful preparation of the dopamine-analogues (**DA2**).

To the best of our knowledge, this is the first time that dopamine-analogues were synthesized in this way starting from eugenol in high yields. In addition to its pharmacological activity, dopamine is also

Chapter 5: The synthesis of primary amines, polymer precursors and surfactants via hydroaminomethylation

able to self-polymerize into thin films.³¹ These materials find application as bio-adhesives. In this regard, You and co-workers³¹ previously investigated analogues of dopamine and their ability to undergo self-polymerization. The linear dopamine-analogue (Figure 5.6, top dopamine-analogue) was one of the compounds that was analyzed (after removal of the methoxy group). This confirms the potential applications of these type of compounds. Furthermore, the synthesis outlined in the You publication entails seven steps in order to obtain the dopamine-analogues, suggesting that our strategy reported here appears to be more effective.

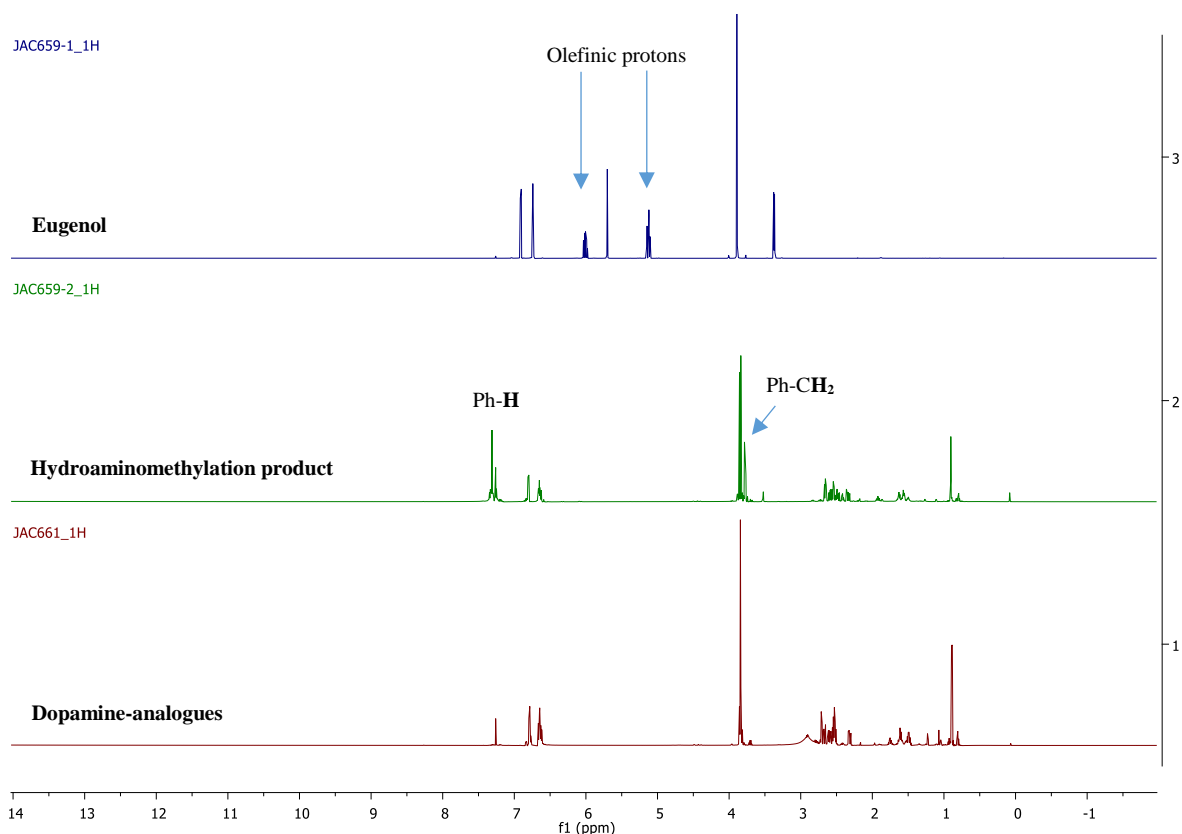


Figure 5.7: ¹H NMR spectra of eugenol (top), hydroaminomethylation product (middle) and dopamine-analogues (bottom)

5.3 The synthesis of novel bio-polymer precursors via hydroaminomethylation

Continuing with the valorization of bio-renewable substrates, we shifted our focus towards undecylenic acid. Undecylenic acid is usually prepared from ricinoleic acid, which is obtained from castor oil.³² In industry, undecylenic acid is converted to 11-aminoundecanoic acid, which is then used for the production of Nylon-11. Furthermore, undecylenic acid is also used as an antifungal agent.³³ The methyl ester of this acid, 10-methyl undecenoate, is also a valuable precursor to polyamides, polyesters, polyurethanes, insect pheromones and lubricants, just to name a few.³⁴⁻³⁸

As a first point of departure, we studied the hydroformylation of 10-methyl undecenoate (Figure 5.8) to the corresponding aldehydes. After the hydroformylation of methyl 10-undecenoate, the

Chapter 5: The synthesis of primary amines, polymer precursors and surfactants via hydroaminomethylation

corresponding aldehydes were isolated as brown oils with a total yield of 84 %. Characterization of the aldehydes was performed using IR (Figure 5.9) and NMR (^1H and ^{13}C) spectroscopy, as well as mass spectrometry.

The IR spectrum of methyl 10-undecenoate is shown in Figure 5.9 (top spectrum). The ester C=O stretch is situated at 1739 cm^{-1} , while the C=C stretch of the olefinic bond occurred at 1640 cm^{-1} . After hydroformylation, the C=C stretch disappears, with the appearance of a new band at 1704 cm^{-1} , assigned to the C=O stretch of the aldehyde (Figure 5.9, bottom spectrum).

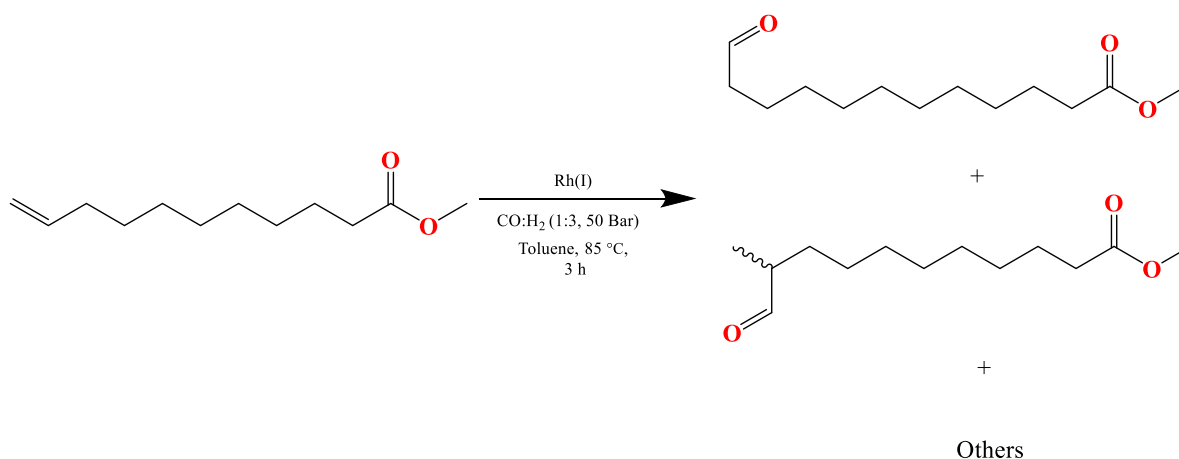


Figure 5.8: Hydroformylation of 10-methyl undecenoate

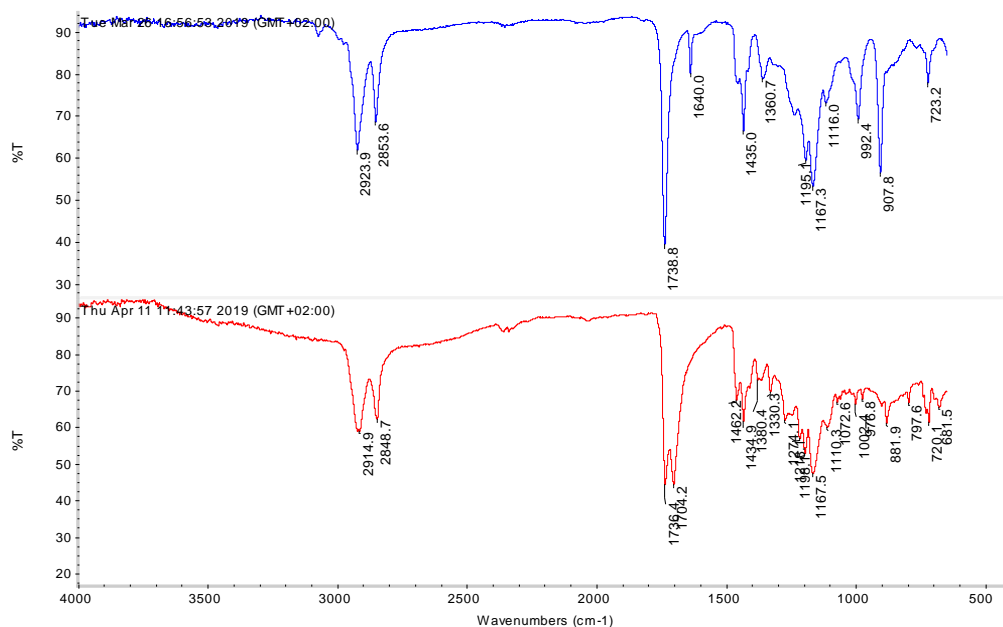


Figure 5.9: IR spectra of methyl 10-undecenoate (top spectrum) and the hydroformylation product (bottom)

^1H NMR spectroscopy lends further credence to the successful conversion of methyl 10-undecenoate to the corresponding aldehydes (Figure 5.10). The olefinic signals, present at ~ 4.95 and ~ 5.80 ppm in the spectrum of methyl 10-undecenoate (Figure 5.10, top spectrum), disappeared, with the concomitant

Chapter 5: The synthesis of primary amines, polymer precursors and surfactants via hydroaminomethylation

appearance of new signals around 9.55-9.75 ppm (bottom spectrum in Figure 5.10). These signals are assigned to the aldehydic protons. Furthermore, for the linear aldehyde, a triplet was observed (9.75 ppm, integrating for one proton), while for the methyl branched aldehyde, a doublet was observed (9.60 ppm, integrating for 0.71 proton). Additionally, a multiplet was observed at 9.55 ppm, integrating for 0.48 protons. Based on this, we can roughly determine the l:b ratio to be 46:54.

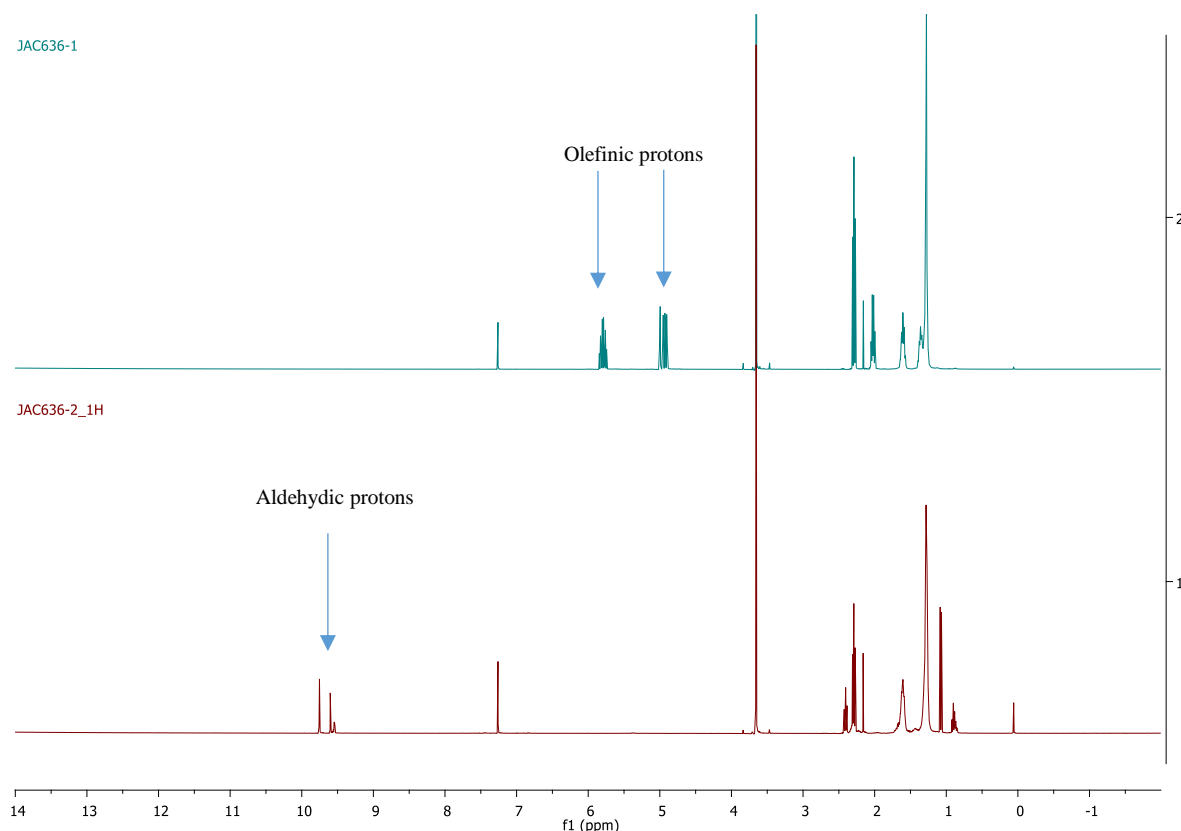


Figure 5.10: ¹H NMR spectra of methyl 10-undecenoate (top spectrum) and the hydroformylation product (bottom) in CDCl₃

The ESI-MS spectrum (direct injection, positive mode) is shown in Figure 5.11. The molecular ion ([M+H]⁺) for methyl 12-oxododecanoate (and its branched counterparts) was not observed. However, the base peak was observed at *m/z* 267.1565, assigned to the potassium adduct of methyl 12-oxododecanoate ([M+K]⁺), corresponding well with the theoretical isotopic pattern.

Following the successful hydroformylation of methyl 10-undecenoate to the corresponding aldehydes, we proceeded towards the evaluation of this substrate in hydroaminomethylation. As amines substrates, we opted to study the hydroaminomethylation of this substrate with amino esters, more specifically, L-proline methyl ester and methyl piperidine-4-carboxylate (Figure 5.12).

The esters of these amino acids were used in order to prevent salt formation. Furthermore, L-proline is known to catalyse the aldol condensation of aldehydes and therefore dimerization of the aldehydes, produced in hydroformylation, can possibly occur.³⁹

Chapter 5: The synthesis of primary amines, polymer precursors and surfactants via hydroaminomethylation

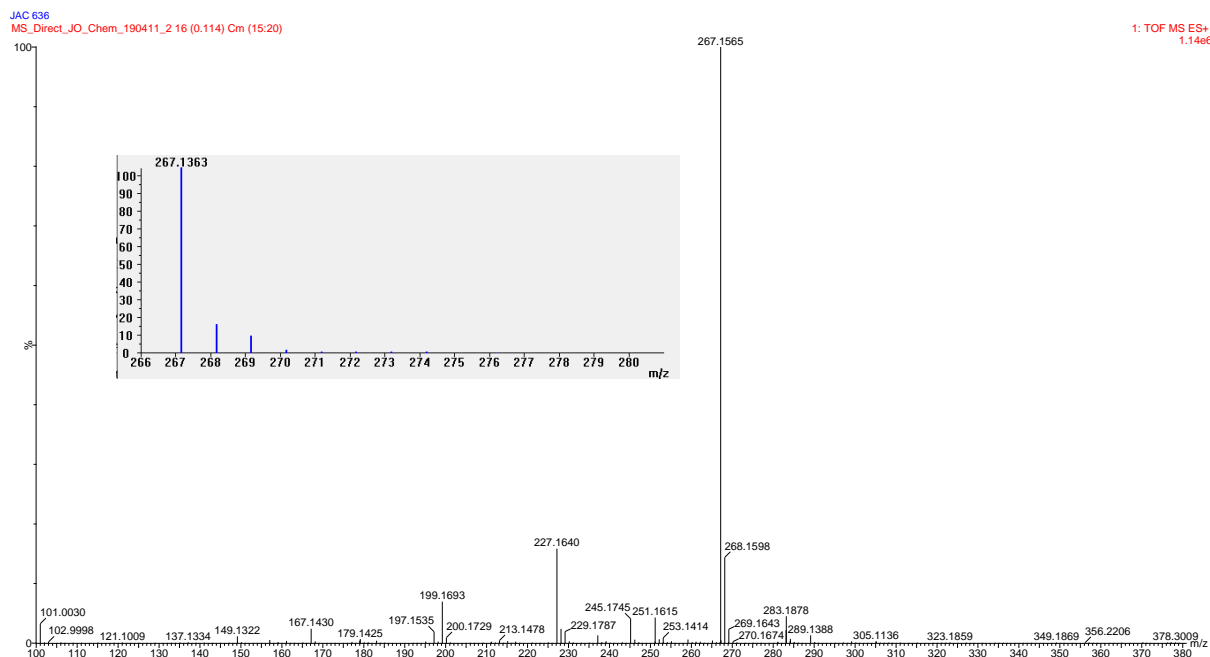


Figure 5.11: ESI-MS (direct injection) spectrum of methyl 12-oxododecanoate and its branched isomers



Figure 5.12: *L*-proline methyl ester and methyl piperidine-4-carboxylate amines for hydroaminomethylation of methyl 10-undecenoate

Owing to its excellent organocatalytic activity, *L*-proline has previously been incorporated into a polymeric matrix, in order to enable the recyclability and reusability of the organo catalyst.⁴⁰⁻⁴¹ However, *L*-proline and piperidine-4-carboxylic acid also have medicinal applications.⁴²⁻⁴⁴ Therefore, the incorporation of these amino acids into biopolymers would be biologically relevant. In this regard, Vorholt and co-workers¹² previously investigated the hydroaminomethylation of methyl oleate with *L*-proline, producing diester monomers as precursors to biopolymers.

Inspired by this, we set out to explore the hydroaminomethylation of methyl 10-undecenoate with *L*-proline methyl ester and methyl piperidine-4-carboxylate (Figure 5.13) to produce a di-functional ester such as the compound, **DE1**. The latter was isolated as a light yellow oil (93 % yield).

Characterization of **DE1** was performed by means of IR and NMR (¹H and ¹³C) spectroscopy and mass spectrometry (ESI-MS, direct injection in the positive mode). In the IR spectrum of **DE1**, a band at 1736 cm⁻¹ was observed. This absorbance was assigned to the two ester moieties. However, confirmation of the successful synthesis of **DE1** was obtained from ¹H NMR spectroscopy (Figure 5.14)

Chapter 5: The synthesis of primary amines, polymer precursors and surfactants via hydroaminomethylation

and mass spectrometry (Figure 5.15). In the ^1H NMR spectrum, the olefinic signals of methyl 10-undecenoate at ~ 4.95 and ~ 5.80 ppm (Figure 5.14, top) disappeared due to the conversion to the corresponding aldehydes. These aldehydes subsequently underwent reductive amination with L-proline methyl ester, as confirmed by the absence of aldehyde signals. Furthermore, three signals are observed at 3.66, 3.69 and 3.72 ppm. These signals are assigned to the methyl groups of the various ester moieties.

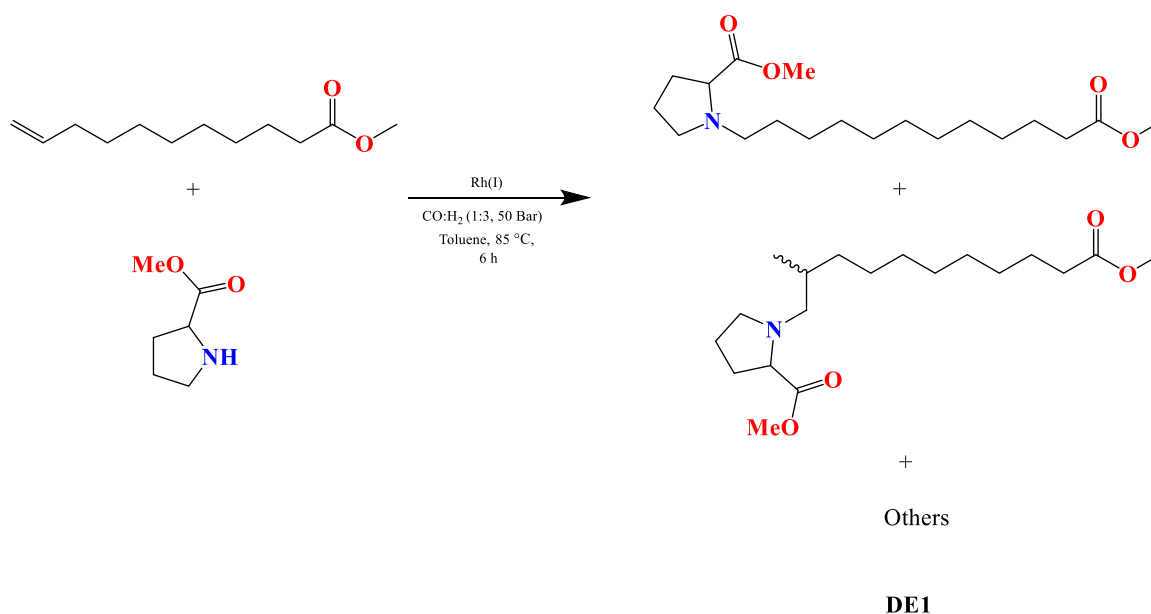


Figure 5.13: Hydroaminomethylation of methyl 10-undecenoate with L-proline methyl ester

The ESI-MS spectrum (direct injection, positive mode) of **DE1** is shown in Figure 5.15. In this spectrum, the molecular ion ($[\text{M}+\text{H}]^+$) and base peak is observed m/z 342.2646. There is excellent agreement between the experimental and the theoretical isotopic pattern.

Therefore, IR and ^1H NMR spectroscopy as well as mass spectrometry confirmed the successful synthesis of **DE1**. The ester derivatives was then converted to the corresponding dicarboxylic acid derivatives (**DC1**) via base mediated hydrolysis followed by subsequent protonation of the potassium salts using hydrochloric acid (1 M) (Figure 5.16).

The hydrolysis of the ester moieties to the corresponding carboxylic acids was confirmed via IR spectroscopy (Figure 5.17). Upon protonation, the dicarboxylic acids precipitated out of the water as a white solid (78 % yield). This compound shows solubility in MeOH and hot EtOH, while it is insoluble in MeCN, acetone and water. Characterization of **DC1** was accomplished by means of IR (Figure 5.17) and ^1H NMR spectroscopy (Figure 5.18).

Chapter 5: The synthesis of primary amines, polymer precursors and surfactants via hydroaminomethylation

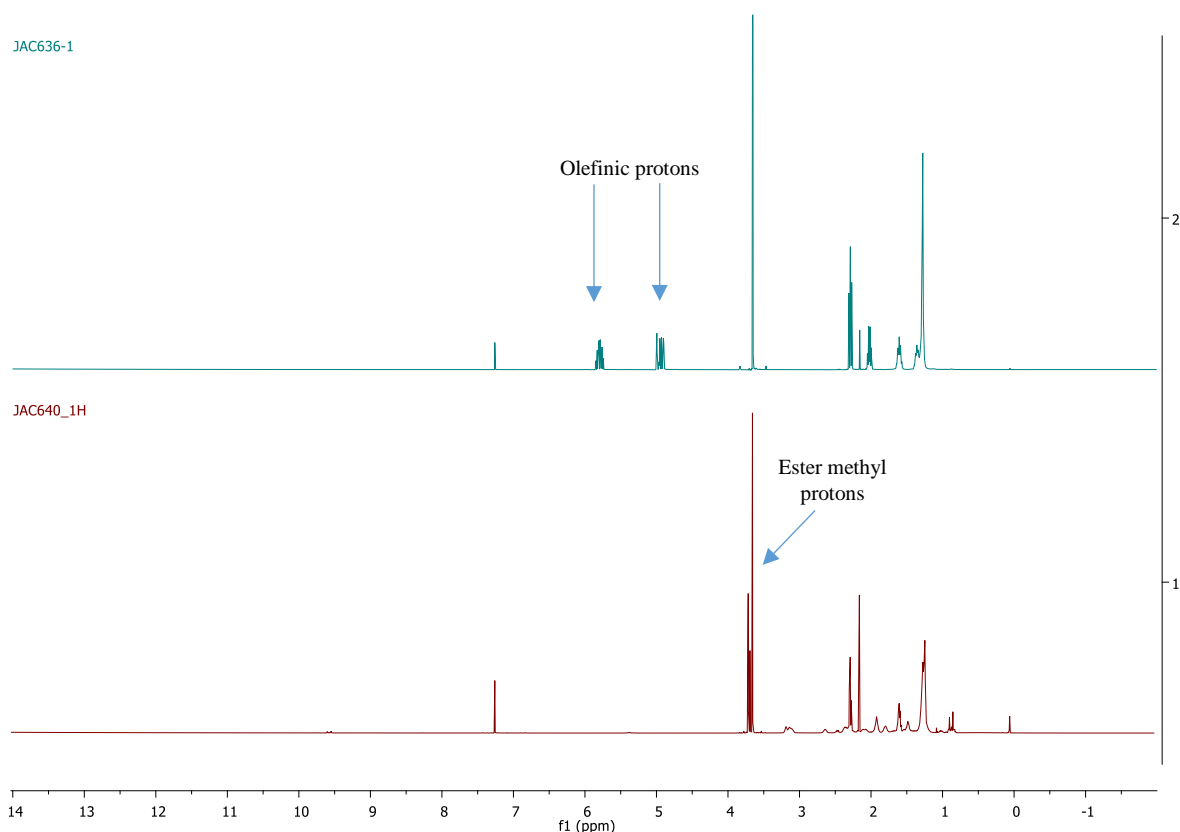


Figure 5.14: ¹H NMR spectra of methyl 10-undecenoate (top spectrum) and the diester obtained from hydroaminomethylation (bottom spectrum)

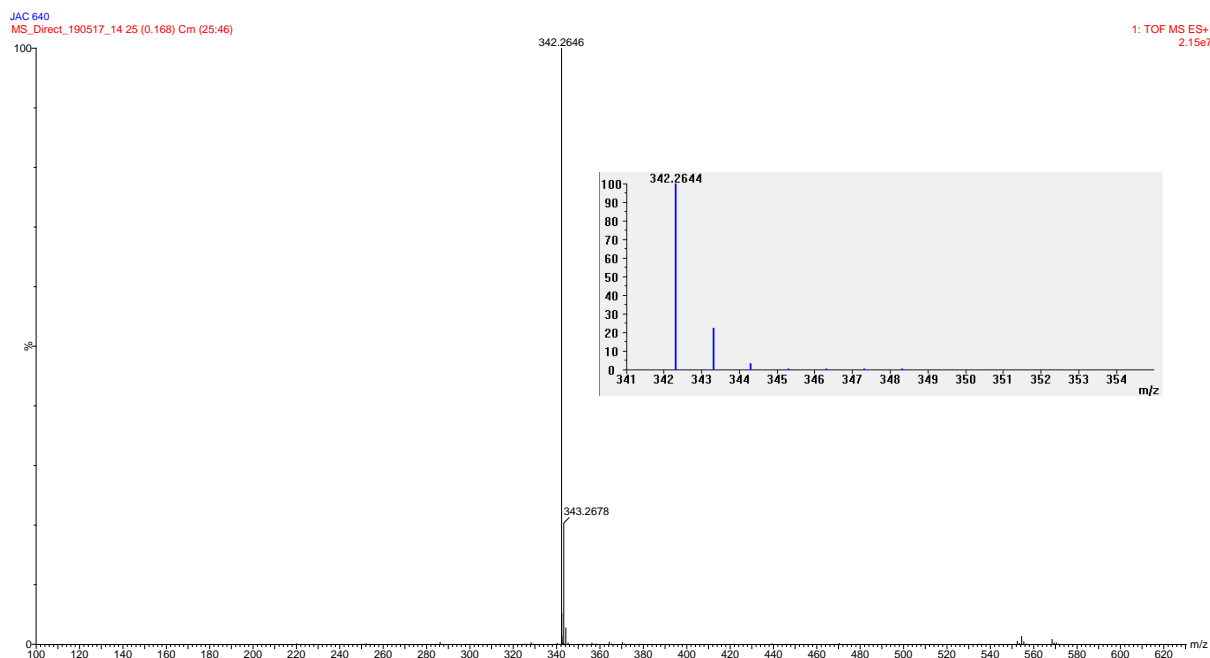


Figure 5.15: ESI-MS spectrum (direct injection, positive mode) of the Diester (DEI)

In Figure 5.17 (top spectrum), the ester moieties can be observed at 1736 cm^{-1} . **DEI** then underwent KOH-mediated ester hydrolysis. This produced a potassium-carboxylate salt, with the IR spectrum shown in Figure 5.17 (middle spectrum). The ester band disappeared as a result of hydrolysis, with the

Chapter 5: The synthesis of primary amines, polymer precursors and surfactants via hydroaminomethylation

appearance of a new band at 1563 cm^{-1} , assigned to the carboxylate moiety. Upon protonation, the carboxylate band disappeared, making way for a new band at 1720 cm^{-1} , as a result of the C=O stretch of the carboxylic acid (**DC1**).

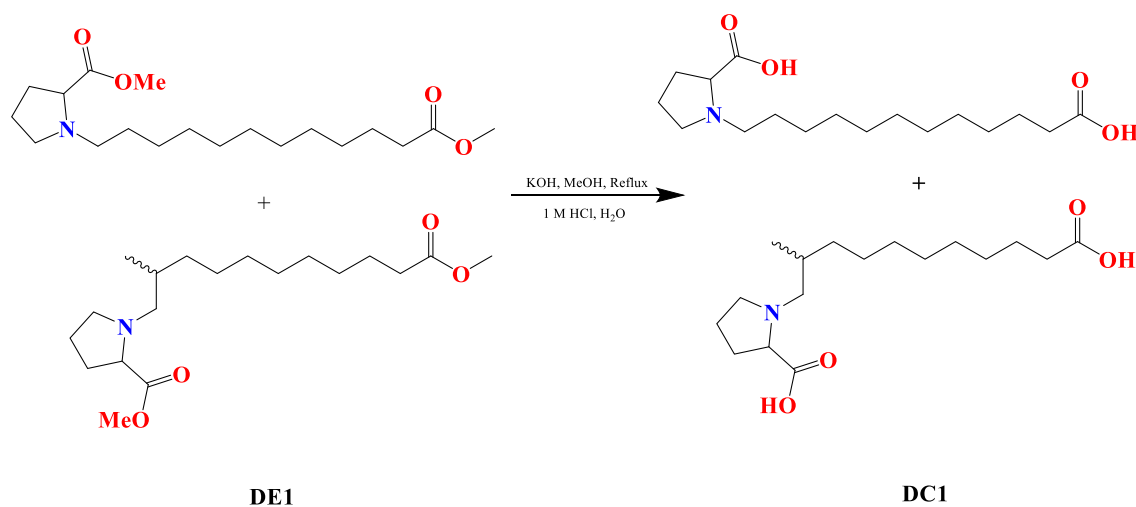


Figure 5.16: Preparation of dicarboxylic acid from diester via base-mediated hydrolysis

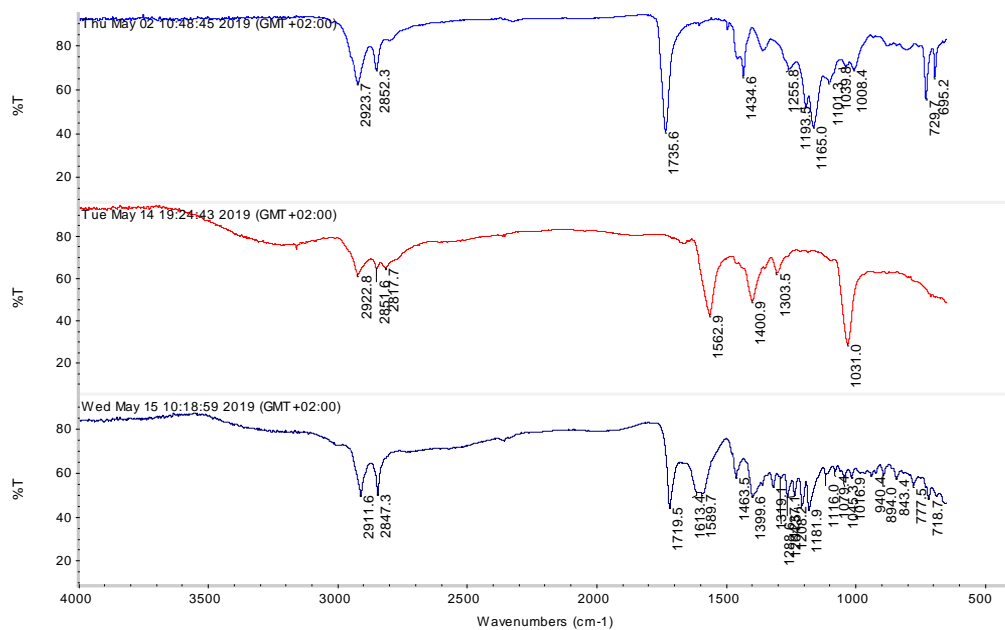


Figure 5.17: IR spectrum of **DE1** (top), potassium carboxylate salt (middle) and **DC1** (bottom)

Similarly, in the ^1H NMR spectrum of **DE1** (Figure 5.18, top), the methyl groups of the esters ($\sim 3.70\text{ ppm}$) disappeared, confirming hydrolysis to the corresponding carboxylic acids (Figure 5.18, bottom).

Furthermore, the ESI-MS (direct injection, positive mode) spectrum of **DC1** is shown in Figure 5.19. In this spectrum, the molecular ion ($[\text{M}+\text{H}]^+$), which is also the base peak, is observed at m/z 314.2344.

Chapter 5: The synthesis of primary amines, polymer precursors and surfactants via hydroaminomethylation

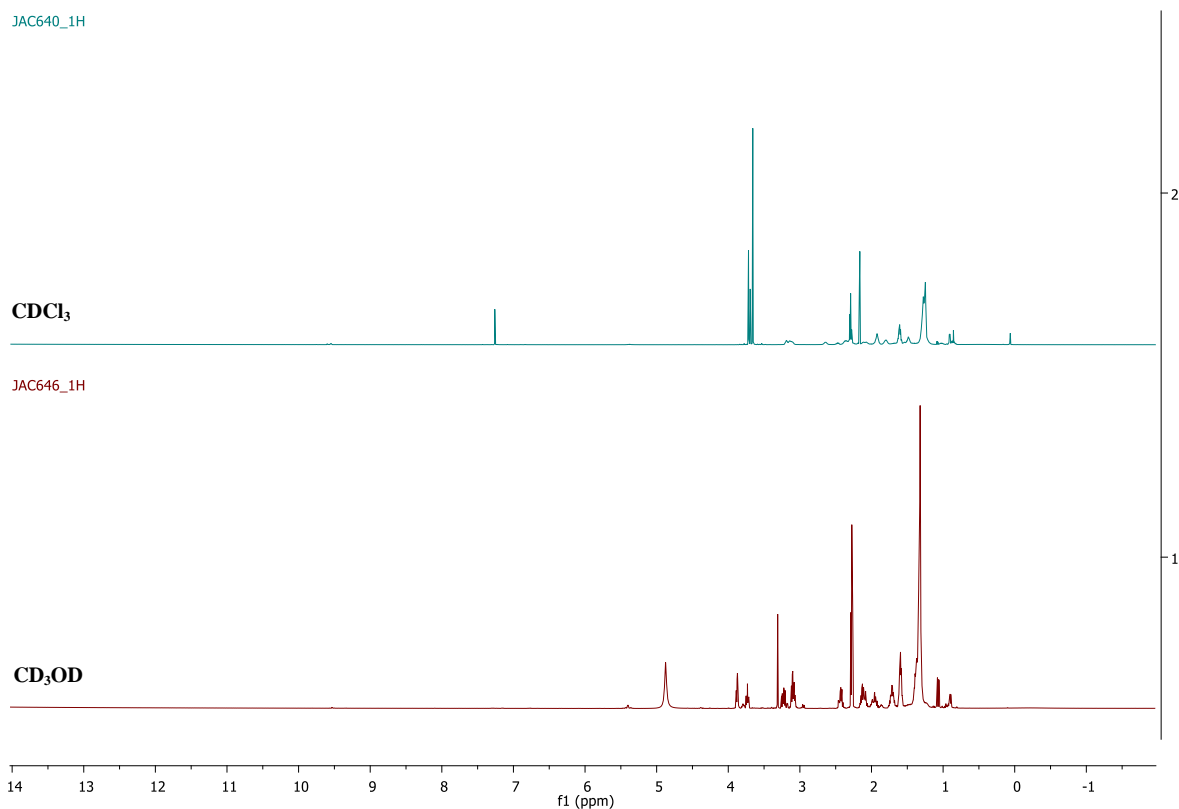


Figure 5.18: ^1H NMR spectra of **DEI** (top) and **DCI** (bottom)

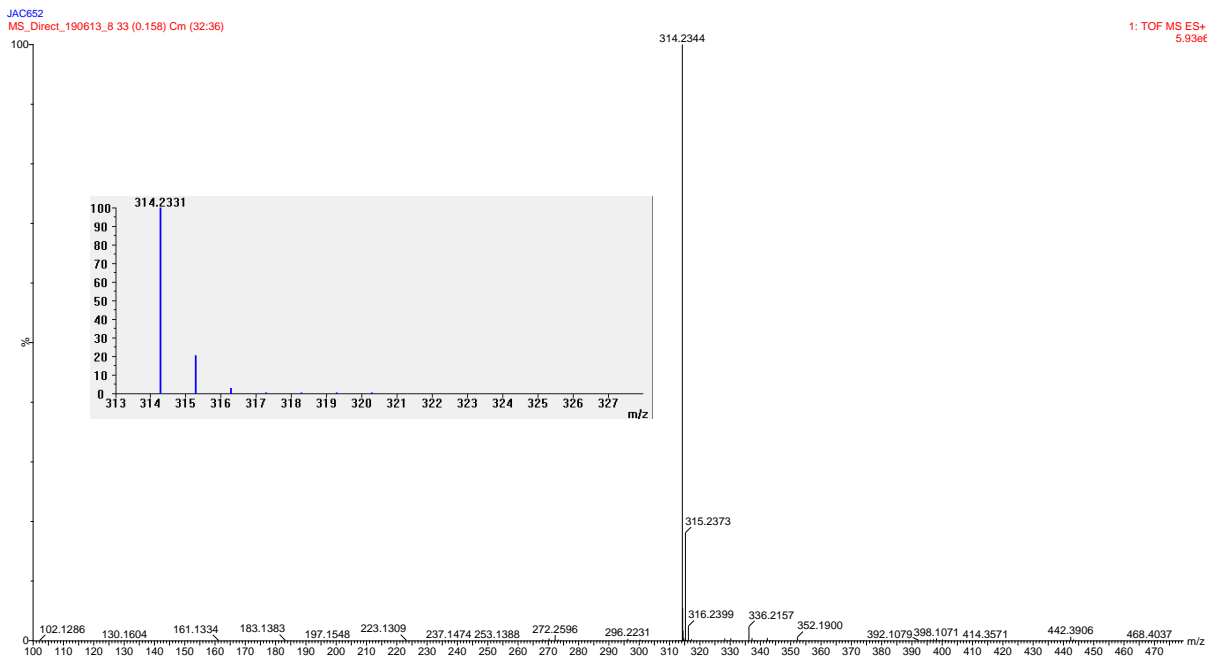


Figure 5.19: ESI-MS (direct injection, positive mode) spectrum of **DCI**

Employing this same methodology, we could synthesize **DC2** (Figure 5.20), which is based on the amino acid, piperidine 4-carboxylic acid (also a white solid, 61 % yield). Characterization of **DC2** was also performed by means of IR, NMR (^1H and ^{13}C) spectroscopy and mass spectrometry.

Chapter 5: The synthesis of primary amines, polymer precursors and surfactants via hydroaminomethylation

Methyl 10-undecenoate is also prone to isomerization, followed by the subsequent hydroaminomethylation of these internal counterparts. This leads to the formation of other branched products, containing ethyl, propyl (and so forth) branches (only the methyl branched product is shown in all figures since it is the major branched product formed). Furthermore, methyl 10-undecenoate can also undergo olefin hydrogenation, producing methyl undecenoate. Therefore, the “others” in the figures represent these products, which are present in trace amounts.

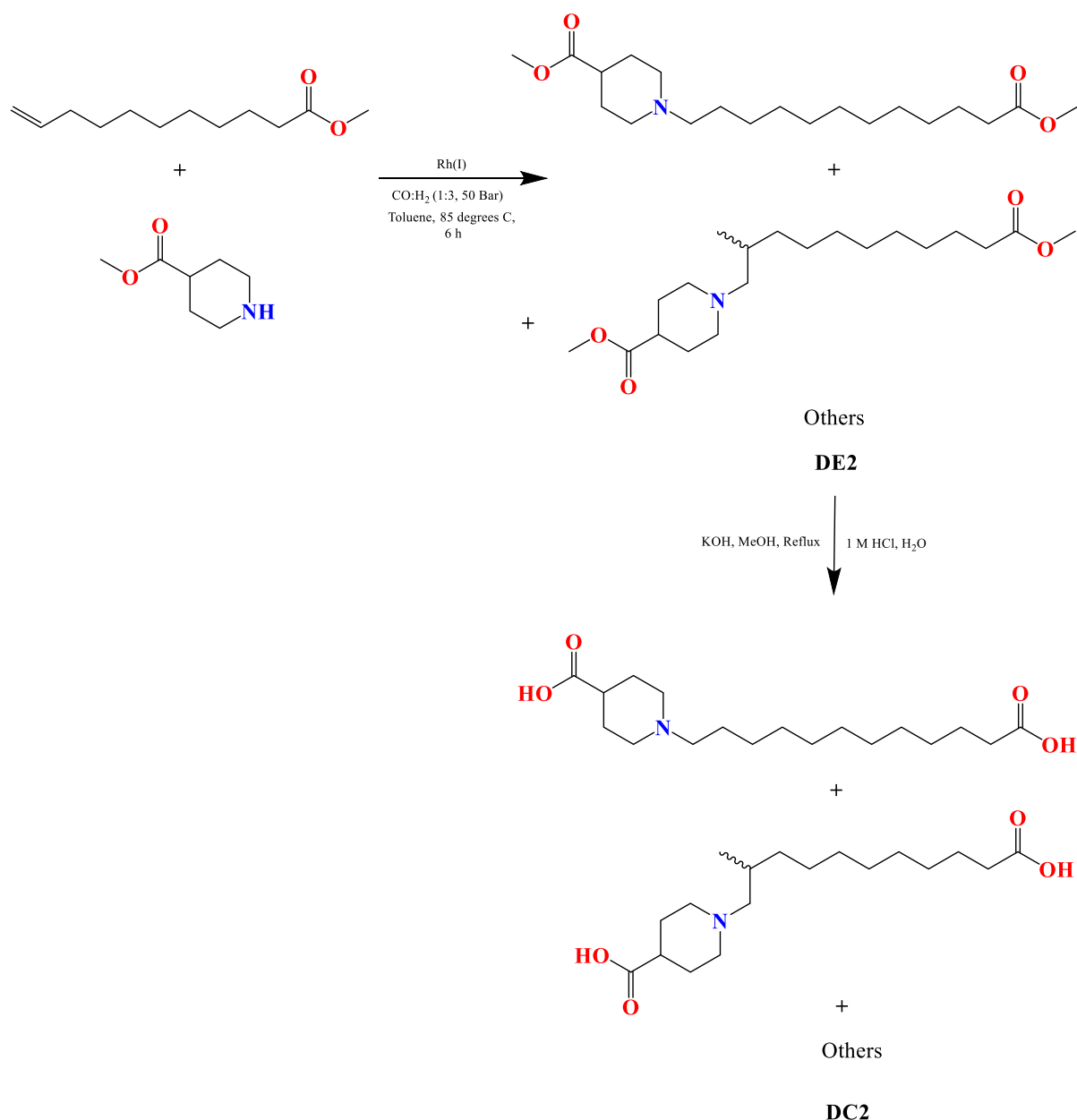


Figure 5.20: Synthesis of DC2 via hydroaminomethylation and KOH-mediated ester hydrolysis

We have therefore successfully demonstrated the synthesis of novel biopolymer precursors (DC1 and DC2) via hydroaminomethylation and base-mediated ester hydrolysis. These biopolymer precursors were synthesized from cheap feedstocks derived from natural sources, as well as from amino acids. In

Chapter 5: The synthesis of primary amines, polymer precursors and surfactants via hydroaminomethylation

conjunction with diamines, novel polyamide-based biopolymers can be synthesized, with potential applications in biomedical fields.

5.4 The synthesis of biosurfactants via hydroaminomethylation

In the previous section, we discussed the use of L-proline and piperidine-4-carboxylic acid in order to synthesize novel biopolymer precursors. However, these amino acids are also potential head-groups for biosurfactants, as shown in Figure 5.21.

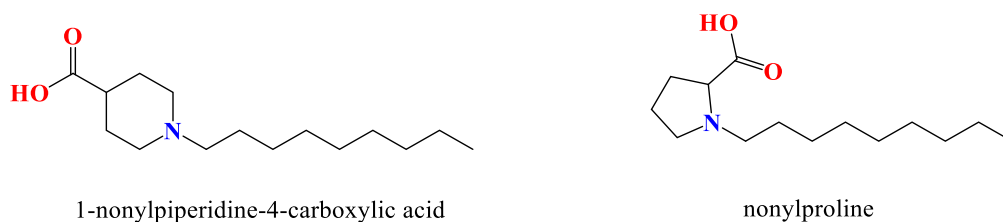


Figure 5.21: *N*-alkylated piperidine 4-carboxylic acid and L-proline

To the best of our knowledge, the synthesis of 1-nonylpiperidine-4-carboxylic acid has not previously been reported. The dodecyl analogue of *N*-nonyl proline is commonly used to perform the chiral separation of aromatic β -amino acids and 3-phenyllactic acid via high-speed counter-current chromatography.⁴⁵⁻⁴⁶ It has also previously been used for the micellar extraction of amino acids.⁴⁷ Furthermore, Jhaumeer-Laulloo and co-workers⁴⁸ previously investigated the interaction of *N*-alkyl prolinates (octyl, decyl and dodecyl) with bovine serum albumin (BSA) and found that these biosurfactants bind more strongly to BSA as the length of the alkyl chain increases. These protein-surfactant binding is of importance in chemical and biological applications.

Generally, these biosurfactants are synthesized via reductive amination of the corresponding aldehydes with the amino acid methyl ester (or ethyl).⁴⁷⁻⁴⁸ As alluded to earlier, the ester versions of these amino acids are used due to the ability of the amino acids to catalyse the aldol condensation of aldehydes. The biosurfactants are then subsequently isolated after base-mediated hydrolysis of the ester moiety. In this regard, KOH or NaOH (or other alkali metals) can be used. This can influence the properties of the resulting biosurfactants.

Our strategy entailed the utilization of olefins which is subsequently hydroformylated to a regio-isomeric mixture of aldehydes. These regio-isomeric mixture of aldehydes then undergo reductive amination with the ethyl ester of piperidine-4-carboxylic acid or L-proline methyl ester to produce the *N*-alkylated amino acid ethyl or methyl esters. These *N*-alkylated amino acid ethyl and methyl esters can be synthesized via a one-pot hydroaminomethylation procedure. Saponification via alcoholic KOH (or NaOH) produce the targeted biosurfactants (Scheme 5.1).

Chapter 5: The synthesis of primary amines, polymer precursors and surfactants via hydroaminomethylation

To the best of our knowledge, these biosurfactants have not previously been synthesized in this way using cheap olefin feedstocks. Although this approach produce a regio-isomeric mixture of the biosurfactants, this is considered not to be a problem since commercially available surfactants are often mixtures. Nevertheless, we employed both reductive amination and hydroaminomethylation to prepare these biosurfactants. The former process leads to the linear product while the latter yields a mixture of regio-isomers. This allow us to elucidate the effect of using mixtures on the properties of the biosurfactants.

In total, five biosurfactants were synthesized via reductive amination and hydroaminomethylation. Three biosurfactants were synthesized based on the piperidine-4-carboxylic acid scaffold (Scheme 5.1). Two of these were synthesized via reductive amination (**BS1** containing the potassium cation and **BS3** containing the sodium cation). **BS2** was synthesized via hydroaminomethylation and therefore consist of a mixture of regio-isomers. Similarly, **BS4** was synthesized via reductive amination and **BS5** via hydroaminomethylation respectively. The synthesis of these biosurfactants were monitored by means of IR and NMR (^1H and ^{13}C) spectroscopy. They were isolated as hygroscopic off-white solids (**BS1-BS3**) or light yellow oils (**BS4** and **BS5**) in high yields (87-94 %).

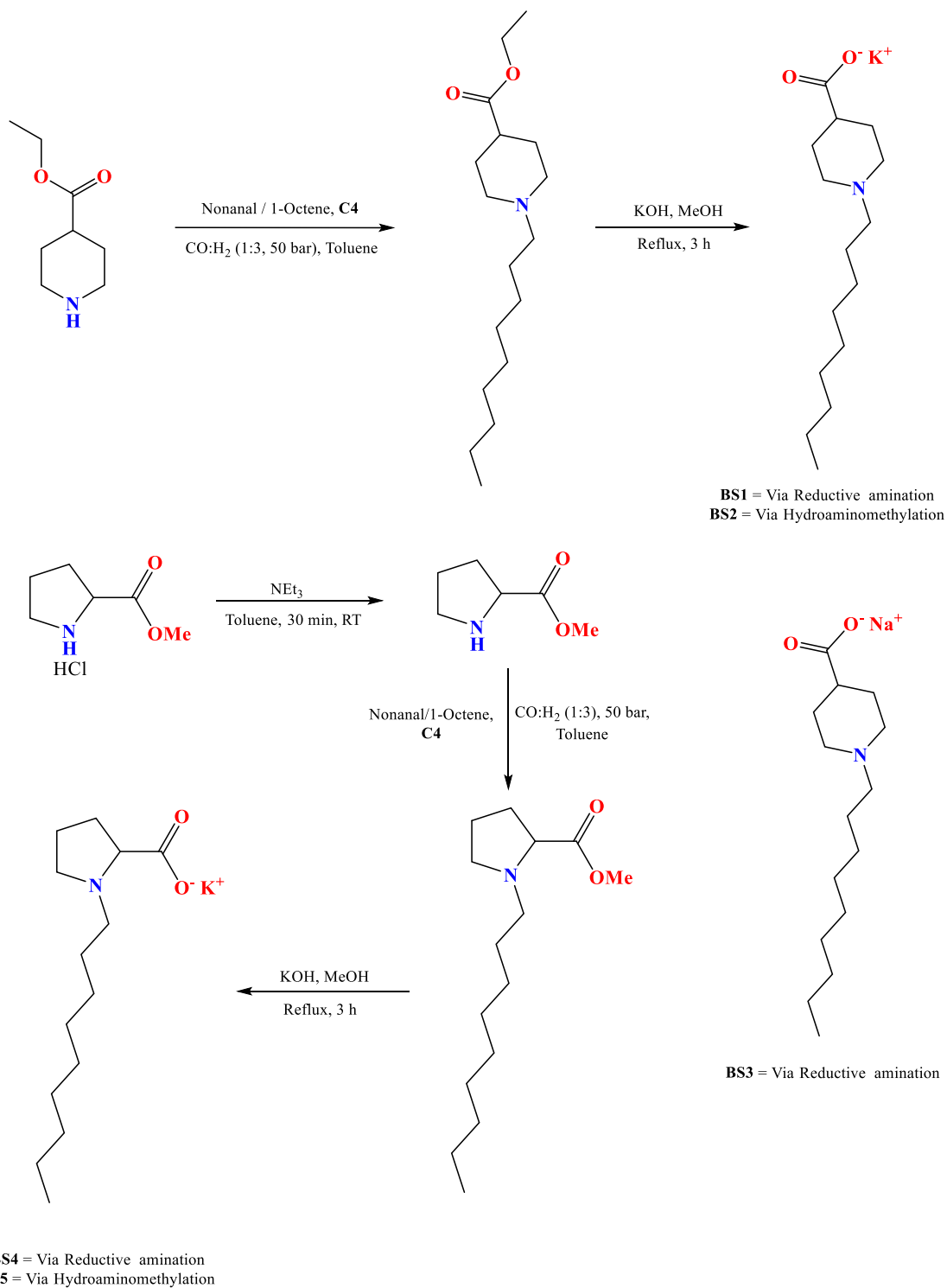
The synthesis and characterization of **BS1** and **BS2** will be discussed as representative examples. The IR spectra of the ester precursors of **BS1** and **BS2** displays the carbonyl stretch of the ester moiety at 1732 cm^{-1} , while the presence of the alkyl chain is confirmed by absorbances at 2853 and 2923 cm^{-1} . Further confirmation regarding the successful synthesis of the ester precursors of **BS1** and **BS2** were obtained from ^1H NMR spectroscopy (Figure 5.22). These ^1H NMR spectra confirms the presence of the ester, piperidyl and alkyl groups. Furthermore, a resonance is observed around ~ 2.88 ppm, which is assigned to the methylene group of the alkyl chain bonded to the piperidyl nitrogen atom. In the ^1H NMR spectrum of the ester precursor of **BS2**, multiple peaks resonated at this chemical shift (~ 2.88 ppm), as a result of the presence of the other regio-isomers.

The last step in the synthesis of the biosurfactants (**BS1** and **BS2**) is the saponification in methanolic KOH. This led to the hydrolysis of the ester moieties with the subsequent formation of a carboxylate (with potassium as the cation). **BS1-BS3** were isolated as off-white solids while **BS4** and **BS5** were isolated as light yellow oils. **BS1-BS5** were isolated in high yields (87-94 %) and were found to be hygroscopic and therefore needed to be stored under N_2 .

The saponification reaction of the esters precursors of **BS1** and **BS2** were monitored by means of IR and NMR (^1H and ^{13}C) spectroscopy and mass spectrometry. The IR spectrum of the ester precursor of **BS1** is shown in Figure 5.23 (top spectrum). The IR spectra of the surfactants, **BS1** and **BS2**, are also shown in Figure 5.23 (middle and bottom respectively). In the top spectrum in Figure 5.23, the ester stretch is situated at 1732 cm^{-1} . After saponification, the ester moiety disappeared, with the appearance

Chapter 5: The synthesis of primary amines, polymer precursors and surfactants via hydroaminomethylation

of a new band at 1552 cm^{-1} which is assigned to the carboxylate moiety. IR spectroscopy thus confirms the successful synthesis of **BS1** and **BS2**.



Scheme 5.1: Synthesis of biosurfactants (**BS1-BS5**)

Chapter 5: The synthesis of primary amines, polymer precursors and surfactants via hydroaminomethylation

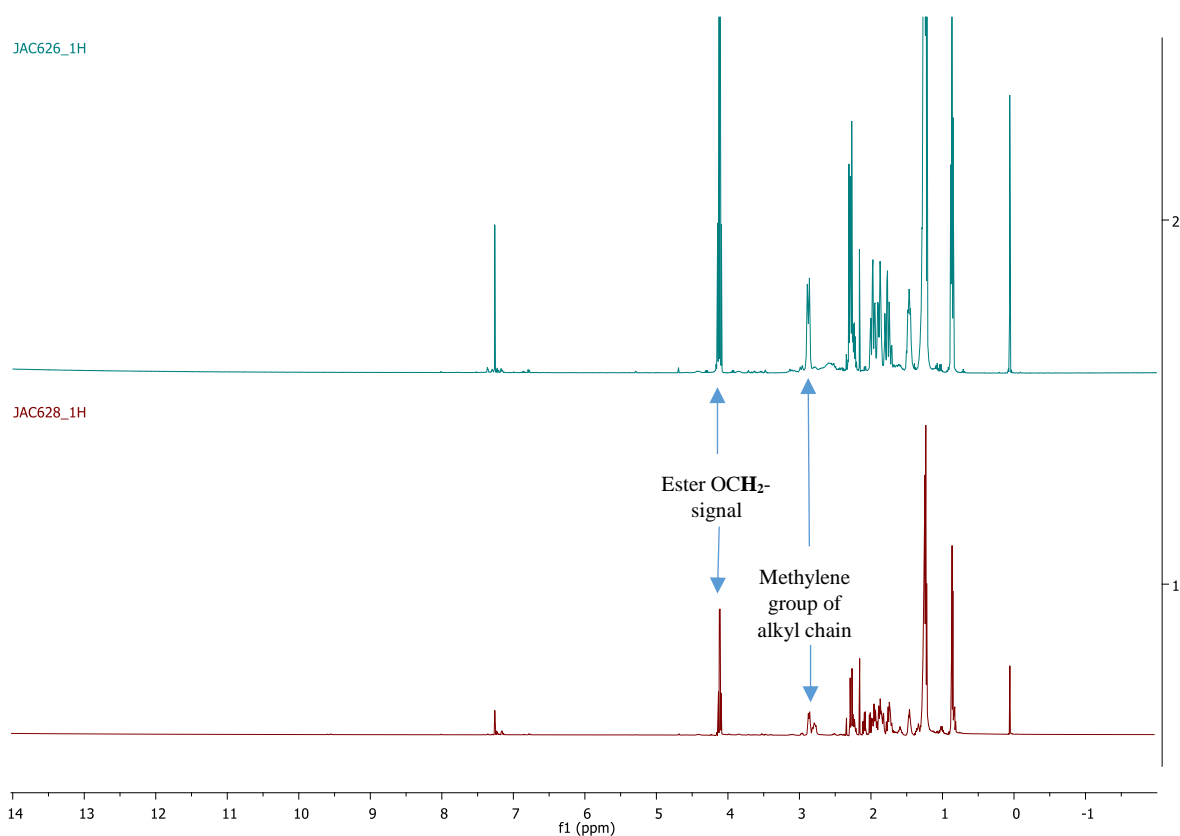


Figure 5.22: ^1H NMR spectra of **BS1** (top) and **BS2** (bottom) ester precursors in CDCl_3

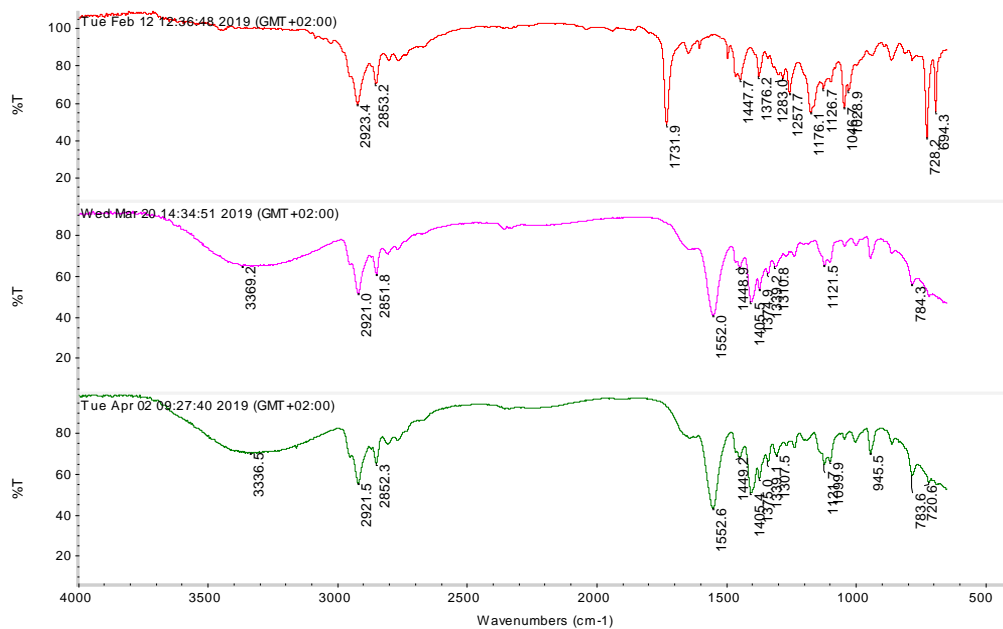


Figure 23: IR spectra of **BS1** ester precursor (top), **BS1** (middle) and **BS2** (bottom)

Further evidence with regards to the successful synthesis of **BS1** and **BS2** is obtained from ^1H NMR spectroscopy (Figure 5.24).

Chapter 5: The synthesis of primary amines, polymer precursors and surfactants via hydroaminomethylation

The ^1H NMR spectra of **BS1** and **BS2** (middle and bottom respectively) clearly shows the absence of the ester moiety (~ 4.12 ppm in the top spectrum in Figure 5.24).

The ESI-MS spectrum (direct injection, positive mode) of **BS2** (Figure 5.25) is shown as a representative example. In this spectrum, the base peak and molecular ion ($[\text{M}+2\text{H}]^+$) is observed at m/z 256.2275. The experimental isotopic pattern is in excellent agreement with the theoretical isotopic pattern.

Utilizing the same methodology, biosurfactants **BS3-BS5** could be synthesized and characterized from their respective precursors.

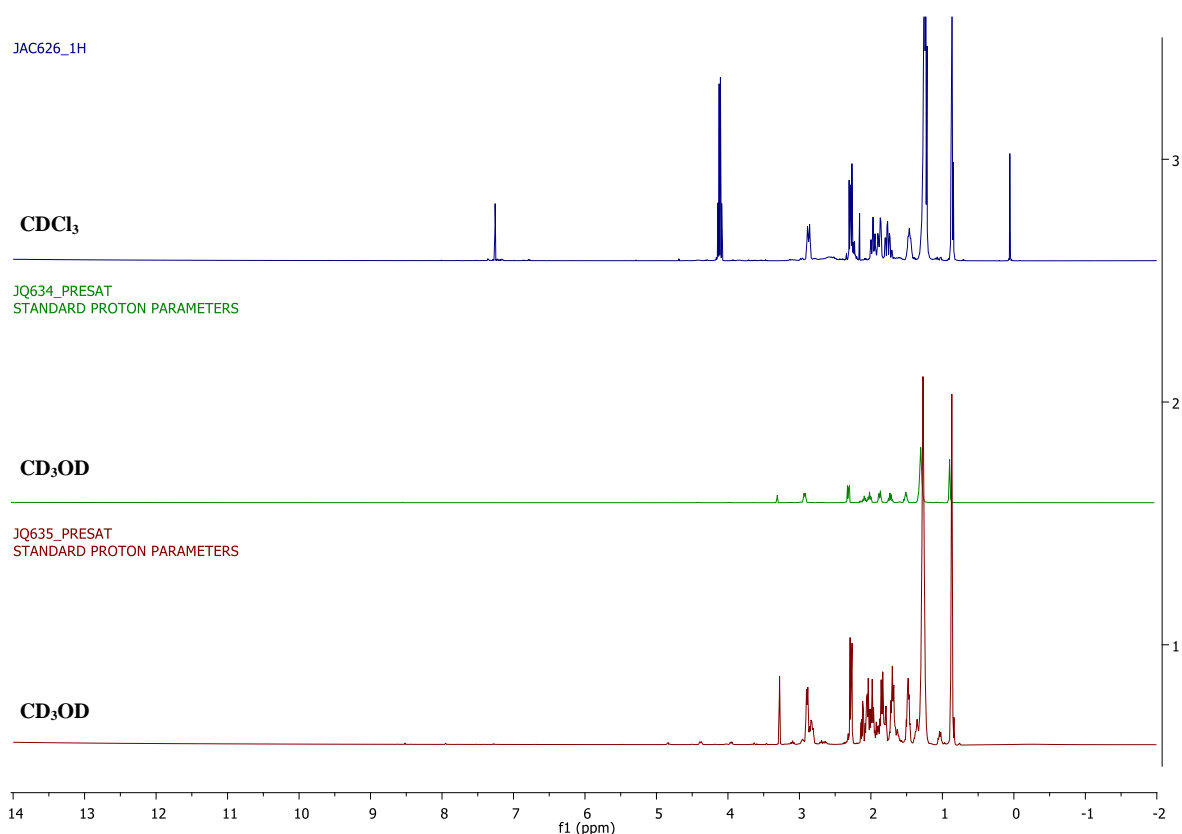


Figure 5.24: ^1H NMR spectra of **BS1** ester precursor (Top), **BS1** (middle) and **BS2** (bottom)

With these biosurfactants in hand, we proceeded to investigate their properties. We were specifically interested in their critical micelle concentration (CMC). Knowledge of the CMC of surfactants are important since this is the concentration at which they are most effective. Various methods exist for the determination of the CMC of surfactants. The most common method to determine the CMC of surfactants is by means of surface tension measurements, since surfactants have the ability to lower the surface tension of water. However, at the CMC, no further decrease in the surface tension of water is observed. Therefore, determination of the concentration of the surfactant at which this occurs, reveals the CMC.

Chapter 5: The synthesis of primary amines, polymer precursors and surfactants via hydroaminomethylation

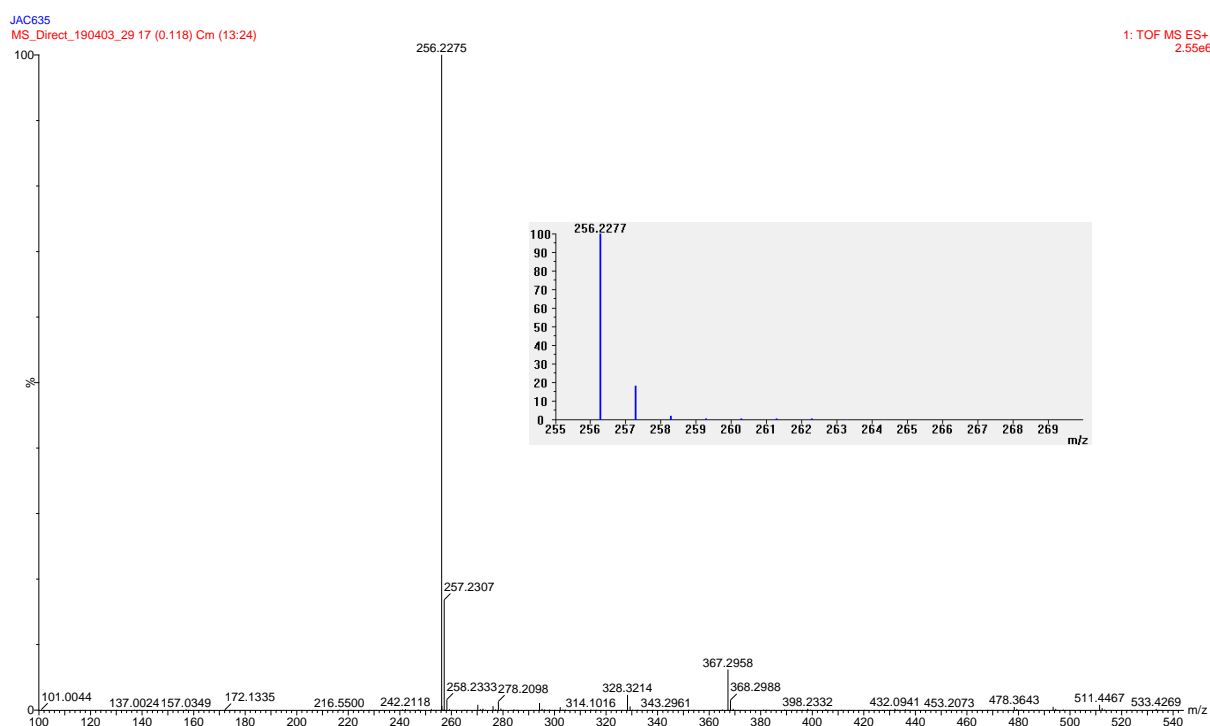


Figure 5.25: ESI-MS spectrum (direct injection, positive mode) of BS2

Other methods to determine the CMC includes density and viscosity measurements, light scattering experiments and conductivity. Similar to surface tension, conductivity is also a common method to determine the CMC of surfactants owing to their ease of operation.

We opted for the conductometric determination of the CMC of the biosurfactants (**BS1-BS5**). In order to confirm the validity of this method, we initially determined the CMC of a known surfactant, SDS (sodium dodecyl sulfate) which has a CMC of 8.4 mM. The determination of the CMC by means of conductivity was conducted at least in duplicate (one of the experiments is shown in Figure 5.26).

Below the CMC, surfactant monomers are mostly situated at the air-water interface, with the hydrophilic head group orientated into the water, while the hydrophobic alkyl chain is protruding outwards into the air. As the concentration of the surfactant is increased, a linear increase in the conductivity is observed. At a certain concentration, the air-water interface will be saturated with surfactant molecules, at which point they will diffuse into the water. At this point, micelles start forming, protecting their hydrophobic chains from the surrounding water environment. This concentration is defined as the CMC. Since micelles are much larger structures in comparison to the individual surfactant monomers, they diffuse much slower through the water and therefore they are less efficient charge carriers. As a result, a drop in the conductivity is observed. The CMC can be determined by identifying the point in the graph where this breaking point occur.

Chapter 5: The synthesis of primary amines, polymer precursors and surfactants via hydroaminomethylation

Therefore, from Figure 5.26, a CMC of 8.3 ± 0.004 mM could be determined for the known surfactant, SDS. This value corresponds quite well with the literature value. The conductometric determination of the CMC of surfactants can thus be regarded as a valid approach.

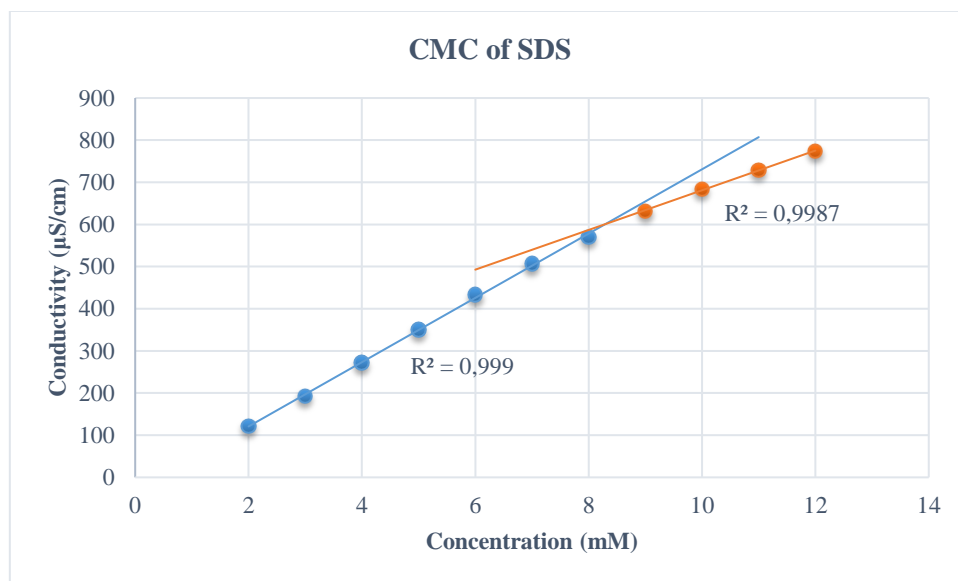


Figure 5.26: Conductivity vs Concentration graph for SDS

The CMC of the biosurfactants (**BS1-BS5**) were then determined by means of this conductometric titration. The structures of **BS1-BS5** is shown in Figures 5.27-5.29. We firstly investigated the influence of the cation (**BS1** vs **BS3**) on the CMC. The CMC of **BS1** was determined as 9.73 ± 0.1 mM and that of **BS3** to be 10.25 ± 0.01 mM. Although not that significant, a slightly higher CMC is obtained for the sodium-based surfactant (**BS3**), compared to the potassium-based surfactant (**BS1**). This is consistent with observations of Kim and co-workers⁴⁹ who concluded that larger cations having a higher binding capacity, decrease the CMC of anionic surfactants. It is therefore expected that if Cs⁺ is used, an even lower CMC should be obtained.

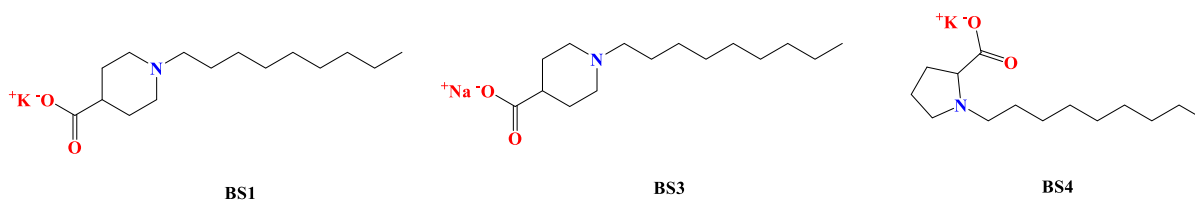
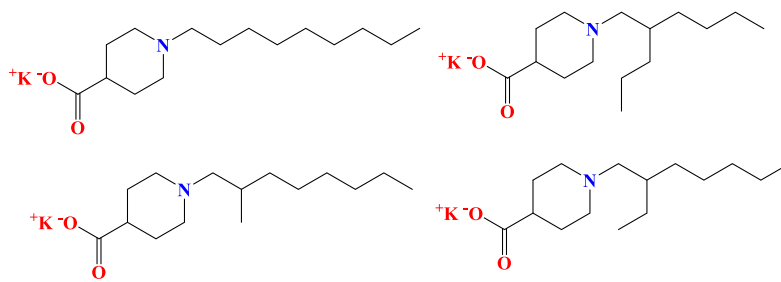


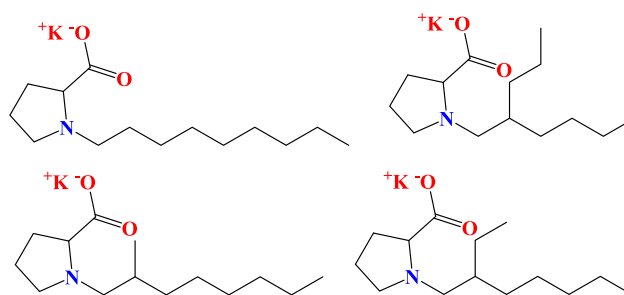
Figure 5.27: Biosurfactants (**BS1**, **BS3** and **BS4**) synthesized via reductive amination

Chapter 5: The synthesis of primary amines, polymer precursors and surfactants via hydroaminomethylation



BS2

Figure 5.28: Mixture of piperidine-4-carboxylate-based biosurfactants (BS2) synthesized via hydroaminomethylation



BS5

Figure 5.29: Mixture of proline-based biosurfactants (BS5) synthesized via hydroaminomethylation

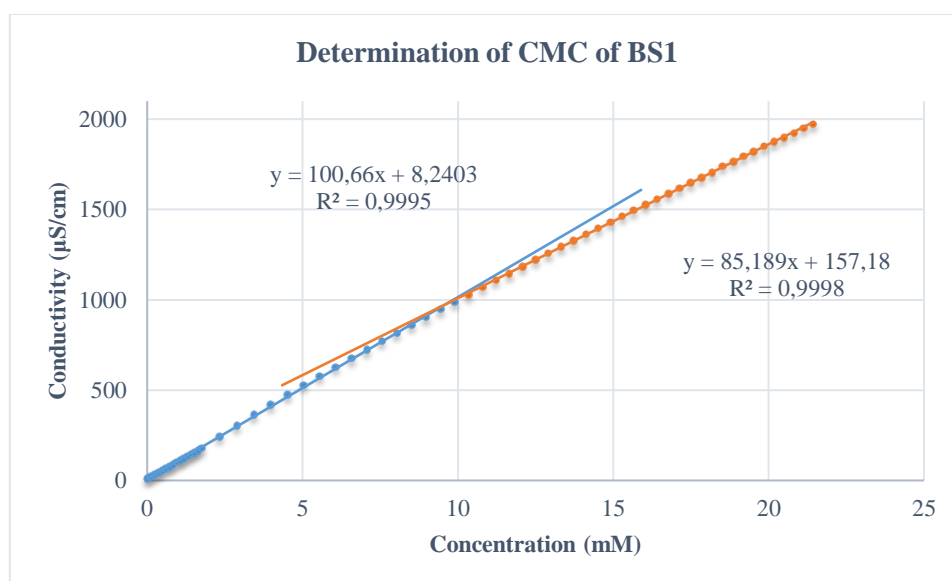


Figure 5.30: Conductivity vs Concentration for BS1

Chapter 5: The synthesis of primary amines, polymer precursors and surfactants via hydroaminomethylation

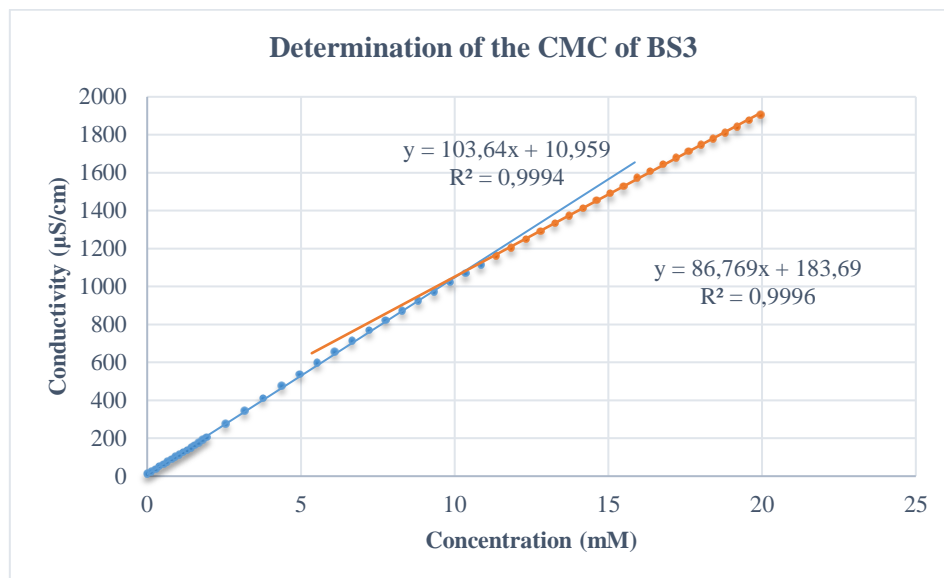


Figure 5.31: Conductivity vs Concentration for BS3

The CMC's of all the biosurfactants prepared are shown in Table 5.1.

Table 5.1: The CMC's of the biosurfactants (BS1-BS5)

Biosurfactant	CMC (mM) ^a
BS1	9.73 ± 0.1
BS2	15.43 ± 0.3
BS3	10.25 ± 0.01
BS4	8.49 ± 0.04
BS5	5.05 ± 0.49

^aDetermined by conductivity

As alluded to earlier, below the CMC, the surfactant monomers reside at the air-water interface and only diffuse into solution once the concentration of the surfactant monomers exceeds the CMC. Therefore, the CMC can be considered as the solubility limit of the surfactant monomer in water.⁵⁰ Micelles will then start forming as a result of the hydrophobic effect.⁵¹⁻⁵² The hydrophobic alkyl chains will rather interact intermolecularly with one another, than to interact with the surrounding water molecules. Results show that the CMC for **BS1**, the biosurfactant containing the linear chain, is lower than the CMC of **BS2**, which consists of a mixture of regio-isomers. The introduction of branching in the aliphatic chain thus led to a higher CMC, consistent with results obtained by Jin and co-workers.⁵³ However, the complete opposite was observed for **BS4** (biosurfactant containing the linear chain) and **BS5** (biosurfactants consisting of a mixture of regio-isomers). Both **BS4** and **BS5** are the surfactants with proline hydrophilic heads. The surfactant containing the branched aliphatic chains (**BS5**) gave the lower CMC. We attribute this to intramolecular interactions between the hydrophobic tails and the hydrophilic head of the same molecule. Thus, the proximity of the alkyl chains to the hydrophilic heads could result in the alkyl chains impeding H-bonding between the hydrophilic proline head and solvent, water. This would lower the solubility of **BS5** in water, resulting in a lower CMC.

Chapter 5: The synthesis of primary amines, polymer precursors and surfactants via hydroaminomethylation

The CMC's of **BS1** and **BS3-BS5** are fairly similar to the well-known surfactant, SDS, even though the alkyl chains in these surfactants are three carbons shorter than the SDS analogue. This is attributed to the hydrophobicity of the pyrrolidyl and piperidyl rings, which is thought to supplement the hydrophobicity of the alkyl tails.

5.5 Conclusion

In this chapter, we have demonstrated the potential of hydroaminomethylation in the synthesis of value-added chemicals.

In industry, fatty amines are usually synthesized via the Nitrile process which involves relatively high temperatures, long reaction times, and in some cases, poor selectivity. By means of hydroaminomethylation and subsequent Pd-catalyzed hydrogenolysis, we demonstrated the efficient synthesis of fatty amines in a facile manner from α -olefins. By varying the length of the α -olefins, fatty amines of different chain lengths can be synthesized. Although these fatty amines are isolated as regio-isomeric mixtures containing linear and branched alkyl chains, primary amines are selectively formed. Subsequent *N*-alkylation of the initially formed secondary amines to tertiary amines are not observed.

Hydroaminomethylation was also used to synthesize biopolymer precursors containing α , ω -carboxylic acid moieties. These α , ω -carboxylic acids can be combined with di-functional amines in order to synthesize novel polyamide biopolymers.

Significantly, we demonstrated the synthesis of biosurfactants via hydroaminomethylation and reductive amination from α -olefins and amino esters. We also showed that the position of the hydrophilic head relative to the hydrophobic tail can have an influence on the CMC. Furthermore, the CMC of most of the synthesized biosurfactants are similar to the well-known surfactant, sodium dodecyl sulfate. This is as a result of the contribution of the pyrrolidyl and piperidyl moieties towards the hydrophobic character of the hydrophobic tail.

5.6 Experimental

5.6.1 General Considerations

All reagents were purchased from either Merck or Sigma Aldrich and were used without further purification unless specifically stated. Solvents were purchased from Merck or Kimix, and were usually dried by conventional distillation or using Pure SolvTM micro solvent purifiers fitted with activated alumina columns. In some cases, simple storing of the solvents over molecular sieves were employed. CO, H₂ and syngas (CO:H₂, 1:1) was purchased from Afrox SA.

Catalytic reactions were performed in a 50 ml Amar pressure reactor equipped with a Teflon liner.

Chapter 5: The synthesis of primary amines, polymer precursors and surfactants via hydroaminomethylation

FTIR spectra were recorded on a Thermo Nicolet Avatar 330 FTIR Spectrometer equipped with a Smart performer (Zn/Se) ATR attachment. NMR spectra were recorded on a Varian Unity Inova NMR Spectrometer (300, 400 and 600 MHz). Mass Spectra were obtained by analysis on a Waters Synapt G2 Spectrometer.

5.6.2 Synthesis of primary amines

Synthesis of *N*-nonylbenzylamine and its branched counterparts

The reactor was charged with toluene (5 mL), **C4** (5.8 mg, 0.008 mmol, 0.5 mol%), 1-octene (179 mg, 0.25 mL, 1.6 mmol) and benzylamine (171 mg, 0.175 mL, 1.6 mmol). The reactor was flushed with CO (~10 bar) three times after which the reactor was pressurised to 50 bar CO:H₂ (1:3). The reactor was then heated to 85 °C for 6 h. After the allotted time, the reactor was cooled and the reactor carefully vented and then opened. The reaction mixture was filtered using a syringe filter and dried over MgSO₄, after which the solvent was removed. It was then dried under vacuum with the isolation of a brown oil (366 mg, 98 %). IR (ATR) 3086, 3062, 3027, 2921, 2852, 729, 696 cm⁻¹. ¹H NMR (400 MHz, CDCl₃) δ_H: 0.89 (m, 3 H, -CH₂-CH₃), 1.26 (m, 12 H, -CH₂-CH₂-(CH₂)₆-CH₃), 1.52 (m, 2 H, -CH₂-CH₂-(CH₂)₆-CH₃), 2.54 (m, 2 H, -CH₂-CH₂-(CH₂)₆-CH₃), 3.80 (s, 2 H, Ph-CH₂), 7.33 (m, 5 H, Ph-H).

Synthesis of *N*-tridecylbenzylamine and its branched counterparts

Synthesized according to the same procedure described for *N*-nonylbenzylamine from 1-dodecene (539 mg, 0.71 ml, 3.2 mmol) and benzylamine (341 mg, 0.35 mL, 3.2 mmol) and isolated in 76 % yield (700 mg) as a brown oil. IR (ATR) 3086, 3062, 3027, 2921, 2851, 728, 696 cm⁻¹. ¹H NMR (600 MHz, CDCl₃) δ_H: 0.89 (m, 3 H, -CH₂-CH₃), 1.28 (m, 20 H, -CH₂-CH₂-(CH₂)₁₀-CH₃), 1.52 (m, 2 H, -CH₂-CH₂-(CH₂)₁₀-CH₃), 2.54 (m, 2 H, -CH₂-CH₂-(CH₂)₁₀-CH₃), 3.80 (s, 2 H, Ph-CH₂), 7.33 (m, 5 H, Ph-H).

Synthesis of *N*-heptadecylbenzylamine and its branched counterparts

Synthesized according to the same procedure described for *N*-nonylbenzylamine from 1-hexadecene (718 mg, 0.92 ml, 3.2 mmol) and benzylamine (341 mg, 0.35 mL, 3.2 mmol) and isolated in 79 % yield (876 mg) as a brown oil. IR (ATR) 3086, 3062, 3027, 2920, 2851, 727, 695 cm⁻¹. ¹H NMR (600 MHz, CDCl₃) δ_H: 0.89 (m, 3 H, -CH₂-CH₃), 1.28 (m, 28 H, -CH₂-CH₂-(CH₂)₁₄-CH₃), 1.52 (m, 2 H, -CH₂-CH₂-(CH₂)₁₄-CH₃), 2.54 (m, 2 H, -CH₂-CH₂-(CH₂)₁₄-CH₃), 3.80 (s, 2 H, Ph-CH₂), 7.33 (m, 5 H, Ph-H).

Synthesis of *N*-nonylamine and its branched counterparts

N-nonylbenzylamine (764 mg, 3.27 mmol) and 10 % Pd/C (200 mg) were added to EtOH (10 ml). The reactor was flushed with H₂ (5 bar) three times after which it was pressurized to 5 bar. The reactor was then heated to 75 °C for 18 h. After the allotted time, the reactor was cooled and the reactor carefully vented and then opened. The solvent was then removed and the colorless oil dried under vacuum

Chapter 5: The synthesis of primary amines, polymer precursors and surfactants via hydroaminomethylation

(421 mg, 90 %). IR (ATR) 2921, 2852, 722 cm^{-1} . ^1H NMR (600 MHz, CDCl_3) δ_{H} : 0.89 (m, 3 H, $-\text{CH}_2-\text{CH}_3$), 1.28 (m, 12 H, $-\text{CH}_2-\text{CH}_2-(\text{CH}_2)_6-\text{CH}_3$), 1.44-1.56 (m, 2 H, $-\text{CH}_2-\text{CH}_2-(\text{CH}_2)_6-\text{CH}_3$), 2.65 (m, 2 H, $-\text{CH}_2-\text{CH}_2-(\text{CH}_2)_6-\text{CH}_3$).

Synthesis of *N*-tridecylamine and its branched counterparts

Synthesized according to the same procedure described for *N*-nonylamine starting from *N*-tridecylbenzylamine (491 mg, 1.7 mmol) and 10 % Pd/C (150 mg) and isolated as a colourless oil (284 mg, 84 %). IR (ATR) 2920, 2852, 721 cm^{-1} . ^1H NMR (600 MHz, CDCl_3) δ_{H} : 0.87 (m, 3 H, $-\text{CH}_2-\text{CH}_3$), 1.24 (m, 20 H, $-\text{CH}_2-\text{CH}_2-(\text{CH}_2)_{10}-\text{CH}_3$), 1.44-1.48 (m, 2 H, $-\text{CH}_2-\text{CH}_2-(\text{CH}_2)_{10}-\text{CH}_3$), 2.31-2.81 (m, 2 H, $-\text{CH}_2-\text{CH}_2-(\text{CH}_2)_{10}-\text{CH}_3$).

Synthesis of *N*-heptadecylamine and its branched counterparts

Synthesized according to the same procedure described for *N*-nonylamine starting from *N*-heptadecylbenzylamine (803 mg, 2.32 mmol) and 10 % Pd/C (250 mg) and isolated as a colourless oil (489 mg, 83 %). IR (ATR) 2920, 2852, 721 cm^{-1} . ^1H NMR (300 MHz, CDCl_3) δ_{H} : 0.89 (m, 3 H, $-\text{CH}_2-\text{CH}_3$), 1.25-1.75 (m, 30 H, $-\text{CH}_2-\text{CH}_2-(\text{CH}_2)_{14}-\text{CH}_3$), 2.47-2.70 (m, 2 H, $-\text{CH}_2-\text{CH}_2-(\text{CH}_2)_{14}-\text{CH}_3$).

Synthesis of 4-[3-(benzylamino)propyl]-2-methoxyphenol and its branched counterparts

Synthesized according to the same procedure described for *N*-nonylbenzylamine starting from eugenol (525 mg, 3.2 mmol) and benzylamine (341 mg, 0.35 mL, 3.2 mmol) and isolated in 93 % yield (849 mg) as a orange-brown oil. IR (ATR) 3085, 3058, 3024, 1597, 1513, 728, 694 cm^{-1} . ^1H NMR (600 MHz, CDCl_3) δ_{H} : 0.79-1.63 (m, 4 H, $\text{Ar}-\text{CH}_2-\text{CH}_2-\text{CH}_2-\text{CH}_2-\text{NH}-\text{CH}_2-\text{Ar}$), 2.32-2.67 (m, 4 H, $\text{Ar}-\text{CH}_2-\text{CH}_2-\text{CH}_2-\text{CH}_2-\text{NH}-\text{CH}_2-\text{Ar}$), 3.79 (s, 2 H, $\text{Ar}-\text{CH}_2-\text{CH}_2-\text{CH}_2-\text{CH}_2-\text{NH}-\text{CH}_2-\text{Ar}$), 3.85 (s, 3 H, $\text{Ar}-\text{OCH}_3$), 6.62-6.66 (m, 2 H, $\text{H}-\text{Ar}-\text{CH}_2-\text{CH}_2-\text{CH}_2-\text{CH}_2-\text{NH}-\text{CH}_2-\text{Ar}$), 6.80-6.81 (m, 1 H, $\text{H}-\text{Ar}-\text{CH}_2-\text{CH}_2-\text{CH}_2-\text{CH}_2-\text{NH}-\text{CH}_2-\text{Ar}$), 7.30-7.35 (m, 5 H, $\text{H}-\text{Ar}-\text{CH}_2-\text{CH}_2-\text{CH}_2-\text{CH}_2-\text{NH}-\text{CH}_2-\text{Ar}-\text{H}$).

Synthesis of 4-(4-aminobutyl)-2-methoxyphenol and its branched counterparts

Synthesized according to the same procedure described for *N*-nonylamine starting from 4-[3-(benzylamino)propyl]-2-methoxyphenol (250 mg, 0.876 mmol) as a light yellow oil (171 mg, 94 %). IR (ATR) 1592, 1513 cm^{-1} . ^1H NMR (600 MHz, CDCl_3) δ_{H} : 0.89-1.63 (m, 4 H, $\text{Ar}-\text{CH}_2-\text{CH}_2-\text{CH}_2-\text{CH}_2-\text{NH}-\text{CH}_2-\text{Ar}$), 2.30-2.71 (m, 4 H, $\text{Ar}-\text{CH}_2-\text{CH}_2-\text{CH}_2-\text{CH}_2-\text{NH}-\text{CH}_2-\text{Ar}$), 3.85 (s, 3 H, $\text{Ar}-\text{OCH}_3$), 6.61-6.67 (m, 2 H, $\text{H}-\text{Ar}-\text{CH}_2-\text{CH}_2-\text{CH}_2-\text{CH}_2-\text{NH}-\text{CH}_2-\text{Ar}$), 6.77-6.80 (m, 1 H, $\text{H}-\text{Ar}-\text{CH}_2-\text{CH}_2-\text{CH}_2-\text{CH}_2-\text{NH}-\text{CH}_2-\text{Ar}$).

5.6.3 Synthesis of novel biopolymer precursors

Synthesis of methyl 12-oxododecanoate and its branched counterparts

Chapter 5: The synthesis of primary amines, polymer precursors and surfactants via hydroaminomethylation

The reactor was charged with toluene (5 mL), **C4** (5.8 mg, 0.008 mmol, 0.5 mol%) and methyl 10-undecenoate (317 mg, 0.36 mL, 1.6 mmol). The reactor was flushed with CO (~10 bar) three times after which the reactor was pressurised to 50 bar CO:H₂ (1:3). The reactor was then heated to 85 °C for 6 h. After the allotted time, the reactor was cooled and the reactor carefully vented and then opened. The solvent was then removed and the resulting brown oil dried under vacuum (306 mg, 84 %). IR (ATR) 2915, 2849, 1736, 1704 cm⁻¹. ¹H NMR (400 MHz, CDCl₃) δ_H: 0.89 (m, 12 H, O=CH-CH₂-CH₂-(CH₂)₆-CH₂-CH₂-COOCH₃), 1.59-1.64 (m, 4 H, O=CH-CH₂-CH₂-(CH₂)₆-CH₂-CH₂-COOCH₃), 2.27-2.43 (m, 4 H, O=CH-CH₂-CH₂-(CH₂)₆-CH₂-CH₂-COOCH₃), 3.66 (s, 3 H, COOCH₃), 9.55-9.75 (m, 1 H, O=CH-). ¹³C NMR (151 MHz, CDCl₃) δ_C: 13.5, 22.2, 25.0, 27.1, 29.3, 29.4, 29.7, 30.6, 34.2, 44.0, 51.6, 174.4, 203.0 ppm. HRMS (ESI + mode, m/z): Calc for [M+K]⁺ 267.1363, found 267.1565.

Synthesis of DE1 and its branched counterparts

L-proline methyl ester hydrochloride (265 mg, 1.6 mmol) was added to toluene (5 ml). NEt₃ (162 mg, 0.223 ml, 1.6 mmol) was then added and stirred for 1 h at room temperature. After the allotted time, the suspension was filtered and the filtrate added to the reactor. The reactor was further charged with **C4** (5.8 mg, 0.008 mmol, 0.5 mol%) and methyl 10-undecenoate (317 mg, 0.36 mL, 1.6 mmol). The reactor was flushed with CO (~10 bar) three times after which the reactor was pressurised to 50 bar CO:H₂ (1:3). The reactor was then heated to 85 °C for 6 h. After the allotted time, the reactor was cooled and the reactor carefully vented and then opened. The reaction mixture was filtered using a syringe filter and dried over MgSO₄, after which the solvent was removed. It was then dried under vacuum with the isolation of a brown oil (506 mg, 93 %). IR (ATR) 2924, 2852, 1736, 1165, 730, 695 cm⁻¹. ¹H NMR (600 MHz, CDCl₃) δ_H: 0.84-1.28 (m, 16 H, -N-CH₂-(CH₂)₈-CH₂-CH₂-COOCH₃), 1.49-1.63 (m, 4 H, -N-CH₂-(CH₂)₈-CH₂-CH₂-COOCH₃, pyrrolidine-**H**), 1.80-2.11 (m, 2 H, pyrrolidine-**H**), 2.28-2.65 (m, 6 H, -N-CH₂-(CH₂)₈-CH₂-CH₂-COOCH₃, pyrrolidine-**H**), 3.10-3.19 (m, 1 H, pyrrolidine-**H**), 3.66 (s, 3 H, -N-CH₂-(CH₂)₈-CH₂-CH₂-COOCH₃), 3.72 (s, 3 H, pyrrolidine-COOCH₃). ¹³C NMR (151 MHz, CDCl₃) δ_C: 25.1, 27.0, 27.2, 27.7, 29.3, 29.4, 29.5, 29.6, 29.7, 30.0, 31.0, 34.3, 51.6, 52.0, 53.7, 53.9, 66.7, 174.5 ppm.

Synthesis of DE2 and its branched counterparts

The reactor was charged with toluene (5 mL), **C4** (5.8 mg, 0.008 mmol, 0.5 mol%), methyl 10-undecenoate (317 mg, 0.36 mL, 1.6 mmol) and methyl piperidine-4-carboxylate (229 mg, 0.216 mL, 1.6 mmol). The reactor was flushed with CO (~10 bar) three times after which the reactor was pressurised to 50 bar CO:H₂ (1:3). The reactor was then heated to 85 °C for 6 h. After the allotted time, the reactor was cooled and the reactor carefully vented and then opened. The reaction mixture was filtered using a syringe filter and dried over MgSO₄, after which the solvent was removed. It was then dried under vacuum with the isolation of a brown oil (521 mg, 92 %). IR (ATR) 2923, 2853, 1734, 1167 cm⁻¹. ¹H NMR (400 MHz, CDCl₃) δ_H: 0.82-1.26 (m, 16 H, -N-CH₂-(CH₂)₈-CH₂-CH₂-COOCH₃),

Chapter 5: The synthesis of primary amines, polymer precursors and surfactants via hydroaminomethylation

1.44-1.63 (m, 2 H, -N-CH₂-(CH₂)₈-CH₂-CH₂-COOCH₃), 1.74-2.01 (m, 4 H, piperidine-**H**), 2.24-2.30 (m, 7 H, -N-CH₂-(CH₂)₈-CH₂-CH₂-COOCH₃, piperidine-**H**), 2.79-2.88 (m, 2 H, -N-CH₂-(CH₂)₈-CH₂-CH₂-COOCH₃), 3.65 (s, 3 H, -N-CH₂-(CH₂)₈-CH₂-CH₂-COOCH₃), 3.66 (s, 3 H, piperidine-COOCH₃). ¹³C NMR (151 MHz, CDCl₃) δ_C: 25.6, 29.5, 29.6, 30.2, 30.9, 31.7, 31.8, 32.0, 32.1, 32.2, 36.7, 37.9, 54.0, 54.2, 55.6, 55.8, 176.9, 178.1 ppm.

Synthesis of DC1 and its branched counterparts

KOH (852 mg, 15.2 mmol) was dissolved in MeOH (8 ml). A solution of **DE1** (1.3 g, 3.79 mmol) in MeOH (2 ml) was added, and refluxed for 6 h. After the allotted time, the solvent was removed and the resulting residue dissolved in water (10 ml). Acidification was then performed to pH = 2 with 10 % HCl, leading to the precipitation of a white solid. This white solid was recovered via filtration and dried under vacuum (932 mg, 78 %). IR (ATR) 2912, 2847, 1720, 1182 cm⁻¹. ¹H NMR (600 MHz, CD₃OD) δ_H: 0.86-1.37 (m, 16 H, -N-CH₂-(CH₂)₈-CH₂-CH₂-COOH), 1.54-1.71 (m, 4 H, -N-CH₂-(CH₂)₈-CH₂-CH₂-COOH, pyrrolidine-**H**), 1.89-2.13 (m, 2 H, pyrrolidine-**H**), 2.23-2.43 (m, 4 H, -N-CH₂-(CH₂)₈-CH₂-CH₂-COOH, pyrrolidine-**H**), 3.04-3.22 (m, 2 H, -N-CH₂-(CH₂)₈-CH₂-CH₂-COOH), 3.68-3.86 (m, 1 H, pyrrolidine-**H**). ¹³C NMR (100 MHz, CD₃OD) δ_C: 24.3, 26.1, 26.9, 27.6, 29.9, 30.1, 30.3, 30.4, 30.5, 30.6, 30.7, 34.9, 56.0, 56.7, 70.5, 173.3, 177.7 ppm. HRMS (ESI + mode, m/z): Calc for [M+H]⁺ 314.2331, found 314.2344.

Synthesis of DC2 and its branched counterparts

Synthesized according to the same procedure described for **DC1** starting from **DE2** (264 mg, 0.74 mmol) and KOH (167 mg, 3 mmol) and isolated as a white solid (149 mg, 61 %). IR (ATR) 2915, 2849, 1728, 1184 cm⁻¹. ¹H NMR (600 MHz, DMSO-d₆) δ_H: 0.80-1.24 (m, 16 H, -N-CH₂-(CH₂)₈-CH₂-CH₂-COOH), 1.46-1.47 (m, 2 H, -N-CH₂-(CH₂)₈-CH₂-CH₂-COOCH₃), 1.59-1.98 (m, 8 H, piperidine-**H**), 2.16-2.19 (m, 3 H, -N-CH₂-(CH₂)₈-CH₂-CH₂-COOCH₃, piperidine-**H**), 2.83-2.85 (m, 2 H, -N-CH₂-(CH₂)₈-CH₂-CH₂-COOCH₃). ¹³C NMR (75 MHz, DMSO-d₆) δ_C: 23.7, 24.5, 25.4, 26.2, 28.3, 28.5, 28.6, 28.8, 28.9, 29.0, 33.7, 38.0, 50.8, 56.0, 174.5, 174.9 ppm. HRMS (ESI + mode, m/z): Calc for [M+H]⁺ 328.2488, found 328.2487.

5.6.4 Synthesis of novel bio-surfactants

Synthesis of ethyl *N*-nonyl piperidine 4-carboxylate

Synthesized according to the same procedure described for *N*-nonylbenzylamine starting from nonanal (228 mg, 0.275 ml, 1.6 mmol) and ethyl piperidine 4-carboxylate (252 mg, 0.247 ml, 1.6 mmol) and isolated as a brown oil (423 mg, 90 %). IR (ATR) 2923, 2853, 1732, 728, 694 cm⁻¹. ¹H NMR (400 MHz, CDCl₃) δ_H: 0.87 (m, 3 H, -N-CH₂-CH₂-(CH₂)₆-CH₃), 1.22-1.29 (m, 15 H, -N-CH₂-CH₂-(CH₂)₆-

Chapter 5: The synthesis of primary amines, polymer precursors and surfactants via hydroaminomethylation

CH₃, -COOCH₂-CH₃), 1.47 (m, 2 H, -N-CH₂-CH₂-(CH₂)₆-CH₃), 1.71-1.81 (m, 2 H, piperidine-**H**), 1.86-2.01 (m, 4 H, piperidine-**H**), 2.22-2.31 (m, 3 H, piperidine-**H**), 2.86-2.89 (m, 2 H, -N-CH₂-CH₂-(CH₂)₆-CH₃), 4.12 (t, *J* = 7.2 Hz, 2 H, COOCH₂-CH₃). ¹³C NMR (75 MHz, CDCl₃) δ_C: 14.2, 14.4, 22.8, 27.1, 27.8, 28.4, 29.4, 29.67, 29.72, 30.0, 41.4, 53.2, 59.2, 60.4, 175.3 ppm.

Synthesis of potassium *N*-nonyl piperidine 4-carboxylate (BS1)

KOH (55 mg, 0.988 mmol) was dissolved in MeOH (8 ml). A solution of ethyl *N*-nonyl piperidine 4-carboxylate (280 mg, 0.988 mmol) in MeOH (2 ml) was added and refluxed for 6 h. After the allotted time, the solvent was removed, producing an off-white solid (251 mg, 87 %). IR (ATR) 2920, 2851, 1553 cm⁻¹. ¹H NMR (600 MHz, CD₃OD) δ_H: 0.90 (m, 3 H, -N-CH₂-CH₂-(CH₂)₆-CH₃), 1.30-1.34 (m, 12 H, -N-CH₂-CH₂-(CH₂)₆-CH₃), 1.51 (m, 2 H, -N-CH₂-CH₂-(CH₂)₆-CH₃), 1.72-1.76 (m, 2 H, piperidine-**H**), 1.87-1.89 (m, 2 H, piperidine-**H**), 2.00-2.04 (m, 2 H, piperidine-**H**), 2.09 (m, 1 H, piperidine-**H**), 2.30-2.33 (m, 2 H, piperidine-**H**), 2.92-2.94 (m, 2 H, -N-CH₂-CH₂-(CH₂)₆-CH₃). ¹³C NMR (75 MHz, CD₃OD) δ_C: 14.4, 23.7, 27.5, 28.8, 30.3, 30.4, 30.7, 30.8, 33.0, 45.7, 54.8, 60.2, 183.8 ppm. HRMS (ESI - mode, m/z): Calc for [M]⁻ 254.2120, found 254.2114.

Synthesis of ethyl *N*-nonyl piperidine 4-carboxylate and its branched counterparts

Synthesized according to the same procedure described for *N*-nonylbenzylamine starting from 1-octene (179 mg, 0.25 ml, 1.6 mmol) and ethyl piperidine-4-carboxylate (252 mg, 0.247 ml, 1.6 mmol) and isolated as a brown oil (408 mg, 87 %). IR (ATR) 2924, 2854, 1732, 729, 694 cm⁻¹. ¹H NMR (600 MHz, CDCl₃) δ_H: 0.84-0.88 (m, 3 H, -N-CH₂-CH₂-(CH₂)₆-CH₃), 1.22-1.26 (m, 15 H, -N-CH₂-CH₂-(CH₂)₆-CH₃, -COOCH₂-CH₃), 1.46 (m, 2 H, -N-CH₂-CH₂-(CH₂)₆-CH₃), 1.71-1.78 (m, 2 H, piperidine-**H**), 1.82-2.11 (m, 4 H, piperidine-**H**), 2.26-2.29 (m, 3 H, piperidine-**H**), 2.77-2.88 (m, 2 H, -N-CH₂-CH₂-(CH₂)₆-CH₃), 4.12 (m, 2 H, COOCH₂-CH₃). ¹³C NMR (151 MHz, CDCl₃) δ_C: 14.2, 14.3, 22.8, 27.1, 27.8, 28.3, 29.4, 29.7, 29.8, 30.6, 41.6, 53.2, 59.2, 60.4, 175.2 ppm.

Synthesis of potassium *N*-nonyl piperidine 4-carboxylate and its branched counterparts (BS2)

Synthesized according to the same procedure described for potassium *N*-nonyl piperidine 4-carboxylate from ethyl *N*-nonyl piperidine 4-carboxylate and its branched counterparts (227 mg, 0.801 mmol) and KOH (45 mg, 0.801 mmol) (212 mg, 90 %). IR (ATR) 2922, 2852, 1553. ¹H NMR (600 MHz, CD₃OD) δ_H: 0.88-0.91 (m, 3 H, -N-CH₂-CH₂-(CH₂)₆-CH₃), 1.30-1.34 (m, 12 H, -N-CH₂-CH₂-(CH₂)₆-CH₃), 1.49-1.54 (m, 2 H, -N-CH₂-CH₂-(CH₂)₆-CH₃), 1.69-1.76 (m, 2 H, piperidine-**H**), 1.82-1.89 (m, 2 H, piperidine-**H**), 2.00-2.03 (m, 2 H, piperidine-**H**), 2.06-2.17 (m, 1 H, piperidine-**H**), 2.30-2.32 (m, 2 H, piperidine-**H**), 2.86-2.93 (m, 2 H, -N-CH₂-CH₂-(CH₂)₆-CH₃). ¹³C NMR (151 MHz, CD₃OD) δ_C: 15.6, 24.9, 28.7, 29.3, 30.1, 31.5, 31.6, 31.9, 32.7, 46.9, 56.4, 61.4, 185.0 ppm. HRMS (ESI - mode, m/z): Calc for [M]⁻ 254.2120, found 254.2110. HRMS (ESI + mode, m/z): Calc for [M+2H]⁺ 256.2277, found 256.2275.

Chapter 5: The synthesis of primary amines, polymer precursors and surfactants via hydroaminomethylation

Synthesis of methyl *N*-nonylprolinate

Synthesized according to the same procedure described for **DE1** from L-proline methyl ester hydrochloride (265 mg, 1.6 mmol) and nonanal (228 mg, 0.275 ml, 1.6 mmol) (399 mg, 98 %). IR (ATR) 2922, 2852, 1733, 1165, 729, 695. ¹H NMR (400 MHz, CDCl₃) δ_H: 0.85-0.88 (m, 3 H, -N-CH₂-CH₂-(CH₂)₆-CH₃), 1.25 (m, 12 H, -N-CH₂-CH₂-(CH₂)₆-CH₃), 1.46-1.49 (m, 2 H, -N-CH₂-CH₂-(CH₂)₆-CH₃), 1.77-1.80 (m, 1 H, pyrrolidine-**H**), 1.89-1.94 (m, 2 H, pyrrolidine-**H**), 2.07-2.12 (m, 1 H, pyrrolidine-**H**), 2.28-2.39 (m, 2 H, pyrrolidine-**H**), 2.59-2.66 (m, 1 H, pyrrolidine-**H**), 3.11-3.20 (m, 2 H, -N-CH₂-CH₂-(CH₂)₆-CH₃), 3.71 (s, 3 H, COOCH₃). ¹³C NMR (151 MHz, CDCl₃) δ_C: 14.2, 22.8, 23.3, 27.7, 28.7, 29.4, 29.5, 29.6, 29.8, 32.0, 51.9, 53.7, 55.4, 66.7, 175.2 ppm.

Synthesis of potassium *N*-nonylprolinate (**BS4**)

Synthesized according to the same procedure described for potassium *N*-nonyl piperidine 4-carboxylate from methyl *N*-nonylprolinate (240 mg, 0.9471 mmol) and KOH (53 mg, 0.9471 mmol) (243 mg, 93 %). IR (ATR) 2921, 2852, 1573. ¹H NMR (400 MHz, CD₃OD) δ_H: 0.88-0.91 (m, 3 H, -N-CH₂-CH₂-(CH₂)₆-CH₃), 1.29 (m, 12 H, -N-CH₂-CH₂-(CH₂)₆-CH₃), 1.52-1.55 (m, 2 H, -N-CH₂-CH₂-(CH₂)₆-CH₃), 1.73-1.89 (m, 3 H, pyrrolidine-**H**), 2.06-2.25 (m, 3 H, pyrrolidine-**H**), 2.74-2.88 (m, 2 H, -N-CH₂-CH₂-(CH₂)₆-CH₃), 3.10-3.15 (m, 1 H, pyrrolidine-**H**). ¹³C NMR (151 MHz, CD₃OD) δ_C: 14.4, 23.7, 27.8, 28.7, 28.9, 30.4, 30.5, 30.6, 30.7, 33.1, 54.7, 56.7, 71.1, 179.9 ppm. HRMS (ESI - mode, m/z): Calc for [M]⁻ 240.1964, found 240.1959. HRMS (ESI + mode, m/z): Calc for [M+2H]⁺ 242.2120, found 242.2119.

Synthesis of methyl *N*-nonylprolinate and its branched counterparts

Synthesized according to the same procedure described for **DE1** from L-proline methyl ester hydrochloride (265 mg, 1.6 mmol) and 1-octene (179 mg, 0.25 ml, 1.6 mmol) (361 mg, 88 %). IR (ATR) 2922, 2852, 1734, 1165. ¹H NMR (600 MHz, CDCl₃) δ_H: 0.85-0.88 (m, 3 H, -N-CH₂-CH₂-(CH₂)₆-CH₃), 1.25-1.29 (m, 12 H, -N-CH₂-CH₂-(CH₂)₆-CH₃), 1.46-1.49 (m, 2 H, -N-CH₂-CH₂-(CH₂)₆-CH₃), 1.77-1.80 (m, 1 H, pyrrolidine-**H**), 1.90-1.92 (m, 2 H, pyrrolidine-**H**), 2.09-2.11 (m, 1 H, pyrrolidine-**H**), 2.30-2.37 (m, 2 H, pyrrolidine-**H**), 2.60-2.65 (m, 1 H, pyrrolidine-**H**), 3.11-3.19 (m, 2 H, -N-CH₂-CH₂-(CH₂)₆-CH₃), 3.71 (s, 3 H, COOCH₃). ¹³C NMR (151 MHz, CDCl₃) δ_C: 14.2, 22.8, 23.3, 27.7, 28.7, 29.4, 29.5, 29.6, 29.8, 32.0, 51.9, 53.7, 55.4, 66.7, 175.2 ppm.

Synthesis of potassium *N*-nonylprolinate and its branched counterparts (**BS5**)

Synthesized according to the same procedure described for potassium *N*-nonyl piperidine 4-carboxylate from methyl *N*-nonylprolinate and its branched counterparts (118 mg, 0.4657 mmol) and KOH (26 mg, 0.4657 mmol) (121 mg, 94 %). IR (ATR) 2921, 2852, 1573. ¹H NMR (600 MHz, CD₃OD) δ_H: 0.88-0.91

Chapter 5: The synthesis of primary amines, polymer precursors and surfactants via hydroaminomethylation

(m, 3 H, -N-CH₂-CH₂-(CH₂)₆-CH₃), 1.29 (m, 12 H, -N-CH₂-CH₂-(CH₂)₆-CH₃), 1.52-1.55 (m, 2 H, -N-CH₂-CH₂-(CH₂)₆-CH₃), 1.73-1.89 (m, 3 H, pyrrolidine-H), 2.06-2.25 (m, 3 H, pyrrolidine-H), 2.74-2.88 (m, 2 H, -N-CH₂-CH₂-(CH₂)₆-CH₃), 3.10-3.15 (m, 1 H, pyrrolidine-H). ¹³C NMR (151 MHz, CD₃OD) δ_C: 14.4, 23.7, 27.8, 28.7, 28.9, 30.4, 30.5, 30.6, 30.7, 33.1, 54.7, 56.7, 71.1, 179.9 ppm. HRMS (ESI + mode, m/z): Calc for [M+2H]⁺ 242.2120, found 242.2119.

5.7 References

1. C. L. Kranemann, B. Costisella and P. Eilbracht, *Tetrahedron Lett.*, 1999, **40**, 7773-7776.
2. T. Rische, K. Müller and P. Eilbracht, *Tetrahedron*, 1999, **55**, 9801-9816.
3. C. L. Kranemann and P. Eilbracht, *Eur. J. Org. Chem.*, 2000, 2367-2377.
4. A. Schmidt, M. Marchetti and P. Eilbracht, *Tetrahedron*, 2004, **60**, 11487-11492.
5. Y. A. El-Badry, A. F. El-Faragy and P. Eilbracht, *Helv. Chim. Acta*, 2013, **96**, 1782-1792.
6. M. Ahmed, C. Buch, L. Routaboul, R. Jackstell, H. Klein, A. Spannenberg and M. Beller, *Chem. Eur. J.*, 2007, **13**, 1594-1601.
7. S. Li, K. Huang, J. Zhang, W. Wu and X. Zhang, *Org. Lett.*, 2013, **15**, 1036-1039.
8. T. O. Vieira and H. Alper, *Chem. Commun.*, 2007, 2710-2711.
9. T. O. Vieira and H. Alper, *Org. Lett.*, 2008, **10**, 485-487.
10. K. Okuro and H. Alper, *Tetrahedron Lett.*, 2010, **51**, 4959-4961.
11. A. Behr, M. Fiene, C. Buß and P. Eilbracht, *Eur. J. Lipid Sci. Technol.*, 2000, **102**, 467-471.
12. A. Behr, T. Seidensticker and A. J. Vorholt, *Eur. J. Lipid Sci. Technol.*, 2014, **116**, 477-485.
13. A. Behr and A. Wintzer, *Chem. Eng. Technol.*, 2015, **38**, 2299-2304.
14. A. J. Vorholt, S. Immohr, K. A. Ostrowski, S. Fuchs and A. Behr, *Eur. J. Lipid Sci. Technol.*, 2017, **119**, 1-10.
15. A. K. Yadav and L. D. S. Yadav, *RSC Adv.*, 2014, **4**, 34764-34767.
16. A. Ariffin, M. N. Khan, L. C. Lan, F. Y. May and C. S. Yun, *Synth. Commun.*, 2004, **34**, 4439-4445.
17. S. Sun, Z. Quan and X. Wang, *RSC Adv.*, 2015, **5**, 84574-84577.
18. A. Mukherjee, D. Srimani, S. Chakraborty, Y. Ben-David and D. Milstein, *J. Am. Chem. Soc.*, 2015, **137**, 8888-8891.
19. R. Porta, A. Puglisi, G. Colombo, S. Rossi and M. Benaglia, *Beilstein J. Org. Chem.*, 2016, **12**, 2614-2619.
20. Y. Saito, H. Ishitani, M. Ueno and S. Kobayashi, *ChemistryOpen*, 2017, **6**, 211-215.
21. C. Gunanathan and D. Milstein, *Angew. Chem.*, 2008, **120**, 8789-8792.
22. K. Shimizu, S. Kanno, K. Kon, S. M. A. Hakim Siddiki, H. Tanaka and Y. Sakata, *Catal. Today*, 2014, **232**, 134-138.
23. B. Zimmermann, J. Herwig and M. Beller, *Angew. Chem. Int. Ed.*, 1999, **38**, 2372-2375.

Chapter 5: The synthesis of primary amines, polymer precursors and surfactants via hydroaminomethylation

24. H. Klein, R. Jackstell, M. Kant, A. Martin and M. Beller, *Chem. Eng. Technol.*, 2007, **30**, 721-725.
25. P. Foley, A. Kermanshahi Pour, E. S. Beach and J. B. Zimmerman, *Chem. Soc. Rev.*, 2012, **41**, 1499-1518.
26. R. Franklin, in *Surfactants from Renewable Resources*, John Wiley & Sons, Ltd., 2010, 21-43.
27. A. de Oliveira Dias, M. G. P. Gutiérrez, J. A. A. Villarreal, R. L. L. Carmo, K. C. B. Oliveira, A. G. Santos, E. N. dos Santos and E. V. Gusevskaya, *Appl. Catal., A*, 2019, **574**, 97-104.
28. S. A. Jagtap, S. P. Gowalkar, E. Monflier, A. Ponchel and B. M. Bhanage, *Mol. Catal.*, 2018, **452**, 108-116.
29. K. C. B. Oliveira, A. G. Santos and E. N. dos Santos, *Appl. Catal., A*, 2012, **445-446**, 204-208.
30. S. Hanna, J. C. Holder and J. F. Hartwig, *Angew. Chem. Int. Ed.*, 2019, **58**, 3368-3372.
31. H. Hu, J. C. Dyke, B. A. Bowman, C. Ko and W. You, *Langmuir*, 2016, **32**, 9873-9882.
32. M. van der Steen and C. V. Stevens, *ChemSusChem*, 2009, **2**, 692-713.
33. D. Shi, Y. Zhao, H. Yan, H. Fu, Y. Shen, G. Lu, H. Mei, Y. Qiu, D. Li and W. Liu, *Int. J. Clin. Pharm. Th.*, 2016, **54**, 343-353.
34. X. Miao, C. Fischmeister, P. H. Dixneuf, C. Bruneau, J. L. Dubois and J. L. Couturier, *Green Chem.*, 2012, **14**, 2179-2183.
35. A. Rybak and M. A. R. Meier, *Green Chem.*, 2007, **9**, 1356-1361.
36. R. J. González-Paz, C. Lluch, G. Lligadas, J. C. Ronda, M. Galià and V. Cádiz, *J. Polym. Sci., Part A: Polym. Chem.*, 2011, **49**, 2407-2416.
37. G. Yu, M. P. Yakovleva and G. A. Tolstikov, *Chem. Nat.*, 2000, **36**, 105-119.
38. S. R. Yasa, S. Cheguru, S. Krishnasamy, P. V. Korlipara, A. K. Rajak and V. Penumarthy, *Ind. Crop. Prod.*, 2017, **103**, 141-151.
39. A. Kumar, M. Dewan, A. De, A. Saxena, S. Aerry and S. Mozumdar, *RSC Adv.*, 2013, **3**, 603-607.
40. A. Lu, T. P. Smart, T. H. Epps, D. A. Longbottom and R. K. O'Reilly, *Macromolecules*, 2011, **44**, 7233-7241.
41. H. A. Zayas, A. Lu, D. Valade, F. Amir, Z. Jia, R. K. O'Reilly and M. J. Monteiro, *ACS Macro Lett.*, 2013, **2**, 327-331.
42. T. M. H. Bach and H. Takagi, *Appl. Microbiol. Biotechnol.*, 2013, **97**, 6623-6634.
43. T. Ponrasu, S. Jamuna, A. Mathew, K. N. Madhukumar, M. Ganeshkumar, K. Iyappan and L. Suguna, *Amino Acids*, 2013, **45**, 179-189.
44. D. Krehan, B. Frølund, P. Krogsgaard-Larsen, J. Kehler, G. A. R. Johnston and M. Chebib, *Neurochem. Int.*, 2003, **42**, 561-565.
45. C. Han, J. Luo, J. Li, Y. Zhang, H. Zhao and L. Kong, *J. Sep. Sci.*, 2016, **39**, 2413-2421.
46. S. Tong, X. Wang, M. Shen, L. Lv, M. Lu, Z. Bu and J. Yan, *J. Sep. Sci.*, 2017, **40**, 1834-1842.

Chapter 5: The synthesis of primary amines, polymer precursors and surfactants via hydroaminomethylation

47. M. Hébrant, P. Burgoss, X. Assfeld and J. Joly, *J. Chem. Soc., Perkin Trans.*, 2001, **2**, 998-1004.
48. N. Joondan, S. B. Moosun, P. Caumul, S. N. Sunassee, G. A. Venter and S. Jhaumeer-Laulloo, *Colloid Polym. Sci.*, 2018, **296**, 367-378.
49. D. H. Kim, S. G. Oh and C. G. Cho, *Colloid Polym. Sci.*, 2001, **279**, 39-45.
50. B. Peterson and C. J. Marzzacco, *Chem. Educator*, 2007, **12**, 80-84.
51. L. Maibaum, A. R. Dinner and D. Chandler, *J. Phys. Chem. B*, 2004, **108**, 6778-6781.
52. N. Kumaraguru and K. Santhakumar, *J. Solution Chem.*, 2009, **38**, 629-640.
53. Z. Jin, Z. Xu, Q. Gong, S. Zhao and J. Yu, *J. Dispersion Sci. Technol.*, 2011, **32**, 898-902.

Chapter 6: Concluding Remarks and Future Prospects

6.1 Concluding Remarks

The main objective of this project was the synthesis of value-added chemicals from relatively cheap feedstocks. In order to accomplish this goal, a range of rhodium (**C1-C5**) and ruthenium (**C6-C8**) complexes were synthesized, bearing imino-pyridine ligands. Complexes **C1-C8** were fully characterized using a range of analytical techniques including IR and NMR (^1H and ^{13}C) spectroscopy, mass spectrometry, elemental analysis and melting point determination.

Complexes **C1-C4** were evaluated as catalyst precursors in the hydroformylation of 1-octene. These complexes contained electron-withdrawing (F) and electron-donating groups (OH and CH_3), however, these substituents had no significant effect on the catalytic activity. We evaluated the influence of pressure, temperature and reaction time on the catalytic activity. High chemoselectivities towards aldehydes were obtained at low temperatures ($\sim 60\text{ }^\circ\text{C}$), albeit at low conversions of the substrate.

We further attempted the hydroformylation of 1-octene using a syngas surrogate, formaldehyde. Although we did not obtain any aldehydic products, the presence of internal octenes and octane indicated that the catalyst is able to decompose formaldehyde. However, the catalyst is only making use of H_2 . Therefore, we postulated the formation of a Rh- H_2 species, with the expulsion of CO.

C4 and **C5** were evaluated as catalyst precursors in the hydroaminomethylation of 1-octene in the presence of secondary (piperidine) and primary amines (aniline and benzylamine). Although these complexes gave a much lower conversion of 1-octene in comparison to the well-known complex, $\text{HRhCO}(\text{PPh}_3)_3$, **C4** and **C5** were found to be superior with regards to the hydrogenation of enamines to the corresponding amines. When we performed the hydroformylation of 1-octene using these complexes, we found that the isomerization of 1-octene was a significant side reaction. However, this was not the case when we performed the hydroaminomethylation of 1-octene in the presence of piperidine. This was attributed to the ability of piperidine to partially inhibit the isomerization of the terminal olefin. This became even more significant when the reaction is performed in the presence of an excess of piperidine. This thus clearly shows the influence of the amine on the chemo- and regioselectivity. The reaction conditions could successfully be optimized to synthesize these amines chemoselectively, proceeding at moderate regioselectivities.

In contrast, isomerization was significant when we performed the hydroaminomethylation of 1-octene in the presence of aniline. This was attributed to the lower basicity of aniline in comparison to

Chapter 6: Concluding Remarks and Future Prospects

piperidine. Aniline is less likely to behave as a ligand and therefore it does not inhibit isomerization. Furthermore, we also found that the hydroaminomethylation of 1-octene in the presence of aniline is much slower due to its lower nucleophilicity. Therefore, careful reaction condition optimization was necessary. When the more basic and nucleophilic amine, benzylamine, was evaluated, the hydroaminomethylation reaction was significantly boosted.

Since rhodium is an expensive metal, there is a need to evaluate the activity of cheaper alternatives. In this regard, we showed that ruthenium is a viable alternative to rhodium, even though slightly higher reaction temperatures are necessary in order to obtain acceptable catalytic activities.

More significantly, we demonstrated the potential of hydroaminomethylation in the synthesis of value-added chemicals from cheap feedstocks. Fatty amines, with carbon chain lengths ranging from C9-C17, were synthesized via hydroaminomethylation and Pd-catalyzed debenzoylation. This synthesis was achieved utilizing cheap olefin feedstocks and an ammonia-surrogate, benzylamine.

We further demonstrated the synthesis of biopolymer precursors via the hydroaminomethylation of methyl 10-undecenoate in the presence of amino esters, L-proline methyl ester and methyl piperidine-4-carboxylate. These compounds were subsequently hydrolysed to the corresponding carboxylic acids.

After the successful utilization of the amino esters in hydroaminomethylation, we realized that they are excellent polar head-groups for surfactants. This allowed us to synthesize biosurfactants via reductive amination and hydroaminomethylation. The CMC's obtained for these biosurfactants corresponded well with that of SDS (sodium dodecyl sulfate), even though they contained an alkyl chain which is three carbons shorter. This illustrated the influence of the nature of the head-groups on the properties of surfactants. We further found that the position of the polar group on the rings can also influence the CMC.

6.2 Future Prospects

Various avenues for further investigation are possible. Although we were unsuccessful in obtaining aldehydes when using formaldehyde, it did reveal that formaldehyde is rather a source of H₂, with the catalyst unable to use the CO. Therefore, a mechanistic investigation by means of ¹H NMR spectroscopy can be performed in order to study the reaction of the complex with formaldehyde. This will hopefully allow us to confirm the formation of Rh-H₂ species. In terms of the catalytic reactions, CO and H₂ can potentially be added to the system in order to evaluate the effect of these gases on the hydroformylation using formaldehyde.

Chapter 6: Concluding Remarks and Future Prospects

In terms of the hydroaminomethylation of 1-octene in the presence of piperidine, aniline and benzylamine, ruthenium needs to be investigated further. This metal is a viable alternative to rhodium, while it is also much cheaper.

All of the complexes used in this study was homogeneous in nature, making their recyclability and reusability almost impossible. Especially using an expensive metal such as rhodium, reusability of the catalyst is necessary in order to improve the efficiency of this system. Since the rhodium complexes contains an OH group, a water-soluble group, such as a PEG moiety, can be attached, in order to perform aqueous-biphasic catalysis. This will potentially allow for the recovery of the catalyst.

There is also the possibility of combining rhodium and ruthenium in order to form a dual-metal catalyst where the rhodium is responsible for hydroformylation and ruthenium for hydrogenation. Since rhodium possess excellent hydroformylation activity, very low catalyst loadings can be used which should lower the cost of the catalyst system.

We have demonstrated the synthesis of primary amines via hydroaminomethylation and Pd-catalyzed debenylation. However, we only focussed on fatty amines and dopamine-analogues. Therefore, the substrate scope can be expanded in order to synthesize other primary amines useful in the pharmaceutical, agrochemical and fine-chemical industries.

The polymerization of diamines and the dicarboxylic acids synthesized in this project can also be performed in order to synthesize novel polyamide polymer.

We showed that the position of the hydrophilic head relative to the hydrophobic tail can have an influence on the CMC of the surfactants. Therefore, in addition to piperidine-4-carboxylic acid, piperidine-3-carboxylic acid as well as piperidine-2-carboxylic acid should also be evaluated. Furthermore, other cations should also be included, such as Cs⁺. According to literature, the larger the cation, the better is its binding to the anion and the lower the CMC.

In addition to the anionic surfactants, cationic surfactants can also be synthesized. *N*-alkylated piperidines were synthesized via the hydroaminomethylation of 1-octene in the presence of piperidine. Further alkylation of the tertiary amine can be performed to form cationic tetra-alkylated amines. These cationic tetra-alkylated amines can also potentially be used as cations for the anionic surfactants, which could lead to surfactants having the properties of both the cationic and anionic surfactant. Additionally, oxidation of *N*-alkylated piperidines can give access to zwitterionic surfactants.